PB82-230939

Volatilization of Organic Pollutants from Water

Toronto Univ. (Ontario)

Prepared for

Environmental Research Lab.
Athens, GA

April 1982

U.S. DEPARTMENT OF COMMERCE
National Technical Information Service
NTIS

PB82-230939

EPA 600/3-82-019

VOLATILIZATION OF ORGANIC POLLUTANTS FROM WATER

by

Donald Mackay, Wan Ying Shiu, Alice Bobra, Jim Billington,
Eva Chau, Andrew Yeun, Cecilia Ng and Foon Szeto

Department of Chemical Engineering
and Applied Chemistry
University of Toronto
Toronto, Canada M5S 1A4

Contract No. R805150010

Project Officer

Samuel W. Karickhoff
Environmental Processes Branch
Environmental Research Laboratory
Athens, Georgia 30613

ENVIRONMENTAL RESEARCH LABORATORY
OFFICE OF RESEARCH AND DEVELOPMENT
U.S. ENVIRONMENTAL PROTECTION AGENCY
ATHENS, GEORGIA 30613

TECHNICAL REPORT DATA
(Please read Instructions on the reverse before completing)

1. REPORT NO. EPA-600/3-82-019	2. ORD Report	3. RECIPIENT'S ACCESSION NO. PB82-230029
4. TITLE AND SUBTITLE Volatilization of Organic Pollutants from Water		5. REPORT DATE April 1982
		6. PERFORMING ORGANIZATION CODE
7. AUTHOR(S) D. Mackay, W.Y. Shiu, A. Bobra, J. Billington, E. Chau, A. Yeun, C. Ng and F. Szeto		8. PERFORMING ORGANIZATION REPORT NO.
9. PERFORMING ORGANIZATION NAME AND ADDRESS Department of Chemical Engineering and Applied Chemistry University of Toronto Toronto, Canada M5S 1A4		10. PROGRAM ELEMENT NO. CCUL1A
		11. CONTRACT/GRANT NO. R805150010
12. SPONSORING AGENCY NAME AND ADDRESS Environmental Research Laboratory--Athens GA Office of Research and Development U.S. Environmental Protection Agency Athens, Georgia 30613		13. TYPE OF REPORT AND PERIOD COVERED Final, 8/77-11/80
		14. SPONSORING AGENCY CODE EPA/600/01

15. SUPPLEMENTARY NOTES

16. ABSTRACT

The volatilization of organic environmental contaminants from water bodies to the atmosphere was investigated. The general aim was to elucidate the factors that control the volatilization process and develop predictive methods for calculating volatilization rates for various compounds from rivers, lakes and other water bodies under various conditions of temperature and wind speed.

The report contains both theoretical and experimental studies and a comprehensive review of the equilibrium physical chemistry and thermodynamics of systems involving hydrophobic organic solutes and water. A result of the thermodynamic analysis is the development of the fugacity approach for calculating multi-phase equilibria applicable to environmental partitioning. The approach can also be applied to calculating multi-resistance transfer as may occur in lakes. Correlations are developed for predicting or checking consistency of data for aqueous solubility, vapor pressure, Henry's law constant and octanol-water partition coefficient.

17. KEY WORDS AND DOCUMENT ANALYSIS

a. DESCRIPTORS	b. IDENTIFIERS/OPEN ENDED TERMS	c. COSATI Field/Group

18. DISTRIBUTION STATEMENT RELEASE TO PUBLIC	19. SECURITY CLASS *(This Report)* UNCLASSIFIED	21. NO. OF PAGES 212
	20. SECURITY CLASS *(This page)* UNCLASSIFIED	22. PRICE

EPA Form 2220-1 (9-73)

DISCLAIMER

This report has been reviewed by the Environmental Research Laboratory, U.S. Environmental Protection Agency, Athens, Georgia, and approved for publication. Approval does not signify that the contents necessarily reflect the views and policies of the U.S. Environmental Protection Agency, nor does mention of trade names or commercial products constitute endorsement or recommendation for use.

FOREWORD

Environmental protection efforts are increasingly directed towards prevention of adverse health and ecological effects associated with specific compounds of natural or human origin. As part of this Laboratory's research on the occurrence, movement, transformation, impact, and control of environmental contaminants, the Environmental Processes Branch studies the microbiological, chemical, and physico-chemical processes that control the transport, transformation, and impact of pollutants in soil and water.

Environmental decisions regarding the control of toxic substances rely heavily on information about the substances' partitioning between the atmosphere, water, soil, sediment, and biota and the effects of degradation processes such as photolysis, chemical oxidation, and hydrolysis. An important factor is the volatilization rate because some compounds that degrade slowly in water are rapidly transformed in the atmosphere. This report examines the volatilization process and presents a predictive method that can be incorporated into evaluative models of compounds in aquatic environments.

David W. Duttweiler
Director
Environmental Research Laboratory
Athens, Georgia

ABSTRACT

The volatilization of organic environmental contaminants from water bodies to the atmosphere was investigated. The general aim was to elucidate the factors that control the volatilization process and develop predictive methods for calculating volatilization rates for various compounds from rivers, lakes and other water bodies under various conditions of temperature and wind speed.

The report contains both theoretical and experimental studies and a comprehensive review of the equilibrium physical chemistry and thermodynamics of systems involving hydrophobic organic solutes and water. A result of the thermodynamic analysis is the development of the fugacity approach for calculating multi-phase equilibria applicable to environmental partitioning. The approach can also be applied to calculating multi-resistance transfer as may occur in lakes. Correlations are developed for predicting or checking consistency of data for aqueous solubility, vapor pressure, Henry's law constant and octanol-water partition coefficient.

The experimental program developed a small-scale laboratory system that is suitable for studying volatilization characteristics of solutes from water under controlled conditions of temperature, concentration, and turbulence, and in the presence of co-solutes or sorbents. The test may be used for volatilization screening purposes. Tests in a 6-m-long by 60-cm-deep wind wave tank were used to study the volatilization of 11 compounds covering a wide range of Henry's law constant. The relevant hydrodynamic data were also obtained. It was concluded that the two-resistance or Whitman model of mass transfer adequately describes the volatilization process. Correlations were developed for the liquid and gas phase mass transfer coefficients as a function of wind speed and solute properties.

Henry's law constant data were obtained for a number of organic solutes using a previously developed gas stripping system. A novel system was also developed that is suitable for the measurement of Henry's law constants in the range of 10^{-7} to 10^{-5} atm m^3/mole. The system essentially involves batch distilling a solute-water mixture.

Determinations of Henry's law constant are also reported for solutes in the presence of dissolved organic humic matter. It is concluded that the dissolved organic matter will rerely be present at concentrations that will significantly affect solubility and hence Henry's law constant.

This report was submitted in fulfillment of Contract No. R805150010 by the University of Toronto under the sponsorship of the U.S. Environmental Protection Agency. This report covers the period August 1977 to November 1980; and work was completed as of November 1980.

CONTENTS

Foreword iii

Abstract iv

Figures vi

Tables viii

1. Introduction 1

2. Conclusions 3

3. Recommendations 6

4. Equilibrium Physical Chemistry 7

5. Mass Transfer Phenomena 57

6. General Model of Laboratory Volatilization Systems 82

7. Experimental and Results 88

8. Discussion 141

9. Calculation of Environmental Volatilization Rates 171

10. References 188

11. Symbols 195

12. Glossary 200

13. Index 201

FIGURES

Number		Page
1	Illustrative Pressure Temperature Diagram for a Pure Compound	18
2	Plot of Total Surface Area Versus Molecular Weight	25
3	Plot of Total Surface Area Versus Molar Volume	26
4	Plot of Total Surface Area Versus Carbon Number	27
5	Plot of Total Surface Area Versus Carbon Plus Chlorine Number	28
6	Relationship Between Vapor Pressure and Boiling Point for Selected Solutes	31
7	Plot of Solubility, Vapor Pressure and Henry's Constant	41
8	Schematic Diagram of Relationships Between Physical Chemical Properties, the Fundamental Quantities which are Inaccessible by Direct Experimental Measurement Being in the Box	53
9	Schematic Diagram of Transport Processes	58
10	Illustrative Fugacity Transport Calculation	67
11	Schematic Diagram of an Element of Water Experiencing Exposure to the Atmosphere and Hence Loss of Solute by Volatilization in a "Roll Cell"	70
12	Diagram Illustrating the Non-additivity of Resistances during Unsteady State Transfer in a Roll Cell	73
13	Diagram Illustrating a Possible Experimental Test of the Two Resistance Theory for Compounds of Various H Values	74
14	Plot of G/A Versus H illustrating Approximately the Regimes Which May Apply during Laboratory Volatilization Experiments	87
15	General Arrangement of the Small Scale Volatilization Apparatus System	100
16	Plan View of the Small Scale Volatilization Tank	101
17	A Typical Plot of Log Concentration Versus Time for a Highly Volatile Solute (Benzene)	102

Number		Page
18	A Typical Plot of Log Concentration Versus Time for a Solute of Intermediate Volatility (2 Butanone)	103
19	A Typical Plot of Log Concentration Versus Time for a Solute of Low Volatility (1 Pentanol)	104
20	Plot of Mass Transfer Coefficients K_{OL} Versus Turbulence for the Small Scale Volatilization Apparatus Illustrating Dependence on Volatility	105
21	Effect of Temperature on K_{OL} for Benzene and Toluene Volatilization in the Small Scale Volatilization System	106
22	Plot of Log $((C-C_\infty)/(C_o-C_\infty))$ Versus Time for Oxygen Transfer in the Small Scale Volatilization System	107
23	Diagram of the Wind Wave Tank	109
24	Typical Plot of Linear and Logarithmic Velocity Profiles	111
25	Variation of Surface Drift Velocity with Fetch in the Wind Wave Tank	112
26	Plot of Final Water Surface Drift Velocity Versus Wind Speed for the Wind Wave Tank Illustrating a Drift Velocity of 2.82% of Wind Speed	113
27	Typical Plot of Log Concentration Versus Time for a Volatile Compound (Benzene) in the Wind Wave Tank	115
28	Plot of Log Concentration Versus Time for Volatilization of a Low Volatility Compound (1 Butanol) in the Wind Wave Tank	116
29	Plot of K_{OL} Versus Wind Speed for Volatilizing Solutes of Various H Values in the Wind Wave Tank	117
30	Schematic Diagram of the Relative Volatility System for Measuring Henry's Law Constants	123
31	Diagram of Henry's Law Apparatus	129
32	Experimental and Correlated Values of K_G for Schmidt Number 0.60	160
33	Experimental and Correlated Values of K_L Connected to a Schmidt Number of 1000	161

TABLES

Number		Page
1.	Illustrative Fugacity Calculation	14
2.	Total Surface Area Correlations	22
3.	Boiling Points, Melting Points and Literature Calculated Vapor Pressures at 25°C	32
4.	Henry's Law Constant Correlations	43
5.	Physical and Chemical Properties of Selected Compounds	47
6.	Solutes Used in the Volatilization Experiments	91
7.	Solute Properties	92
8.	Small Scale Volatilization Test Results	98
9.	Volatilization of Mixtures	99
10.	Mass Transfer Coefficients Fom the Wind Wave Tank	120
11.	Volatilization Results of Mixtures in the Wind Wave Tank	121
12.	Results from the Relative Volatility Apparatus	125
13.	Solubility Results	127
14.	Henry's Law Constants Results	131
15.	Hydrodynamic Results	150
16.	Wind Wave Tank Mass Transfer Rates for Benzene and Toluene	152
17.	Wind Wave Tank Gas Phase Controlled Mass Transfer Coefficients	155
18.	Environmental and Laboratory Values of K_L and K_G	156
19.	Constants for Infinite Dilution Activity Coefficients	162
20.	Calculated and Experimental Results from the Relative Volatility Apparatus	164

SECTION 1

INTRODUCTION

This report contains a description of the results of a three-year research program into the volatilization of environmental contaminants from water bodies to the atmosphere. The general objective was to elucidate the dominant factors controlling the volatilization process and develop a predictive method by which volatilization rates can be calculated for various compounds under various environmental conditions.

It is evident that the environmental management of toxic substances requires a knowledge of the substances' partitioning properties between the atmosphere, water, soil, sediments, and biota, and also the reaction rates of processes such as biodegradation, photolysis, chemical oxidation and hydrolysis which may occur in each environmental compartment. The overall rate of reaction of the substance, which directly controls its half-life or persistence in the environment is the sum of the various individual rates of reaction in each compartment, which are each determined by concentrations of the substance and prevailing degradative rate constants as influenced by microbial populations, incident solar radiation, temperature, pH, and other variables. In many cases, contaminants are introduced into one compartment of the environment, for example, water, in which there may be relatively slow degradation. The primary degradative process for that compound may occur in an adjacent compartment such as the atmosphere. The result in such cases is that the overall persistence of the substance and the concentrations which it achieves in the environment are controlled by the rate at which the material can move from the compartment into which it was first introduced, to the compartment in which it primarily degrades. For example, certain hydrocarbons may be introduced as effluents to the water environment in which they are subject to very slow or zero rates of hydrolysis, oxidation and biodegradation. Their physical-chemical properties are such that they volatilize into the atmosphere where they become subject to photolytic degradation rates. In such cases, the environmental rate of destruction of the compound may be primarily controlled by the volatilization rate.

An adequate understanding of a substance's environmental dynamics can thus only be obtained by assembling some form of model in which the accumulation in, reaction in, and transfer between various compartments is taken into account. The real environment is exceedingly complex and it is possible to model only very limited sections of it with any degree of validity. An example could be a stretch of river or a small pond. In such cases, for local management purposes, it may be desirable to estimate the prevailing volatilization rates of contaminants for that particular environment. For example, attempts have been made to assemble mass budgets for contaminants in water

bodies such as the Great Lakes of Lake Zurich (1,2). Of more general applicability and of greater use for regulatory purposes are the "evaluative" models first proposed by Baughman and Lassiter (3), which have been implemented for 12 contaminants by Smith et al. (4). In this study, the dynamics of the behaviour and movement of these toxic substances was calculated for hypothetical aquatic environments consisting of defined volumes of ponds or rivers. This concept has recently been extended to the "Exposure Analysis Modeling System" developed at the U.S. Environmental Protection Agency's Environmental Research Laboratory, Athens, Georgia (5).

In these modelling efforts it is apparent that accurate estimates of volatilization rate are required for certain categories of compounds. The object of this study was then to undertake an experimental program to elucidate the nature of the volatilization process and develop a predictive method which can be used in such evaluative models or in models of actual sections of the environment.

In this report, the approach taken is first to discuss the equilibrium physical-chemistry or thermodynamics of these substances. This is largely the estimation of the Henry's Law constant or air-water partition coefficient, which applies to a given substance. Relationships between this constant and other quantities are explored. This is followed by a discussion of the kinetic or mass transport phenomena aspects of the issue and is largely concerned with measurements of mass transfer coefficients. Finally, a general approach towards calculation of volatilization rates in the environment is presented by combining physical-chemical properties with transport phenomena information and environmental data. Some validating experiments are also described.

SECTION 2

CONCLUSIONS

An experimental and theoretical study has been undertaken of the process of volalilization of organic compounds from water bodies to the atmosphere. Comprehensive reviews are presented of the relevant equilibrium physical density and mass transport phenomena from which the following conclusions are drawn.

The fugacity concept which has been increasingly used in engineering calculations of multi-phase equilibria has been extended to treat environmental partitioning. It is believed that its use facilitates partitioning calculations which are an important component of the assessment of compounds of environmental concern. The use of the fugacity concept has also been successfully applied to multi-resistance transfer problems as may occur in lakes.

From a consideration of the physical chemical principles underlying aqueous solubility, vapor pressure, Henry's Law Constant (i.e., air-water partition coefficient) and octanol water partition coefficient (i) forms of correlation are suggested (based largely on previous work) for solubility as a function of solute melting point, total surface area, molecular weight, molar volume and carbon number; (ii) a correlation is presented for vapor pressure as a function of boiling & melting point; (iii) correlations are presented for Henry's Law constant and (iv) correlations are presented between solubility and octanol-water partition coefficient.

The equations governing the volatilization process in various configurations of laboratory systems have been assembled and it has been shown that they reduce to four limiting regimes of equilibrium control, liquid phase resistance control, gas phase resistance control and non-volatile systems. Some confusion has existed in the literature by applying equations applicable in one regime to results obtained from another.

The experimental program has resulted in the development of a small scale laboratory system suitable for the study of the volatilization characteristics of solute under controlled conditions of concentration, temperature, turbulence and the presence of co-solutes or sorbents. Tests with a series of twenty organic solutes (covering a wide range of Henry's Law Constants) demonstrated the validity of the two resistance model of volatilization and suggested that the preferred method of taking into account solute molecular size as it influences the gas and liquid mass transfer coefficients is by use of the solute's dimensionless Schmidt number (i.e., phase viscosity divided by the product of density and diffusivity) raised to the power of -0.67 for the gas and -0.5 for the liquid. This approach also incorporates a temperature dependence.

It was also concluded that in dilute solutions solute mixtures volatilize without significant interactions between the solutes, thus greatly facilitating multicomponent volatilization calculations.

The effect of temperature is complicated by the possible influence of evaporating or condensing water which could not be adequately quantified in this study.

A wind wave tank 6 meters long by 1.2 meters deep was constructed and operated to study the volatilization of eleven compounds covering a wide range of Henry's Law Constants. Relevant hydrodynamic data were also obtained, especially velocity profiles from which full stream and function velocities, surface roughness and roughness Reynolds Number were calculated. It is concluded that function velocity is the primary determinant of mass transfer coefficient in gas and liquid phases.

The liquid and gas phase mass transfer coefficients K_L and K_G m/s have been correlated for both laboratory and environmental conditions as follows.

Laboratory	$K_L = 68.2\times10^{-6} U_\infty^{1.5} Sc_L^{-0.5}$	
Environment	$K_L = 34.1\times10^{-6} (6.1+0.63U_{10})^{0.5} U_{10} Sc_L^{-0.5}$	(all in units of m/s)
Laboratory	$K_G = 92.4\times10^{-5} U_\infty^{1.5} Sc_G^{-0.67}$	
Environment	$K_G = 46.2\times10^{-5} (6.1+0.63U_{10})^{0.5} U_{10} Sc_G^{-0.67}$	

where U_∞ is the free stream velocity (m/s) (generally at a height of 30 cm), U_{10} is the 10 metre environmental wind velocity (m/s), Sc_L and Sc_G are the dimensionless liquid and gas Schmidt Numbers i.e. (viscosity devided by density and molecular diffusivity in consistent units).

More complex forms involving roughness Reynold's Number terms have also been developed which give a slightly better fit of the data, but the extra complexity is not regarded as justified at present. These equations which have a sound basis in fluid mechanics predict that environmental mass transfer coefficients will be lower than laboratory values because of the generally lower drag coefficients which in turn cause lower friction velocities in the environment. It is believed that at short fetches when the wind is actively accelerating the water surface layers there are higher drag coefficients and friction velocities, greater turbulence and hence more rapid mass transfer. This observation is borne out from an examination of the few available environmental mass transfer coefficients, which are reproduced well using the correlations.

There remains some doubt about the K_L and K_G values at low wind speeds (which were not studied in this work) and it is suspected that the correlations will require some modification to be more accurate at these conditions.

The use of the Schmidt number quantifies the effects of molecular size and temperature.

The data generated in the wind wave tank for eleven solutes covering a range in Henry's Law Constants provide further evidence validating the two resistance approach.

A preliminary experiment into the effect of interfacial films on volatilization is described and a theoretical framework is suggested (based on previous work) which is believed to be capable of describing this phenomenon.

A novel system is described for the measurement of Henry's Law Constants in the range of 10^{-7} to 10^{-5} atm m^3/mol which involves measuring the relative volatility of the solute and water. It is thus complimentary to the gas stripping technique which is better applied to compounds of higher Henny's Law constant. Determinations are presented for the solutes alone and in the presence of dissolved organic (humic) matter. The aqueous solubility of selected organic compounds was also measured in the presence of similar organic matter using a generator column technique. It is concluded that dissolved organic matter present at concentrations likely to be encountered environmentally does not significantly affect solubility and hence Henry's Law constant. Allowance must be made for sorbents and high concentrations of electrolytes as may be encountered in certain environments.

The results of the program suggest that volatilization rates can be calculated for most environmental conditions with an acceptable accuracy. Some aspects of these calculations applied to rivers and lakes are reviewed.

It is suggested that when the environmental volatilization characteristics of a solute are to be determined the optimal strategy is to obtain data for:

aqueous solubility
vapor pressure and boiling point
Henry's Law Constant
octanol water partition coefficient
molar volume (experimentally or by additive volumes)
(and hence Schmidt Numbers)

The physical chemical data should be subjected to an internal consistency check. An example is given for naphtahlene.

Volatilization rates can then be measured in the small scale (6 liter) system to obtain K_{OL} estimates at the required temperature, preferably with simultaneous measurement of K_{OL} for solutes of similar Henry's Law Constant (e.g. toluene, an alcohol or oxygen) and the values again checked for consistency with the two resistance model. If desired distilled water, salt water or other natural waters containing organic or mineral matter can be used at any desired temperature and humidity level.

The resistance to volatilization as characterised by K_L and K_G combined with the appropriate fugacity capacities can then be compared with other resistances as may for example be offered by depths of water column to establish an overall resistance and hence a steady state flux.

SECTION 3

RECOMMENDATIONS

For any compound of environmental concern, reliable aqueous solubility, vapor pressure, Henry's Law Constant and octanol water partition coefficient data should be sought and the values checked for internal consistency.

Of particular interest are data for highly hydrophobic compounds such as PCB's which have apparently anomalous solubility-octanol water partition coefficient relationships.

The correlations developed here for solubility, vapor pressure and hence Henry's Law Constants should be improved to achieve higher accuracy by improving (i) the activity coefficient - molecular area relationship and (ii) the boiling point-vapor pressure relationship. To achieve this accurate vapor pressure data are required for higher boiling organic solutes. Ultimately, it is believed that these properties can be predicted with acceptable accuracy from molecular structure.

The further systematic study of the effects of temperature, co-solutes and turbulence on volatilization rates of various organic solutes is justified to provide additional validation of the predictive equations derived here, especially at low wind speeds.

A study of the effect of surface organic microlayers or films of various compositions and various thickness is desirable to test the theoretical approach suggested here.

In situ measurement of volatilization rates from ponds is desirable to validate the predictions developed here.

Further experimentation using the "relative volatility" method for determining Henry's Law Constants is desirable, especially for solutes in which water is quite soluble and for which the assumption that the Henry's Law Constant is simply the ratio of vapor pressure to solubility is believed to be erroneous. The magnitude of this error and corrective methods should be studied.

SECTION 4

EQUILIBRIUM PHYSICAL CHEMISTRY

CRITERIA FOR EQUILIBRIUM BETWEEN PHASES

Volatilization of a substance from a water body to the atmosphere occurs only when the concentration of the substance in the atmosphere is lower than the (hypothetical) concentration which is in equilibrium with its concentration in the water body. Determining whether or not volatilization occurs and the direction of transfer between the two phases thus requires knowledge of the equilibrium concentrations in the two phases. Further, in kinetic expressions developed later, the conventional approach is to postulate that the rate at which material moves between phases is proportional to the displacement from equilibrium. Equilibrium data are thus critically important in controlling the direction and rate of transfer.

When a solute, such as benzene, achieves equilibrium between air and water phases, it adopts different concentrations in each phase. The ratio of these concentrations, i.e. the air-water partition coefficient can be expressed in various forms, the most convenient being the Henry's Law constant (H atm m^3/mol) which is the ratio of partial pressure in the atmosphere (P atm) to concentration in water (C mol/m^3).

In environmental studies, several such partition coefficients are useful, for example, bioconcentration factors between water and aquatic biota, octanol-water partition coefficient, and sorption coefficients. For each solute, there can be therefore, a partition coefficient for each pair of environmental phases. It is more illuminating and intellectually more satisfying to discuss these equilibrium partitioning situations in terms of the fundamental quantity which controls the differing concentrations. In his classical studies of phase equilibrium thermodynamics, Gibbs showed that diffusive equilibrium of a solute between two phases occurs when the system is at maximum entropy, or for constant temperature and pressure conditions is at minimum free energy, or when the chemical potential of the solute in in both phases are equal. This topic is discussed fully in standard texts in thermodynamics, for example that by Prausnitz (6). Later, Lewis introduced the more convenient criterion for equilibrium between phases of fugacity. Whereas chemical potential has units of energy per mole which is conceptually difficult to grasp, fugacity has units of pressure and can be viewed as the escaping tendency which a substance exerts from any given phase. In the atmosphere, the fugacity is normally equal to the partial pressure of the substance. Equilibrium is achieved between two phases when the escaping tendency from one phase exactly equals that from the other. There is

inevitably transfer or exchange between the two phases, however, the net rate of exchange is zero. A most convenient property of fugacity is that it is usually linearly related to concentration, at least at the low concentrations which normally apply to environmental contaminants. It is thus possible to write a fugacity concentration relationship of the form

$$C = fZ$$

where C is concentration in (mol/m^3), f is fugacity (atm) and Z is a fugacity capacity with units mol/m^3 atm.

It may be helpful for conceptual purposes to consider the analogous situation of equilibrium of heat between two phases. Heat achieves equilibrium between two phases at different heat concentrations expressed as J/m^3. The criterion of equilibrium in this case, is that the temperature of the two phases are equal. Temperature, like fugacity, is a potential quantity which determines the state of the phases with respect to equilibrium. The relationship between heat concentration and temperature is the simple heat capacity relationship,

$$C_H = TZ_H$$

where C_H is heat concentration (J/m^3), Z_H is a volumetric heat capacity (J/m^3K) (which is actually the product of the more commonly used mass heat capacity and the phase density), and T is temperature (K). Whereas heat tends to accumulate in the phases where its heat capacity is largest, mass tends to accumulate in phases where its fugacity capacity is largest. It transpires that hydrophobic organics thus tend to partition into lipid phases where their Z value is large. This topic has been reviewed by Mackay (7).

If there are two phases, (subscripted 1 and 2) then equilibrium of a solute will be reached when the fugacity of the solute is equal in both phases

$$\text{i.e. } f_1 = f_2$$
$$\text{thus } C_1/Z_1 = C_2/Z_2$$
$$\text{or } \quad C_1/C_2 = Z_1/Z_2 = K_{12}$$

It is apparent then that the dimensionless partition coefficient controlling the distribution of the substance between the two phases (K_{12}) is thus merely the ratio of the fugacity capacities. The elegance of this approach is apparent if one considers a ten phase system in which there are potentially 10 x 9 or 90 partition coefficients which may apply. These partition coefficients are, of course, constrained in value with respect to each other. There are, however, only 10 fugacity capacities, and the 90 partition coefficients are merely all possible ratios of these 10 values. Expressing equilibrium in terms of these fugacity capacities is also more convenient because it separates the escaping tendencies of each phase and facilitates the calculation of these quantities from other related thermodynamic data. Usually, much of the uncertainty about the value of an air-water partition coefficient lies in the value of Z in the water.

The approach taken here is to calculate Z values for solutes mainly in the atmosphere, in aqueous solution, in sorbed state, in octanol

solution, and in biota. The ratios of these quantities then give the required partition coefficients, in particular, the related Henry's Law constant, which is of primary interest in volatilization calculations.

It is believed that the "fugacity approach" for elucidating the partitioning, reaction and transport characteristics of environmental contaminants, which has been developed as part of this research program, may be of value in the environmental management of toxic substances. It has the advantage of being conceptually simple, of being applicable at various levels of complexity, and of providing guidance as to the required accuracy of physical, chemical, reaction and transport data which may be sought by regulatory agencies prior to commercial manufacture and use. Most substances will partition into a few environmental compartments, be degraded by a few processes and be subject only to a few significant transport routes. Obviously then, relatively high accuracy is required for only a few properties, but which few is not apparent until a preliminary assessment has been undertaken. A particularly attractive and economic option is thus to estimate physical property data, then refine these estimates by experiment as the need for refinement is demonstrated. It is hoped that this section will be of value in this subject area by assembling a reasonably complete account of the phase equilibrium thermodynamics of aqueous solutions of organic compounds, with some attempt at correlation and estimation of environmentally relevant properties.

FUGACITY CAPACITIES

The Atmosphere

In the vapor phase the fugacity is rigorously expressed by

$$f = y \phi P_T \simeq P$$

where y is the mole fraction, P_T is the total pressure (atm) (here atmospheric pressure) and ϕ is the fugacity coefficient which is dimensionless and is introduced to account for non-ideal behaviour. Fortunately at atmospheric pressure ϕ is usually close to unity and can thus be ignored. The exceptions are solutes such as carboxylic acids which associate in the vapor phase. The fugacity is thus equivalent in most cases to the partial pressure P (atm). It should be noted here that this equation assumes the solute to be in truly gaseous form, not associated with particulates. Now concentration C (mol/m^3) is related to partial pressure through the gas law as

$$C = n/V = P/RT = f/RT = fZ$$

Thus Z_A for vapors is simply 1/RT where RT has a value of about 24 atm/(mol/liter) or 0.024 m^3atm/mol, corresponding for example to R of 82 x 10^{-6} m^3atm/mol K and T of 293 K or 20°C. Z_A is independent of the nature of the solute or the composition of the vapor (for non-association solutes and low or atmospheric pressure condition) and has a value of typically 41 mol/m^3atm. The temperature dependence of Z is obvious.

Water Bodies

In aqueous solution the fugacity is given by

$$f = x\gamma P^s$$

where x is the mole fraction, P^s is the vapor pressure of the pure liquid solute at the system temperature and γ is the liquid phase activity coefficient on a Raoult's Law convention (not a Henry's Law convention). By this convention when x is unity γ is also unity and f becomes the pure component vapor pressure. Generally for non-ionizing substances γ increases as x decreases to an "infinite dilution" value as x tends to zero. This relationship between x and γ is often of the form

$$\ln \gamma = K(1-x)^2$$

In most environmental situations x is quite small thus ln γ can be equated to K without serious error. This near-constancy in γ leads to the very convenient near linear relationship between C and f, reflected as a constant value of Z.

The relationship between f and C to give Z_W can be obtained by writing for infinite dilution conditions

$$Z = C/f = C/P = 1/H = x/vf = 1/v\gamma P^s$$

where v is the molar volume (m^3/mol) of the solution which is approximately 18×10^{-6} m^3/mol. For water Z_W is thus simply the reciprocal of the Henry's Law Constant H. This is in accord with the definition of H which is the constant by which liquid concentration is multiplied to give partial pressure P, which is here equal to fugacity, i.e.

$$P = HC$$

Since H is of such importance in volatilization calculations it is desirable to elucidate certain conditions under which this simple approach may be applied incorrectly.

First, these equations are applicable only if the solute is in truly dissolved forms at a concentration less than or equal to saturation. Often the solute is present environmentally in solution in a sorbed form associated with biota or suspended mineral or organic matter. Very hydrophobic compounds such as PCBs or PNAs may be present in colloidal form at a total concentration in excess of their solubility. Such forms of solute are effectively in another phase and do not contribute to the solution fugacity. It is thus essential to ensure that a measured concentration is truly dissolved, or if this is not the case, calculate the fraction which is dissolved.

Second, as discussed later, there are several methods of measuring or estimating H (and hence Z for water). In principle these reduce to the direct or indirect measurement of P and C at equilibrium or to the separate calculation of P as the saturation vapor pressure (P^s) and C the solubility of the solute (C^s). This latter method is very convenient since solubilities and vapor pressures are widely available in the literature. Unfortunately the pure solute may undergo a phase transition (melting, boiling or crystalline) near environmental temperatures thus the published P^s and C^s data may refer to different phases. For example the solubilities published for naphthalene are usually of the solid, while the vapor pressures are of the liquid. In the case of PCBs the solubilities are usually of the pure isomers, most of which are solid, whereas the vapor pressures are of the liquid mixtures which are essentially subcooled. Both measurements must refer to the same phase or erroneous results will be obtained.

Techniques are emerging by which γ can be calculated from molecular structure. If such data are available H can be deduced as $v\gamma P^s$ provided that data are available for P^s, the <u>liquid</u> solute vapor pressure at the system temperature. This vapor pressure may be experimentally inaccessible if the solute is solid or gas at this temperature i.e. the system temperature lies outside the range from triple point to critical point. In such cases P^s is a hypothetical quantity whose value can be inferred by extrapolating the liquid vapor pressure curve below the triple point or above the critical point. It is erroneous to use a solid vapor pressure in this calculation.

This issue is discussed in more detail later.

Sorbed Phases

The importance of calculating Z for sorbed phases lies in the necessity of discriminating between truly dissolved and sorbed material as are often measured in total by environmental analyses. The approach taken below differs from that presented previously by Mackay (7) and it is believed to be simpler and more rigorous.

Sorption equilibrium are usually expressed as equations or isotherms relating dissolved to sorbed concentrations. Examples are the Freundlich, Langmuir or Linear equations. For most hydrophobic compounds at concentrations well below their solubilities the Linear equation is adequate (Karickhoff et al, 8), namely

$$X = K_p C$$

where X is the sorbed concentration, here expressed in moles solute per 10^6 g (Mg) sorbent (wet or dry) and K_p is a sorption coefficient with units of m^3 water per 10^6 g sorbent. The equation is often expressed in mass concentration units (X in g/Mg or μg/g and C in g/m^3 or mg/L) in which case an identical numerical value is obtained.

If the sorbent concentration expressed as volume fraction is S and its density is ρ (g/cm^3 or Mg/m^3) then its concentration is Sρ Mg/m^3 (or g/cm^3). This concentration is typically 10^{-5} g/cm^3 or 10 mg/L thus it is convenient to record data as g/m^3 or $10^6 S\rho$.

The concentration of sorbed material (C_s) expressed as mol per m^3 of sorbent is thus $X\rho$ mol/m^3.

At equilibrium, the fugacities of the sorbed and dissolved material must be equal, thus if Z_s is the sorbed phase fugacity capacity

$$f = HC = C_s/Z_s$$

thus

$$Z_s = C_s/HC = X\rho/H(X/K_p) = K_p\rho/H$$

the group $K_p\rho$ is dimensionless and is actually the partition coefficient expressed as a mols per unit volume ratio.

If in 1.0 m^3 of solution containing a low concentration of sorbent of volume fraction S the fugacity is f then the concentration of dissolved material is Zf or f/H mol/m^3 thus there are f/H mol dissolved. The sorbed concentration is fZ_s or C_s mol per m^3 of sorbent or a total of fZ_sS mol or $fK_p\rho S/H$. The total amount is thus

$$f/H + fK_p\rho S/H \quad \text{or} \quad f/(1 + K_p\rho S)H$$

and the fractions dissolved and sorbed become

dissolved $\quad [(f/H)]/[f/(1 + K_p\rho S)H] = 1/(1 + K_p\rho S)$

sorbed $(fK_p\rho S/H)/f/(1 + K_p\rho S)H = K_p\rho S/(1 + K_p\rho S)$

If the sorbent concentration is expressed as S' g/m^3 (or mg/l) this is equivalent to $10^6 S\rho$ and the group $K_p\rho S$ in these equations becomes the more conventional group $10^{-6}K_pS'$.

This analysis can be applied also to sorption on atmospheric particulate matter but caution must be exercised in situations when the sorbed solute is physically trapped or enveloped in the particle. This may occur, for example, to polynuclear aromatics formed during combustion and associated with (or inside) soot particles. Such materials are unable to exert their intrinsic fugacity outside the limits of the particle and thus are not in a truly equilibrium situation.

For biota a bioconcentration factor K_B is used instead of the partition coefficient. If it can be expressed as a ratio of the concentration in the biota (e.g. fish) on a wet weight basis in which case it is identical to K_p. If expressed on a wet volume basis it is rigorously analogous to the group $K_p\rho$ where ρ is the fish density but since ρ is near unity the difference is dimensional rather than numerical. If a dry weight or lipid content basis is used a suitable concentration factor must be applied.

In summary the term Z for sorbing phases is $K_p\rho/H$ and the problems become that of estimating K_p; usually some relationship being sought to the solute's octanol-water partition coefficient.

Octanol Phase

The importance of Z for octanol (Z_o) lies in the utility of the octanol water partition coefficient K_{ow} as an indicator of hydrophobicity as documented in the many studies of Leo and Hansch (9, 10).

Following the example of water, it can be shown that Z_o is $1/v_o\gamma_o P^s$ where γ_o is the activity coefficient of the solute in octanol and P^s is the vapor pressure of the liquid solute at the system temperature and v_o is the molar volume of octanol saturated with water.

Of greatest interest is the octanol-water partition coefficient K_{ow} expressed as a concentration ratio (mol/m^3) or (g/m^3) i.e. C_o/C_w when the fugacities are equal.

$$K_{ow} = C_o/C_w = Z_o/Z_w = v_w\gamma_w/v_o\gamma_o$$

the vapor pressures cancelling. For most hydrophobic organic compounds γ_o appears to be fairly constant in the range 1 to 10 and of course v_w and v_o are also constant. The value of K_{ow} is thus dominated by γ_w. Since γ_w controls aqueous solubility it follows that solubility and K_{ow} are closely related. This issue is discussed in more detail later.

Pure Solid and Liquid Phases

For pure substances (solid or liquid) the fugacity is the vapor pressure of the pure substance. This situation rarely occurs environmentally

but is interesting thermodynamically and is included here for completeness. The concentration C of the material is the inverse of the molar volume v (m^3/ mol). The saturation vapor pressure of the pure substance (solid or liquid) P^s is approximately equal to the fugacity at environmental pressures, except for some associating species such as carboxylic acids. Z is thus given by

$$H = f/C = P^s/v \quad Z = C/f = 1/P^s v$$

The temperature dependence of Z arises primarily from the variation in P^s which is conventionally quantified by Antoine Equations

$$\ln P^s = A - B/(T + C)$$

The temperature dependence of v is slight and can be obtained from density-temperature data.

Illustrative Calculation of Fugacities

If a system of i phases is in equilibrium each phase having a volume V_i m^3 and a fugacity capacity Z_i then the concentration in each phase C_i is fZ_i where f is the prevailing common fugacity. The amount of material in each phase M_i is thus C_iV_i or fZ_iV_i and the total amount M_T is $f\Sigma Z_iV_i$. If the total amount is known, the fugacity can thus be calculated as

$$f = M_T/\Sigma Z_iV_i$$

Hence the individual values of C_i and M_i can be deduced.

For example if we consider a system consisting of air, water, suspended solids and biota containing a fixed amount of a hydrophobic organic compound it is possible to deduce the partitioning behaviour as illustrated below in Table 1.

TABLE 1. ILLUSTRATIVE FUGACITY CALCULATION

Compartment	Volume V m^3	Fugacity capacity Z mol/m^3atm	ZV mol/atm	C mol/m^3	M mol
Air	10000	41	410×10^3	410×10^{-6}	4.1
Water solution	1000	500	500×10^3	5000×10^{-6}	5.0
Suspended solids	0.015	5×10^6	75×10^3	50	0.75
Aquatic biota	0.005	3×10^6	15×10^3	30	0.15
Total			1000×10^3		10.0

Volumes are assumed as given in Table 1. If the substance has a vapor pressure of 0.02 atm and an aqueous solubility of 10 mol/m^3 its Henry's Constant H is 0.02/10 or 0.002 atm m^3/mol thus Z_w becomes 500 mol/m^3 atm. Z for the atmosphere is typically 41 mol/m^3 atm. If the suspended solids have a density of 2 g/cm^3 and are present at 30 mg/L or g/m^3 the volume fraction S is 15 x 10^{-6} thus V_s becomes SV_w or 0.015. If the biota have a density of 1 g/cm^3 and a concentration of 5 mg/L or g/m^3 the volume fraction is 5 x 10^{-6} and V_B is 0.005. A substance of K_{ow} equal to 50000 may have a K_p of approximately 5000 and a K_B of 6000, thus Z_s is 5000 x 2/0.002 or 5 x 10^6 and Z_B is 6000 x 1/0.002 or 3 x 10^6. These K_p and K_B data could be measured experimentally or deduced from correlations.

The individual and total values of ZV can then be calculated. If the total amount of material M_T is 10 mols, the fugacity can then be deduced as $M_T/\Sigma ZV$ or 10^{-5} atm. The individual concentrations can then be deduced as fZ_i or C_i and the individual amounts as C_iM_i. In this case the compound partitions fairly equally in amount between the air and water, with the air having a larger volume by a factor of 10. The concentrations in the suspended solids and biota are very high but in amount they are 9% of the total. In the aqueous phase the total concentration of 5.9 mol/m^3 is 85% in solution 13% sorbed on suspended solids and 2% bisorbed.

The concentration of 50 mol/m^3 on the solids is equivalent to 25 mol/Mg, a factor of K_p (i.e. 5000) greater than the water concentration of 5 x 10^{-3} mol/m^3. Likewise the biotic concentration of 30 mol/m^3 is a factor of K_B (i.e. 6000) greater than the water concentration.

Summary

This example illustrates the general procedure which can be followed when calculating concentrations in environmental compartments. It is of fundamental importance to volatilization calculations in several respects.

Before any estimate can be made of the rate or even direction of transfer between air and water phases it is essential to have concentration data which can be translated properly into the appropriate fugacities in order to determine the phase of lowest fugacity into which material will tend to transfer.

A knowledge of the breakdown of the total aqueous (and indeed atmospheric) concentrations into truly dissolved and sorbed forms is essential.

The actual amounts present in each phase provide a useful indication of the importance of the partitioning. In this example the highest concentrations on a mass per unit mass basis are in the biota from which an erroneous deduction can be made that biota contain most of the solute. Generally it is only in the case of highly hydrophobic compounds present in very turbid waters that an appreciable quantity of the material in the water column is sorbed. A useful rule of thumb is that the sorbed and dissolved forms are approximately equal when the sorbent is at a concentration of $10^6/K_p$ parts per million.

AQUEOUS SOLUBILITY

Theoretical Background

It often seems strange that aqueous solubility plays such an important role in volatilization calculations since most compounds are (fortunately) present in the environment at levels well below their solubility limits. The importance lies in the fact that the Henry's Law Constant or the partitioning coefficient into the air is inversely proportional to solubility

$$\text{i.e.} \quad H = P^s/C^s.$$

Compounds of low vapor pressure (such as DDT) can have high H values and thus tend to volatilize despite their low vapor pressures because of their low solubility. Certainly, a low vapor pressure impedes the absolute volatilization rate but if the compound is sparingly soluble it is likely to be present at a low concentration and very little of it may have to volatilize in order that the concentration drops by a significant factor. The volatilization "half life" of a substance thus tends to be reduced by increasing P^s and decreasing C^s. In a homologous series of increasing molecular weight there is a tendency for P^s and C^s to fall and the overall effect on H is not clear. Conceptually it may be useful to regard solubility as the inverse of hydrophobicity thus decreasing solubility or increasing hydrophobicity tends to drive a solute out of solution by volatilization.

The solubility of a pure, non-ionizing, sparingly soluble liquid solute can be expressed by writing the fugacity equation for the pure liquid and the solution yielding

$$f = P^s = x\gamma_w P^s \qquad \text{thus} \quad x = 1/\gamma_w$$

where x is mole fraction, γ is activity coefficient and P^s is vapor pressure. Converting to mol/m^3 units using the water molar volume v_w (18×10^{-6} m^3/mol) gives

$$C^s = x/v_w = 1/\gamma_w v_w$$

It is assumed here that the concentration of solute in water is so low that the molar volume of the solution equals that of water and that the solubility of water in the liquid solute is negligible.

For solid solutes the equation is more complex since the fugacity is that of the solid f_s whereas the vapor pressure P^s remains that of the liquid, here termed f_R for convenience. It follows that

$$f = f_s = x\gamma_w f_R \qquad \text{thus} \quad x = (f_s/f_R)/\gamma_w$$

$$\text{and} \quad C^s = (f_s/f_R)/\gamma_w v_w$$

The group (f_s/f_R) is termed the fugacity ratio and is essentially the ratio of the vapor pressures of the solid to the subcooled liquid. It is unity at the triple point but less than unity below that temperature. Its importance lies in the observation that it causes a marked reduction in

solubility of solid organic compounds when compared to similar liquid compounds. Further, the higher the melting point the lower the fugacity ratio (because the slope of the solid P-T line is greater than that of the liquid P-T line on a phase diagram as is illustrated in Figure 1.

It can be shown (Prausnitz 6) that the fugacity ratio (f_s/f_R) can be expressed as

$$\ln(f_s/f_R) \simeq -\Delta H_F(1/T - 1/T_M)/R$$

where ΔH_F is the enthalpy of fusion (J/mol), T and T_M are the system and solute melting point temperatures (K) and R is the gas constant (8.3 J/mol K). Since the entropy of fusion ΔS_F at the melting point is $\Delta H_F/T_M$ and is found to be fairly constant it is convenient to write

$$\ln(f_s/f_R) \simeq -\Delta S_F(T_M - T)/RT$$

Yalkowsky (11) has shown that for many organic compounds ΔS_F is approximately 13.6 entropy units, thus $\Delta S_F/R$ is approximately 6.8, thus

$$\ln(f_s/f_R) = -6.8(T_M - T)/T = 6.8(1 - T_M/T)$$

or at 25°C, i.e. T = 298 K,

$$\ln(f_s/f_R) = -0.023(T_M - 298)$$

or

$$\log(f_s/f_R) = -0.01\ (T_M - 298)$$

Now since $\ln C^s$ is $\ln(f_s/f_R) - \ln\gamma_w - \ln v_w$ it follows that solubility can be estimated if data for T_M and γ are available. Yalkowsky and Valvani (12) have shown that $\ln\gamma_w$ varies linearly with computed total surface area using the solubility data for polynuclear aromatics. Techniques for correlating activity coefficients and hence solubility are discussed in more detail later in this section. Such correlations are invaluable for predicting solubility and checking experimental values.

As part of this work a similar approach was taken for PCBs using TSA data kindly supplied by Yalkowsky and Valvani, the method being given in a recently published paper on this topic (Mackay et al 13).

For gaseous solutes i.e. when the system temperatures exceed the triple point, the vapor pressure becomes hypothetical and the pure solute has a fugacity equivalent to its partial pressure. Solubility data are usually reported as Henry's Law Constants, Bunsen or Ostwald coefficients.

In summary, the aqueous solubility of a non-ionizing sparingly soluble compound is dependent on two quantities, its activity coefficient in aqueous solution (γ_w) which is a measurement of its hydrophobicity and if the compound is solid at the system temperature the solubility also depends on melting point. Theoretically based methods are available to correlate solubility as influenced by these quantities. The final equation for C^s using $18 \times m^{-6}\ m^3/mol$ for v_W is thus

$$\ln C^s = 6.8(1 - T_M/T) - \ln \gamma_W + 10.95$$

FIGURE 1

ILLUSTRATIVE PRESSURE, TEMPERATURE

DIAGRAM FOR A PURE COMPOUND

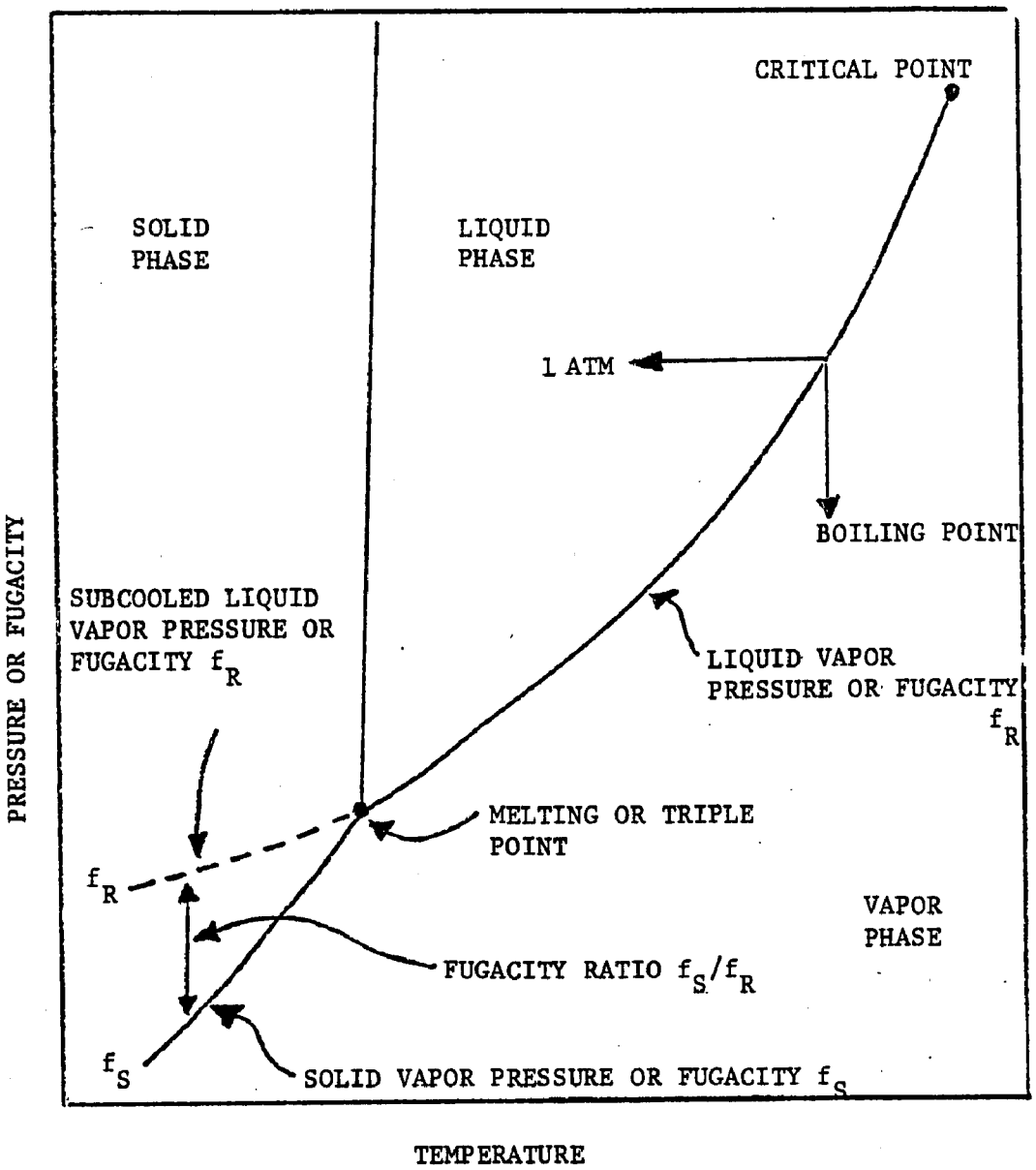

If the solute is totally miscible or even quite soluble in water i.e. greater than 5% mole fraction, this simple analysis breaks down because the solute phase properties are influenced by the dissolved water. This usually occurs when γ_w has a value less than 20. Fortunately, when considering environmental volatilization such compounds are rarely of interest because they volatilize very slowly as can be demonstrated by a simple calculation.

If the compound is present at a concentration of 1 g/m^3 and has a molecular weight of 100 g/mol its molar concentration is 0.01 mol/m^3 equivalent to a mole fraction (x) of 0.01/55000 or 2×10^{-7}. If its activity coefficient is 20 and its vapor pressure is 0.025 atm then its fugacity f is the product of these three quantities or 1×10^{-7} atm. The vapour pressure of water under these conditions may be 0.02 atm thus the equilibrium ratio of solute to water in the air is 5×10^{-6} which is 25 times the aqueous concentration. It follows that to evaporate most of the solute in a water body requires evaporation of about 1/25th of the water present, a process which will take a considerable time except in shallow ponds. Further, compounds of this type, which include alcohols, phenols, esters, ketones, etc. tend to be biodegradable or subject to hydrolysis thus volatilization is usually a less significant environmental pathway.

If values for γ are desired the best approach is to use vapor-liquid equilibrium data as reviewed by Reid et al (14). Group contribution methods outlined in that reference can be used to estimate γ_w to a sufficient degree of accuracy for most environmental purposes.

Effect of Co-solutes on Solubility

It is well established that the solubility of a compound is influenced by the presence of other dissolved compounds. Suspended matter is best treated as a sorption phenomenon.Of primary environmental interest are three classes of compounds, electrolytes, other dissolved organics and surfactants.

Most electrolytes cause a "salting out" effect, i.e. they reduce the solubility of the organic solute. The mechanism by which this occurs is not entirely clear but it appears that these electrolytes alter the water structure to reduce the volume of the "holes" available for incorporation of organic solutes. The conventional approach for correlating this behaviour is to use the Setschenow equation (15) to describe the relationship between solubility and electrolyte concentration in terms of a single constant which is essentially the slope of the plot of log of the ratio of solubility in electrolyte solution to that in pure water against molarity. The constant depends on the electrolyte and on the molar volume of the solute organic and can be correlated using the McDevitt-Long approach (16). An example of the use of these methods has been reported by Aquan-Yeun et al (17).

To give a general indication of the magnitude of this effect, most hydrocarbons have a solubility in sea water (approximately 30 g/L electrolyte) of 70 to 80% of their pure water values. This may be important in marine or estuarine waters, the implication being that since the solubility is reduced by some 25% the Henry's Law Constant will be increased by a similar amount, thus possibly promoting faster volatilization. In practice this effect is probably not very important for two reasons. Most compounds which volatilize rapidly have high Henry's Law Constants and (as is discussed later) volatilize under liquid phase diffusion control which proceeds at a rate independent of

that constant. Only when the compound volatilizes slowly under gas phase control does this effect become significant. From an environmental quality viewpoint the electrolyte concentrations necessary to significantly affect solubility are so large that these electrolytes in themselves probably have a more significant detrimental effect on environmental processes. Finally, the concern is occasionally expressed that in estuaries the mixing of salt and fresh water will reduce the solubility of a dissolved compound to a level such that it precipitates. This is very unlikely since it requires that the solute be present at close to its solubility (which fortunately rarely occurs) and the dilution by sea water inevitably results in a drop in concentration.

Surface active materials "solubilize" organic solutes, which is of course the principle of detergency as reviewed in the many texts on interfacial phenomena such as Davies and Rideal (18). This phenomenon is perhaps best regarded as partitioning into a separate phase which is stabilized by the surfactant and can act as a partitioning reservior. Such "phases" tend not to form appreciably below a critical micelle concentration (cmc). Below the cmc the solubility is only slightly increased, however above the cmc when micelles form they are capable of accommodating solutes, especially organic solutes similar in composition to the organic part of the surfactant, thus apparently increasing the solubility. This topic has been reviewed by Makenjee and Mysels (19) and recent data given on solubilization of aromatic hydrocarbons by Almgren et al (20).

The simplest approach is to assume that below the cmc, solubility (and hence Henry's Law Constant) is unaffected by the presence of surfactants. Above the cmc the situation is very complex and although it is possible to assemble partition equilibria equations using what are essentially micelle-water partition coefficients it seems unlikely that this appraoch could be used for environmental modelling or prediction purposes because of the doubtful nature, number and concentrations of the natural and anthropogenic surfactant molecules and the various solutes present which will compete for accommodation in the micelles. Fortunately the use of biodegradable detergents has substantially reduced their environmental concentrations to levels, usually below the cmc.

More difficult is the problem of assessing the effect on solubility of other organic solutes. A common procedure for preparing an aqueous solution of a sparingly soluble compound is to first dissolve it in an organic liquid such as methanol or acetone and then mix this solution with water. It is thus possible to obtain solutions in water at concentrations exceeding the water solubility. It can be argued therefore that the solubility of say napththalene in water can be increased by adding some methanol or acetone. The extension of this argument to environmental conditions is that the presence of natural or anthropogenic organic material will increase the solubility of the solute and thus reduce the Henry's Law Constant. Most natural waters contain concentrations of dissolved and suspended organic matter, notably fulvic and humic acids whose chemical structures are poorly characterised. It is suspected that these compounds may enhance solubility although definitive solubility determinations are lacking. The real issue is the magnitude of this effect rather than its existence. Accordingly some experiments were undertaken to measure the magnitude of this effect. This involved measuring the solubility of organic solutes in the presence of low concentrations of other organic compounds, including fulvic acid, using a modified "generator column" technique. The results of this study and their implications are discussed later.

A final concern is the observation that when saturated solutions of sparingly soluble organic solutes are prepared there may be solubilization or "accommodation" of concentrations of the solute in the range up to 10 g/m^3 in the form of colloidal or emulsified particles. This was first noticed by Peake and Hodgson (21) for hydrocarbons. Membrane filtration removes some (but not all) of this material and the apparent solubility depends on the filtration efficiency. This effect is responsible for many erroneous solubility data reported in the literature. Preparation of solutions of such solutes is best done under conditions such that no colloid material forms. Further, when very small organic particles are present the solubility may be enhanced because of the interfacial curvature effect. Although important in areas such as petroleum reservoir engineering such effects are of marginal environmental interest because they can only occur at saturation. A system of unsaturated solution and a separate phase of organic solute in particle form is inherently unstable and will tend to move towards true solution. The effect is thus unlikely to be important in natural waters where most solutes are present at concentrations several orders of magnitude below their solubilities.

There has been a considerable amount of erroneous solubility data published in the literature, especially for sparingly soluble compounds such as hydrocarbons and halogenated hydrocarbons. The errors usually arise from either analytical difficulties associated with the quantification of small quantities of solute (which may sorb appreciably on glass surfaces) or the improper preparation of saturated solutions. Fortunately modern "generator column" techniques coupled to liquid chromatographic analysis are capable of high accuracy. Such methods are described later.

Activity Coefficient Correlations and Predictions

As was discussed earlier in this section, the aqueous solubility of a hydrophobic organic solute depends on two factors, its melting point and entropy of fusion (which controls the fugacity ratios f_S/f_R) and the activity coefficient γ_W. The former quantity can be estimated using Yalkowsky's value for the entropy of fusion. The latter (γ_W) is a function of molecular size and the nature of the solute interaction with water. Estimation and correlation techniques for γ_W are developing, the simplest approach being to examine the variation in γ_W for a homologous series and develop equations or "rules" in which molecular fragments are regarded as being responsible for contributions. This approach has been successfully used to correlated octanol -water partition coefficient and to estimate γ for some systems of engineering interest, a review being given by Reid et al (14). Here we examine the status of such techniques and undertake some further development.

Greatest success has been obtained in correlating $\ln \gamma_W$ with total molecular surface area (TSA, which is conventionally expressed in square angstroms) using an equation of the type

$$\ln \gamma_W = A + B\ (TSA)$$

Table 2 lists values of A and B for various homologous series, the studies being reported in several publications by Yalkowsky and co-workers. Unfortunately, the computation of TSA is a relatively sophisticated procedure and some doubt may arise as to actual values depending on the conformation of the molecule. There is therefore an incentive to correlate γ_W with a more

TABLE 2

TOTAL SURFACE AREA CORRELATIONS FOR AQUEOUS SOLUBILITY AND ACTIVITY COEFFICIENT CORRELATIONS AS $\ln\gamma = A + B\ (TSA)$ *

Solute Series	Number of Compounds	K_1	K_2	K_3	A	B	Reference
Alkanes	18	0.73	0.0323	--	2.92	0.0744	128
Alcohols	55	3.8	0.0317	--	4.15	0.0730	128
Polynuclear aromatics	31	1.42	0.0282	0.0095	1.33	0.0649	12
Halobenzenes	35	3.30	0.0423	0.0103	3.00	0.0974	129
Polychlorinated biphenyls	35	3.20	0.354	--	2.78	0.0815	13

* See explanation on following page.

Explanation of Table 2

For the first four series Yalkowsky and Valvani report the solubilities as a function of total surface area (TSA) in square angstroms as follows

$$\log S = K_1 - K_2(TSA) - K_3(MP)$$

where S is solubility at 25°C (mol/L), MP is melting point (°C), K_1, K_2 and K_3 are regression constants, the K_3 term being included only if the melting point exceeds 25°C. K_3 is equivalent to the constant 6.8 developed here divided by 298 K and by 2.303 to convert to base 10 logarithms i.e. 0.0099.

Substituting 0.0099 for K_3 and converting S to C^s, MP to T_M, and using natural logs gives

$$\ln C^s = 2.303(K_1+3) - 2.303K_2(TSA) - 2.303\text{x}0.0099(T_M-273)$$

$$= 2.303(K_1+3) - 2.303K_2(TSA) - 0.0228T_M + 6.22$$

The equivalent form used here is

$$\ln C^s = -\ln\gamma_W - \ln V_w + 6.8(1-T_M/T)$$

which at 298 K and with V_w equal to 18 x 10^{-6} m^3/mol gives

$$\ln C^s = - A - B(TSA) + 10.93 + 6.80 - 0.0228T_M$$

It follows that

$$A \cong 11.51 - 2.303\ (K_1+3)$$

$$B \cong 2.303\ K_2$$

A specimen calculation involving these quantities is given at the end of Section 4.

accessible quantity such as molecular weight, carbon number, molar volume or some calculated combination of the contributions of the various groups or molecular fragments present. Here we examine the feasibility of these approaches by illustrating the correlation of TSA with such accesible quantities.

Figure 2 is a plot of TSA versus molecular weight for selected homologous series, which shows satisfactory correlation within a series, but not between series. Figure 3 is similar and shows TSA plotted against molar volume, which is best expressed as molecular weight divided by liquid density at the normal boiling point. Additive atomic volumes can also be used to calculate molar volume. Figure 4 shows TSA plotted against carbon number which is again fairly successful provided that the number of atoms such as chlorine or oxygen is zero or constant. Clearly for a series such as the PCBs carbon number is a useless correlating quantity. The use of the sum of carbon and chlorine number is then preferable as illustrated in Figure 5.

Regression equations can be obtained for each series, resulting in a net correlation between γ_w and the accessible quantity (Q) which may have the form:

$$\ln \gamma_w = A + B\ (TSA)$$

$$TSA = C + D\ (Q)$$

$$\ln \gamma_w = A + BC + DB\ (Q)$$

or more complex expressions can be used. From plots such as Figures 2,3,4 and 5 or the corresponding regression equations it is possible to estimate γ_w and hence solubility for a compound for which no experimental data are available.

An attractive sequel to this data compilation is to develop a group contribution procedure which would be applicable to a wide range of compounds. Some preliminary steps were taken towards this end as part of this study but the results were not sufficiently accurate to justify publication. Further work is planned and it is believed that the ultimate objective of calculating solubility from molecular structure and melting point is attainable with accuracy sufficient for most environmental purposes.

FIGURE 2

PLOT OF TOTAL SURFACE AREA VERSUS MOLECULAR WEIGHT

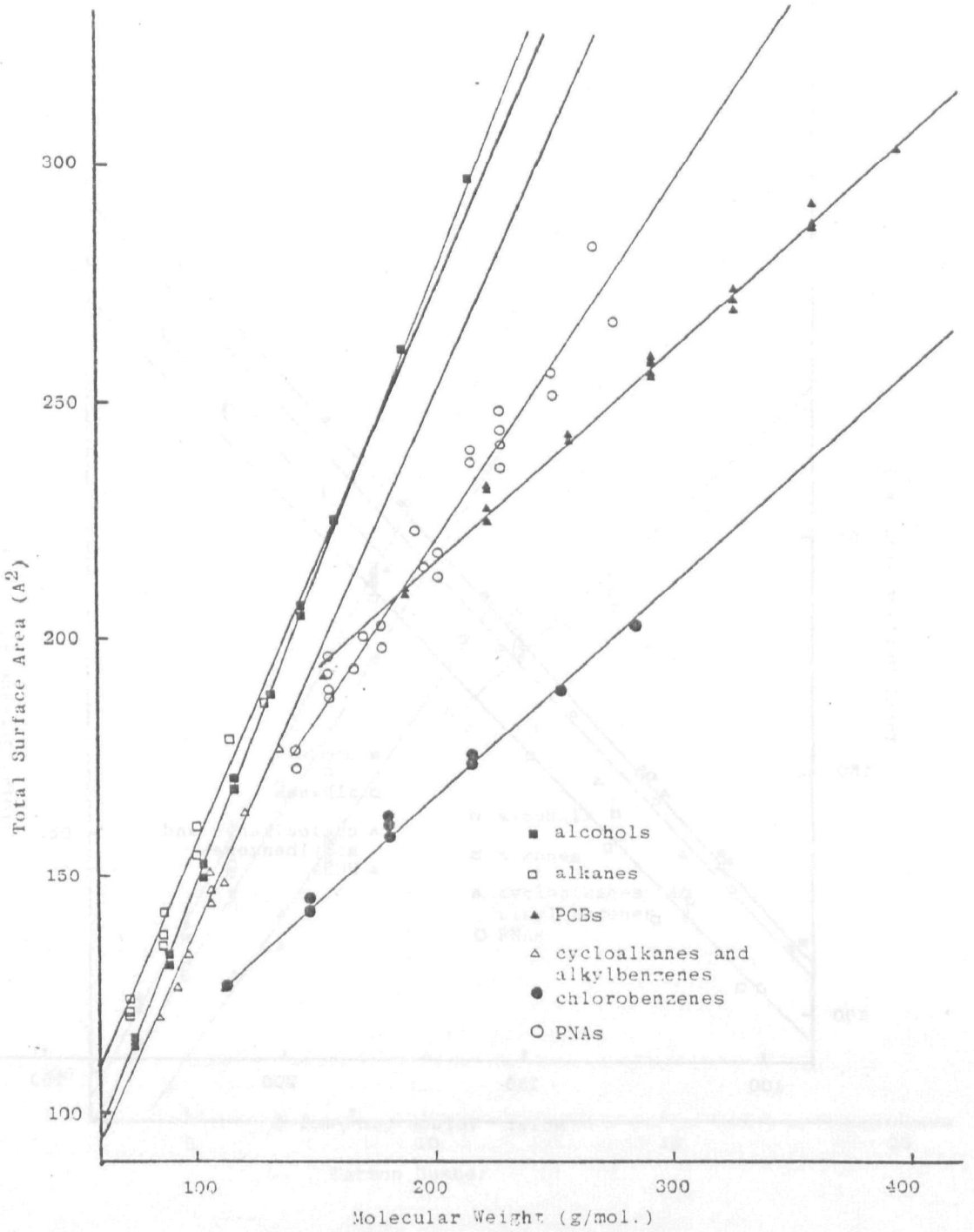

FIGURE 3

PLOT OF TOTAL SURFACE AREA VERSUS MOLAR VOLUME

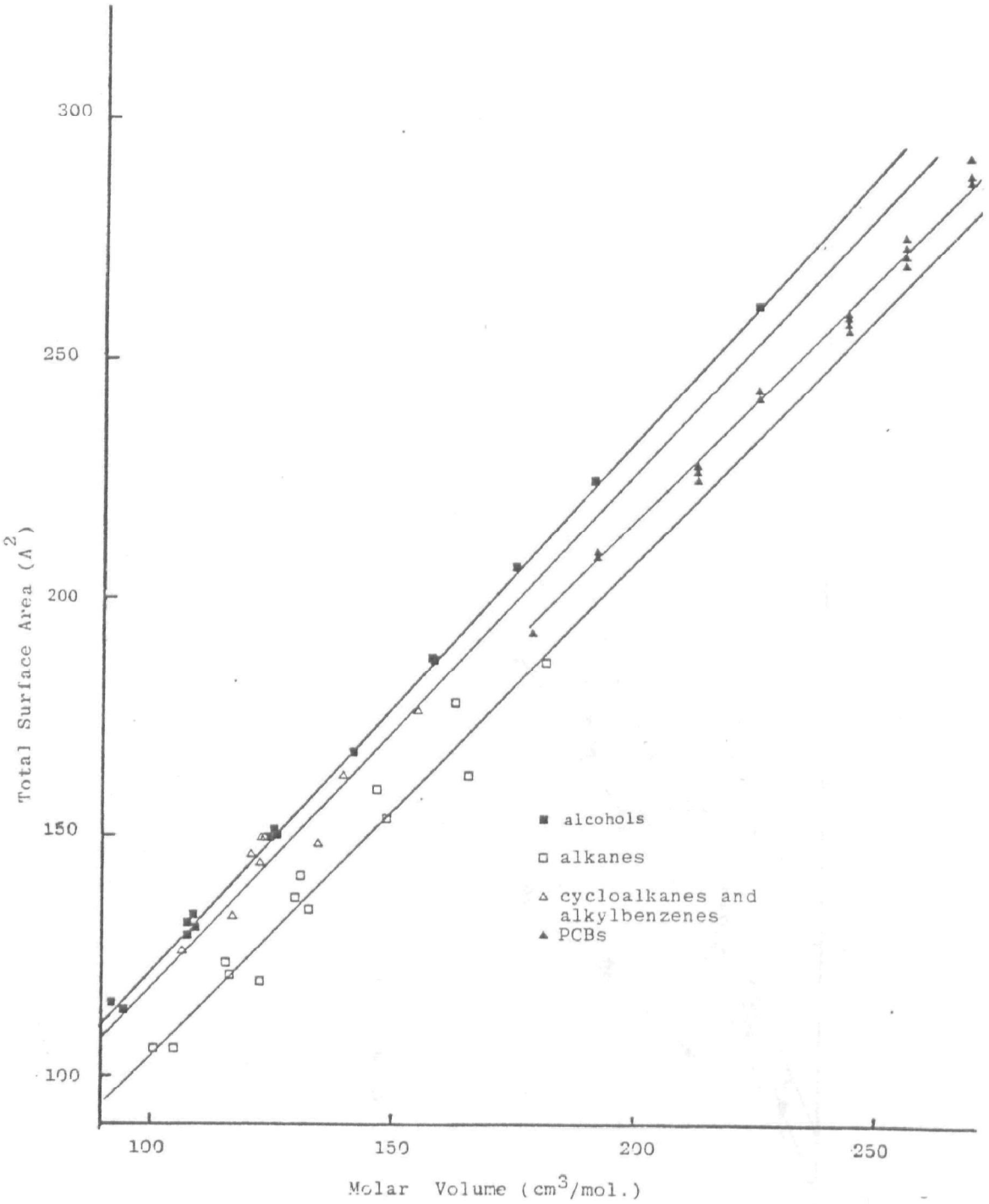

FIGURE 4

PLOT OF TOTAL SURFACE AREA VERSUS CARBON NUMBER

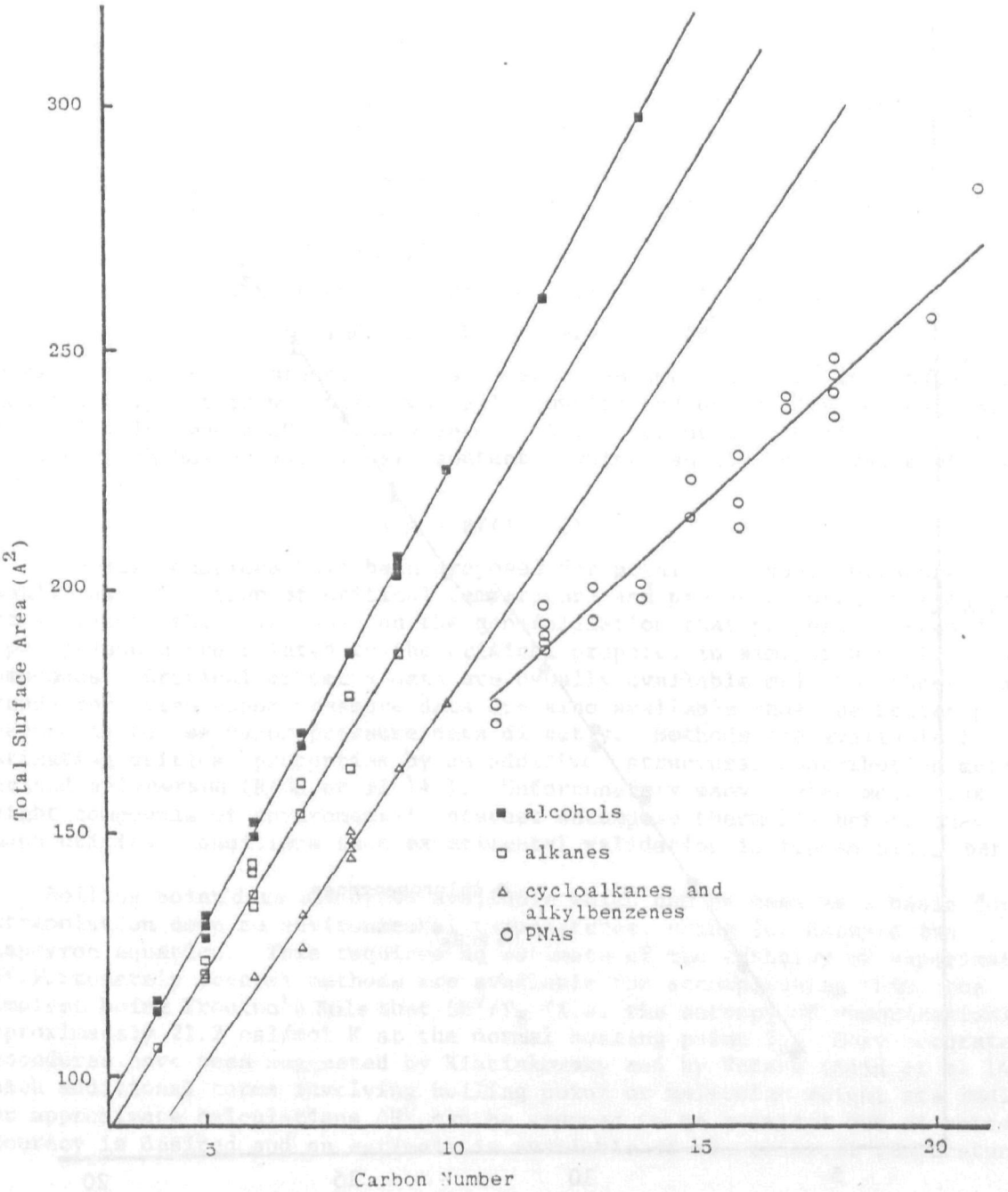

FIGURE 5

TOTAL SURFACE AREA VERSUS CARBON PLUS CHLORINE NUMBER

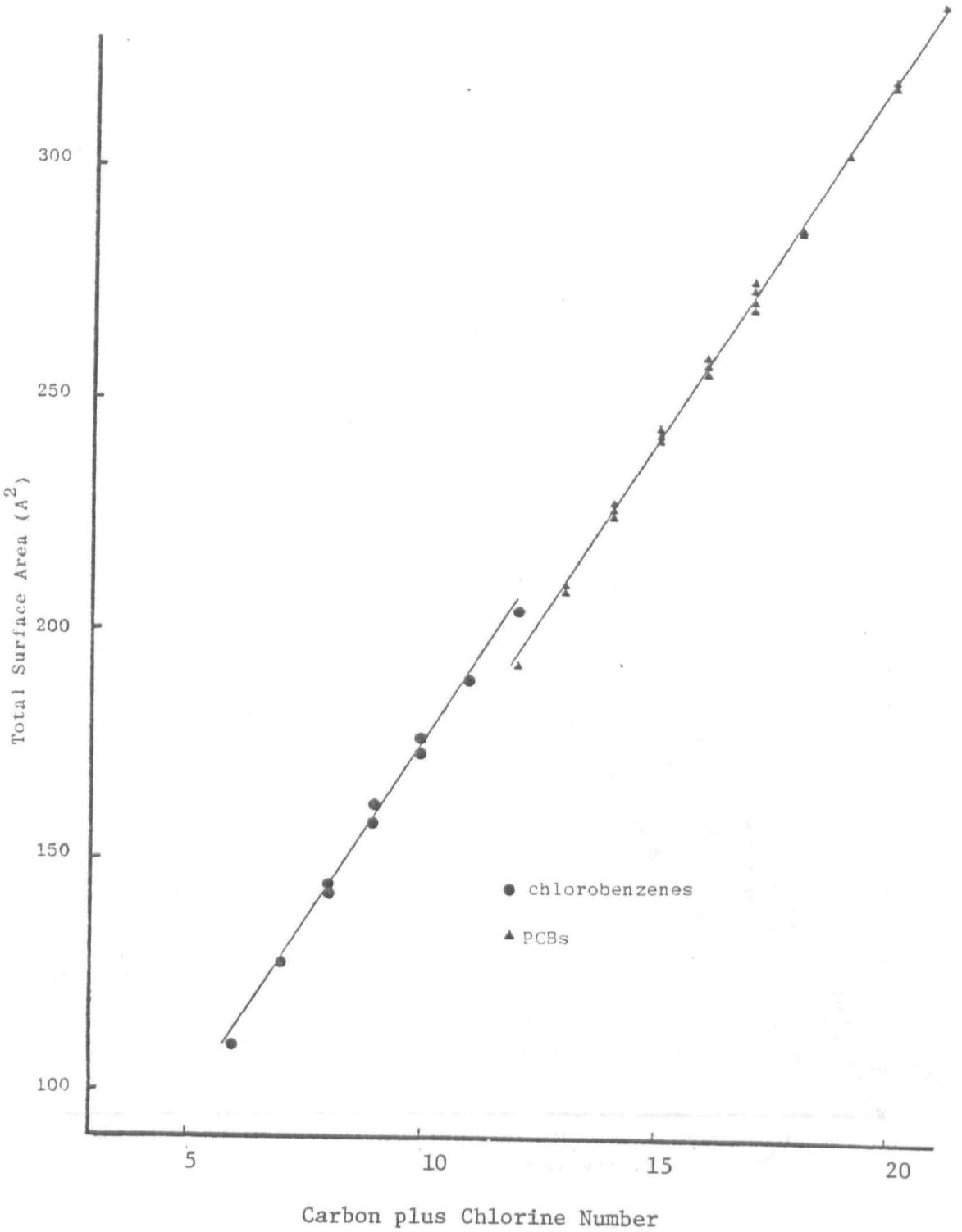

VAPOR PRESSURE

The vapor pressure of a solute is clearly of considerable significance in any assessment of volatilization and reliable data are very desirable but unfortunately often lacking, especially if the solute has a low vapor pressure which is difficult to measure accurately. A detailed treatment of correlating equations for vapor pressure has been given by Reid et al (14) and only some salient points are presented here.

Figure 1 is a typical pressure-temperature diagram for a pure solute. The range of environmental temperatures may lie anywhere on this diagram relative to the important phase transition points which are the triple point (which is essentially the melting point, the critical point and the normal boiling point). Ideally data should be available for vapor pressure of solid or liquid over the range of environmental temperatures but estimation is often necessary.

The Clausius-Clapeyron equation in its simple form relates vapor pressure to temperature as a function of enthalpy of vaporization ΔH^V

$$d\ln P/dT = \Delta H^V/RT^2$$

from which the Clapeyron equation can be derived by integration

$$\ln P = A - B/T \quad \text{where B is } \Delta H^V/R$$

where A and B are constants. This equation assumes that ΔH^V is constant with changing temperature which is generally invalid and especially so near the critical point where ΔH^V becomes zero. A more accurate equation is that of Antoine which has an additional constant C which usually has a value of -40 to -60 K,

$$\ln P = A - B/(T + C)$$

Several equations have been proposed for predicting vapor pressure, usually as a function of critical temperature and pressure using corresponding states theory which is based on the generalization that properties such as vapor pressure are related to the critical property in similar ways for all compounds. Critical property data are usually available only for those compounds for which vapor pressure data are also available thus the better proceedure is to use vapor pressure data directly. Methods are available for estimating critical properties by an additive structural contribution method devised by Lydersen (Reid et al 14). Unfortunately many higher molecular weight compounds of enviromental interest decompose thermally before they reach critical conditions thus experimental validation is impossible.

Boiling point data are often available which can be used as a basis for extrapolation down to environmental temperatures, using for example the Clapeyron equation. This requires an estimate of the enthalpy of vaporization, ΔH^V. Fortunately several methods are available for accomplishing this, the simplest being Trouton's Rule that $\Delta H^V/T_B$ (i.e. the entropy of vaporization) is approximately 21.2 cal/mol K at the normal boiling point T_B. More accurate procedures have been suggested by Kistiakowsky and by Vetere (Reid et al 14) in which additional terms involving boiling point or molecular weight are included. For approximate calculations ΔH^V can be assumed to be constant but if better accuracy is desired, and an estimate is available of the critical temperature,

the Watson equation can be used to express ΔH^V as a function of temperature

$$(\Delta H_1^V/\Delta H_2^V) = \left|(1-T_1/T_c)/(1-T_2/T_c)\right|^{0.38}$$

where subscripts 1 and 2 refer to the values at two temperatures T_1 and T_2 and T_c is the critical temperature (K).

A simple approximation for vapor pressure (P atm) as a function of temperature T and boiling point T_B using Trouton's Rule and the Clapeyron equation is,

$$\ln P = -B\,(1/T - 1/T_B) = -(\Delta H^V/R)(1/T - 1/T_B)$$

$$= -(21.2\ T_B/R)(1/T - 1/T_B) = 10.6(1 - T_B/T)$$

$$\text{or } \ln P_M = 10.6\ (1 - T_B/T_M)$$

This can be used to estimate the liquid vapor pressure down to its value P_M at the melting or triple point (T_M). Below this temperature the enthalpy of sublimation should be used. This can be estimated approximately using Yalkowsky's observation (11) which is essentially Waldens' Rule,that the entropy of fusion of most rigid organic compounds is 13.5 cal/mol K. Long chain molecules with n flexible links have higher entropies of fusion expressed as 13.5 + 2.5 (n-5).

Applying a similar equation to the solid-vapor pressure curve (below the triple point) gives

$$\ln(P/P_M) = -(\Delta H^S/R)(1/T - 1/T_M)$$

where ΔH^S is the heat of sublimation and is given approximately by

$$\Delta H^S = 21.2\ T_B + 13.5\ T_M$$

$$\text{or } \Delta H^S/R = 10.6\ T_B + 6.8\ T_M$$

Combining these equations to eliminate P_M yields

$$\ln P = 10.6\ (1 - T_B/T) + 6.8\ (1 - T_M/T)$$

The first term gives the liquid (and subcooled liquid) vapor pressure at any temperature T and the second term (which is also negative) gives the additional reduction in vapor pressure due to solid phase formation. The second term is ignored if the environmental temperature exceeds the melting point, i.e. $T > T_M$. For correlation purposes a plot of lnP versus T_B/T should thus be linear for liquids. Solids should also fall on the line if the vapor pressure is connected to the higher subcooled liquid value by adding the term $6.8\ (1 - T_M/T)$ to ln P.

Figure 6 is a plot of this type for 30 compounds listed in Table 3 illustrating the general validity of the method.

FIGURE 6

RELATIONSHIP BETWEEN VAPOR PRESSURE AND

BOILING POINT FOR SELECTED SOLUTES

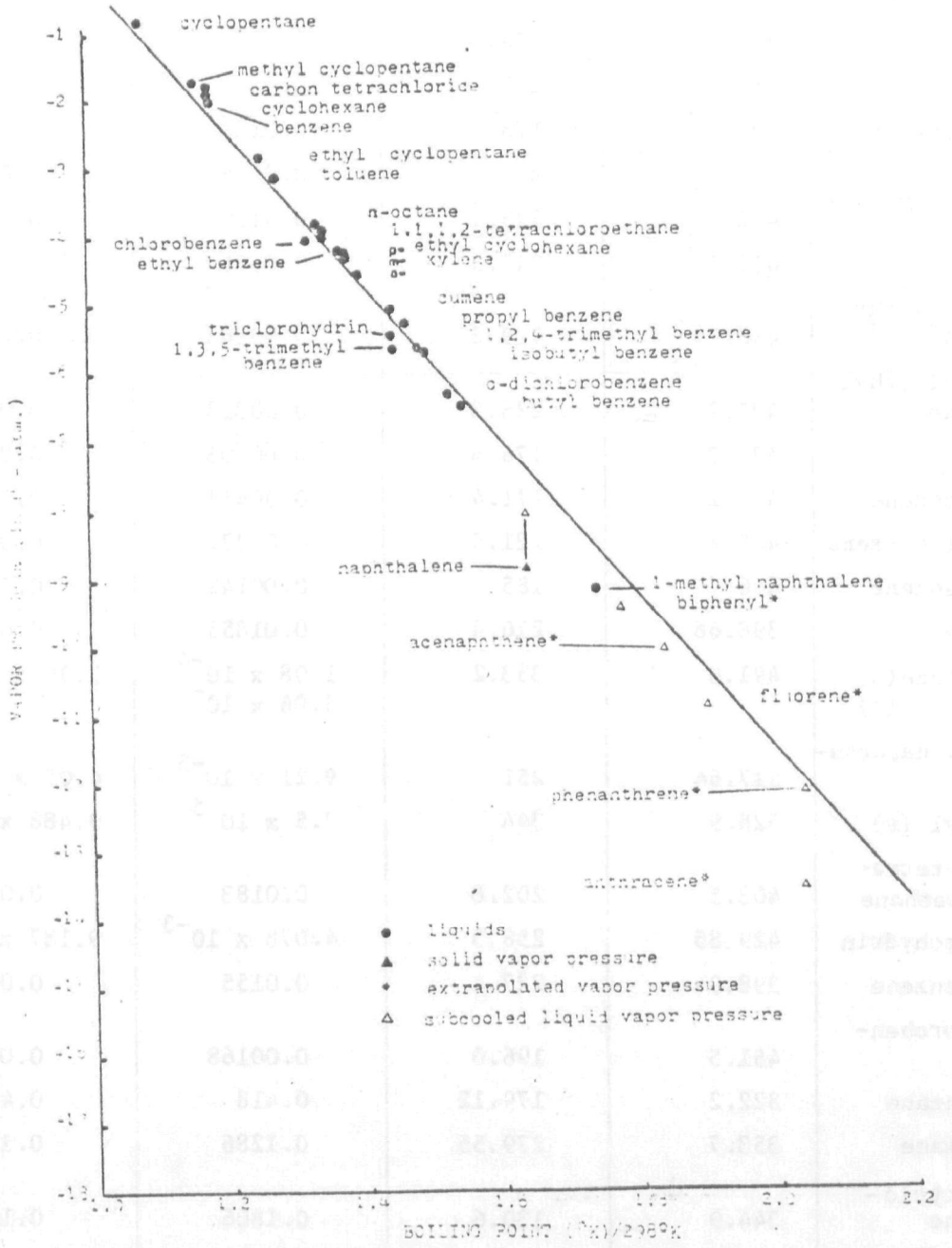

TABLE 3. BOILING POINTS, MELTING POINTS AND

LITERATURE & CALCULATED VAPOR PRESSURES AT 25°C

Compound	Boiling Pt. K	Melting Pt. K	Vapor Pressure (atm) Literature	Vapor Pressure (atm) Calculated
benzene	353.099	278.5	0.125	0.141
toluene	383.6	178	0.037	0.048
ethyl benzene	409.2	178	0.013	0.019
p-xylene	411.0	286.2	0.0115	0.018
m-xylene	412.0	225.1	0.0109	0.017
o-xylene	417.4	247.8	0.0086	0.014
1,2,4-trimethyl benzene	442.35	229.2	0.00267	0.006
1,3,5-trimethyl benzene	437.7	228.3	0.00318	0.007
cumene	437.7	176.4	0.00605	0.007
propylbenzene	432.2	171.4	0.00451	0.008
isobutyl benzene	445.8	221.5	0.00271	0.005
butyl benzene	456	185	0.00142	0.0036
n-octane	398.66	216.4	0.01855	0.028
naphthalene (s) (l)	491.0	353.2	1.08×10^{-4} 3.06×10^{-4}	2.96×10^{-4}
1-methyl naphthalene	517.64	251	9.21×10^{-5}	4.05×10^{-4}
*biphenyl (s)	528.9	344	7.5×10^{-5}	9.488×10^{-5}
1,1,1,2-tetrachloroethane	403.5	202.8	0.0183	0.0235
trichlorohydrin	429.85	258.3	4.078×10^{-3}	9.187×10^{-3}
chlorobenzene	398.9	227.4	0.0155	0.0276
o-dichlorobenzene	451.5	196.0	0.00168	0.0043
cyclopentane	322.2	179.12	0.418	0.423
cyclohexane	353.7	279.55	0.1286	0.138
methyl cyclopentane	344.9	130.6	0.1806	0.189
ethyl cyclopentane	376.4	134.56	0.0526	0.0615

(continued)

TABLE 3. (CONTINUED)

Compound	Boiling Pt. K	Melting Pt. K	Vapor Pressure (atm) Literature	Vapor Pressure (atm) Calculated
ethyl cyclo-hexane	402.9	161.68	0.01688	0.024
carbon tetra-chloride	349.7	250.0	0.149	0.159
*phenanthrene (s)	612	374	4.53×10^{-6}	2.489×10^{-6}
*anthracene (s)	613	489.2	1.42×10^{-6}	1.73×10^{-7}
*fluorene (s)	568	389	1.64×10^{-5}	8.46×10^{-6}
*acenaphthene (s)	550.5	369.2	3.97×10^{-5}	2.476×10^{-5}

* extrapolated vapor pressure

Interestingly, Almgren et al (20) have recently shown that a degree of correlation exists between aqueous solubility and boiling point, of aromatic hydrocarbons, most of which are solid, namely

$$-\log S = 0.0138\ T_B + 0.76$$

where S the solubility has units of mol/L and T_B is in ^oC. This correlation is not very accurate, having a typical error in S of a factor of 2 and occasionally as high as 10 but it indicates that both solubility and boiling point depend on molecular size.

The overall picture which emerges is that molecular size and structure and the presence of interactive groups such as alcohol or amine groups control the molecular's critical properties, larger molecules having higher critical temperatures and pressures. These properties in turn control the vapor pressure of the liquid. Molecular shape also plays a strong role in controlling melting point and hence the solid vapor pressure. Molecular area appears to control the aqueous activity coefficient and hence directly controls solubility of liquids and jointly with melting point controls the solubility of solids. It is thus not surprising that a correlation exists between boiling point and solubility since both depend on the same molecular properties.

Finally, it is worth commenting on experimental methods for determining vapor pressure. Little difficulty is encountered if the vapor pressure exceeds 1 mm Hg since an isoteniscope can be used. For lower vapor pressures effusion rate or evaporation rate methods have been used but they are now regarded as excessively complex and unreliable. The preferred approach is to flow a stream of gas through a vessel containing the volatile solute either as liquid or as a solid coated on packing under conditions such that saturation is achieved. The effluent gas is then analysed for the concentration of the solute by one of several methods including trapping on a sorbent column, absorption in a liquid or combustion to yield CO_2 which is subsequently analysed by IR spectrometry. Such methods have been described by Spencer and Cliath (22), Sinke (23) and Macknick and Prausnitz (24).

It must be emphasized that the foregoing analysis applies only to non-electrolytes.

HENRY'S LAW CONSTANT

UNITS AND SYSTEMS

In this report H is consistently presented in units of atm m^3/mol, but other systems are used, for example, pressure can be expressed in mm Hg or Pa and concentration in g/m^3, mg/L or mole fraction. The correct SI unit is Pa m^3/mol which reduces to J/mol. It is often convenient to calculate H as the dimensionless ratio of concentrations (e.g. (mol/m^3)/(mol/m^3)) which can be derived from H simply by dividing by the group RT thus converting pressure into concentration using the gas law

$$\text{i.e.} \quad n/v = P^s/RT$$

The gas constant is 82 x 10^{-6}atm m^3/mol K thus RT is typically 0.024 atm m^3/mol. If H is expressed in Pa m^3/mol or J/mol, R is 8.3 J/mol K.

Another system of expressing H is as the ratio of partial pressure to mole fraction or

$$P = H_M X$$

Examination of the fugacity equation shows that H_M is equivalent to $\gamma_w f_R$ (atm). At low concentrations the molar volume of water v_w is 18 x $10^{-6}m^3$/mol thus at a concentration C mol/m^3 the mole fraction of solute X is C v_w thus H is equivalent to ($H_M v_w$).

Gas solubilities are occasionally reported as the Bunsen or absorption coefficient which is the volume of gas at 0°C and 1 atm which is dissolved in one volume of water. It can be shown to be 273 R/H. The Ostwald coefficient is similar except that the gas volume is at the system temperature and the solute partial pressure. It is thus RT/H or the reciprocal of the partition coefficient.

A final and unusual system is to express H as a relative volatility with respect to water. This is later shown to be useful experimentally. The relative volatility α is usually expressed for a binary system as

$$\alpha = y\,(1 - x)/x(1 - y) \simeq y/x$$

where x and y are the liquid and vapor mole fractions of solute. In dilute solution this reduces to y/x which can be shown by the fugacity equations to be $\gamma_w f_R/P_T$ or $\gamma_w P^s/P_T$ where f_R is the reference fugacity, equivalent to the liquid vapor pressure P^s (possibly subcooled) and P_T is the total pressure. As was shown earlier H is equal to $v_w \gamma_w f_R$ or $v_w \gamma_w P^s$ thus α equals $H/P_T V_w$. Considering for simplicity an air-free system, the H for water between pure water and

the vapor phase is P^s_w/C_w, i.e. the ratio of water vapor pressure to its concentration C_w which is 55,000 mol/m^3 or $1/v_w$. The group $P_T v_w$ is thus the Henry's Law Constant for water H_w and α is the ratio of the solute to water Henry's Law Constants, i.e.

$$\alpha = H/H_w$$

Addition of air to the system does not alter this conclusion since air merely increases the total pressure P_T and correspondingly reduces the mole fraction y, leaving the vapor phase fugacities of water and solute unchanged.

The usefulness of this approach is that for systems of relatively low H, water provides a convenient "benchmark" since if H is lower than H_w, i.e. $\alpha < 1$, volatilization will tend to increase solute concentration (as occurs with ethylene glycol). Only if α exceeds 1.0 will volatilization cause a concentration drop. Knowledge of α thus provides a convenient method of rapidly estimating volatilizating tendency.

CALCULATION OF H.

Although H is commonly referred to as the ratio of vapor pressure to solubility, it is more correct to express it as the ratio of partial pressure to aqueous concentration thus allowing its value to change at undersaturated conditions. Provided that the solubility is low, little change in H with concentration is expected.

Temperature has a profound effect on H mainly because of its effect on vapor pressure and to a lesser extent, because of the solubility effect. Expressing H in logarithmic form yields,

$$\ln H = \ln P^s - \ln C^s$$

Applying a Clapeyron-type relationship to both P^s and C^s yields,

$$\ln H = -\Delta H^v/RT + \Delta H^s/RT + \text{Constant}$$

For naphthalene ΔH^v the enthalpy of vaporization is approximately 10,000 cal/mol,(Reid et al 14), whereas the enthalpy of solution ΔH^s is about 5000 cal/mol (Schwartz 25) thus the combined effect is about 5000 cal/mol or a $(-\Delta H^v + \Delta H^s)/R$ value of 2500 K. An increase in temperature from 0°C to°25 C corresponding to $(1/T_1 - 1/T_2)$ of 0.0003 thus results in an increase in H by a factor of 2.2 corresponding approximately to a 4.6 fold increase in P^s and a 2.2 fold increase in C^s. A convenient "rule of thumb" is thus that H approximately doubles over a 25° temperature rise.

An aspect of calculating H which has been briefly referred to earlier, and has been the cause of erroneous deductions is the possibility of combining a solid vapor pressure with a liquid solubility or an activity coefficient calculated from molecular size with a solid vapor pressure. This issue is clarified below.

When H is expressed as P^s/C^s it is essential that both P^s and C^s refer to the same state of solid or liquid, ideally solid state data should be used below the triple point and liquid state data above. Extreme care must be taken when using literature vapor pressure correlations since these may be

for liquids extrapolated to below-melting temperatures. Occasionally liquid mixtures exist below the melting point temperature of either pure substance, the classic example being PCBs. Most PCB solubility data are for pure solid isomers but the vapor pressures are for liquid mixtures.

If an activity coefficient γ_w is used to calculate H the correct pressure to use is the reference fugacity or the liquid or subcooled liquid vapor pressure.

H is usually a smooth, continuous function of temperature through the melting point whereas P^s and C^s experience abrupt changes in slope, the gradients of both increasing by an amount corresponding to the enthalpy of fusion. But since H is the ratio (or difference in logs) it does not experience this abrupt change.

A final pitfall in the calculation of H arises when the solute is appreciably soluble in water or when water is soluble in the liquid solute.* The assumption that H equals P^s/C^s is valid only if the solute vapor pressure P^s is not appreciably reduced by water dissolving in the pure liquid solute phase. For example, considering a system in which the pure solute vapor pressure is 0.100 atm and the aqueous solubility is 100 mol/m^3, the value of H is apparently 10^{-3} atm m^3/mol. It is possible that the solute phase contains dissolved water to the extent of a mole fraction of 0.1 in which case the solute will not exert the full vapor pressure P^s of 0.100 atm thus H may be lower, possibly 0.9×10^{-4} atm m^3/mol.

If subscripts s and w apply to the solute activity coefficient γ and mole fraction x in the solute and water phases respectively then it follows that at equilibrium

$$x_s\gamma_s = x_w\gamma_w$$

Writing the 2 suffix Margules equation for γ as a function of mole fraction (Reid et al 14) gives in terms of a constant K

$$\ln\gamma_s = K(1-x_s)^2$$

$$\ln\gamma_w = K(1-x_w)^2$$

Here x_s and γ_s are close to unity, x_w is small and γ_w is large. The group of interest is $\gamma_s x_s$ which is the factor by which the vapor pressure is reduced. Eliminating K and γ_w in favor of γ_s yields after rearrangement

$$\ln x_s + \ln\gamma_s = \ln x_w + (1-x_w)^2 \ln\gamma_s/(1-x_s)^2$$

thus $$\ln\gamma_s = (\ln s_w - \ln x_s)/(1-(1-x_w)^2/(1-x_s)^2)$$

and $$\ln\gamma_s + \ln x_s = \frac{(1-x_s)^2 \ln x_w - (1-x_w)^2 \ln x_s}{(1-x_s)^2 - (1-x_w)^2} = F$$

or $$\ln(x_s\gamma_s) = F \quad \text{and} \quad x_s\gamma_s = \exp(F)$$

*In the case of a solute such as ethanol which is miscible with water, the group P^s/C^s has no meaning and H must be measured experimentally or calculated from $v_w \gamma_w P^s$, the value of γ_w being obtained from another source.

The quantity F is normally small and negative and becomes zero when x_s becomes unity, ie the water content of the solute phase becomes zero. F can be calculated from a knowledge of x_w the mole fraction solubility of the solute in water and x_s, where $(1-x_s)$ is the mole fraction solubility of water in the solute. For example if x_w is 0.1 and x_s is 0.9 then F is -0.07 and $x_s\gamma_s$ is 0.93 resulting in a 7% reduction in vapor pressure and hence in H.

When x_s approaches unity the equation can be approximated as

$$F \approx (1-x_w)^2 \ln x_s \approx (1-x_w)^2(1-x_s)$$

and ultimately if x_w is very small

$$F \approx \ln x_s$$

from which $x_s\gamma_s = \exp(F) \approx 1+F \approx x_s$

The most important influence on $x_s\gamma_s$ is thus x_s with the γ_s effect being secondary.

In the case of solutes such as alcohols x_w may be small e.g. 0.01 but $(1-x_s)$ may be quite large e.g. 0.3 in which case F may become apparently positive (e.g. 0.073) and the Henry's Law constant is increased (i.e. by a factor of 1.073). Such systems can not be represented by a Margules one constant equation and the best approach is simply to reduce P^s by the factor x_s. This approach is used later in the experimental section of this report.

In summary, for solutes which have an appreciable miscibility with water the simplest approach is to assume that P^s is reduced by the factor x_s, If x_s is less than 0.95, ie water achieves a solubility greater than 5 mol percent, it is advisable to calculate $x_s\gamma_s$ more rigorously.

METHODS OF DETERMINING H

Two methods are discussed here, the first being an approach discussed earlier in which the relative volatility α is measured to give the ratio of H for the solute to that of water (H_w).

At 15°C, for example, the vapor pressure of water is 0.0168 atm and its molar volume is 18×10^{-6} m^3/mol thus H_w is 3.03×10^{-7} atm m^3/mol. Only if H is significantly greater than this is volatilization likely to be important.

It is very easy to measure α for dilute systems since all that is required is that a volume of solution be distilled at the temperature of interest and the concentration change measured. Specifically, if a solution of V_1 m^3 of water containing solute of concentration C_1 mol/m^3 is distilled to leave a residue of V_2 m^3 and concentration C_2 mol/m^3 thus yielding a distillate of D m^3 of concentration C_D mol/m^3 then a mass balance yields,

$$V_1 = V_2 + D \qquad \text{(total)}$$

$$V_1C_1 = V_2C_2 + D\,C_D \qquad \text{(solute)}$$

If the vapor leaving the solution is in equilibrium with the liquid its concentration will be α C where C is the liquid concentration.

Writing the differential equation for the concentration decay gives,

$$dV\ (\alpha\ C) = d(VC) = VdC + CdV$$

thus $dV/V = dC/C(\alpha - 1)$.

Integrating between limits of V_1, C_1 and V_2, C_2 yields,

$$\ln(V_1/V_2) = \ln(C_1/C_2)/(\alpha - 1)$$

or $\alpha = 1 + \ln(C_1/C_2)/\ln(V_1/V_2)$

This has the correct properties that if the solute is involatile ($\alpha = 0$) C_D is zero and C_1V_1 equals C_2V_2 thus (C_1/C_2) equals (V_2/V_1) and the log term becomes -1. When α is unity there is no concentration change and C_1 equals C_2 making the log term zero. Usually α exceeds unity and may typically have a value of 5 thus when (V_1/V_2) is 2.0 (i.e. half the liquid is distilled), C_1/C_2 is 16 or the concentration drops to 6.2% of its initial value.

If the concentrations of the initial solution (C_1) the residue C_2 and the distillate (C_D) are measured along with the respective volumes a mass balance can be done to validate the distillation. The value of α can then be calculated accurately. If α is high, only a small fraction of the volume V, should be distilled. Highest accuracy is probably attained when C_2 is about half C_1 which implies that

$$V_2/V_1 \simeq \exp\ [-\ 0.69/(\alpha - 1)]$$

Thus if α is 3, i.e. H is 10^{-6}, V_2/V_1 should be 0.71
if α is 10, i.e. H is 3×10^{-6}, V_2/V_1 should be 0.93
if α is 30, i.e. H is 10^{-5}, V_2/V_1 should be 0.97.

As α becomes large,

$$V_2/V_1 \simeq 1 - 0.69/(\alpha - 1)$$

thus the fraction distilled becomes very small and only a small amount of water need be evaporated in order to substantially deplete the solution of solute. This phenomenon was noticed by Acree et al (26) for aqueous solutions of DDT and at that time was wrongly attributed to a "codistillation" phenomenon. In fact DDT has a fairly high Henry's Law Constant relative to water thus α is large and only slight water evaporation is necessary to remove most of the DDT. This was demonstrated by Mackay and Walkoff (27) who first elucidated the physical chemical principles which in modified form are detailed here.

In view of the simplicity of this method compared to the difficulty of measuring Henry's Law Constants for these relatively involatile compounds by conventional methods, some experimental work was done to develop a suitable test method. This method described later as the "relative volatility method" is a simple method of obtaining an estimate of H for compounds which have H values in the range 10^{-7} to 10^{-4} atm m^3/mol range.

A second "gas stripping" method is also described which is more suitable for compounds of higher H values. Details of this method have been described previously by Mackay et al (28) but it has been extended in this study. The principle is to sparge a gas stream of G m^3/s through a volume

Vm^3 of water containing an initial concentration C_1 mol/m^3 of solute under conditions such that the exit gas stream is saturated with solute, the partial pressure being HC atm and the concentration HC/RT mol/m^3. A differential equation for the volume yields,

$$GHC/RT = -VdC/dt$$

This includes the assumption that HC is small compared to atmospheric pressure. Integration yields,

$$C = C_1 \exp(-GHt/RTV)$$

A plot of $\ln(C/C_1)$ against t yields a straight line of slope -GH/RTV from which H can be deduced. This method becomes inconveniently slow when H is small. For example, if G is $10^{-5}m^3/s$, V is $10^{-3}m^3$ and RT is 0.024, as is typical of laboratory scale systems the group in the exponent becomes approximately 0.4 Ht. To achieve a reasonable concentration drop (say by a factor of 10) requires that this group have a value of 2.3 which implies that Ht be approximately 6 or t is 6/H. For compounds of H values above about 10^{-4} such an extent of concentration drop can be achieved in a reasonable time of one day. When H is 10^{-5} the time required becomes about one week which is inconveniently long. It is thus in the region of 10^{-5} that the two methods overlap in applicability.

A convenient method of illustrating the dependence of H on physical chemical properties is Figure 7 which is a wide range plot of log P^s versus log C^s. Since H is P^s/C^s a line of constant H is a 45° diagonal on that figure. The regimes corresponding to different ranges of H (which are later shown to correspond to different controlling resistances for diffusive mass transfer) can be easily identified. The figure illustrates that compounds of very low P^s and low C^s may have similar values of H to those of high P^s and high C^s for example, p-dichlorobenzene and methylene chloride have similar values of H. The extreme compounds are those of very low H such as water, phenol or diols and those of very high H such as oxygen or alkanes.

CORRELATIONS FOR H

For preliminary or approximate assessment purposes, it may be useful to have a correlation for H in terms of readily available properties such as boiling point and molecular weight. Several approaches are possible, based on the fundamental dependence of H on vapor pressure P^s and solubility C^s, namely

$$H = P^s/C^s \text{ or } \ln H = \ln P^s - \ln C^s$$

As was discussed earlier, $\ln P^s$ can be expressed as a function of boiling point as

$$\ln P^s = 10.6(1 - T_B/T) + 6.8(1 - T_M/T)$$

The solubility can be correlated best in terms of total surface area (TSA) corrected for the fugacity ratio in the form

$$\ln C^s = -A - B(TSA) + 6.8(1 - T_M/T) + 10.93$$

FIGURE 7

PLOT OF SOLUBILITY, VAPOR PRESSURE AND HENRY'S CONSTANT

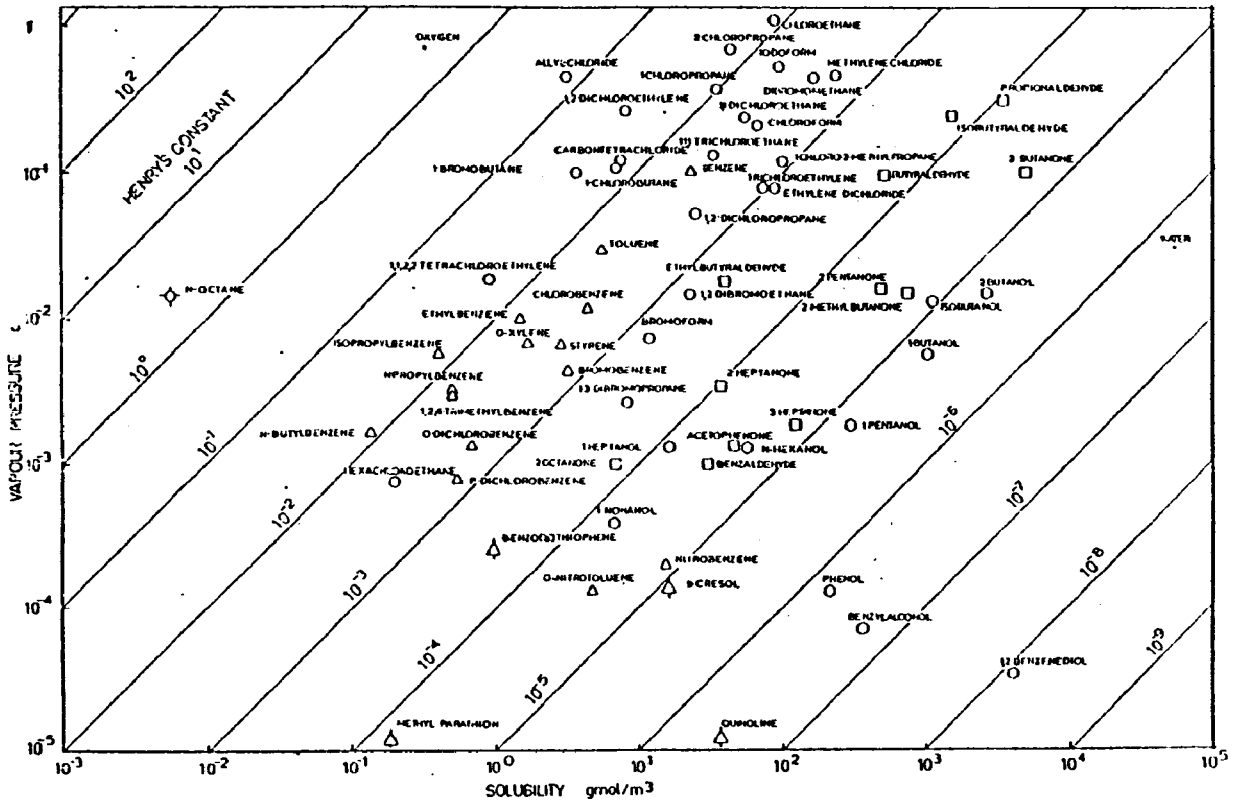

Combining these expressions to give one for ln H eliminates the fugacity ratio term giving

$$\ln H = 10.6\ (1 - T_B/T) - 10.93 + A + B(TSA)$$

The significance of this elimination is that H can be correctly defined as the ratio of the solid vapor pressure to solid solubility or liquid vapor pressure to solid solubility or liquid vapor pressure to liquid solubility, but not a mixture of solid and liquid values. Although P^s and C^s show discontinuities in slope at T_M, H has a continuous slope.

The values of A and B presented earlier in the solubility section can be used or TSA can be related to molar volume, molecular weight or carbon number for a homologous series. Finally, Almgren's correlations (20) for solubility can also be used thus yielding a correlation for H in terms of only melting and boiling points. Writing Almgren's equation in units of K, mol/m^3 and natural logarithms yields

$$\ln C^s = -0.0318(T_B - 273) + 5.15$$

Thus $$\ln H = 10.6(1 - T_B/T) + 6.8(1 - T_M/T) + 0.0318(T_B - 273) - 5.15$$

This equation can be used to give approximate values for H, however the preferred procedure is to obtains experimental data for the homologous series and interpolate or extrapolate. It is unlikely that a sufficiently accurate correlation can be established for H for a wide range of compounds.

As a test of these correlations, data were gathered for a selected group of compounds for which reliable H data and TSA data are available. Values of H were then calculated from the TSA, boiling point correlation and from Almgren's correlation and presented in Table 4. The mean factor by which the (TSA and BP) value differs from the experimental value is 3.2, the corresponding number for the Almgren correlation being 13.0. Neither is accurate enough for any but the most approximate purposes. This expression of the results is somewhat "pessimistic" since much of the error is attributable to a few compounds (especially first six). A better approach is to use TSA and BP as a mechanism of interpolation or extrapolation from data for homologs. It is believed that such an approach will give values consistently within a factor of two of the correct value. Occasionally a fortuitously high P^s and low C^s combine to give a large error in H.

TABLE 4

HENRY'S LAW CONSTANT CORRELATIONS

Compound	M.W. g/mol	Solubility mol/m^3	Vapor Pressure atm	Boiling Point K	Melting Point K	TSA $Å^2$	Henry's Law Constant-atm m^3/mol Literature*	TSA and BP	Almgren
naphthalene	128.19	0.27	1.1×10^{-4}	491	353.2	155.8	4.8×10^{-4}(e)	1.74×10^{-3}	1.76×10^{-3}
1-methyl naphthalene	142.2	0.20	7.8×10^{-5}	517.6	251	172.5	3.9×10^{-4}(c)	2.0×10^{-3}	1.6×10^{-2}
1-ethyl naphthalene	156.2	0.07	2.5×10^{-5}	531.7	259.2	187.4	3.6×10^{-4}(c)	3.2×10^{-3}	1.3×10^{-2}
2-methyl naphthalene	142.2	0.18	8.9×10^{-5}	514.6	307.6	176.3	4.9×10^{-4}(c)	2.8×10^{-3}	4.6×10^{-3}
biphenyl	154.21	0.05	7.4×10^{-5}	528.9	344	182.0	4.1×10^{-4}(e)	2.5×10^{-3}	1.9×10^{-3}
acenaphthene	154.21	0.03	4.0×10^{-5}	550.5	369.2	175.0	1.5×10^{-4}(e)	7.3×10^{-4}	9.8×10^{-4}
fluorene	166.2	0.011	1.63×10^{-5}	568	389	193.6	1.5×10^{-3}(c)	1.3×10^{-3}	5.8×10^{-4}
phenanthrene	178.23	6.6×10^{-3}	4.5×10^{-6}	612	374	198.0	3.9×10^{-4}(e)	3.6×10^{-4}	6.9×10^{-4}
o-dichloro benzene	147.01	0.99	1.9×10^{-3}	453.5	256	142.7	1.9×10^{-3}(e)	3.84×10^{-3}	1.9×10^{-2}
m-dichloro-benzene	147.01	0.84	3.0×10^{-3}	446	248.3	144.7	3.6×10^{-3}(c)	6.1×10^{-3}	2.3×10^{-2}
p-dichloro-benzene	147.01	0.57	8.9×10^{-4}	447	326.1	144.7	2.4×10^{-3}(e)	5.9×10^{-3}	3.9×10^{-3}
bromobenzene	157.02	2.61	5.0×10^{-3}	429	242.18	133.1	2.4×10^{-3}(e)	3.6×10^{-3}	2.8×10^{-2}
1,2,3,5-tetra-chlorobenzene	215.9	0.017	-	519	327.5	175.8	1.6×10^{-3}(e)	9.4×10^{-3}	2.8×10^{-2}
fluorobenzene	96.11	16.16	0.10	358.1	231.8	113.6	612×10^{-3}(c)	6.7×10^{-3}	4.6×10^{-2}
iodobenzene	204.01	0.88	1.3×10^{-3}	461.3	241.79	141.9	1.4×10^{-3}(e)	2.7×10^{-3}	2.5×10^{-2}
n-octane	114.23	5.78×10^{-3}	1.86×10^{-2}	398.66	216.21	178.4	3.219(c)	5.4	5.7×10^{-2}
2,2-dimethyl-butane	86.17	0.214	0.420	322.74	173.13	135.1	1.967(c)	3.2	2.0×10^{-1}
n-pentane	72.15	0.534	0.675	309.07	143.3	124.0	1.265(c)	2.3	4.2×10^{-1}
2,24-trimethyl pentane	114.23	0.0214	6.49×10^{-2}	372.24	165.62	163.1	3.038(c)	4.4	2.0×10^{-1}
2,2,5-trimethyl pentane	114.23	0.0101	2.18×10^{-2}	397.1	167.22	186.6	2.165(c)	10.46	1.7×10^{-1}

* c - calculated; e - experimental

OCTANOL-WATER PARTITION COEFFICIENT

It is universally accepted that a knowledge of octanol water partition coefficient (K_{ow}) is essential for predicting the environmental fate of organic contaminants. The pioneering work of Hansch and Leo and co-workers (9, 10, 30) and other groups have demonstrated that K_{ow} can be used as an indicator of hydrophobicity or lipophilicity and thus serves to quantify the tendency for solute partitioning into cell membranes where the solute may have some physiological effect. It has thus been widely used in drug design. Its application to environmental prediction has been successfully developed by Neely et al (31) to bioaccummulation or bioconcentration in fish, by Karickhoff et al (8) to characterise sorption to organic matter in sediments and by many other workers.

An attractive feature of K_{ow} is that methods are available for calculating it from a knowledge of molecular structure by adding increments to log K_{ow} attributable to various functional groups. Such calculations can be quite accurate when the process is essentially interpolation or modest extrapolation but it is suspected that significant extrapolation is inaccurate. This latter issue is unfortunately of considerable environmental relevance since many compounds of environmental interest have high molecular weights, are sparingly soluble in water and have high K_{ow} values which are very difficult to measure experimentally.

The purpose of considering K_{ow} here is to demonstrate that its value can be closely related to aqueous solubility using the fugacity equations derived earlier. It is thus a useful physical chemical property which can help to validate (or invalidate) other property data and the ability to calculate it from a knowledge of molecular structure may make it possible to estimate other physical chemical properties.

The relationship between solubility C^s mol/m^3 and K_{ow} was first noted by Hansch et al (30) and later Chiou et al (32) correlated the approximately inverse relationship between C^s and K_{ow}. The issue has also been discussed by Mackay (33), Tulp and Hutzinger (34) and Kenega and Goring (35).

Recalling the equations derived earlier

$$C^s = 1/(\gamma_w v_w) \text{ for liquid solutes}$$

$$C^s = \exp(6.8(1-T_M/T))/\gamma_w v_w \text{ for solid solutes}$$

$$K_{ow} = v_w \gamma_w / (v_o \gamma_o)$$

Equating $\gamma_w v_w$ in these equations yields

$$K_{ow} = 1/C^s \gamma_o v_o \text{ for liquids}$$

$$K_{ow} = \exp(6.8(1-T_M/T))/C^s \gamma_o v_o \text{ for solids}$$

Writing in logarithmic form gives

$$\ln K_{ow} = -\ln C^s - \ln\gamma_o - \ln v_o \text{ for liquids}$$

$$\ln K_{ow} = 6.8\ (1 - T_M/T) - \ln C^s - \ln\gamma_o - \ln v_o \text{ for solids}$$

The molar volume of pure octanol is 157 x 10^{-6} m^3/mol. In K_{ow} determinations the octanol is water saturated to a mole fraction of approximately 0.26, thus the molar volume of the mixture is lower, ie 115 x 10^{-6} m^3/mol, thus ln v_o is -9.07. If K_{ow} and C^s data are available γ_o can thus be calculated.

Correlation

Data for 56 compounds are presented in Table 5. From the K_{ow} and C^s data γ_o was calculated for each compound. The tabulated γ_o results are remarkably constant for most compounds but there are two exceptional groups. The aromatic carboxylic acids and 2,4-D (regarded as suspect) have low γ_o values which indicates some form of solute association in octanol solution. The mean γ_o value of approximately 0.48 is an order of magnitude smaller than those of the other compounds. The second group is of compounds of molecular weight greater than 290 including some PCBs and DDT in which γ_o is larger. Segregating these groups for separate treatment gives a mean value of γ_o for the remaining 45 compounds of 4.835 thus ln γ_o is 1.576. The overall correlations become

$$\ln K_{ow} = 7.494 - \ln C^s \quad \text{for liquids}$$

$$\ln K_{ow} = 7.494 - \ln C^s + 6.8\ (1-T_M/T) \text{ for solids}$$

The root mean square of the deviation in log K_{ow} for the 45 points is 0.216 corresponding to a factor of 1.64 in K_{ow}. The correlation coefficient for the calculated and literature values of log K_{ow} is 0.988.

Discussion of the Correlation

A useful procedure for calculating K_{ow} or C^s emerges from these equations. Structurally similar molecules such as phenanthrene and anthracene should have similar γ_o values. Eliminating γ_o from the equations yields at 298 K.

$$K_{ow1}/K_{ow2} = (C_2^s/C_1^s)\ \exp(-0.023\ (T_{M1} - T_{M2}))$$

If either or both are liquids T_{M1} and/or T_{M2} is replaced by the system temperature, usually 25°C. The ratio of solubilities (C_2^s /C_1^s) for anthracene (1) and phenanthrene (2) is 17.7 but the melting point difference (T_{M1} - T_{M2}) is 115° thus the exponential term becomes 0.071 and the expected K_{ow} ratio is 17.7 x 0.071 or 1.26, close to the observed value.

An important implication is that in correlating the partitioning behaviour of organic solutes from water or its subsequent toxic effects it is best to use K_{ow} since it is a more direct measurement of γ_w. Solubility should only be used if the fugacity ratio term is also included, i.e, the correlation should be with ($C^s f_s/f_R$) not C^s. This better correlation has been observed for sorption by Karickhoff et al (8). The preferred units of solubility are mol/m^3 or mole fraction not g/m^3 or ppm. For long chain flexible molecules the entropy of fusion will be higher resulting in a larger coefficient on the melting point term, and the rules devised by Yalkowsky can be used to estimate this effect (11).

The K_{ow}, C^s relationship for carboxylic acids is best treated by assign-

ing a value of 0.48 to γ_o thus the coefficient 7.494 in the equations should be replaced by 9.804.

The higher molecular weight compounds present a more serious problem which may have significant envirionmental implications. Several authors have speculated that very high molecular weight compounds do not show the expected lipophilicity that is indicated from their calculated K_{ow} values. Examples are high molecular weight chlorinated alkanes reported by Zitko (36) and squalene reported by Albro and Fishbein (37), as discussed by Tulp and Hutzinger (34). It has been speculated that lipophilicity is related to calculated K_{ow} by a near linear equation at low K_{ow}, i.e. below log K_{ow} of 5 or 6 but a negative quadratic term becomes dominant thereafter depressing the lipophilicity. There is pharmacological support for this claim (Hansch 38). An alternative explanation suggested by the data is that the calculated K_{ow} values are in error and that above a molecular weight of approximately 290, K_{ow} tends to level off because both γ_o and γ_w increase with increasing molecular size. It is possible that γ_o shows a tendency to increase as a result of the solute molecule becoming "less soluble" in octanol. An equation relating γ_o to molecular weight could be easily devised if sufficient accurate data were available.

The most significant implication is that if high molecular weight solutes display this unusual behaviour with octanol they may also display it with lipids, but to a different degree. If this is the case, the K_{ow}-lipophibicity relationship may break down above log K_{ow} of about 6. Sugihara et al (39) reported evidence of such an effect. Whether this is due to kinetic or thermodynamic effects is not known. Clearly this is an area requiring further study since if very high molecular weight compounds do not bioconcentrate to the extent expected they may prove to be safer environmentally than is expected from extrapolation of the behaviour of lower molecular weight compounds.

Table 5 Physical and chemical properties of selected compounds

Compound	M.W.	M.P. (°C)	S Solubility g/m³	C^S mol/m³	f_S/f_R	Literature log k_{ow}	γ_o	Calculated log k_{ow}
benzene	78.12	5.5	1780	22.79	1.0	2.13	2.83	1.90
toluene	92.15	-95.0	515	5.59	1.0	2.69	3.18	2.51
ethyl benzene	106.17	-94.97	152	1.43	1.0	3.15	4.30	3.10
o-xylene	106.17	-25.18	175	1.65	1.0	3.12	4.00	3.04
1,2,4-trimethyl benzene	120.20	-43.8	57	0.47	1.0	3.65	4.14	3.58
propyl benzene	120.20	-99.5	55	0.46	1.0	3.68	3.95	3.59
isopropyl benzene	120.20	-96.0	50	0.42	1.0	3.66	4.53	3.63
naphthalene	128.19	80.55	31.7	0.25	0.28	3.37	4.15	3.30
1-methyl naphthalene	142.20	-22.0	28.5	0.20	1.0	3.87	5.87	3.95
2-methyl naphthalene	142.20	34.58	25.4	0.18	0.80	3.86	5.36	3.90
1,3-dimethyl naphthalene	156.23	<25	8.0	0.05	1.0	4.42	6.46	4.55
1,4-dimethyl naphthalene	156.23	7.66	11.4	0.07	1.0	4.37	5.08	4.39
1,5-dimethyl naphthalene	156.23	81.0	3.38	0.02	0.28	4.38	4.60	4.35
2,3-dimethyl naphthalene	156.23	105	3.0	0.02	0.16	4.40	2.94	4.18
2,6-dimethyl naphthalene	156.23	108.0	2.0	0.013	0.15	4.31	5.01	4.32

Table 5 continued:

	M.W.	M.P.	S	C^s	f_S/f_R	Literature log k_{ow}	γ_o	Calculated log k_{ow}
1-ethyl naphthalene	156.23	-13.88	10.7	0.068	1.0	4.39	5.21	4.42
1,4,5-trimethyl naphthalene	176.2	64.0	2.1	0.012	0.41	4.90	3.75	4.79
biphenyl	154.21	71.0	7.0	0.045	0.35	4.09	5.30	4.14
acenaphthene	154.21	96.2	3.93	0.025	0.20	4.03	6.40	4.15
fluorene	166.23	116.0	1.98	0.012	0.13	4.18	6.06	4.27
phenanthrene	178.24	101.0	1.29.	7.2×10^{-3}	0.18	4.46	7.36	4.64
anthracene	178.24	216.2	0.073	4.1×10^{-4}	0.01	4.45	9.63	4.73
9-methyl-anthracene	196.3	81.5	0.261	1.33×10^{-3}	0.28	5.15	12.96	5.65
9,10-dimethyl-anthracene	206.3	182.0	0.056	2.7×10^{-4}	0.03	5.67	1.91	5.25
pyrene	202.26	156.0	0.135	6.7×10^{-4}	0.05	4.88	8.66	5.12
fluoranthrene	202.26	111.0	0.26	1.3×10^{-3}	0.14	5.22	5.72	5.29
1,2-benzofluorene	216.28	187.0	0.045	2.1×10^{-4}	0.02	5.75	1.85	5.32
chrysene	228.3	255.0	0.002	8.8×10^{-6}	0.005	5.91	6.47	6.01
triphenylene	228.3	199.0	0.043	1.9×10^{-4}	0.019	5.45	3.10	5.24
tetracene	228.3	357.0	5.7×10^{-4}	2.5×10^{-6}	0.0005	5.91	2.23	5.54
1,2-benzo-anthracene	228.3	162.0	0.014	6.13×10^{-5}	0.04	5.91	7.68	6.10
3,4-benzopyrene	252.32	176.5	0.0038	1.5×10^{-5}	0.03	6.50	5.87	6.57
perylene	252.32	277.0	0.0004	1.6×10^{-6}	0.003	6.50	5.50	6.53

Table 5 continued:

	M.W.	M.P.	S	C^S	f_S/f_R	Literature log k_{ow}	γ_o	Calculated log k_{ow}
3-methyl cholanthrene	268.36	178.0	0.0029	1.1×10^{-5}	0.03	7.11	1.91	6.69
benzo(ghi) perylene	276.34	277.0	0.00026	9.4×10^{-7}	0.003	7.10	2.35	6.77
indan	118.18	-51.4	109.1	0.92	1.0	3.33	4.41	3.29
chloroform	119.38	-63.5	7950	66.6	1.0	1.97	1.40	1.43
tetrachloro-ethylene	165.83	-19.0	400	2.41	1.0	2.60	9.06	2.88
carbon tetrachloride	153.82	-22.99	800	5.20	1.0	2.64	3.83	2.54
fluorobenzene	96.11	-41.2	1553	16.16	1.0	2.27	2.89	2.05
chlorobenzene	112.56	-45.6	472	4.19	1.0	2.84	3.00	2.63
bromobenzene	157.02	-30.82	410.6	2.61	1.0	2.99	3.41	2.84
iodobenzene	204.01	-31.27	340 (30°)	1.67	1.0	3.25	2.93	3.03
p-dichlorobenzene	147.01	53.1	79	0.54	0.53	3.38	3.54	3.24
4,4'-dichloro-biphenyl	223.11	149	.062(20°)	2.8×10^{-4}	0.05	5.58	4.31	5.57
<u>high activity coefficient compounds</u>								
2,4,5,2'5'-penta-chlorobiphenyl	326.4	77	0.010(24°)	3.1×10^{-5}	0.30	6.11	65.87	7.24*
2,4,5,2',4',5'-hexa-chlorobiphenyl	360.9	103	0.00095(24°)	2.6×10^{-6}	0.17	6.72	104.01	8.06*
methoxychlor	345.66	94	0.12	3.5×10^{-4}	0.21	5.08	43.15	6.03*
p,p'-DDT	354.49	109	0.0031	8.7×10^{-6}	0.13	6.19	84.10	7.48*
malathion	330.36	2.85	145(20°)	0.44	1.0	2.89	25.52	3.61*

Table 5 continued:

	M.W.	M.P.	S	C^s	f_S/f_R	Literature log k_{ow}	γ_o	Calculated log k_{ow}
parathion	291.27	6.1	24	0.08	1.0	3.81	16.42	4.35*
low activity coefficient compounds								
2,4-D	221.04	141	890	4.03	0.07	2.81	0.24	1.50 (2.49)
salicylic acid	138.12	159	1800(20°)	13.03	0.04	2.26	0.15	0.75 (1.75)
benzoic acid	122.13	122.4	2700(18°)	22.11	0.09	1.87	0.49	0.86 (1.87)
phenyl acetic acid	136.16	77	16600(20°)	121.92	0.27	1.41	0.76	0.60 (1.60)
phenoxyacetic acid	152.16	99	12000(10°)	78.86	0.13	1.26	0.79	0.47 (1.47)

( ) values in bracket are calculated log k_{ow} using the preferred value of 0.48 for γ_o.

* values in which poor agreement between correlated and experimental data is evident.

RELATIONSHIPS BETWEEN PHYSICAL CHEMICAL PROPERTIES

The elucidation and regulation of the environmental behaviour and effects of existing and new contaminants is a fascinating scientific and social problem. There is no doubt that before any assessment can be made for a particular compound, sufficiently accurate physical chemical data must be available. Most toxic substance regulatory schemes thus require information on solubility, vapor pressure, boiling and melting point, K_{ow}, sorption coefficients, as well as reactivity or degradability data. Essentially, the required physical chemical data are fugacity capacities. Interestingly, it is not clear how accurate these data must be until some general indication of environmental behaviour is obtained in which the important processes or compartments are identified. This issue has been discussed in some detail by Mackay (7).

The establishment of procedures for calculating these data from solely a knowledge of molecular structure would be invaluable for two reasons. It would permit economies in that certain properties of certain compounds need only be calculated rather than measured. It would enable experimental data to be checked for validity and any obviously erroneous data could be identified. Part of this procedure would undoubtedly involve relating one measured quantity to another, for example vapor pressure to boiling point or solubility to K_{ow} as have been discussed earlier.

This brief section is an exploratory review of the state of the art in this area which has the purpose of elucidating some of the existing and potential procedures. It is first useful to list the properties which are directly and readily accessible or inaccessible by experiment.

Directly and Readily Accessible Properties

- Molecular Structure
- Solid and Liquid Vapor Pressure, melting and boiling points
- Aqueous Solubilities
- K_{ow}
- Henry's Law Constant

Properties which are not directly accessible

- Activity coefficients in water, octanol or lipid phases
- Fugacities

Properties which are potentially accessible but present difficulties in direct measurement

- Critical Properties (Temperature and Pressure)
- Enthalpies and Entropies of fusion and vaporization
- Other Phase Transition properties e.g. crystalline transitions

The linkages between these properties is illustrated in Figure 8 which shows that the fundamental physical chemical quantities are the activity coefficients in water and in an organic phase (such as octanol or lipid)

and the solid and liquid fugacities and their ratio, which are essentially the vapor pressures. If these data are known as a function of temperature it is possible to calculate all the experimentally measurable quantities using established thermodynamic relationships. Conversely, it is possible (and necessary in practice) to estimate these inaccessible properties from experimental measurements.

The important conclusion is that most of these quantities are mutually dependent, thus not all quantities need be measured. For example only two of - vapor pressure, solubility and Henry's Law Constant need be measured since the third can be calculated, or better, all three can be measured and checked for consistency.

Consistency checks are also possible between K_{ow} and solubility or between vapor pressure and boiling point.

A very significant development would be the ability to calculate the activity coefficient and fugacities from molecular structure. This would enable data to be validated and avoid the necessity for some experimental measurement, although it is accepted that there is ultimately no substitute for experimenal data. This capability is emerging. Examples are the correlations of activity coefficient with molecular surface area by Yalkowsky and Valvani (12), the calculation of K_{ow} from molecular structure by Hansch and Leo (10). Ultimately the development of this predictive ability could be a step towards further structure -property-activity deductions involving estimation of sorption (from K_{ow} and organic content), reactivity using linear free energy relationships (e.g. hydrolysis) and ultimately even biological processes such as biodegradation or toxicity. In the long term it is possible that the environmental behaviour and effects of contaminants will become predictable from molecular structure. To achieve this a sound foundation of verified physical chemical property data is essential.

FIGURE 8

SCHEMATIC DIAGRAM OF RELATIONSHIPS BETWEEN PHYSICAL CHEMICAL PROPERTIES, THE FUNDAMENTAL QUANTITIES WHICH ARE INACCESSIBLE BY DIRECT EXPERIMENTAL MEASUREMENT BEING IN THE BOX

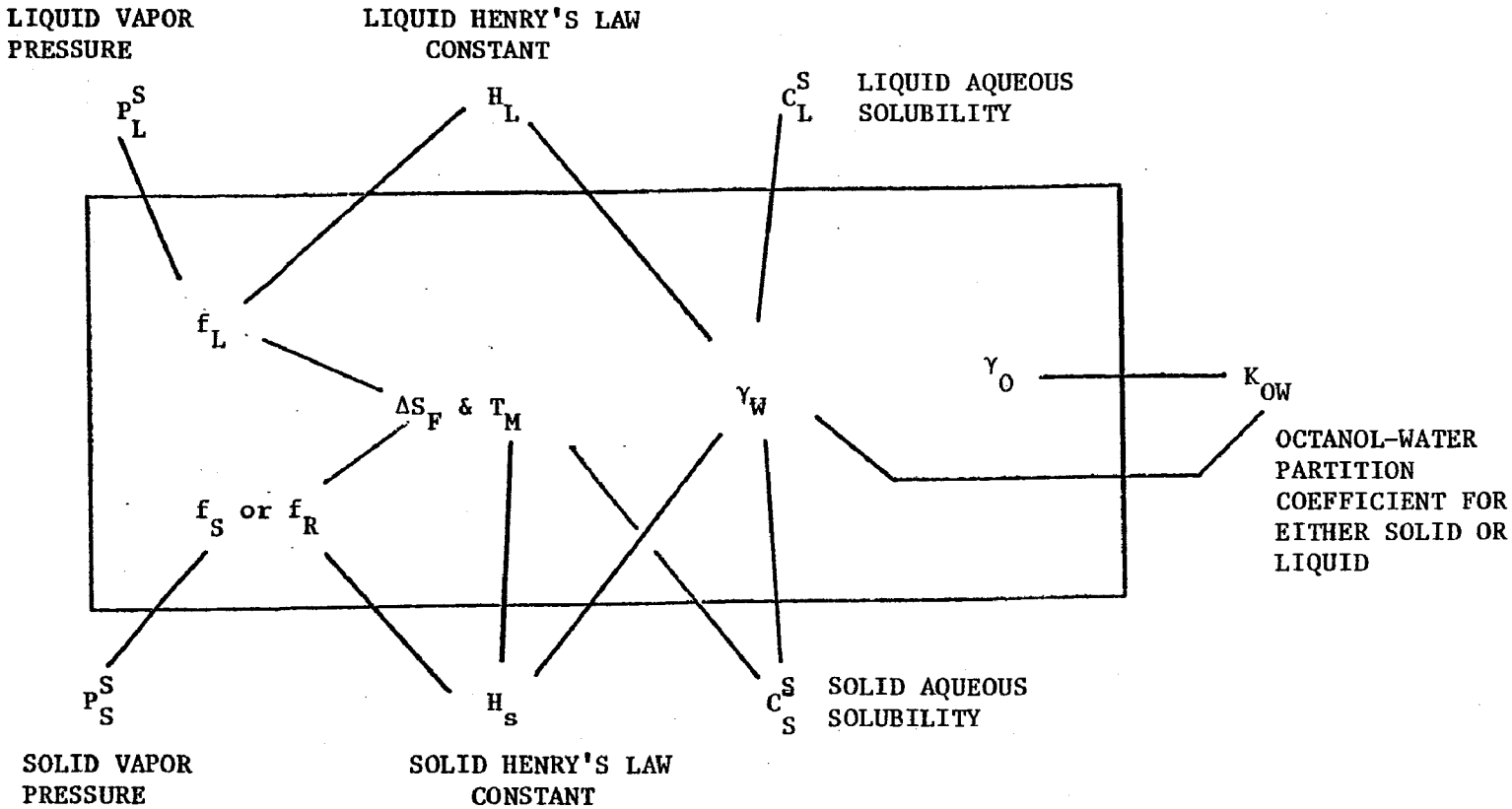

SPECIMEN CALCULATION AND CRITICAL REVIEW OF AQUEOUS PHASE PROPERTIES

To illustrate the concepts discussed in this section a calculation for naphthalene is outlined below.

Properties (experimentally obtained)
Molecular weight 128.2 g/mol.
Total Surface Area 155.8 sq. angstroms
Melting point (T_M) 353.2K (80.2°C)
Boiling point 491 K (218°C)
Aqueous solubility at 25°C 34.4 g/m^3 (0.268 mol/m^3)
Vapor Pressure at 25°C solid 1.14×10^{-4} atm (f_S)
liquid 3.08×10^{-4} atm (f_L)
Henry's Law Constant 4.8×10^{-4} atm m^3/mol
Octanol Water Partition Coefficient 2300

(1) Fugacity ratio at 25°C (298K)

$$f_S/f_R = \exp(6.8(1-T_M/T)) = 0.28$$
(experimental = 0.35)

(2) Activity Coefficient

$$\ln\gamma = A + B(TSA) = 11.44$$

thus $\gamma = 93100$ (Table 2)

(3) Aqueous solubility

$$C^S = (f_S/f_R)/\gamma v_W = 0.28/93100 \times 18 \times 10^{-6} = 0.167 \text{ mol/m}^3$$
(experimental = 0.268)

Yalkowsky correlation (Table 2) for MP = 80.2°C

$$\log S = K_1 - K_2(TSA) - K_3(MP)$$
$$= 1.42 - 0.0282(TSA) - 0.0095(MP) = -3.73$$

thus S is 0.000184 mol/L or 0.184 mol/m^3

Almgren's correlation gives

$$-\log S = 0.0138T_B + 0.76 = 3.77 \quad (T_B \text{ in °C})$$

thus S is 0.00017 mol/L or 0.17 mol/m^3

(4) Vapor Pressure from boiling and melting point

(i) liquid $\ln P = 10.6(1 - T_B/T) = -6.87$

$P = 10.4 \times 10^{-4}$ atm (experimental 3.06×10^{-4})

(ii) solid $\ln P = 10.6(1 - T_B/T) + 6.8(1 - T_M/T) = -8.13$

$P = 2.96 \times 10^{-4}$ atm (experimental 1.08×10^{-4})

(5) Henry's Law Constants

H calculated from P^s and C^s is 4.25×10^{-4} atm m^3/mol

(experimental = 4.8×10^{-4})

$$\ln H = 10.6(1\ T_B/T) - 10.93 + A + B(TSA) = -6.36$$

$$H = 1.7 \times 10^{-3} \text{ atm m}^3/\text{mol} \quad (\text{experimental } 0.48 \times 10^{-3})$$

The discrepancy here is due to a combination of an overestimated vapor pressure and an underestimated solubility.

Almgren's correlation

$$\ln H = 10.6(1 - T_B/T) + 6.8(1 - T_M/T) + 0.0318(T_B - 273) - 5.15$$

$$= 8.13 + 6.93 - 5.15$$

$$= 6.35$$

$$H = 1.76 \times 10^{-3} \text{ atm m}^3/\text{mol}$$

(6) Solubility-Octanol Water Partition Coefficient

$$\ln K_{OW} = 7.494 - \ln C^s - 0.023(T_M - T)$$

here C^s is 0.0268 mol/m^3 thus

$$\ln K_{OW} = 7.54$$

$$\log K_{OW} = 3.27 \qquad K_{OW} = 1883 \qquad (\text{experimental } 2300)$$

Discussion

It is apparent from this example that correlated values of solubility, vapor pressure, Henry's Law Constant and octanol-water partition coefficient can be in error by factors of two or more. At the present state of the art such correlations must be used with caution. Since experimental values are also suspect in many cases there is a compelling incentive to check the experimental data by comparing values of f_S, f_L, γ_W and γ_O obtained by different methods and critically reviewing their likely errors.

For example, naphthalene is judged on the basis of the accuracy of the determinations and correlations to have the following basic values.

quantity	units	recommended value	lower limit	upper limit
f_S	atm	1.14×10^{-4}	1.00×10^{-4}	1.40×10^{-4}
f_L	atm	4.0×10^{-4}	2.5×10^{-4}	4.5×10^{-4}
γ_W	-	59100	57400	60900
γ_O	-	4.02	3.82	4.22
f_S/f_L	-	0.285	0.25	0.31

quantity	units	recommended value	lower limit	upper limit
C^s	mol/m^3	0.268	0.260	0.276
K_{OW}	-	2300	2200	2400
H	$atm\ m^3/mol$	4.25×10^{-4}	3.90×10^{-4}	4.83×10^{-4}

A compilation of this type is invaluable in highlighting the quantities which are less accurately known. A judgement can then be made as to whether or not more accurate values are required for environmental assessment purposes. As data in this form become available, better correlations can be developed thus facilitating the calculation of properties of other solutes in the series with greater accuracy.

SECTION 5

MASS TRANSFER PHENOMENA

MECHANISMS OF TRANSFER

Figure 9 illustrates the processes which may occur when a solute transfers from a water body to the atmosphere.

First it may be incorporated in sediments or biota and require some time for desorption into the water column.

Second, it may have to diffuse vertically through the water column until it reaches the near surface layer, i.e. within a mm of the interface. In fast flowing shallow rivers this process is probably fairly rapid but in deep quiescent water it is slower. The solute may encounter stratified regimes during its vertical journey in which there are different diffusive velocities. This occurs particularly in lakes where there may be a well defined fairly well mixed surface layer or epilimnion and a deeper more quiescent hypolimnion. Such stratification is normally the result of density differences arising from temperature variation but in sea water and estuaries there may be contributions arising from the differing salinities, and hence densities, of the water.

Third, the solute must pass through the near-interfacial liquid layer to the interface.

Fourth, it must penetrate the interface.

Fifth, it must pass through the near-interfacial gas layer.

Sixth, it must then diffuse to the bulk of the atmosphere.

In addition to these processes the solute may be carried vertically by rising bubbles generated for example by anaerobic processes or it may rise or fall in association with suspended mineral, organic or biotic matter. This gives rise to a possibly complex situation in which the material is moving up and down simultaneously by differing mechanisms and at different rates and it is not immediately clear what the net effect will be.

At the surface it is possible that the material may accumulate in a surface organic microlayer containing organic material of natural and anthropogenic origin. This layer may influence the transfer rate in several respects. If coherent, it can damp turbulence in the form of capillary waves thus reducing transfer rates, (Davies & Rideal [18]). It may also block

FIGURE 9

SCHEMATIC DIAGRAM OF TRANSPORT PROCESSES

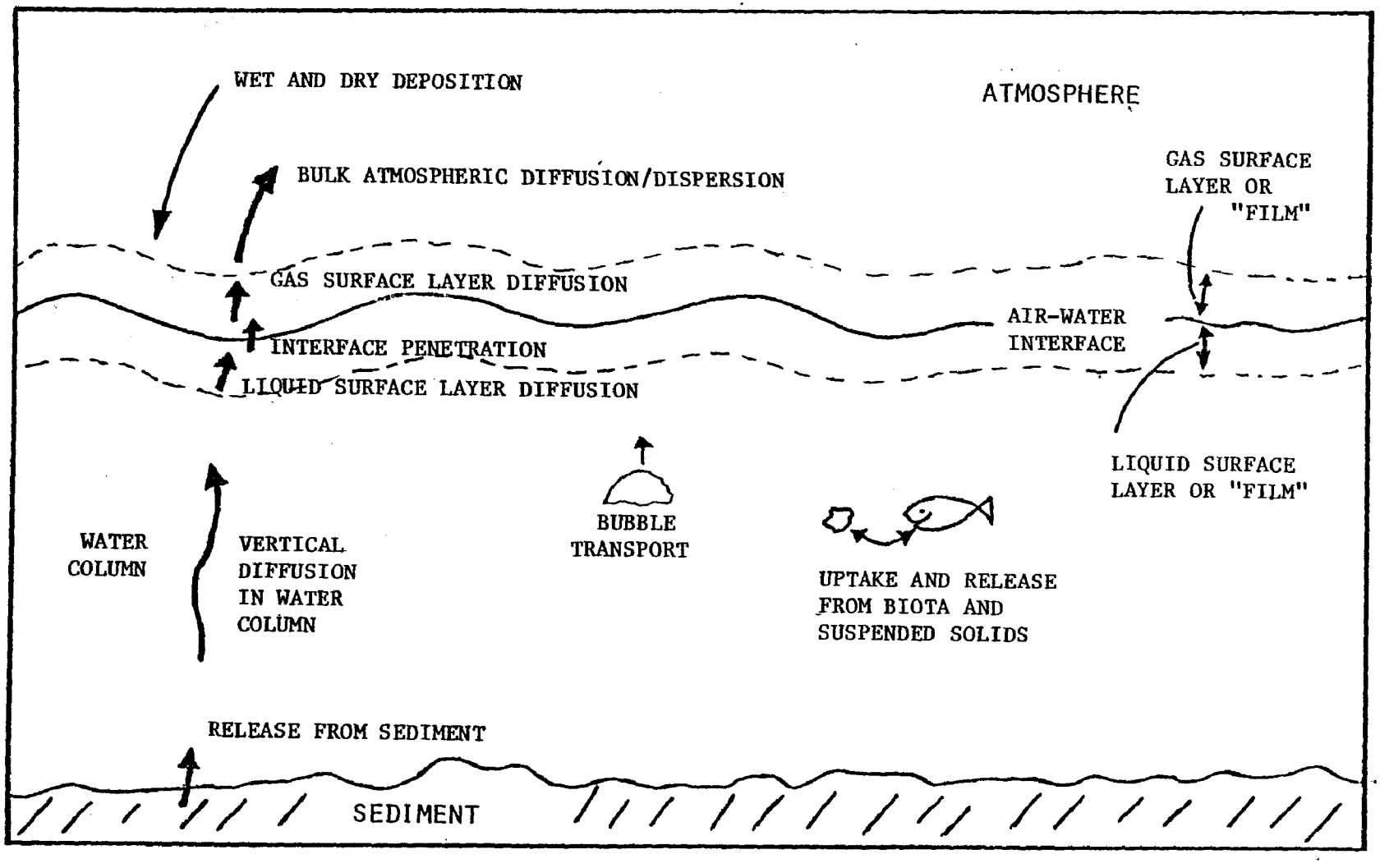

the transfer process by forming a layer of less penetrable surface active materials. This layer is probably in motion relative to the water column at approximately 3% of the prevailing wind speed. As a result, a solute may diffuse vertically through the water column at one location, enter the microlayer and be swept horizontally to another location at a velocity of typically 0.1 to 1.0 km/h. The result may be the transfer of the solute preferentially to the banks of rivers or small lakes.

As bubbles arrive at the surface they tend to form a thin skin consisting primarily of the interfacial material which ruptures as the bubble bursts through the surface, generating a number of small droplets which may be propelled permanently into the atmosphere. This occurs particularly in situations such as aeration vessels where exceptionally high rates of bubbling are induced. This mechanism serves to introduce involatile materials such as electrolytes and microorganisms into the atmosphere in addition to volatile material. Only in locations where there is abnormal bubbling activity is this likely to be important for the volatilizing compounds considered here.

Finally, it should be noted that the solute may become associated with particulate matter in the atmosphere and be redeposited in the water. It may also dissolve in rain water or associate with snow and return to the water in the form of wet deposition. It is most unlikely that there are high rates of exchange in both directions. A substance which volatilizes generally does so because of its tendency to partition into air rather than water. Having volatilized it will tend to achieve a lower atmosphere concentration because of dilution. If then contacted with water in the form of rain it can not then achieve an aqueous concentration equal to that of the water body it left. Rain must thus contain a lower concentration of the volatilized solute than that of the water from which volatilization took place. Rainfall will thus lend to dilute the water body concentration, possibly approximately making up for the concentrating effect of evaporation.

In the event that the solute enters the system primarily by air, as is the case with SO_2, there may of course be substantial wet deposition, but one would then expect negligible volatilization. The situation with substances such as PCBs which have poorly defined sources and partition characteristics is less clear.

There is a possibility that a solute may sorb on to atmospheric particulate matter and then be deposited either naturally by gravity or by washout. Only if the rate of deposition is high is this likely to be important. Generally, particulate matter is at much higher concentrations in water than in air thus if the compound has a strong sorbing tendency it will tend to remain in the water rather than volatilize since it will be associated with the suspended aquatic matter.

The general conclusion is that it seem unlikely that a substance will undergo simultaneously significant transfer rates in both directions. Rainfall should have a negligible effect on a volatilizing compound, especially because of the low rates and its intermittent nature. Movement by associa-

tion with suspended matter will tend to be either consistently vertically down in the case of compounds which sorb strongly, the ultimate destination being sediments, or it will be unimportant for other compounds.

From a thermodynamic viewpoint the overall tendency will be to equalize fugacity or chemical potential and in a closed system no natural process can appreciably delay that process..

DIFFUSION PROCESSES

Diffusion Within A Phase

Within a single phase, diffusion tends to transfer material from regions of high to low concentration which corresponds to high and low fugacity. This is essentially a manifestation of the tendency of any fluid to mix, ultimately reaching a homogeneous composition. The simplest mathematical representation of diffusion is Fick's first law which applies to steady state (i.e. time independent) conditions. It is analogous to Fourier's law for heat transfer, Ohm's law for electricity transfer, and Newton's law for momentum transfer, in that it postulates that the flux is proportional to the gradient in the driving force. For mass diffusion, concentration is the driving force and the proportionality constant is the mass diffusivity. The equation can be expressed in differential or intergrated form as shown below.

$$N = - D\, dC/dy = - D\Delta C/\Delta y$$

where N is mass flux (mol/m^2s), D is diffusivity (m^2/s), C is concentration (mol/m^3) and y is distance in the direction of diffusion (m). The mass flux is thus the product of two types of terms. The diffusion and distance terms express the kinetics of the system and can be regarded as characterizing the rate of mixing or the velocity which with the elements of the fluid move. The concentration difference term is an expression of the departure of the system from equilibrium conditions and is therefore thermodynamic in nature and time independent.

In a stagnant fluid, in which there is no bulk motion (a condition which is achieved only with difficulty in the laboratory and rarely in the environment), the diffusivity is the molecular diffusivity which is typically 10^{-5} cm^2/s for liquids and 10^{-1} cm^2/s for gases. It can be shown from the kinetic theory of gases that the gas diffusivity equals 1/3 of the root mean square velocity times the mean free path. As a result, high diffusivities result from high molecular velocities (which are caused by high temperatures) and large internal spacing between the molecules, which arise from low pressures. For liquids, no such simple relationship can be devised. For solids, the diffusivity is normally regarded as negligible. Diffusivity is thus dependent upon the nature of the diffusing molecule. Larger heavy molecules tend to have lower velocities and thus have lower diffusivities. This is important environmentally in calculating diffusion rates of one compound from that of another, for example, in calculating the diffusion rate of PCB molecule from that observed for oxygen. Diffusivities are temperature and pressure dependent and are influenced by the presence of other species in solution.

Correlations are available for calculating these diffusivities as reviewed in the text by Reid, Sherwood and Prausnitz (14). Usually the Wilke-Chang correlation is used for liquids and the Chapman-Enskog correlation for gases.

In environmental and industrial situations, the fluids (air or water) are normally in motion thus diffusion can occur by two distinct and additive mechanisms, molecular diffusion as described above, and turbulent diffusion which can be regarded as transport of material by means of an element or eddy of fluid which moves from one region to another. There is relatively poor information about the size and velocity and frequency of these eddies, largely because they vary greatly in size and configuration and are very difficult to observe because of their intermittent nature. Eddies may range from a fraction of a millimeter to many meters in dimension and they may be superimposed upon each other. There is a considerable amount of literature in atmospheric and oceanographic physics on turbulent diffusion processes and many empirical approaches have been used to calculate these diffusivities, (for example, Csanady, 40).

It is noteworthy that in the bulk of environmental fluids turbulent diffusivities are normally several orders of magnitude greater than molecular diffusivities, thus, in many situations, the molecular term can be ignored. Turbulent diffusivities are virtually impossible to predict from theoretically first principles. They can only be measured by simultaneously measuring mass fluxes and concentration gradients and correlating the results.

Fortunately there is a close linkage or analogy between turbulent diffusion of mass, heat and momentum thus generalised correlations are possible in which data from one transport process can be used to predict the behaviour of another (Bird, Stewart and Lightfoot 41).

The source of turbulence or eddies is of considerable importance, since if the strength of the source can be measured it may be possible to predict its effect in generating turbulence elsewhere. The source is usually a region of relatively high fluid velocity gradient. Examples are the interaction of a river current with the bottom in which the roughness at the bottom induces eddies, which move upwards towards the surface tending to decay as they progress. Even smooth surfaces induce turbulence above a certain critical velocity, usually characterized by the Reynolds number. Only at low velocities does flow become nonturbulent or laminar. In the atmosphere, pressure and thermal effects cause winds which are variable in direction and velocity. The turbulent diffusivity in the atmosphere depends on wind velocity and particularly on the thermal structure near the ground. The turbulence experienced at, for example, a lake surface, is thus very dependent on the temperature and velocity conditions in the overlying air. In lakes most turbulence may be formed by the interaction of wind with the water surface resulting in the formation of waves and surface currents. Residual currents arising from rivers may also play a significant role. Estuaries and tidal regions, may also contain significant currents which induce turbulent motion. Finally, under some conditions, the turbulence induced by biota may be significant, for example, in sediments benthic organisms may play a significant role in in transporting material between the sediment and the water column.

When mass diffuses close to a phase boundary, for example, at a solid-liquid or air-liquid interface, gravitational and interfacial forces prevent eddies from moving directly across the interface vertically, although an eddy in one phase may induce eddying in the other phase. For example, wind may induce turbulence at and below the surface of a lake. The result is that turbulent vertical diffusivities tend to approach zero at an interface, thus much of the resistance to mass transfer (the resistance being inversly proportional to the diffusivity) tends to be located within a few millimeters of phase boundaries. From the viewpoint of the diffusing molecule, it finds that it can move relatively easily from the bulk of the phase to a region a few millimeters from the interface having been carried by relatively large turbulent eddies but its subsequent journey to the interface is made on smaller and slower eddies and may ultimately be made by slow molecular diffusion. In calculating the rate of flux, it is often possible to ignore the time taken to get to the near-interfacial region and concentrate on interfacial transfer in both phases. Unfortunately then, the interfacial region is often the most critical and where it is most difficult to make precise measurements of concentration, distance or even position. This is particularly true in air-water systems, where the interface may be moving vertically as a result of wind and wave action. In applying Fick's law, there is thus no accurate data for D, the diffusivity or Δy, the diffusion path length. It is then convenient to lump these two unknown quantities together in a single unknown term, called a mass transfer coefficient, which can be regarded as $D/\Delta y$, and is defined as follows:

$$N = D\ \Delta C/\Delta y = K\ \Delta C \text{ where } K = D/\Delta y$$

A considerable volume of data exists on mass transfer coefficients in various phases, geometries, turbulence levels and for various compounds. Ultimately any volatilization rate predictions depends heavily on such correlations.

It is noteworthy that there remains considerable doubt about the actual microscopic mechanism during mass transfer between air and water phases. It is generally accepted that eddies of fluid move to the surface, are exposed to unsteady state molecular diffusive mass transfer for some unknown time, and then move back to the bulk. This model is consistent with observations that the mass transfer coefficient depends on the molecular diffusivity, but the dependence is not linear as one would expect if K was simply $D/\Delta y$. Empirically, K is often expressed as a power of D, usually D to the power in the range 0.5 to 0.8. This is regarded as evidence that the diffusion process is a combination of turbulent transport of the eddy (which is independent of D) followed by an unsteady state diffusion at the surface dependent on D, and possibly even a steady state period. This unsteady state transfer can be characterized by Fick's second law, which essentially gives the differential relationship between the concentration, time and distance. Solutions of this equation suggest that the mass transfer should be proportional to the square root of diffusivity. The full details of such considerations are given in texts on mass transfer, for example, by Sherwood et al (42).

A further complication is that turbulent diffusion is not necessarily or even usually isotropic, i.e. it is not equal in all directions. If eddies were spherically symmetrical, one would expect diffusion to be equal in all

directions, however, the eddies are subject to gravitational forces and tend to move horizontally with a greater ease than vertically, especially if the fluid is horizontally stratified or confined. Vertical diffusion is thus often an order of magnitude less than horizontal diffusion in water. Similar, but not as profound differences, exist in atmospheric diffusion. Vertical diffusion may be particularly slow under conditions where the fluid has a temperature (and hence a density) gradient. In most fluids, as temperature increases, density decreases (water below 4°C being the notable exception), thus, an element of fluid propelled vertically upwards into a fluid region of higher temperature tends to be slowed and fall back by virtue of its greater density. Such fluids in which temperature increases with height tend to be very stable and even stagnant, the buoyancy effects damping out any tendency for vertical diffusion. Examples of this are thermoclines in lakes and temperature inversions in the atmosphere. In the opposite situation in which temperature falls with increasing height, an eddy moving vertically tends to be assisted by buoyancy forces and thus, vertical diffusion may be enhanced. The net result is that the mass transfer processes are strongly influenced by the thermal condition of the fluid in which transfer is taking place. This thermal condition may be a result of recent temperature history, but may also be influenced by evaporation of water.

In summary, diffusion within a phase is readily characterized by Fick's law by which fluxes can be calculated from diffusivities, concentration differences and diffusion path lengths. The diffusivity term can be regarded as the sum of a molecular term (for which adequate correlations exist) and a turbulent term which is very complex and can only be measured experimentally and correlated empirically. In the near interface regions, there is considerable doubt about the value of diffusivity path length and indeed position, thus it is conventional to lump the diffusivity and distance terms into a mass transfer coefficient. These diffusivity or mass transfer coefficient terms depend on turbulence level, the molecules properties, including its molecular diffusivity, and the only approach available is to develop an empirical procedure for calculating them from easily measurable quantities such as wind speed or river depth, which are essentially characterisations of the strength of the turbulence source.

Diffusion Between Phases

When a solute diffuses through a region of different phases or of one phase in which it experiences different diffusivities (and hence velocities) it is essential to develop a method of determining how each zone affects the overall diffusion rate. Often one process is so fast that it affects the overall rate to a negligible extent. This is illustrated schematically in Figure 10 which shows a solute diffusing at steady state from a high terminal fugacity f_1 to a low terminal fugacity f_4 through three zones which may be different phases (eg. air and water) or stratified layers.

There is presumably a continuous trend in fugacity between f_1 and f_4 which must be linear in regions of constant diffusivity if steady state applies.

An important assumption here is that at the boundary between phases or regions within a phase the fugacities are equal i.e. there are no fugacity discontinuities. This is regarded as a reasonable assumption since if a fugacity difference did exist over a microscopically small distance diffusion would be very fast because of the large gradient. This assumption is equivalent to the "equilibrium existing at the interface" assumption made in the Whitman Two Resistance Theory and elsewhere.

Fick's Law can be written for each phase as

$$N = - D_i \Delta C_i / \Delta y_i \text{ or } - K_i \Delta C_i$$

But in each zone $C_i = Z_i f_i$

Thus $N = - D_i Z_i \Delta f_i / \Delta y_i \text{ or } - K_i Z_i \Delta f_i$

It is convenient to replace the "conductivity" terms $D_i Z_i / \Delta y_i$ and $K_i Z_i$ by their reciprocals or "resistances" r_i i.e.

$$r_i = \Delta y_i / D_i Z_i \text{ or } 1/K_i Z_i$$

thus $N = \Delta f_i / r_i$

$$N = (f_1 - f_2)/r_A = (f_2 - f_3)/r_B = (f_3 - f_4)/r_C$$

from which $r_A = (f_1 - f_2)/N$, $r_B = (f_2 - f_3)/N$ etc.

hence $(r_A + r_B + r_C) = (f_1 - f_4)/N$

and $N = (f_1 - f_4)/(r_A + r_B + r_C)$

If each resistance can be predicted, the total can be obtained, the dominant resistance determined and the flux calculated. The values of intermediate fugacities can than be determined.

The most important feature of this analysis is that the resistance terms depend not only (as is obvious) on the diffusivities or mass transfer coefficient but also (and less obviously) on the Z values or fugacity capacities. The reason for this latter dependence is that in regions of low Z only a low concentration is necessary to achieve the required fugacity, thus only on low concentration gradient is achievable, thus the mass flux tends to be constrained to a low value. Mass diffuses most rapidly where it can achieve high concentrations and hence concentration gradients. Low Z values thus cause high resistances. The importance of this effect lies in the observation that in many cases Z is sufficiently high in a phase that the resistance becomes small and hence can be neglected. Control of the overall diffusive process then lies in another phase.

This general conclusion reduces to the Whitman Two Resistance Theory (43) for air-water exchange. If r_L and r_G are liquid and gas resistances equivalent to $1/K_L Z_L$ and $1/K_G Z_G$ then since f_L is C_L/Z_L and f_G is P_G

$$N = (C_L/Z_L - P_G)/(1/K_L Z_L + 1/K_G Z_G)$$

But Z_L is 1/H and Z_G is 1/RT thus

$$N = (C_L H - P_G)/(H/K_L + RT/K_G)$$

This equation is conventionally written in the equivalent forms

$$N = K_{OL}(C_L - P_G/H) \quad \text{where} \quad 1/K_{OL} = 1/K_L + RT/HK_G$$

or

$$N = K_{OG}((C_L H - P)/RT) \quad \text{where} \quad 1/K_{OG} = 1/K_G + H/RTK_L$$

The terms K_{OL} and K_{OG} are overall liquid and gas mass transfer coefficients which are related since

$$K_{OL} = HK_{OG}/RT$$

compounds of high H values which tend to partition into the air phase because of their high vapor pressure and/or low solubility usually have negligible gas phase resistances (RT/HK_G) because they are able to establish high gas phase concentrations. Such systems are termed liquid phase controlled. Conversely compounds of low H are usually gas phase controlled. The resistances are equal when

$$1/K_L = RT/HK_G \text{ or when } H/RT = K_L/K_G$$

Illustration Of Multiphase Diffusion

Consider a solute diffusing through a system of (A) a water body of depth Y of 2 m and diffusivity D of 0.001 m^2/s, (B) a liquid film of mass transfer coefficient K_L of 0.0001 m/s and (C) a gas film of mass transfer coefficient K_G of 0.01 m/s. The concentration at the bottom is 0.1 mol/m^3 and in the atmosphere it is 10^{-6} atm. The temperature is 10°C at which the solute solubility C_s is 20 mol/m^3 and its vapor pressure P^S is 0.002 atm.

Then Henry's constant H is P^S/C_S or 0.0001 atm. m^3/mol, thus Z_L is 10000. Z_G is 1/RT or $1/82 \times 10^{-6} \times 283$ or 43.

The resistances are thus

$$r_A = Y/DZ_L = 2/0.001 \times 10000 = 0.20 \text{ atm. } m^2 s/mol$$

$$r_B = 1/K_L Z_L = 1/0.0001 \times 10000 = 1.00 \text{ atm. } m^2 s/mol$$

$$r_C = 1/K_G Z_G = 1/.01 \times 43 = 2.33 \text{ atm. } m^2 s/mol$$

The total resistance r_T is thus 3.53

The total fugacity difference is from the bottom value f_1 of C/Z_L or 0.1/10000 or 10^{-5} atm to the atmospheric value f_2 of 10^{-6} atm i.e. a change in Δf of 9×10^{-6} atm.

The flux N is thus $\Delta f/r_T = 9 \times 10^{-6}/3.53$ or $2.55 \times 10^{-6} mol/m^2 s$

The intermediate fugacities can also be calculated from $\Delta f = Nr$

i.e. $\Delta f_A = 2.55 \times 10^{-6} \times 0.2$ or 0.51×10^{-6} atm

$\Delta f_B = 2.55 \times 10^{-6} \times 1.0$ or 2.55×10^{-6} atm

$\Delta f_C = 2.55 \times 10^{-6} \times 2.33$ or 5.94×10^{-6} atm

Total 9.00×10^{-6} atm

The intermediate fugacities are thus

Between the water column and the water film 9.49×10^{-6} atm

Between the water film and air film 6.94×10^{-6} atm

In this case most of the resistance (66%) lies in the air film, 28% lies in the water film and 6% lies in the bulk of the water phase. The calculation can be done for any number of phases with little increase in complexity.

These quantities are illustrated in Figure 10. Note that the fugacity profile varies continuously over the diffusing regions whereas the concentration profile undergoes a discontinuity at the air-water interface.

FIGURE 10

ILLUSTRATIVE FUGACITY TRANSPORT CALCULATION

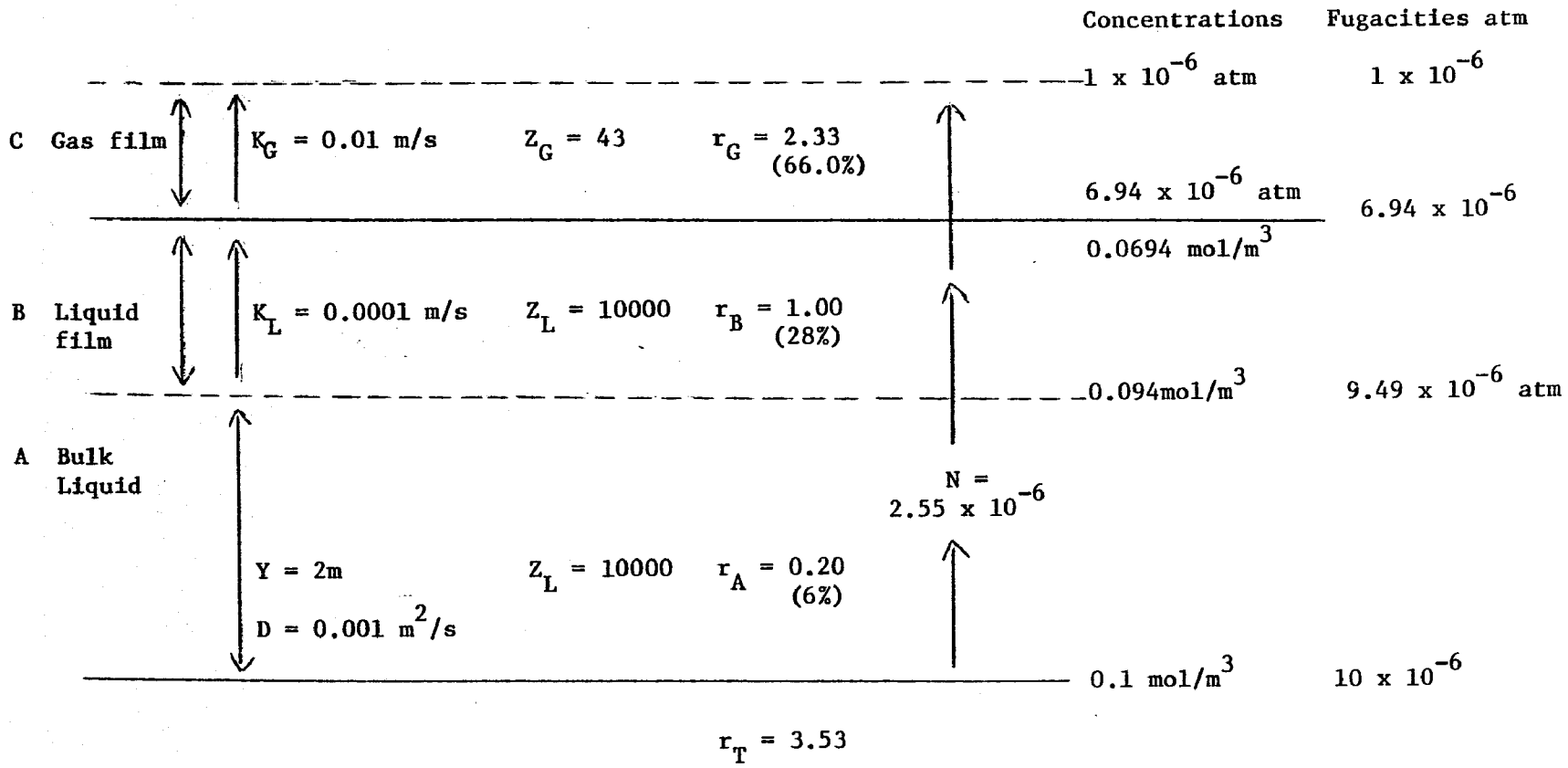

PREDICTION AND CORRELATION OF ENVIRONMENTAL MASS TRANSFER COEFFICIENTS

(a) Mass Transfer Coefficients

There have been numerous studies in which mass transfer coefficients have been measured in various contacting geometries. Much of the incentive has been to assist the design of chemical process equipment such as distillation columns where the size and efficiency are directly controlled by these coefficients. A convenient review of this topic is the text by Sherwood et al (42). Less effort has been devoted to environmental mass transfer and the predictive capability is somewhat poorer, partly because environmental systems have more complex and variable fluid flow characteristics. Reviews relevent to this area have been compiled by Csanady (40) and Thibodeaux (44).

Since the 1920's several approaches towards predicting and correlating mass transfer coefficients have been advanced, all based on a conceptual model of the physical processes which control mass transfer. One of the principal difficulties is that for environmental conditions the physical mechanism of transfer is still not clear, and until this is clarified it is doubtful if a comprehensive, accurate predictive capability will emerge.

The film theory presented by Whitman (43) and by Lewis and Whitman (45) was the earliest model to quantify the absorption of gases into turbulent liquids. They postulated that laminar or stagnant films of gas and liquid exist at the interface between the two phases. These films experience little convective motion while turbulent motion and rapid mixing keep the concentration of the solute uniform in the bulk phases. It follows that the solute that transfers through one film must also pass through the other and the two films can be considered as two diffusional resistances in series. The rate of transfer at steady state can thus be calculated from the film thickness (Z) and the molecular diffusivity (D) and the mass transfer coefficient K becomes D/Z. This approach is still used in some oceanographic and limnology literature in which the mass transfer resistance is expressed as an equivalent stagnant film thickness.

It is generally accepted that this sample model is invalid, principally because there is insufficient time for steady state diffusion to be established. This is manifested experimentally as a non linear relationship between K and D, i.e. generally if D increases by a factor of four, K only doubles or trebles.

This model is however invaluable as a means of combining the two phase resistances to give an overall resistance. This "two resistance" version of the model is generally accepted as valid in process equipment provided that it claims no particular relationship between resistance and diffusivity. It is less generally accepted in environmental situations partly because of concern about the role of surface organic microlayers and accumulation of certain solutes at the surface at concentrations different from the bulk. For example the interface can be viewed as a temporary storage or sorption region from which solute molecules may leave according to some form of thermal activation process, as occurs on solid surfaces. Undoubtedly several conceptual models of inter-phase transfer processes can be postulated and used as a correlating or predictive tool by fitting appropriate constants to the model equations. The evidence available suggests, however, that diffusion

models most faithfully express the physical reality.

After Lewis and Whitman the next significant step was taken by Higbie (46) who postulated that elements of fluid moved to the surface, experienced unsteady state transfer for a short time t then moved back to the bulk. Application of Fick's Second Law yields an expression for K

$$K = \sqrt{4D/\pi t}$$

Dobbins pioneered the application of unsteady state mass transfer theory to environmental conditions of oxygen transfer to water bodies (48). Danckwerts (47) later introduced the concept of a surface renewal rate or frequency S yielding

$$K = \sqrt{DS}$$

When t is large of S small these models reduce to the Whitman Two Film model. Toor and Marchello (49), King (50), Harriot (51) and Ruckenstein (52) have proposed models which are similar in concept. These models predict that

$$K \alpha D^{0.5} \text{ when exposure time is short}$$

$$K \alpha D^{1.0} \text{ when exposure time is long}$$

Typically an intermedidate condition exists and a power of 0.67 is frequently used. This dependence is very important environmentally since it is useful to relate transfer rates of one compound to those of another, such as oxygen.

One of the most appealing models is based on the "roll cell" concept developed by Fortescue and Pearson (53) Ruckenstein (52) and Ruckenstein and Sucier (54). A version of this model is illustrated in Figure 11. It oan be regarded as a microscopic version of the Langmuir circulations which result from the interaction of wind and waves and cause clearly defined downwelling regions. An element of fluid at the water surface moves at a few percent of the wind speed (say 15 to 20 cm/s) when the wind speed is 5 m/s or 18 km/h. The element is exposed to unsteady state transfer (volatilization) losing solute to the atmosphere above. After some time t in which it may have moved some centimeters or meters it is propelled back to the bulk of the liquid to be replaced by another element. This propulsion may be associated with internal circulation in waves. Horizontal movement of the element is a factor of 10 to 100 faster than vertical movement thus the roll cell is elongated. It is possible that several scales of roll cells exist superimposed on each other. The relative ease of horizontal movement compared to vertical movement results in a higher horizontal than vertical eddy diffusivity as is observed experimentally in dye tracer studies (Csanady 40).

The nature and dimensions of environmental roll cells are not known and it seems likely that it is impossible to simulate then precisely in the laboratory. It would not be surprising if over a large fetch a stable relatively long roll cell pattern developed which would not be observed at short fetches as inevitably apply to laboratory systems. This would result in laboratory tests overestimating mass transfer rates since the exposure time is shorter in the laboratory and the average mass transfer coefficient

FIGURE 11

SCHEMATIC DIAGRAM OF AN ELEMENT OF WATER EXPERIENCING EXPOSURE TO THE ATMOSPHERE AND HENCE LOSS OF SOLUTE BY VOLATILIZATION IN A "ROLL CELL"

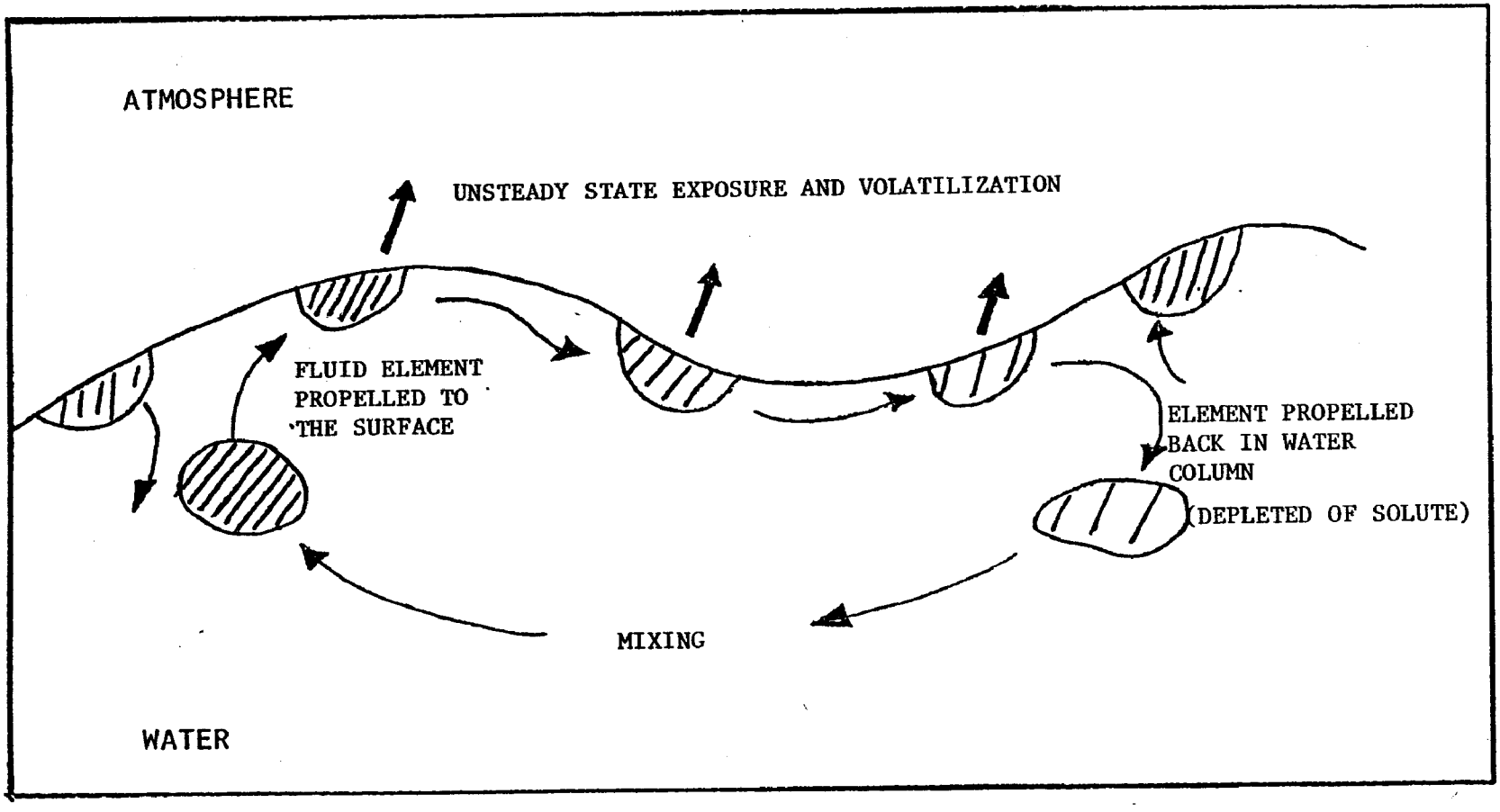

correspondingly higher as is indicated by the Higbie equation presented earlier.

(b) Verification of the Two Resistance Model

The 5 conditions under which the additivity of individual phase resistances is valid has been theoretically treated by King (55). They are:

1. H must be a constant.
2. There must be no significant resistance present other than those represented by K_L and K_G.
3. The hydrodynamic conditions for the case in which the resistances are to be combined must be identical to the measurements of the individual phase resistances.
4. The mass transfer resistances of the two phases must not interact.
5. The ratio $H\ K_G/K_L$ must be constant at all points of the interface.

Most of these conditions are intuitively obvious but the last two deserve some discussion. If unsteady state exchange from roll cells exists this implies that the flux from the water is greatest from the freshly exposed element, and least just before the "aged" element returns to the water bulk. The local K_L thus varies along the roll cell. If there is negligible gas phase resistance an average K_L will apply. If there is an air phase resistance equal in magnitude to that of the average water phase resistance then it will add equally to all points of the roll cell. This is illustrated in Figure 12 with hypothetical quantities for a compound of H/RT of unity. If the first half of the roll cell (A) has a K_L of 10, doubling it will give an average K_L of 7.1 (by penetration theory) thus K_{LB} must be 4.2. Assuming a uniform K_G of 7.1 and adding the resistances (i.e. reciprocals of K) to give an overall K yields 4.15 for A, 2.64 for B, the average of which is 3.39. This is less than the value calculated by merely adding the average K_L and K_G. The reason is that when K_L drops (at the end of the cell) the overall resistance does not drop in proportion. The net effect is a 5% error in flux, i.e. the actual flux is 5% less than is expected from adding the resistances. This effect is thus relatively small given the uncertainties in the values of K but it does indicate that conditions may exist when additivity is not precisely correct. One implication is that deducing K_G of K_L from K_{OG} or K_{OL} for a two phase resistant system may give different values from that of one phase resistant systems.

The closest experimental verification of the additivity of resistances has been by Goodgame and Sherwood (56) who studied transfer of CO_2,NH_3 and acetone to water in an agitated vessel . The experimental design with gas and liquid stirring was quite removed from an environmental air-water interface thus it is unwise to assume that the two resistance concept has been verified for environmental conditions. Accordingly a small scale apparatus was designed, built and operated in this project to provide additional verification. Although it can be argued that the evidence supporting the two resistance concept is overwhelming it was judged to be worthy of further verification in this project because its validity is the key assumption in volatilization calculations and any discrepancies should be exposed. In addition a small scale test apparatus can be used to test the dependence of K on diffusivity under various turbulence conditions as

well as the effects of temperature and extent and direction of evaporation.

A convenient method of verifying the two resistance concept is to measure the mass flux and hence K_{OL} for compounds of a wide range of H. Rearranging the transfer coefficient equation yields.

$$(1/K_{OL}) = (1/K_L) + (RT/H)(1/K_G)$$

If K_L and K_G are constant, a plot of $(1/K_{OL})$ versus (RT/H) should yield a line of slope $(1/K_G)$ and intercept (at RT/H = 0) of $(1/K_L)$ as illustrated in Figure 13.

(c) Effect of Waves

As has been indicated, considerable difficulties have been experienced quantifying interphase transfer rates even from solids to fluids in which the interface is well defined. In air-water systems the presence of a mobile wavy interface introduces an additional dimension of complexity. The characteristics of wind waves have been reviewed in the text by Kinsman (57) and only a brief account is possible here in which some of the more relevant references are cited.

When wind blows across a solid surface its velocity at the surface must be zero i.e. there is "no slip". This implies that a steep velocity gradient exists immediately above the surface. Since air has a small but finite viscosity there is thus transfer of momentum and thus a force or stress exerted by the wind on the surface, tending to drag it in the wind direction. If the surface is liquid it will be dragged by the wind thus creating a surface current which is generally observed to be 2 to 5% of the wind speed. Above a wind speed of about 3 m/s waves develop of a few centimeters in length. These waves provide a roughness which further increases the drag resulting in growth of waves to a steady amplitude and wavelength. This process of wave build up may occur over hundreds of kilometers resulting in large gravity waves. A typical large lake or ocean surface is covered with multiple wave spectra which are remnants of wind action in remote locations. At higher wind speeds whitecapping may occur as the wave crests are blown over and at very high wind speeds waves may break and generate spray. No mathematical description of these processes is entirely satisfactory.

An important point is that it is believed that is is the small "capillary" waves which are most important from a mass transfer viewpoint. Large waves of period 5 to 10 s are probably not important in this respect because the air "rides" with them. There is no doubt that the wind influences the water which in turn influences the air phase etc., a complex equilibium being reached and a level of turbulent mixing achieved dependent on wind speed and fetch. There is also an area increase but this is quite small since the ratio of wave height to length is usually about 0.143 (Kinsman 57) thus the factor increase in area is approximately $\sqrt{(1^2 + 0.143^2)}$ or 1.01 i.e. 1%. In breaking wave conditions this may be considerably higher.

The commonest method of defining the velocity of the air is the logarithmic velocity profile

$$U = (U^*/K)\ln(Z/Z_o)$$

FIGURE 12

DIAGRAM ILLUSTRATING THE NON-ADDITIVITY OF RESISTANCES

DURING UNSTEADY STATE TRANSFER IN A ROLL CELL

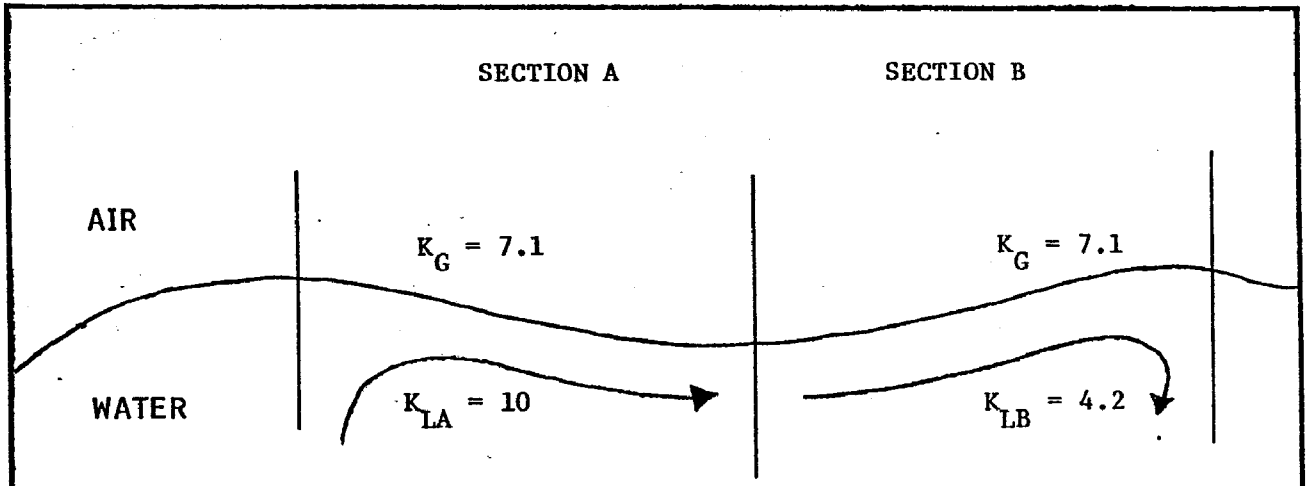

$$K_{L,\,MEAN} = 7.1$$

$$\frac{1}{K_{OLA}} = \frac{1}{K_{LA}} + \frac{1}{K_G} = \frac{1}{10} + \frac{1}{7.1} = \frac{1}{4.15}$$

$$K_{OLA} = 4.15$$

$$\frac{1}{K_{OLB}} = \frac{1}{K_{LB}} + \frac{1}{K_G} = \frac{1}{4.2} + \frac{1}{7.1} = \frac{1}{2.64}$$

$$K_{OLB} = 2.64$$

$$\text{AVERAGE } K_{OL} = \underline{\underline{3.39}}$$

$$\text{BUT } \frac{1}{K_{OL}} = \frac{1}{K_L} + \frac{1}{K_G} = \frac{1}{7.1} + \frac{1}{7.1} = \frac{1}{3.55}$$

$$\text{AVERAGE } K_{OL} = \underline{\underline{3.55}}$$

FIGURE 13

DIAGRAM ILLUSTRATING A POSSIBLE EXPERIMENTAL TEST OF THE TWO RESISTANCE THEORY FOR COMPOUNDS OF VARIOUS H VALUES

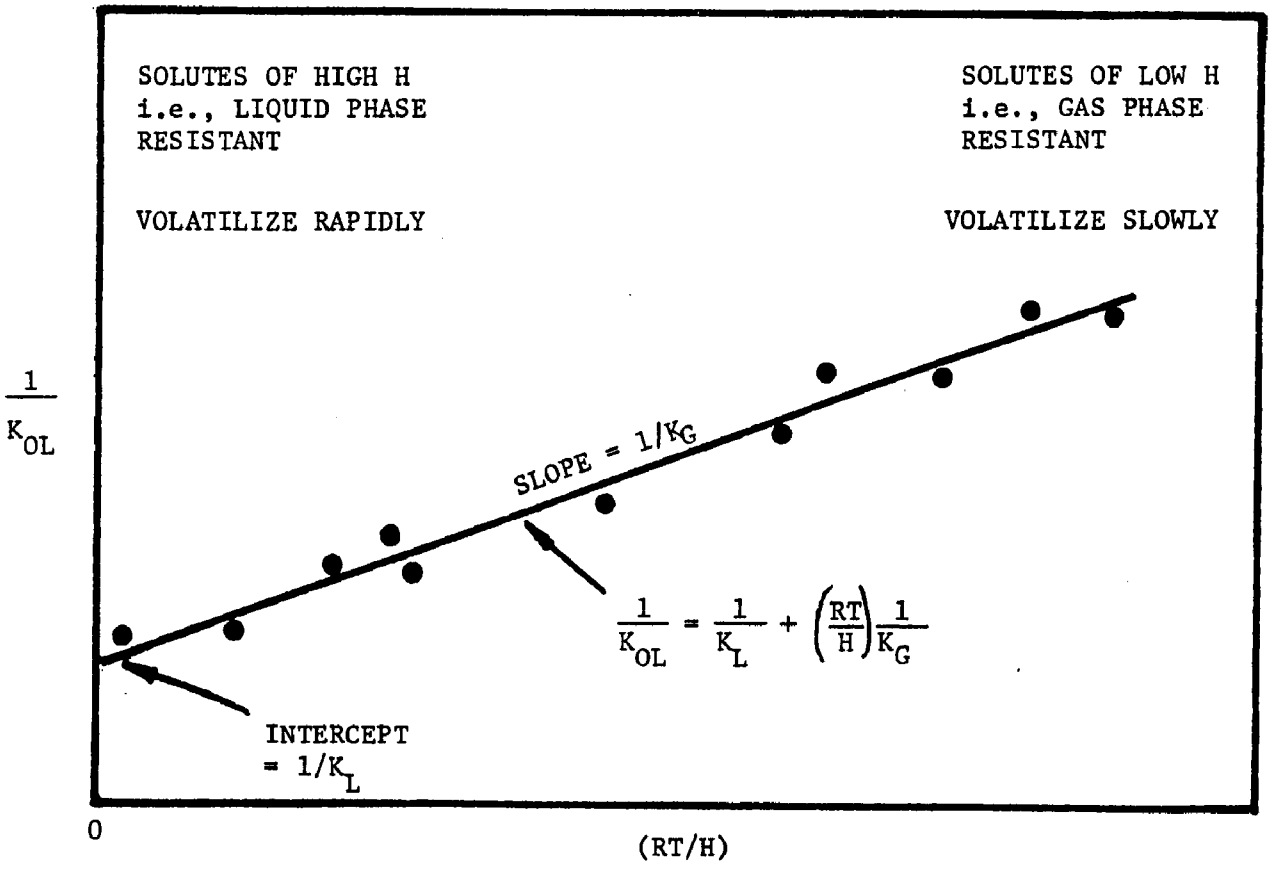

where U is velocity (m/s), K is the von Karman constant (taken as 0.4), Z is the height, Z_o the "surface roughness" and U^* is the "friction velocity" which is equivalent to

$$U^* = (\tau/\rho_A)^{0.5}$$

where τ is the stress of the air on the surface (N/m^2) and ρ_A is the air density (kg/m^3). A plot of velocity versus ln(Z) generally gives a straight line of slope (U^*/K) and intercept ln Z_o when U is extrapolated to zero. For example Z_o may be 0.001 m, U^* may be 1.0 m/s thus at various heights Z the following velocities will apply.

Z	U
0.001m (1 mm)	0
0.003m (3 mm)	2.75
0.01m (1 cm)	6.32
0.03m (3 cm)	8.50
0.10 (10 cm)	11.5
1.0	17.3
10.0	23.0

Clearly most of the velocity gradient lies in the few centimeters above the water surface. A height of 10 m is the standard for wind speed measurement but there is little gradient above 2 m.

The friction velocity U* is best conceived of as being related to the force which the air exerts on the water rather than as a velocity. The surface roughness Z_o can be conceived of as being related to the height of the small capillary waves on the water surface which are caused by the wind and tend to assist the wind to drag the water surface. Both quantities are thus indicative of the degree of turbulence or mixing induced at the water surface by the air and it seems reasonable that their product should correlate well with mass transfer coefficients. Cohen et al (58) combined these quantities with the air density ρ_A and viscosity (μ_A) to give the dimensionless roughness Reynolds Number Re*

$$Re = Z_o\ U^*\ \rho_A/\mu_A$$

and correlated it with K_L. Schlichting (59) has shown that for Re* exceeding 2.3 the surface can be regarded as aerodynamically rough whereas below 0.17 it is smooth, with a transition region between. Environmental conditions are in the transition and rough region except at very low wind speeds where the water surface becomes glassy.

It is not feasible to measure U* or Z_o routinely in the environment thus a method must be sought of relating these quantities to a conveniently measurable quantity such as the 10 meter wind speed U_{10}. Two approaches are possible, both of which use the dimensionless drag coefficient (or wind stress coefficient) C_D which is defined from

$$\tau = C_D \rho_A U_{10}^2$$

But since $\tau = \rho_A U^{*2}$

$$C_D = (U^*/U_{10})^2$$

A considerable literature exists on values of C_D at various wind velocities. Typically it has a value of 10^{-3} under oceanic conditions thus a typical friction velocity will be 3% (i.e. $\sqrt{10^{-3}}$) of the 10 meter wind speed. This is usually close to the actual water surface drift velocity. The available data indicate that C_D tends to increase slightly with wind speed and several correlations have been attempted, for example Wu (60) has suggested that

$$C_D = 5.0 \times 10^{-4} (U_{10})^{0.5}$$

with the value of C_D levelling off above 15 m/s at a value of 26×10^{-4}. Smith (61) has recently suggested that

$$C_D = 10^{-4}(6.1 + 0.63U_{10})$$

for winds from 6 to 22 m/s, which has the merit that C_D does not become zero at zero wind speed.

Unfortunately, C_D is also dependent on fetch, i.e., the distance from the point at which the air flow meets the water surface. This distance can be a few meters in a laboratory tank or hundreds of kilometers at sea. The reason for this dependence is that when an air flow meets a water surface the air starts to drag the water and to generate waves. This process continues with wave height building up until a steady or equilibrium condition is reached. During the acceleration phase more energy is transmitted from air to water. This results in a higher value of U^* and hence a higher value of C_D. Wu (62) has suggested that C_D can be correlated as a function of the dimensionless Froude Number F which is a function of the wind speed U_Z at height Z above the water surface, and the gravitational constant g (m/s^2)

$$F = U_z/(gZ)^{0.5}$$

Laboratory systems tend to have smaller values of Z than do oceanic conditions thus the Froude numbers are higher, resulting in higher values of C_D. The effect of low fetch at constant wind speed is thus to alter the velocity profile generally increasing the velocities near the surface and thus probably increasing K_L.

Charnock (63) argued on dimensional grounds that Z_o should be proportional to U^{*2} or equivalently that the group

$$Z_o\ g/U^{*2} \text{ or "a"}$$

will be constant. This can be tested by plotting Z_o versus U^{*2}/g to obtain a

slope of a. Wu (62) has suggested a value of 0.0156 for a and other workers have obtained similar values, for example Smith (61) obtained 0.010.

The implication of this assumption is to establish a relationship between C_D and F since,

$$C_D = (U^*/U_{10})^2 = [K/\ln(Z/Z_o)]^2$$

$$= [K/\ln(Zg/aU^{*2})]^2$$

$$= [K/\ln(Zg/C_D\ a\ U_{10}^2)^2] = [K/\ln(1/aF^2C_D)]^2$$

where $F = U_{10}/(Zg)^{0.5}$

This relationship is implicit in C_D but can be plotted to facilitate solution. Wu's correlation between C_D and F is essentially this equation. Its usefulness is that under laboratory conditions measurements can be made of U_Z and Z at various values of Z and C_D, & U* and Z_o deduced from the logarithmic velocity profile. The Charnock relationship can then be tested, which is equivalent to testing the C_D - F relationship. If these relationships hold it can be argued that the laboratory conditions can be related to environmental conditions since the same underlying principles apply. Further, it becomes necessary only to measure U_Z at Z of say 10 cm, calculate F, then C_D and hence U*, Z_o and Re*. If K_L and K_G data are available for both laboratory and environment they can be tested to determine if they are the same function of Re*.

This lengthy procedure can be shortened by substituting the Charnock relationship directly into Re* i.e.

$$Re^* = \rho_A U^* Z_o/\mu_A = \rho_A U^{*3} a/g\mu_A$$

But $U^* = U_{10} C_D^{0.5}$

Thus $Re^* = \rho_A\ U_{10}^3\ a\ C_D^{1.5}/g\mu_A$

where C_D can be estimated from one of the correlations and a can be taken as 0.0156.

An alternative approach suggested by Cohen et al (58) is to use the logarithmic velocity profile to calculate Z_o from U* and C_D namely

$$Z_o = Z \exp(-K\ U_Z/U^*) = Z \exp(-KC_D^{0.5})$$

The difference between these equations is relatively small given the uncertainties in the variables. For example when U_{10} is 15 m/s, C_D from the Wu correlations is 1.9×10^{-3} with the Smith correlation yielding 1.6×10^{-3}. Taking 1.8×10^{-3} as C_D gives U* of 0.64 m/s. The Charnock equation gives Z_o to be 6.5×10^{-4} m whereas the logarithmic profile value is 8.5×10^{-4} m.

The effect is to change Re* by some 30%. Since K_L is a fairly weak function of Re* (for example Cohen et al (58) found it to be to the power of 0.195) the effect is tolerable. The important requirement is that Re* be calculated and correlated consistently. These equations are very simplified expressions of exceedingly complex phenomena and can only be used as correlating guides for treating experimental data.

The Charnock relationship is an attractive approach since it has been supported by environmental observations and its use is thus preferred here.

In summary, the approach adopted here is to measure velocity profiles K_L and K_G, test the Charnock relationship, calculate U*, Z_o and C_D and hence Re*, correlate Re* with K_L and K_G and examine if this correlation agrees with other data.

Since a dimensionless number approach is used it is preferable to render K_L and K_G dimensionless either as a Stanton Number (St) (by dividing by a velocity) or as a Sherwood Number by dividing by a diffusivity and multiplying by a length. It is tidier to use diffusivity only once in the Schmidt Number (Sc) thus the Stanton Number is preferred. Two velocities can be selected, the friction velocity U* or the free stream velocity U_Z. Both can be tested and the better approach used.

The ultimate correlating equation is thus

$$St = A\ Re^{*B}\ Sc^{C}$$

where

$$St_L = K_L/U^* \text{ or } K_L/U_Z$$

$$St_G = K_G/U^* \text{ or } K_G/U_Z$$

$$Re = \rho_A U^* Z_o/\mu$$

$$= \rho_A\ U_{10}^3\ a\ C_D^{1.5}/g\mu$$

and

$$Sc_L = \mu w/\rho_w D_w$$

$$Sc_A = \mu_A/\rho_A D_A$$

This approach is regarded as being hydrodynamically justifiable but it suffers from a practical disadvantage in that few environmental scientists (who are equally concerned with other processes such as reactions, sorption and accumulation by biota) have the necessary background in fluid mechanics to appreciate these subtleties. It is thus convenient to transpose these equations into simpler versions containing only 10 meter wind speed, possibly at the expense of loss of some rigor and accuracy. Thus simpler versions also have a useful role in that they will tend to be more readily used.

A final problem is the effect of fetch on K_G as a result of the air stream gradually building up a concentration of the volatilizing substance. Previous work by Mackay and Matsugu (64) showed that fetch influences K_G albeit weakly and they suggested, based on earlier work, a dependence of the type

$$K_G \propto X^{-0.11}$$

where X is the fetch (m). To verify this power requires data from systems of widely varying fetch, in fact to generate a two fold reduction in K_G requires a 545 fold increase in X which is difficult experimentally. The only feasible approach is to compare laboratory water evaporation data with oceanic data at similar wind speeds. This system is entirely gas phase controlled since there is no need for water to diffuse to the liquid surface.

The series of wind wave tank experiments described later thus had the objective of providing volatilization data which could be used to generate expressions for K_L and K_G from which K_{OL} can be calculated. Clearly it is desirable to test this hypothesis by measuring volatilization rates over a range of Henry's Law Constants and compare the experimental values and those calculated from the correlating equations.

(d) Surface Films

It is well established that most environmental water bodies are covered with a thin layer of organic-rich material consisting of proteinaceous and lipid material. In extreme cases this layer may be augmented by surfactants or oil of anthropogenic origin. Such layers can have a profound effect on the fluid mechanics of the interface, they may accumulate organic and metallic contaminants and depress volatilization rates.

The role of surface films in altering volatilization rates is complex and difficult to study and quantify. No attempt is made here to review the subject comprehensively or to undertake experimental investigations. The aim is merely to assemble a multiple resistance model based on the fugacity capacity concepts developed earlier and speculate on its possible future application to studies of surface films. The subject merits more detailed consideration than can be given here.

Liss (66) has comprehensively reviewed recent literature of the effects of surface films on gas exchange across the air-sea interface. Liss and Martinelli (67) have described laboratory experiments involving oil films. The general conclusions are that natural (glycoprotein and polysaccharide) material petroleum and surfactants to retard air-water exchange. The extent of retardation is very dependent on the coherence or coverage of the film and its thickness. Most natural films are unable to achieve the coherence necessary to retard transfer significantly. Even a 1 mm oil film only reduces oxygen transfer to 40% of its oil free value but a 30 μm has the same effect on water transfer. The conclusion is that when the transfer resistance is vapor phase controlled (as in the case of water) the effect of surface films is larger. In essence, the film creates an additional or enhanced liquid phase resistance which adds (slightly) to the already present liquid phase resistance for oxygen and substantially to the previously vapor-only resistance for water vapor. Whether or not this effect will apply to all vapor phase resistant systems is not clear.

Nguyen Ly et al (68) have developed a model in which the film is considered as a separate layer with a finite thickness, diffusivity and solubility (i.e. fugacity capacity). Typically, for detergent films the calculated thickness was 10^{-5} cm and the diffusivity 10^{-8} cm^2/s. The resultant mass transfer coefficient K_L is 10^{-3} cm/s or 3.6 cm/h which is of the same order of magnitude as K_L.

Writing the transfer equation in the form of series resistances using fugacity capacity (2) shows that the film will have the most profound effect when Z is small, i.e., the solute is relatively insoluble in the film and thus unable to establish a substantial concentration gradient specifically the total resistance r_T is

$$r_T = r_L + r_F + r_V$$
$$= 1/K_L Z_L + \delta/D_F Z_F + 1/K_V Z_V$$

where subscripts L, F and V refer to liquid, film and vapor phases and δ is the film thickness.

The ratio of transfer rates with and without the film present is thus the inverse of the corresponding resistances or

$$r_V/(r_V + r_F) = 1/(1 + \delta K_V Z_V/Z_F D_F)$$

For water transfer r_L is negligible thus this ratio becomes

$$r_L/(r_L + r_F) = 1/(1 + \delta K_L Z_L/Z_F D_F)$$

and a value of 15 cm^{-1} is indicated for $(K_L Z_L/Z_F D_F)$ since the ratio becomes 0.4 when δ is 0.1 cm.

A set of reasonable values which would reproduce the experimental data are

D_F	10^{-5} cm^2/s	or	10^{-9} m^2/s
K_L	3×10^{-4} cm/s	or	3×10^{-6} m/s
K_V	1 cm/s	or	10^{-2} m/s

For water $Z_F = 10^4$ mol/m^3atm, $Z_V = 41$ mol/m^3atm

For oxygen $Z_F/Z_L = 2$ corresponding to an oil-water partition coefficient of 2, oxygen being more soluble in oil than water. Z_L is approximately 1.5 corresponding to H for oxygen in water of 0.65 atm m^3/mol thus Z_F is approximately 3.0.

If these estimates are close to the correct values it becomes clearer why oil retards water transfer more than oxygen transfer. For water r_V is approximately 2.4 m^2s/mol. For oxygen r_L is approximately 2.5×10^5, a factor of 10^5 greater thus a much thicker oil film is necessary to establish a comparable resistance. This is compensated for, however, by the much greater solubility of water in the oil compared to oxygen resulting in a low H and a higher Z_F by a factor of some 300. The net result is that an oil film a factor of only 30 greater is necessary to create a resistance equal to that experienced by the oxygen in the water in the absence of oil.

It follows that surface films will have their greatest effect when the liquid resistance is low i.e., when Z_L is large or the solute Henrys Law Constant is low and the solute can establish high concentrations in water. The retarding effect will be enhanced if Z_F is low, i.e., the solute is less soluble in the surface film. Since most compounds of interest here are organic they will probably partition preferentially into a surface film resulting in high Z_F values, necessitating very thick films to achieve significant retardation. From a knowledge of the partition properties of the solute and an indication of the composition of the surface film it should be possible to estimate Z_F. D_F apparently varies from its molecular diffusivity value of 10^{-5} cm^2/s to 10^{-8} cm^2/s for close packed surfactant films. The thickness δ is amenable to measurement. In principle, it may be possible to develop a method of calculating the film resistance but this is presently not feasible.

In summary, there may be two quite different mechanisms of surface film retardation, introduction of a diffusive resistance as discussed above and damping of capillary waves resulting in hydrodynamical changes. Only some preliminary experiments could be undertaken here in which an attempt was made to determine if a surface film significantly reduced benzene volatilization rates.

SECTION 6

GENERAL MODEL OF LABORATORY VOLATILIZATION SYSTEMS

There has been some confusion in the literature about the relationship between laboratory volatilization systems with different geometries and air-water contacting arrangements. Some systems involve beakers which may or may not be stirred, over which air may or may not be blown by a fan. Others involve wind tunnels or sparged systems in which a bubble swarm is directed through a pool of water. It is the purpose of this section to develop a general volatilization rate equation and demonstrate that it reduces to simplified forms describing specific types of contacting. The danger is that an equation for one type of system may be wrongly applied to another.

If we consider a water volume of V m^3 and area A m^2 contacted with a flow of air of G m^3/s and containing a solute of concentration C mol/m^3 and a Henry's Constant H atm m^3/mol, the partial pressure of the solute in the gas is an average of P atm. In cases of interest here the direction of transfer is water to air thus C exceeds P/H, i.e. the fugacity of the solute is greater in the water than in the air. Using the mass transfer relationship derived earlier with overall mass transfer coefficients, K_{OL} and K_{OG} m/s the mass flux N mol/m^2s can be related to the concentration driving force, to the increase in solute partial pressure in the gas $(P - P_1)$ where P_1 is the inlet and P the outlet partial pressure and to the change in solute concentration with time.

$$NA = G(P - P_1)/RT = -V\, dC/dt = AK_{OG}(CH - P)/RT$$
$$= AK_{OL}(C - P/H)$$

This contains the inherent assumption that all the area experiences the same concentration driving force which is to a first approximation valid in most cases. In the interests of simplicity, the derivation is continued with the assumption that P_1 is zero, i.e. the incoming air contains no solute.

These equations can be rearranged to eliminate P, i.e.

$$P = -(RTV/G)\, dC/dt = (RTV/AK_{OG})(dC/dt) + CH$$

Rearranging yields,

$$dC/dt = GHC/\left((RTV)(1 + G/K_{OG}A)\right)$$

Integrating from $C = C_o$ at time zero yields,

$$C = C_o \exp\left(- GHt/\left((RTV)(1 + G/K_{OG}A)\right)\right)$$

or in terms of the individual coefficient K_L and K_G

$$C = C_o \exp\left(- GHt/\left((RTV)(1 + G/K_GA + GH/K_LART)\right)\right)$$

The relative magnitudes of the three summed terms in the denominator control which of four regimes may apply. The principal determinants are the prevailing values of H (which is controlled by the value of the solute), G the gas flow rate and A the interfacial area. Although K_L and K_G vary they do not vary over as wide a range. The following simplified or limiting versions apply.

(a) Near-equilibrium conditions

If $G/K_{OG}A << 1$ the general equation simplifies to

$$C = C_o \exp(-GHt/RTV)$$

Under this condition mass transfer is essentially complete and P equals HC. This condition occurs when the transfer area and coefficients are large thus promoting fast and complete transfer but the gas rate G is restricted such that the gas becomes saturated prior to leaving the system.

When H is large, i.e. there is marked preferential partitioning into the vapor, it may be difficult to achieve equilibrium except with a very small gas rate G. This corresponds to a condition in which head space analysis or gas purging are very effective. Intermittent rather than continuous operation may be preferable. Such solutions obviously volatilize very quickly and volatilization is a significant environmental pathway.

The system of this type has been described by Mackay et al ([28]) in which air is sparged into a column of water at a slow rate such that the exit gas is saturated. It is a useful method of measuring H directly,particularly for solutes such aromatic hydrocarbons for which solubility and vapor pressure data may not exist or may be suspect because of the low values. A plot of the logarithm of concentration versus time will have a slope of $-GH/RTV$ from which H can be calculated from the known values of the other terms.

It is essential to confirm experimentally that the inequality assumption is valid. This can be done by reducing A thus increasing $G/K_{OG}A$. This may involve a change in V if for example, the height of the liquid is reduced, thus the test should be if the apparent H as obtained from the slope is dependent on height.

(b) Liquid Phase Diffusion Control

If $GH/K_LART >> (1 + G/K_GA)$ the general equation simplifies to

$$C = C_o \exp(-K_LA\ t/V)$$

Under these conditions the volatilization rate is controlled by the diffusion rate through the liquid layer immediately below the interface. Interestingly, the rate becomes apparently independent of H which gives rise to the possibility of the erroneous conclusion that even very involatile (low H) solutes (such as NaCl) will be volatilized according to this equation. In practice when H is small the inequality stated above cannot be achieved

thus this condition will never apply.

This condition will tend to occur when H is fairly large, i.e. $H >> K_L RT/K_G$ or about 0.0002 atm m^3/gmol, which implies a fairly volatile, insoluble solute. It is also favoured by large values of G, resulting in the volatilized solute becoming very rapidly diluted in the exit gas stream. This is most easily accomplished in a wind tunnel and applies for example to the conditions described by Cohen et al ([58]). This is an ideal method of measuring K_L under various turbulence (wind speed) conditions, where A is well-defined. The rate of concentration drop is controlled by area, K_L and the volume of water.

Convenient solute systems for measuring K_L are by oxygen transfer (in either direction) or by volatilization of a solute such as benzene or toluene.

(c) Gas Phase Diffusion Control

If $G/K_G A >> (1 + GH/K_L ART)$ which is essentially equivalent to $H/RT << K_L/K_G$, the general equation reduces to

$$C = C_o \exp(-K_G AHt/RTV)$$

Under these conditions the volatilization rate is controlled by the diffusion rate through the gas layer immediately above the interface. It tends to occur for systems of very low H implying high solubility and/or low vapor pressure. Since the ratio K_L/K_G is typically 0.01 and RT is 0.024 for this situation to apply, $H << 0.0024$. This results in a very low value for the entire term in the exponent and thus very slow volatilization. Indeed, the water may volatilize faster than the solute unless the inlet gas is saturated with water. The "half life" for volatilization is likely to be many hours or even days in a small laboratory apparatus. This condition or conditions close to it may occur during volatilization of ionizing gases such as SO_2, lower molecular weight soluble organics such as alcohols and possibly some pesticides such as dieldrin.

In view of the experimental difficulties associated with operating under these conditions it may be preferable to measure the reverse process, i.e. absorption from the vapor, by introducing the solute vapor into a recycling gas stream and monitoring the increase in concentration in the water. This could be done easily for SO_2 or acetone. The form of the equation describing the absorption process can be obtained by solution of the mass flux equation with appropriate boundary conditions.

A convenient method of measuring K_G or $K_G A$ for a given apparatus is to measure the water evaporation rate which is totally vapor phase controlled, there being no necessity for the water to diffuse to the interface.

(d) Non-Volatile Systems

When H becomes smaller than H for water, i.e. less than approximately 6×10^{-7} the group in the exponent becomes very small and evaporation under environmental conditions will tend to increase rather than decrease the solute concentration.

The Henry's Law Constant for water thus forms a convenient criterion for determining if volatilization is significant environmentally.

An instructive method of illustrating these simplied versions is on a plot of G/A against H or H/RT as illustrated in Figure 14. The four regions correspond to the inequality assumption. It is essential when designing and interpreting volatilization experiments to have a clear concept of where the conditons will be on this "map". Apparently anomalous results can be obtained by misapplication of these equations.

For example, it is convenient to use oxygen transfer rate (reaeration) data as a means of estimating K_L for other solutes in rivers since a considerable literature on reaeration rates exists. Tsivoglov (69,70) demonstrated that the inert gases could be used as "tracers" or "surrogates" for oxygen transfer estimation. Rathbun (71) later used volatile hydrocarbons in a similar manner. The advantage of using these solutes instead of oxygen is that their presence at the experimental concentrations is "unnatural" whereas oxygen is ubiquitous and is generated and consumed by biological processes thus masking the concentration changes attributable to air-water exchange. Smith et al (72) have also measured ratios of transfer coefficients of other solutes to that of oxygen. Normally the ratio of the solute and oxygen transfer coefficients is 0.2 to 0.5 reflecting the slower diffusion of the larger solute molecule. For some solutes very low ratios were obtained, i.e. less than 0.1 or 0.01 which cannot be attributable to diffusion differences.

Examination of these cases in the light of these equations,shows clearly that when H becomes low the term (GH/K_LART) becomes small thus the implicit assumption that $(GH/K_LART) >> 1 + G/K_GA$ becomes invalid and the rate of volatilization falls because a gas phase resistance becomes significant. It is clearly incorrect to estimate the volatilization rate of such solutes from reaeration rate data because the controlling processes differ.

A popular and simple method of estimating volatilization tendency is to follow the concentration decay of a solute experienced in a water solution of a solute from a beaker. Depending on the presence or nature of induced agitation or mixing and air flow over the surface, the values of G, K_G and K_L can vary considerably and it is not immediately clear which regime applies. Increasing the air flow rate can cause a change from equilibrium control to diffusion control corresponding to a vertical movement in Figure 14.

Finally, there is interest in calculating volatilization rates in "artificial" environments such as lagoons, aerated lagoons,spray towers and biological oxidation units. The general equations derived here can be applied to such systems but care is necessary to ensure that the correct equations are applied. Perhaps the safest approach is to apply the general equation initially, using one of the simplified forms as experience demonstrates its validity.

FIGURE 14

PLOT OF G/A VERSUS H ILLUSTRATING APPROXIMATELY THE REGIMES WHICH MAY APPLY DURING LABORATORY VOLATILIZATION EXPERIMENTS

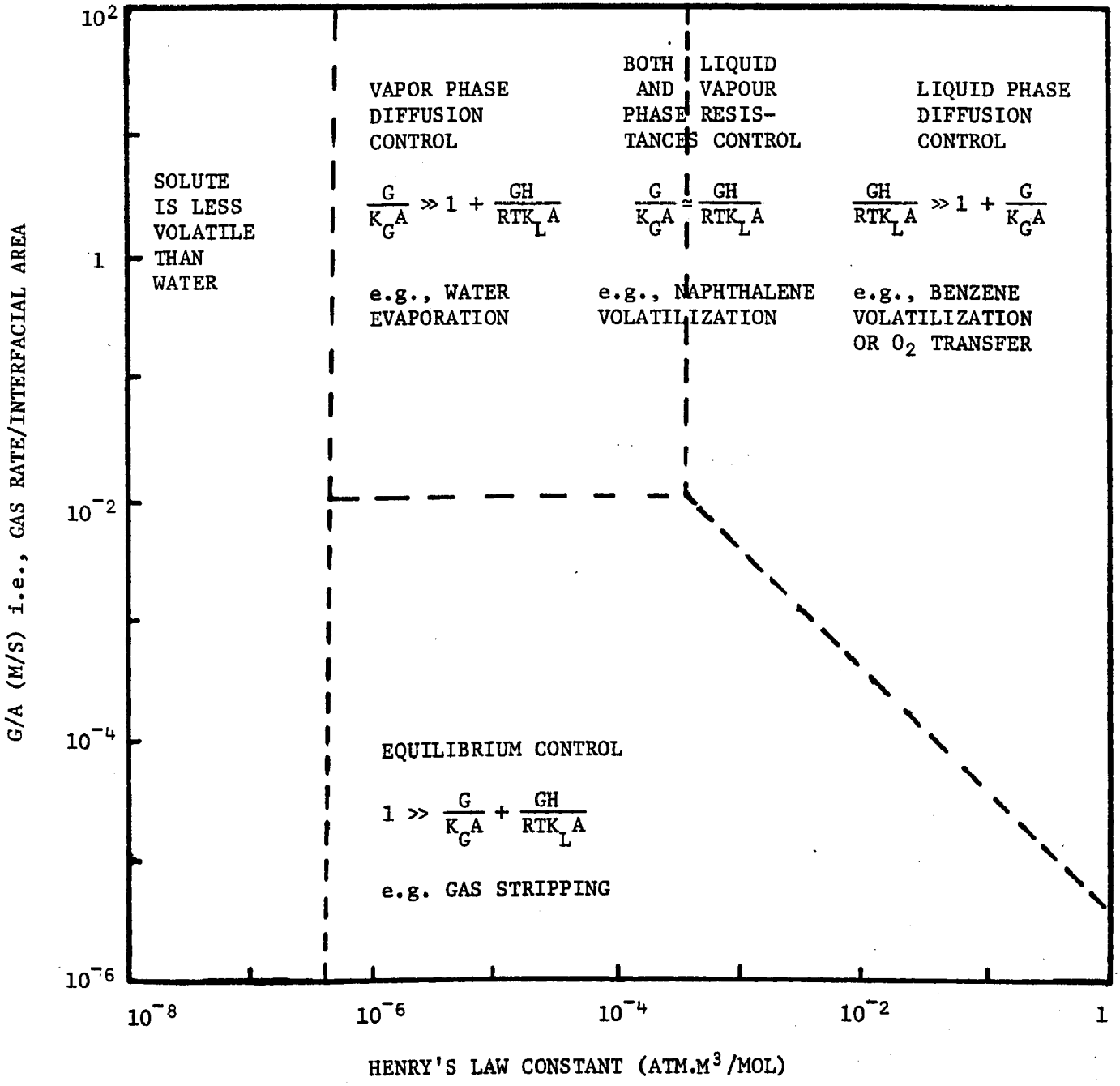

SECTION 7

EXPERIMENTAL

INTRODUCTION AND ORGANIZATION

This section consists of a description of several experimental systems used in the study. For each, the apparatus is described with appropriate diagrams followed by the experimental procedures used. Analytical procedures were common to several of the studies and are thus grouped at the end. The results including assessment of errors and unusual difficulties are also discussed. It should be noted that much of the experimental effort was devoted to improving and adapting the systems often by trial and error in order to obtain precise experimental data. Details of these less productive but essential efforts are generally omitted in the interests of brevity.

The approach adopted is to describe the small (30 cm diameter) volatilization system, the wind wave tank, the relative volatility system, the measurement of Henry's Law Constants, the measurement of solubility and finally the analytical techniques.

There were several objectives of this experimental program.

In the case of the small volatilization system the aim was to study the volatilization rates of compounds with a wide range of Henry's constant to determine whether the two resistance approach is valid. Although the evidence is substantial that this is so, the assumption is so important that further validation is believed to be justified. The effect of solute molecule "size" was also investigated to develop a procedure for taking this factor into account. Other variables examined include temperature and whether solute mixtures behave independently or interact. A final objective was to devise a simple test for screening the volatilization characteristics of new solutes.

Work in the wind wave tank emphasized higher velocities for which there are few data published. Again the two resistance model was tested. The primary aim was to develop equations which can predict both laboratory and environmental mass transfer coefficients in a rigorous manner. This requires novel interpretive analyses of these and other data since no entirely satisfactory theoretical framework exists with which to approach this problem.

The aim in the relative volatility and Henry's Law Constant work was to devise methods for measuring H reliably over the range of interest above 5×10^{-7} atm m^3/mol, and obtain new data.

The solubility measurements and some Henry's Constant measurements sought to elucidate the extent to which the presence of natural organic matter influences these properties at typical environmental levels.

SMALL SCALE VOLATILIZATION APPARATUS

Volatilization tests were carried out in a small scale system in which the process of environmental air-water transfer was simulated. It is shown schematically in Figure 15 and is similar in principle to an apparatus developed by Mackay et al (73) for dispersant effectiveness.

The core of the apparatus testing was a 30 cm ID, 30 cm deep glass tank containing 6.0 L of water (approximately 10 cm deep) containing, in solution, the compound under study. The tank was covered by a 1.25 cm thick, 40 x 40 cm plexiglass lid with a rubber gasket to prevent air leakage. It was immersed in a constant temperature bath.

Three thermometers were inserted at the centre of the tank through the lid. One was placed in the water, giving the bulk water temperature. The other two were used to measure the air humidity, one giving the air dry-bulb temperature and the other, which was wrapped with a piece of cotton cloth continuously soaked by dipping it in a small beaker of water, giving the wet-bulb temperature. A sampling port was located 2 cm from the tank wall to enable water samples to be taken by a syringe.

Wind-induced waves were generated at the air-water interface by blowing air from a blower into the tank. The air flowrate and thus the turbulence level was controlled by a 3.2 cm diameter gate valve and measured by passing the air through an orifice meter 2.54 cm in diameter connected to a water manometer.

Air entered the tank through a 5 cm diameter PVC 90° elbow inserted through the lid and at a height of 10 cm above the water surface, and flowed tangentially along the wall of the tank in a swirling motion. It left the tank through a 5 cm diameter pipe located vertically beside the elbow and extending 6 cm below the lid. The exit air was directed to a fume hood by a 3.2 cm flexible plastic hose. The relative locations of the pipes, thermometers and sampling port are shown in a plan view of the tank in Figure 16.

The evaporation of water at the air-water interface in the tank may influence the mass transfer behaviour of the compounds under study, thus provision was made for humidity control. In most tests the air was saturated with water vapor by passing it through a humidification column prior to entering the tank. This 20.3 cm ID plexiglass column was packed with 3.8 cm ceramic Raschig rings to a height of 1.2 m. The blower was located at the bottom of the column. Air having a maximum flowrate of 17,000 cm^3/s passed up the column. Simultaneously, water was injected at the lap in a spray located 24 cm above the packing at a flowrate of 100 cm^3/s. The water collected at the bottom of the column drained into a 40 cm x 20 cm x 25 cm reservoir from which it was returned to the top of the column by a pump.

To prevent any increase in air temperature due to heat generation in the blower, it was wrapped with copper cooling coils through which cold water was passed. A second coil was immersed in the water reservoir. The air (and water) temperatures of the column were adjusted by varying the cooling coil water flowrate.

The saturated air leaving the top of the column was passed through the gate valve and the orifice meter to the tank, where the flowrate was controlled and measured.

In some experiments, the mass transfer process was studied using unsaturated air, in which case, instead of passing the air through the humidification column, it was directly blown into the tank.

The volatilization rates of twenty organic compounds across the air-water interface were determined. The compounds listed in Table 6 and Table 7 covered a wide range of Henry's Law Constants (10^{-2} to 10^{-6} atm.m^3/mol).

The overall liquid phase mass transfer coefficients (K_{OL}) for each compound were determined individually with air saturated with water vapor at four different turbulence levels and at ambient temperature (22 ± 2° C). The experimental procedure for a typical run is outlined below.

The saturated solution of the compound under study was prepared by stirring an excess quantity of the compound in distilled water for a minimum of four hours. Six liters of distilled water having a low concentration (less than 100 ppm) of the compound was prepared in the glass tank by diluting the saturated solution. The degree of dilution (10, 100, or 1000 times) depended on its response factor in the gas chromatograph.

The plexiglass lid with the rubber gasket was immediately fitted in place to minimize the loss of the compound. A stirring rod was then used to stir the diluted solution to ensure homogeneity of the aqueous solution. Water was then passed through the cooling coils around the blower and in the reservoir to maintain the air flow at ambient temperature. The pump and blower were then switched on and the tank and the plexiglass lid were checked to ensure a complete seal at the rim. The air flowrates were adjusted by the gate valve to the required value.

Five minutes were allowed for the air flow and water waves in the tank to stabilize, after which water samples were taken at selected times. Sampling intervals depended on the rate of volatilization of the specific compound and varied from ten minutes to two hours. Duplicate water samples of 5.5 ml were obtained by syringes through the sampling port and stored in 5.5 ml sampling bottles. The samples were analyzed immediately by gas chromatography or if analyzed later were stored in a refrigerator with tightly sealed caps to avoid vapor loss.

A typical experiment lasted for two to ten hours depending on the rate of volatilization. To reduce experimental error, a concentration drop of at least 80% (i.e. a factor of 5) was desirable. Thus, a preliminary run was performed for each compound to determine the sampling time and the length of the experiments.

When the mass transfer rates of two or more compounds were studied simultaneously, the same procedure described above was followed. Compounds were used in mixtures only when gas chromatographic analysis was capable of detecting and quantifying them separately.

TABLE 6

SOLUTES USED IN THE VOLATILIZATION EXPERIMENTS

	Small Scale Apparatus	Wind Wave Tank	H at 25°C atm m^3/mol
Carbon Tetrachloride	√	√	1.6×10^{-2}
Toluene	√	√	6.7×10^{-3}
Benzene	√	√	5.5×10^{-3}
Chorobenzene	√	√	3.7×10^{-3}
1,2-dichloropropane	√	√	2.1×10^{-3}
0-dichlorobenzene	√		1.9×10^{-3}
Bromobenzene	√		2.1×10^{-3}
1-Choro-2-Methylpropane	√		1.2×10^{-3}
1,2-dibromoethane	√	√	6.3×10^{-4}
Bromoform	√		6.2×10^{-4}
1,3-dibromopropane	√		3.2×10^{-4}
3-heptanone	√		1.5×10^{-5}
2-heptanone	√	√	1.0×10^{-4}
4-methyl-2-pentanone	√		3.1×10^{-5}
2-butanone	√		4.3×10^{-5}
2-pentanone	√	√	3.7×10^{-5}
2-butanol	√		3.9×10^{-5}
1-pentanol	√	√	1.5×10^{-5}
Acetophenone	√		1.1×10^{-5}
Cyclohexanol	√		8.7×10^{-6}
2-methyl-1-propanol		√	5.6×10^{-5}
1-butanol		√	1.1×10^{-5}

Note. Further physical property data are given in Table 7.

TABLE 7

PROPERTIES OF THE SOLUTES USED IN THIS STUDY

ESTIMATED VALUES ARE DESIGNATED WITH AN ASTERISK*

Compound	Molecular Weight	Vapor Pressure (atm) 20°C	Vapor Pressure (atm) 25°C	Aqueous Solubility mol/m^3 20°C	Aqueous Solubility mol/m^3 25°C	Solubility of water in solute at 25°C (mol frn)	Henry's Law Constant atm m^3/mol. 20°C	Henry's Law Constant atm m^3/mol. 25°C
Benzene	78.11	0.100	0.125	22.4	22.8	7×10^{-4}	4.39×10^{-3}	5.49×10^{-3}
Toluene	92.13	0.029	0.0374	5.39	4.85	5×10^{-4}	5.18×10^{-3}	6.71×10^{-3}
Chlorobenzene	112.56	0.012	0.0156	4.44	4.19	2×10^{-3}	2.61×10^{-3}	3.72×10^{-3}
Bromobenzene	157.02		0.056		2.61	2×10^{-3}	2.0×10^{-3}	2.08×10^{-3}
o-Dichlorobenzene	147.01	0.00132	0.00193	0.68	0.99	4×10^{-4}	1.8×10^{-3}	1.95×10^{-3}
Carbon-tetrachloride	153.84	0.118	0.148 0.118	5.20	7.54 5.10	7×10^{-4}	2.27×10^{-2}	1.56×10^{-2}
1,2-Dichloro-propane	113.0	0.052	0.066	25.0		2×10^{-3}	2.07×10^{-3}	
1-Chloro-2-methyl propane	92.57		0.119		99.0	4×10^{-3}	1.0×10^{-3}	1.2×10^{-3}
1,2-Dibromoethane	187.9	0.0144	0.0143	23.0	22.94	4×10^{-3}	5.0×10^{-4}	6.32×10^{-4}
1,3-Dibromo-propane	201.9		0.0027		8.4	2×10^{-3}	3.0×10^{-4}	3.18×10^{-4}
Bromoform	252.7	0.0060	0.00737		12.0	1×10^{-3}	5.0×10^{-4}	6.15×10^{-4}
1-Butanol	74.12	0.0058	0.010	1040	1040	0.5	7×10^{-6}	1.65×10^{-5}
2-Butanol	74.12	0.0158	0.023	1686 2712		0.76	6×10^{-6}	
1-Pentanol	88.15		0.0034	307 (22°)		0.33	8×10^{-6}	
2-Methyl-1-propanol	74.12	0.0079	0.0095	1280		0.51	1.0×10^{-5}	
Cyclohexanol	100.16	0.00132	0.00145	1260		0.58	2.5×10^{-6}	
2-Pentanone	86.14	0.016	0.016	500	500	0.14	3.67×10^{-5}	4.88×10^{-5}
2-Heptanone	114.18	0.0034		38.0	38.0	0.11	1.01×10^{-4}	

TABLE 7 CONTINUED

Compound	Molecular Weight	Vapor Pressure (atm) 20°C	Vapor Pressure (atm) 25°C	Aqueous Solubility mol/m^3 20°C	Aqueous Solubility mol/m^3 25°C	Solubility of water in solute at 25°C (mol frn)	Henry's Law Constant atm m^3/mol. 20°C	Henry's Law Constant atm m^3/mol. 25°C
3-Heptanone	114.18		0.00184	125.2		0.047	2.0×10^{-4}	
4-Methyl-2-pentanone	100.16	0.0079	0.0095	190		0.097	4.60×10^{-5}	
Acetophenone	120.16		4.87×10^{-4}		45.8	0.01		1.06×10^{-5}
2-Butanone (Methyl ethyl ketone)	72.12	0.102	0.129	3702 3328	3134	0.055	2.92×10^{-5} 3.23×10^{-5}	4.35×10^{-5}
Oxygen	32.0	-	-	-	-	-	-	-
Water	18.0	-	-	-	-	-	-	-
Air	29	-	-	-	-	-	-	-
Carbon dioxide	44	-	-	-	-	-	-	-
Radon								

TABLE 7

PROPERTIES OF THE SOLUTES USED IN THIS STUDY

ESTIMATED VALUES ARE DESIGNATED WITH AN ASTERISK*

Compound	Diffusivities (cm^2/s) in air 20°C	in air 25°C	in water x 10^6 20°C	in water x 10^6 25°C	Schmidt Numbers in air 20°C	in air 25°C	in water 20°C	in water 25°C	Molar Volume at N. BP. cm^3/mol
Benzene	0.0797	0.0817	9.57	10.9	1.892	1.898	1049	827	96
Toluene	0.0732	0.0751	8.45	9.63	2.060	2.065	1188	931	118.2
Chlorobenzene	0.0705	0.0724	8.05	9.69	2.139	2.142	1247	925	116.9
Bromobenzene	0.0691	0.0709	7.95	9.58	2.182	2.187	1263	936	119.3
o-Dichlorobenzene	0.0643	0.0659	7.704	8.78	2.345	2.353	1303	1021	137.8
Carbon-tetrachloride	0.0695	0.0713	8.22	9.90	2.169	2.175	1221	906	112.8
1,2-Dichloro-propane	0.0716	0.0734	8.09	9.75	2.106	2.113	1241	920	115.8
1-Chloro-2-methyl propane	0.0719	0.0739	8.04	9.69	2.097	2.104	1249	925	117.1
1,2-Dibromoethane	0.0724	0.0742	8.92	10.8	2.083	2.090	1126	830	98.4
1,3-Dibromo-propane	0.0663	0.0680	7.9	9.52	2.275	2.281	1271	942	120.6
Bromoform	0.0710	0.0728	8.87	10.7	2.125	2.130	1132	838	99.5
1-Butanol	0.0778	0.0798	8.65	10.4	1.938	1.943	1161	861	103.6
2-Butanol	0.0778	0.0798	8.65	10.4	1.938	1.943	1161	861	103.6
1-Pentanol	0.0703	0.0721	7.70	9.62	2.145	2.151	1304	932	125.8
2-Methyl-1-propanol	0.0778	0.0798	8.65	10.4	1.938	1.943	1161	861	103.6
Cyclohexanol	0.0693	0.0711	7.71	9.29	2.176	2.181	1302	965	125.6
2-Pentanone	0.0723	0.0741	7.99	9.62	2.086	2.093	1257	932	118.4
2-Heptanone	0.0591	0.0606	6.26	7.54	2.552	2.559	1604	1189	177.6

TABLE 7 CONTINUED

Compound	Diffusivities (cm^2/s) in air 20°C	25°C	in water x 10^6 20°C	25°C	Schmidt Numbers in air 20°C	25°C	in water 20°C	25°C	Molar Volume at N.BP. cm^3/mol
3-Heptanone	0.0591	0.0606	6.26	7.54	2.552	2.559	1604	1189	177.6
4-Methyl-2-pentanone	0.0661	0.0678	7.21	8.68	2.281	2.287	1393	1033	140.6
Acetophenone	0.0649	0.0666	7.21	8.683	2.32	2.329	1393	1033	140.4
2-Butanone (Methyl ethyl ketone)	0.0805	0.0825	9.05	10.9	1.866	1.880	1109	823	96.2
Oxygen			18.0				558		25.6
Water					0.77	0.60			18.9
Air			18.0						29.9
Carbon dioxide			17.7				570		34.0
Radon									

Experiments in which the effects of temperature and humidity were examined involved blowing air directly into the tank instead of through the humidification column. The temperature of the water bath in which the glass tank was immersed was adjusted by an immersion heater or a cooler as required. The dry-bulb temperature of the unhumidified air was kept at 25° C. The experimental procedure was identical to that described previously. During the run, water temperature, wet and dry-bulb temperatures were checked and adjusted if necessary.

The oxygen transfer rate across the air-water interface was studied by first depleting the water of oxygen by bubbling nitrogen gas. A YSI Model 53 Oxygen Monitor connected to a Heath-Built Model EUW-20A Servo-Recorder was used to indicate the percent saturation of oxygen in water. The instruments were first calibrated by immersing the oxygen probe in a beaker of water saturated with air. After calibration the oxygen probe was inserted through the plexiglass lid and immersed 5 cm below the water surface to monitor the decrease in oxygen concentration. When oxygen saturation was less than 20% (about 2 ppm), nitrogen bubbling was stopped and the blower was switched on, the flowrate adjusted and the increase in oxygen concentration was recorded. The concentration was at least 80% of saturation before the experiment was terminated. At the end of the test, the oxygen concentration was allowed to reach a steady value to confirm the saturated concentration calibration. These tests were repeated at four different flowrates.

The air flow geometry was designed to simulate wind effects on water in the environment. Above a critical air flowrate, water waves were observed. This was found to occur at a turbulence level of 2 to 3 cm H_2O pressure drop across the orifice meter. Below this turbulence level, a flat water surface moving along with the air flow was observed. At turbulence levels of 3 to 7 cm H_2O, steady and smooth waves having heights of 4 to 7 cm were noted. At still higher turbulence levels (> 7 cm H_2O) the water surface was rough, waveheight did not increase significantly, a small quantity of air bubbles was found in the bulk of the water. It is believed that this contacting geometry is the best small scale simulation that can be obtained, being more typical in turbulence intensity than stirred systems and more reproducible than beaker-fan systems.

The conditions were selected to study mass transfer within the kinetic area in Figure 14 . The non-volatile region has been omitted because experiments conducted in this regime are of little interest and are of long duration. The turbulence levels were chosen largely on the basis of oxygen transfer rates to cover the range of environmental interest. Taking the gas flowrate (G) from the flowrate through the orifice meter and the surface area (A) as the flat water surface area, the ratios G/A were calculated and found to be 0.15 to 1.00 m/s which indicates equilibrium was not reached in these experiments. For a given G/A ratio or turbulence level, when compounds of different Henry's Law Constant (H) values were tested in the apparatus, the volatilization process moved from vapor phase diffusion control for low H to liquid phase diffusion control for high H. Between is a transition region in which resistances in both phases were significant.

The twenty organic compounds were tested at four levels of turbulence of 3, 4, 6 and 8 cm H_2O pressure drops across the orifice meter. For compounds with high Henry's Law Constant, such as benzene, samples were taken every 10-20

minutes over two hours. For compounds with low Henry's Law Constants, for example, acetophenone samples were taken every 1 - 2 hours over 10 hours. During the experiments, slight variation of water, air temperatures was unavoidable but were kept at 20 ± 2° C. The wet and dry-bulb thermometers indicated that the air was essentially saturated with water vapor.

Applying an overall mass balance on the system assuming negligible solute oncentration in the bulk of the vapor phase, results in the equation (as detailed earlier) where C_o is the initial aqueous solute concentration and C the concentration at time t; A and V are the surface area and volume of water respectively. Due to wave motion at the surface of the interface, determination of the actual surface area is difficult, thus A was taken as the flat water surface area.

The overall mass transfer coefficients (K_{OL}) were determined by plotting In (C/C_o) against t, the slopes of these plots being obtained by linear regression. A typical plot of ln C/C_o versus t is shown in Figures 17 to 19 for compounds of high, intermediate and low volatility. Table 8 groups all the experimental mass transfer coefficients, the compounds being listed in order of decreasing Henry's Law Constants. The dependence of transfer coefficients on turbulence levels is shown in Figure 20.

Five different groups of organic compounds were selected and studied in mixtures. The tests were conducted at air and water temperatures of 20 ± 2° C with saturated air and at two different turbulence levels, corresponding to 4 and 6 cm H_2O. The results are shown in Table 9. The mass transfer coefficients were calculated individually.

The effects of temperature and humidity were studied by keeping the air dry-bulb temperature constant at 25° C for all runs. A wet-bulb temperature of 16 ± 1° C was measured. Water temperatures of 25°C, 20°C and 15°C were tested using a mixture of toluene and benzene as volatilizing solutes at a turbulence level of 4 cm H_2O. The experimental data were analyzed as described above, the mass transfer coefficients being presented graphically in Figure 21.

The transfer of oxygen in the laboratory was tested at water and air temperatures of 20 ± 2° C using air saturated with water vapor transfer at four different turbulence levels as illustrated in Figure 22.

As oxygen was transferred from air to the water phase, the following equation results from an overall mass balance:

$$\ln[(C - C_S)/(C_O - C_S)] = -K_{OL}\, At/V$$

where C_O is the initial concentration at time zero and C_S is the final saturation concentration at infinite time.

TABLE 8

MASS TRANSFER COEFFICIENTS IN THE SMALL SCALE VOLATILIZATION SYSTEM.

UNITS ARE cm/h. VALUES IN PARENTHESES ARE CORRELATED.

Compound	K_{OL} values at stated orifice plate pressure drop			
	3 cm H_2O	4 cm H_2O	6 cm H_2O	8 cm H_2O
carbon tetrachloride	10.07 (8.54)	14.50 (15.5)	27.73 (28.1)	36.71 (39.9)
toluene	8.31 (8.59)	19.72 (15.6)	30.28 (28.3)	36.35 (40.1)
benzene	10.48 (9.12)	19.8 (16.6)	32.25 (30.0)	44.15 (42.6)
chlorobenzene	10.48 (8.28)	22.83 (15.0)	24.13 (27.3)	31.54 (38.7)
1,2-dichloropropane	5.59 (8.26)	13.58 (14.9)	25.47 (27.2)	34.06 (38.6)
0-dichlorobenzene	8.19 (8.01)	15.40 (14.5)	22.47 (26.4)	31.03 (37.4)
bromobenzene	12.41 (8.18)	20.35 (14.8)	31.67 (26.9)	40.35 (38.2)
1-chloro-2-methyl-propane	10.22 (8.0)	17.87 (14.5)	28.43 (26.3)	41.66 (37.3)
1,2-dibromoethane	9.94 (7.91)	16.98 (14.4)	25.34 (26.0)	33.35 (36.9)
bromoform	7.46 (7.90)	11.09 (14.3)	23.46 (26.0)	32.48 (36.8)
1,3-dibromopropane	7.60 (6.93)	12.82 (12.6)	25.12 (22.8)	34.00 (32.4)
3-heptanone	7.20 (5.72)	13.96 (10.4)	19.96 (18.9)	23.00 (26.7)
2-heptanone	6.33 (4.66)	11.44 (8.45)	14.22 (15.3)	22.93 (21.7)
4-methyl-2-pentanone	7.22 (3.40)	13.37 (6.18)	16.45 (11.2)	20.00 (15.9)
2-butanone	5.40 (2.92)	7.78 (5.30)	11.73 (9.61)	15.92 (13.6)
2-pentanone	7.52 (3.16)	9.81 (5.72)	14.18 (10.4)	17.99 (14.7)
2-butanol	1.90 (3.4)	3.30 (6.22)	4.10 (11.3)	4.49 (15.9)
1-pentanol	1.64 (1.66)	2.44 (3.02)	3.21 (5.48)	4.84 (7.77)
acetophenone	1.10 (1.17)	2.28 (2.12)	2.95 (3.85)	3.76 (5.47)
cyclohexanol	0.35 (0.33)	0.44 (0.59)	0.47 (1.07)	0.68 (1.52)
oxygen	17.3 (13.4)	32.0 (24.3)	46.0 (44.0)	54.0 (62.4)

TABLE 9

VOLATILIZATION OF MIXTURES

Compounds	K_{OL} (cm/h) at h = 4 cm H_2O		K_{OL} (cm/h) at h = 6 cm H_2O	
	Single	Mixture	Single	Mixture
benzene	19.8	19.0	32.2	29.0
toluene	19.7	19.1	30.3	28.9
benzene	19.8	19.0	32.2	29.0
toluene	19.7	19.1	30.3	28.9
bromoform	11.1	10.5	23.5	22.4
benzene	19.8		32.2	29.0
bromoform	11.1	10.5	23.5	22.4
1, 2 dichloropropane	13.6	13.4	25.5	20.4
3 heptanone	14.0	8.1	20.0	14.0
2 pentanone	11.4	7.0	14.2	11.0
2 butanol	3.3	1.7	4.1	2.8
1 pentanol	2.4	2.0	3.2	2.4

FIGURE 15

GENERAL ARRANGEMENT OF THE SMALL SCALE VOLATILIZATION APPARATUS SYSTEM

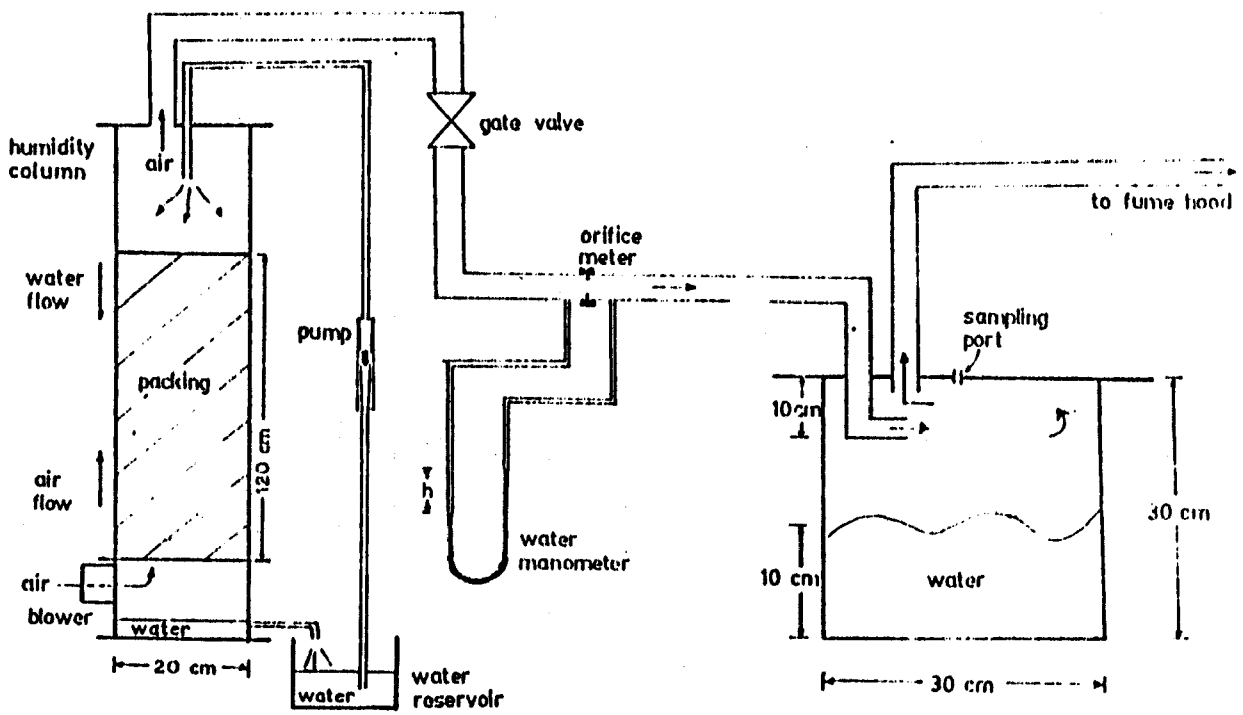

FIGURE 16

PLAN VIEW OF THE SMALL SCALE VOLATILIZATION TANK

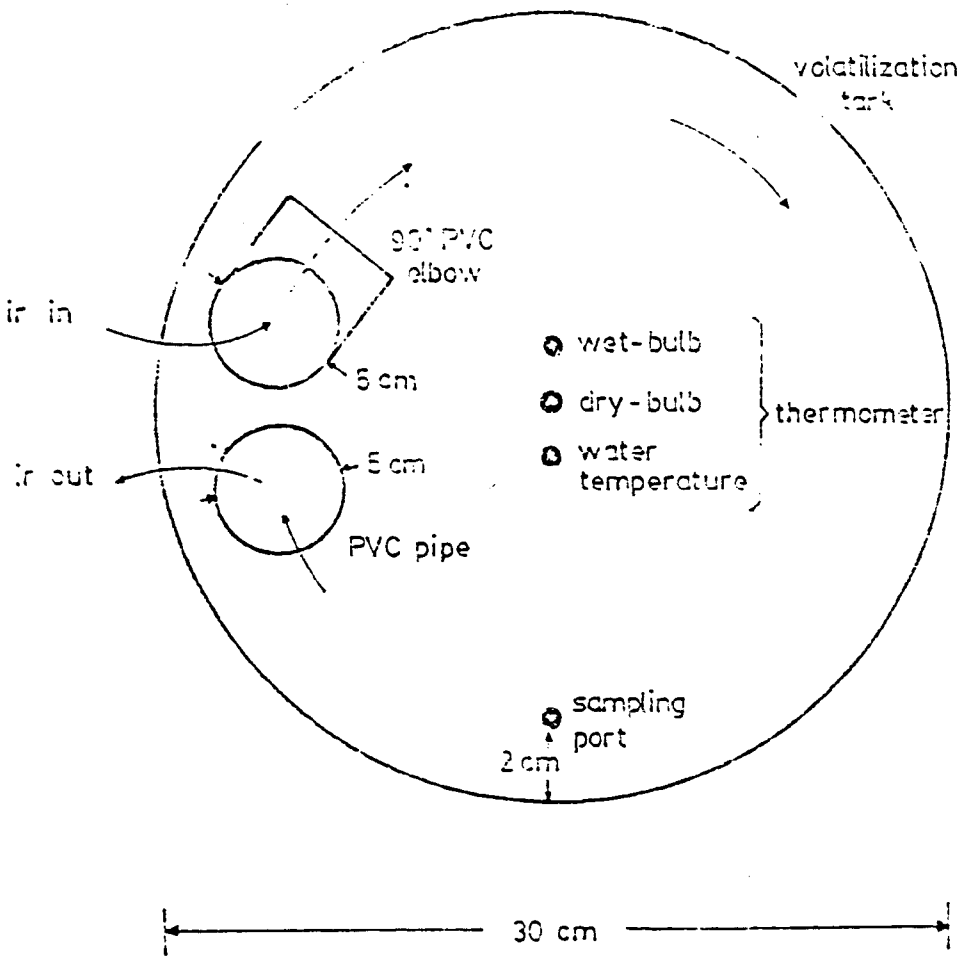

FIGURE 17

A TYPICAL PLOT OF LOG CONCENTRATION VERSUS TIME FOR A HIGHLY VOLATILE SOLUTE (BENZENE)

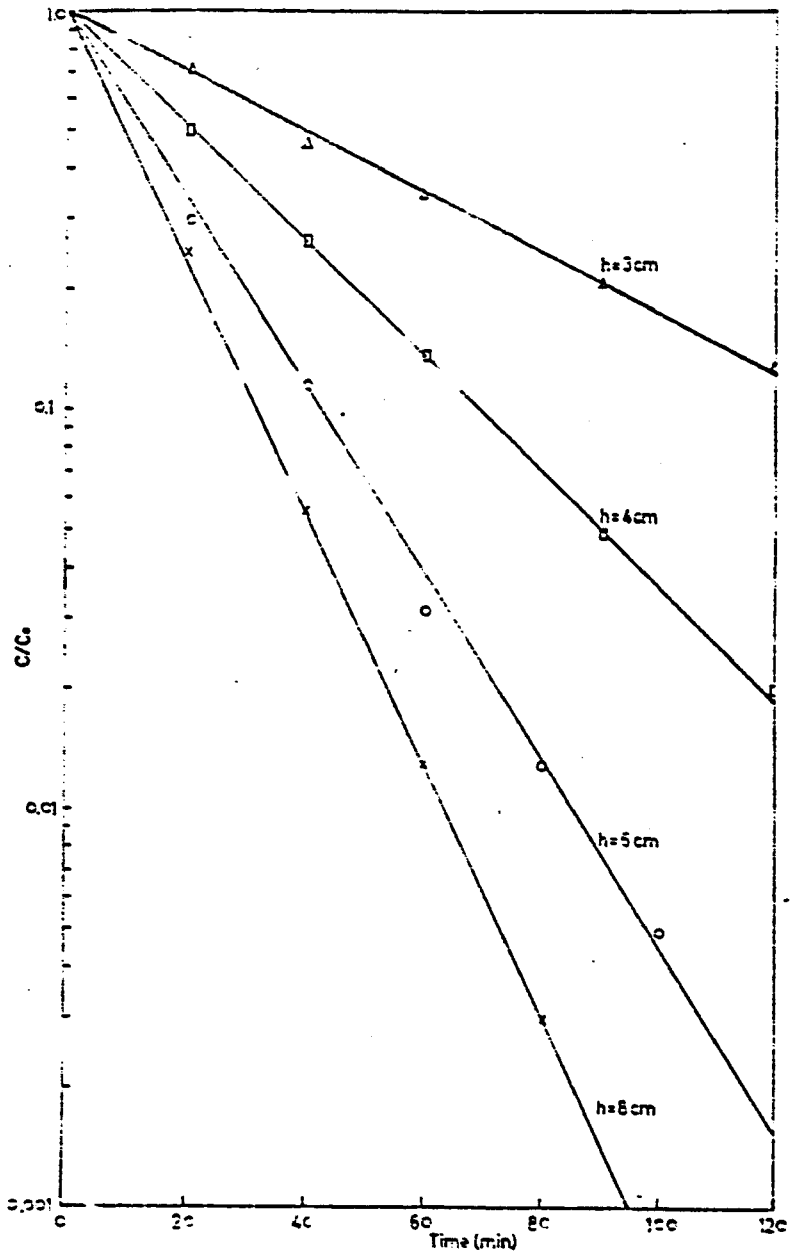

FIGURE 18

A TYPICAL PLOT OF LOG CONCENTRATION VERSUS TIME FOR A SOLUTE OF INTERMEDIATE VOLATILITY (2 BUTANONE)

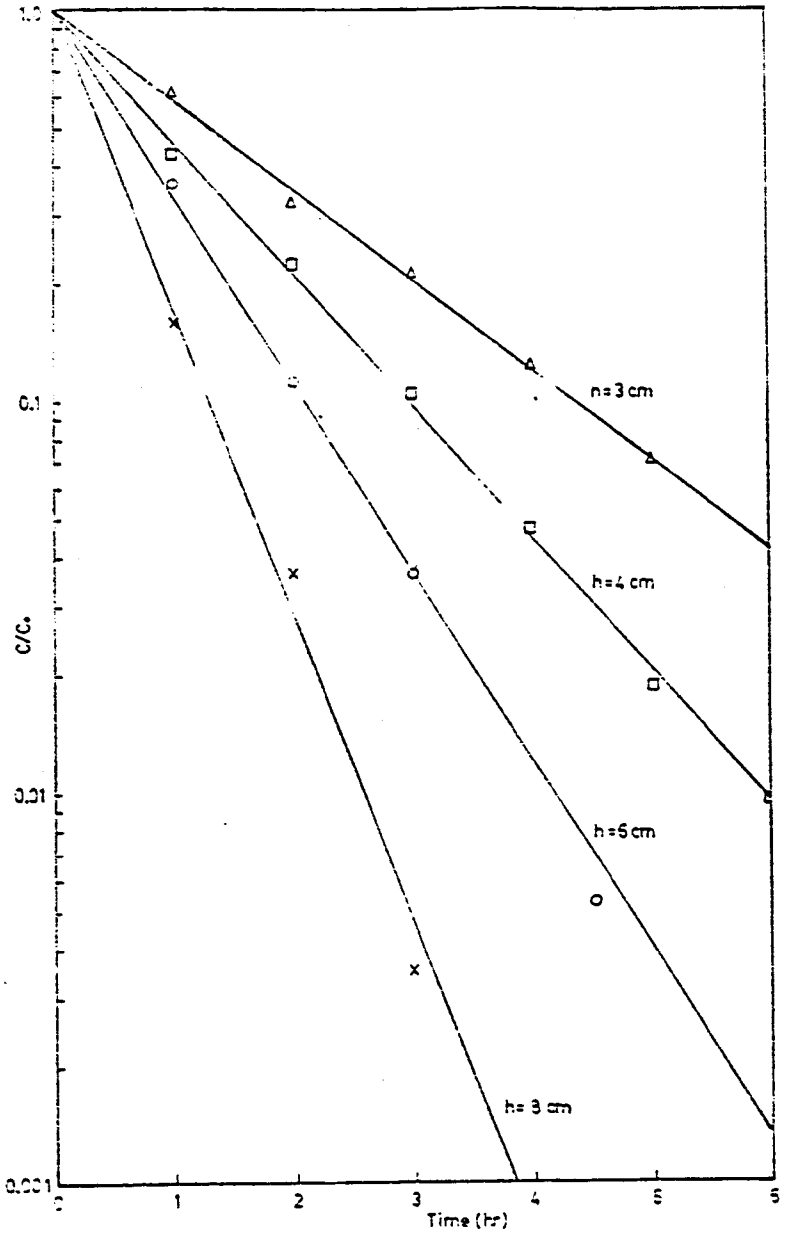

FIGURE 19

A TYPICAL PLOT OF LOG CONCENTRATION VERSUS TIME

FOR A SOLUTE OF LOW VOLATILITY (1 PENTANOL)

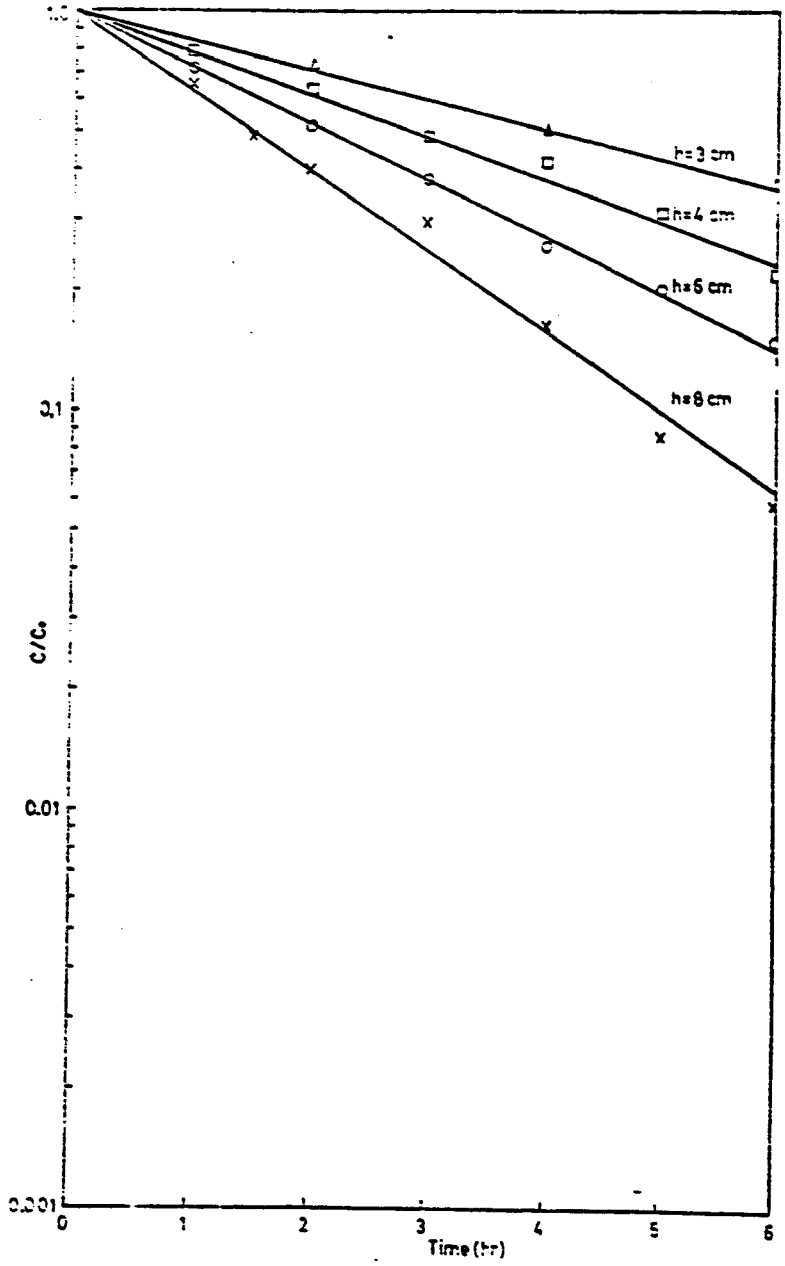

FIGURE 20

PLOT OF MASS TRANSFER COEFFICIENTS K_{OL} VERSUS TURBULENCE FOR THE SMALL SCALE VOLATILIZATION APPARATUS ILLUSTRATING DEPENDENCE ON VOLATILITY

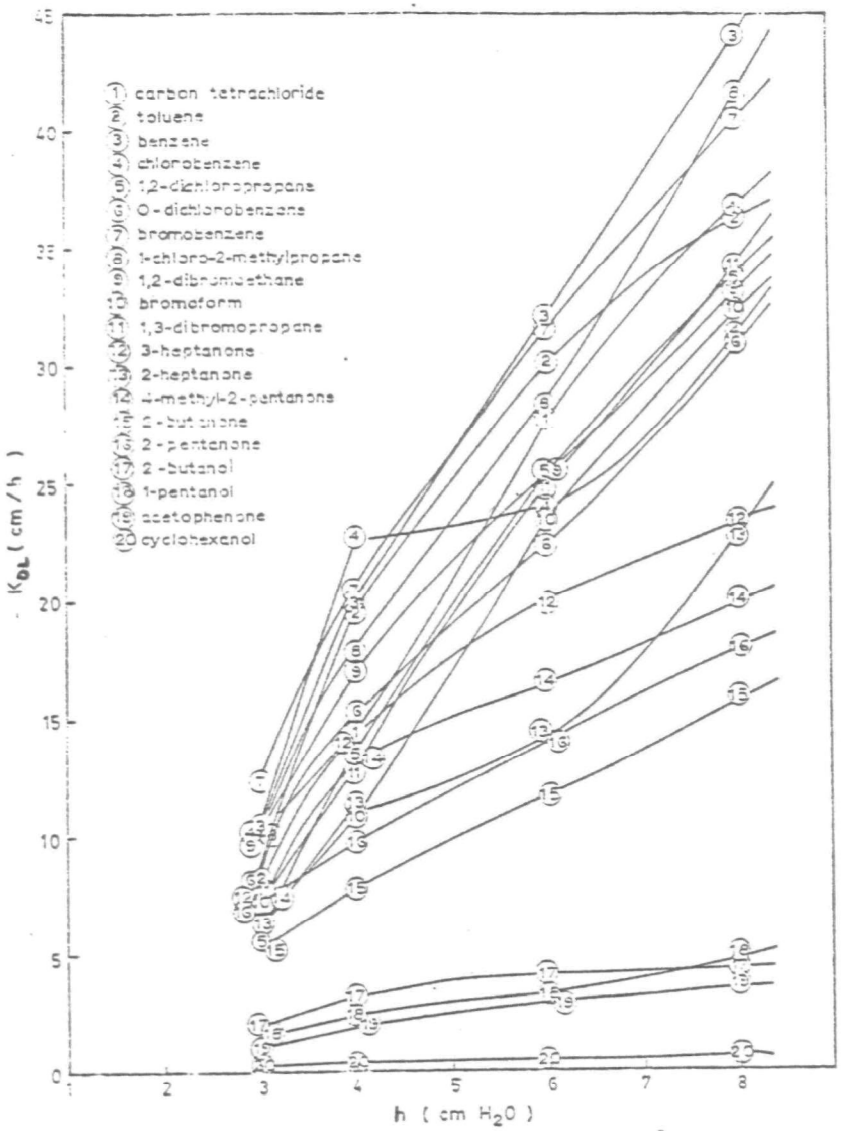

FIGURE 21

EFFECT OF TEMPERATURE ON K_{OL} FOR BENZENE AND TOLUENE VOLATILIZATION IN THE SMALL SCALE VOLATILIZATION SYSTEM

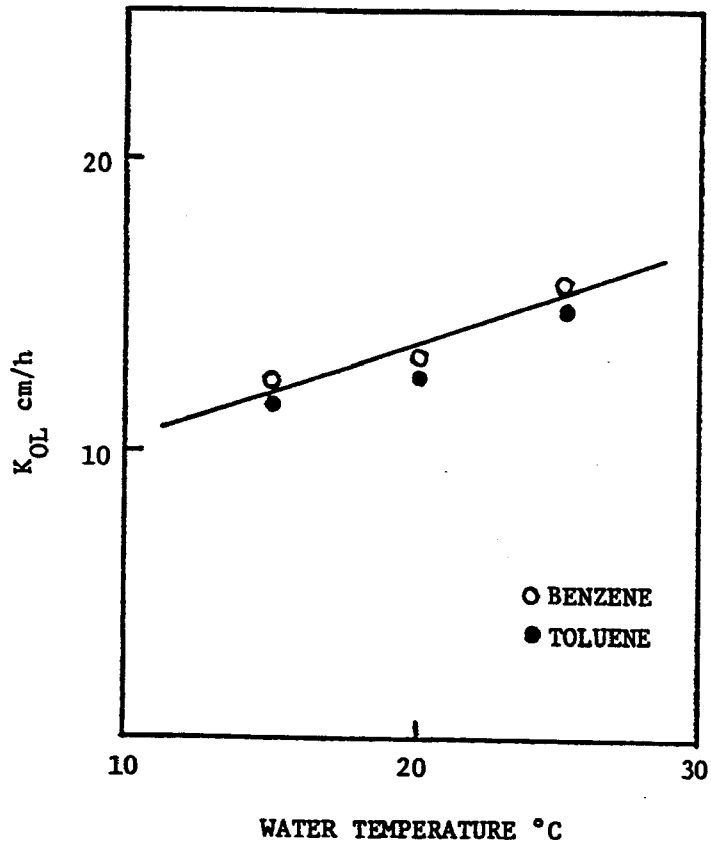

FIGURE 22

PLOT OF LOG $((C - C_\infty)/(C_o - C_\infty))$ VERSUS TIME FOR OXYGEN TRANSFER IN THE SMALL SCALE VOLATILIZATION SYSTEM

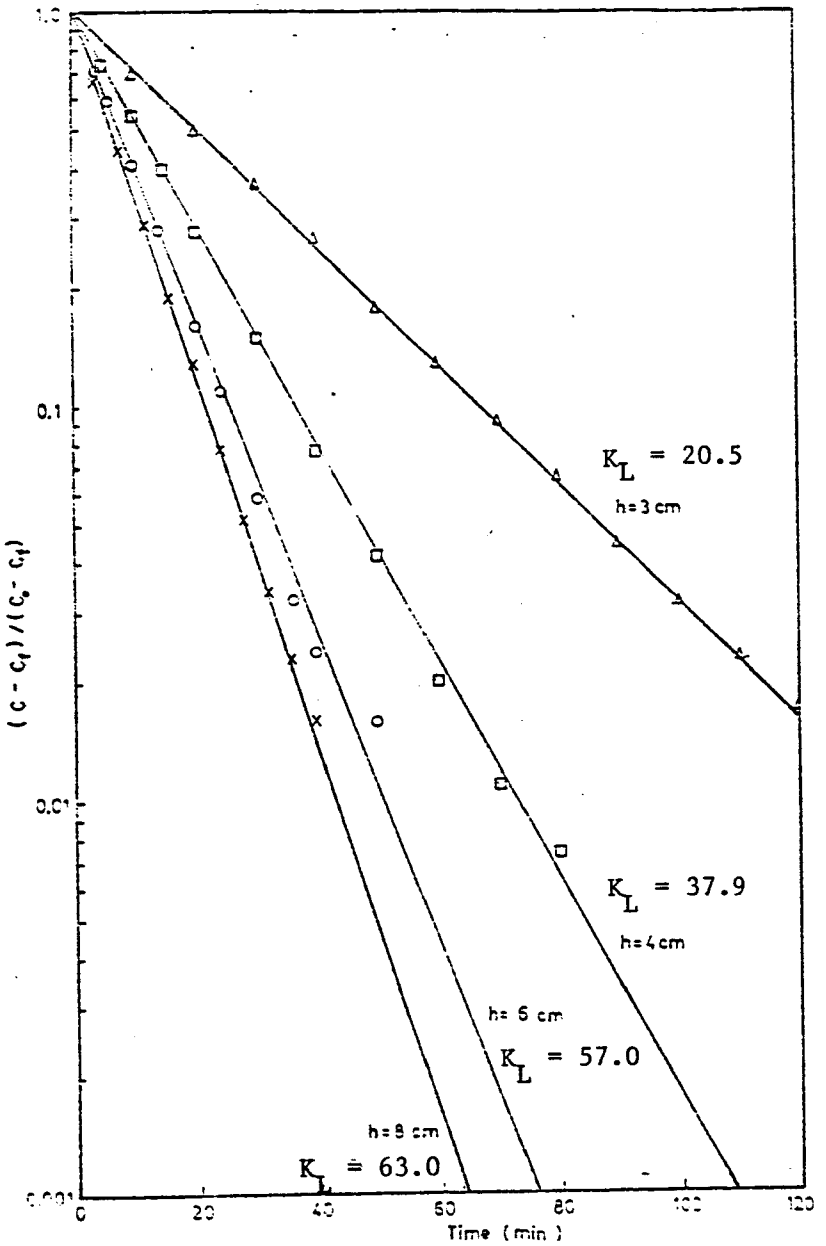

WIND WAVE TANK

The wind-wave tank system used for the volatilization study is shown in Figure 23 . It consisted of an upwind or air-entry section, a water tank, and a downwind section in which an Aerovent LS-248 fan was located. One side of the water tank was made of steel plate while glass sheet was used for the front side to permit viewing of waves and taking other measurements. The top of the tank was removable and was constructed of acrylic sheet to facilitate observations. Air gaps were taped to prevent leakages.

The upwind section was equipped with a diffuser to decrease the turbulence of the air flow at the entrance. A honeycomb structure consisting of glued thin wall paper tubes, 4 cm in diameter and 23 cm in length, was installed at the inlet converging section and just upstream of the outlet diffuser to even out the swirling motion of the fan. An aluminum plate 50 cm long was attached to the end of the upwind section and inclined at an angle of 5° to the water surface to provide a smooth transition between the adjoining air and water flow. Air speed was varied by inserting screens of different porosity in front of the fan.

A fibre mat wave absorber was attached to the downwind end of the tank to dissipate the wave energy and minimise reflection. It also acted as a barrier to stop water spilling out from the tank during high wind speed runs.

To maintain a uniform concentration along the tank, a recirculation system consisting of a 1.5 HP pump (Dayton, Teel pump) and a gate valve for adjusting the recirculating rate was connected to the two ends of the water tank. Two stirrers (Canlab high-torque stirrers) were mounted on the tank to enhance the mixing process. A stirrer speed of 400 r.p.m. was found to give satisfactory mixing with minimum disturbance and no surface vortex formation. The propeller shafts were made of 316 stainless steel, were 40 cm in length and were 9 mm in diameter. The propellers used were axial flow three bladed marine-type propellers, type 316 stainless steel, placed 30 cm below the water surface.

Air velocity profiles were measured at two locations, A and B which were 1.5 m and 4.2 m from the leading edge of the tank, using a pitot-static tube of Prandtl design which was mounted on a motor driven transverse mechanism. The height of the pitot tube from the water surface was measured by a cathetometer. The pressure differential was measured using a differential pressure transducer (Decker 306) and a recorder (Honeywell, Electronik 196). The pressure transducer was calibrated using a zero displacement type micromanometer (Airflow Development Ltd., portable Airflow Testing Set Mark IV).

The drift velocity of the wind driven current was measured using pieces of wax paper 5 mm in diameter. The tank was divided into thirteen sections and the time for the wax paper to travel through each of them was measured using an electronic stop-watch.

The transfer rates of eleven organic chemicals at various wind speeds were measured. Tap water was used for the experiments. A sump pump was used to dissolve the chemicals. For compounds which were denser than water saturated solutions were first prepared in large vessels and then diluted in the water

FIGURE 23

DIAGRAM OF THE WIND WAVE TANK

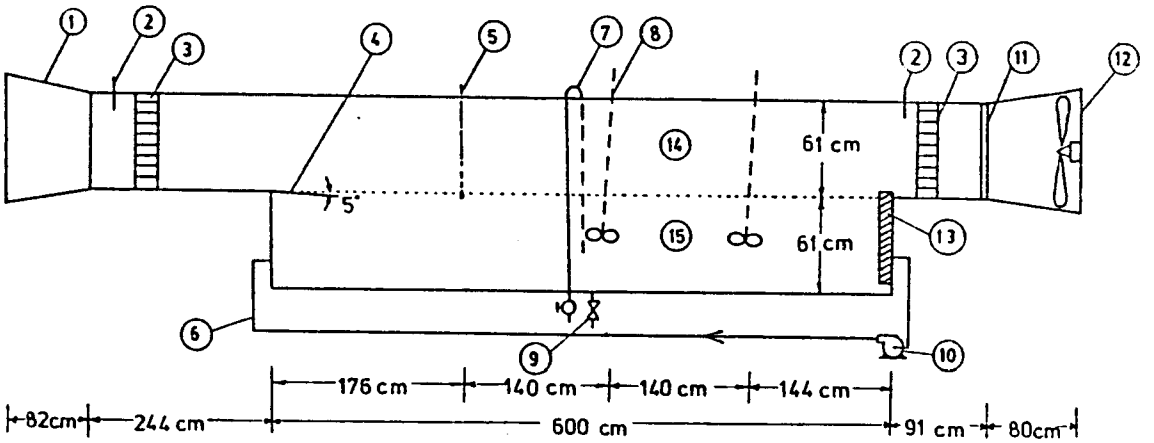

1. Diffuser
2. Humidity Measurement
3. Air Flow Grid
4. Beach
5. Interfacial Temperature Measurement
6. Recirculation System
7. Sampling Port
8. Stirrer
9. Drain
10. Recirculation Pump
11. Air Flow Controlling Screen
12. Aerovent LS-248 Fan
13. Wave Absorber
14. Wind Tunnel
15. Water Tank

tank. Direct mixing in the tank was feasible for soluble compounds which were less dense than water. Water samples (50 mL) were siphoned from the tank usually at one hour intervals however the duration between sampling was increased up to four hours for experiments of less volatile compounds which ran over 50 hours. The analytical procedure is described later.

The evaporation rate of water at different wind speeds was measured using a constant water level apparatus which operated on the "chicken-feeder" principle i.e. the volume of water added to the tank to maintain a constant level was measured. Air humidity was measured at the upwind and downwind ends of the tank and the interfacial temperature was estimated using a thermometer (accurate to 0.1°C) dipped just below the water surface. The length of the experiments was usually 48 hours to give a reasonable estimate of the transfer coefficient.

Velocity profiles were measured in the wind wave tank for speeds from 5 to 13 m/s. A steep increase in velocity adjacent to the air-water interface was found and a uniform velocity occurred in most parts of the profile. A typical velocity profile is shown in Figure 24 . The profiles indicate that the air flow generally develops the behaviour characteristic of turbulent flow in a boundary layer over roughened surfaces.

The velocity profiles were fitted to a logarithmic law as described earlier, the values of the free stream velocity U^{∞}, the friction velocity U^{*} and the surface roughness Z_o being calculated. Figure 24 also gives a typical logarithmic profile.

Longitudinal profiles of surface velocity for different flow conditions are plotted in Figure 25. The drift current appears to increase linearly with the wind speed and a ratio of 0.0282 can be established from the data. A plot of drift velocity versus wind speed is shown in Figure 26.

The development of wind waves with fetch can be distinguished into several regions. The fist part is the wave generation section which consisted of the glassy surface near the leading edge of the tank in which two-dimensional waves are formed at the end of the section. The second region of linear instability followed in which the amplitude increases while the frequency is approximately constant. The third section is the non-linear growth region in which the growth in amplitude takes place at a slower rate while the frequency of dominant waves decreases with fetch. For still larger fetches white caps and water droplets may form and an equilibrium wave pattern

FIGURE 24

TYPICAL PLOT OF LINEAR AND LOGARITHMIC VELOCITY PROFILES

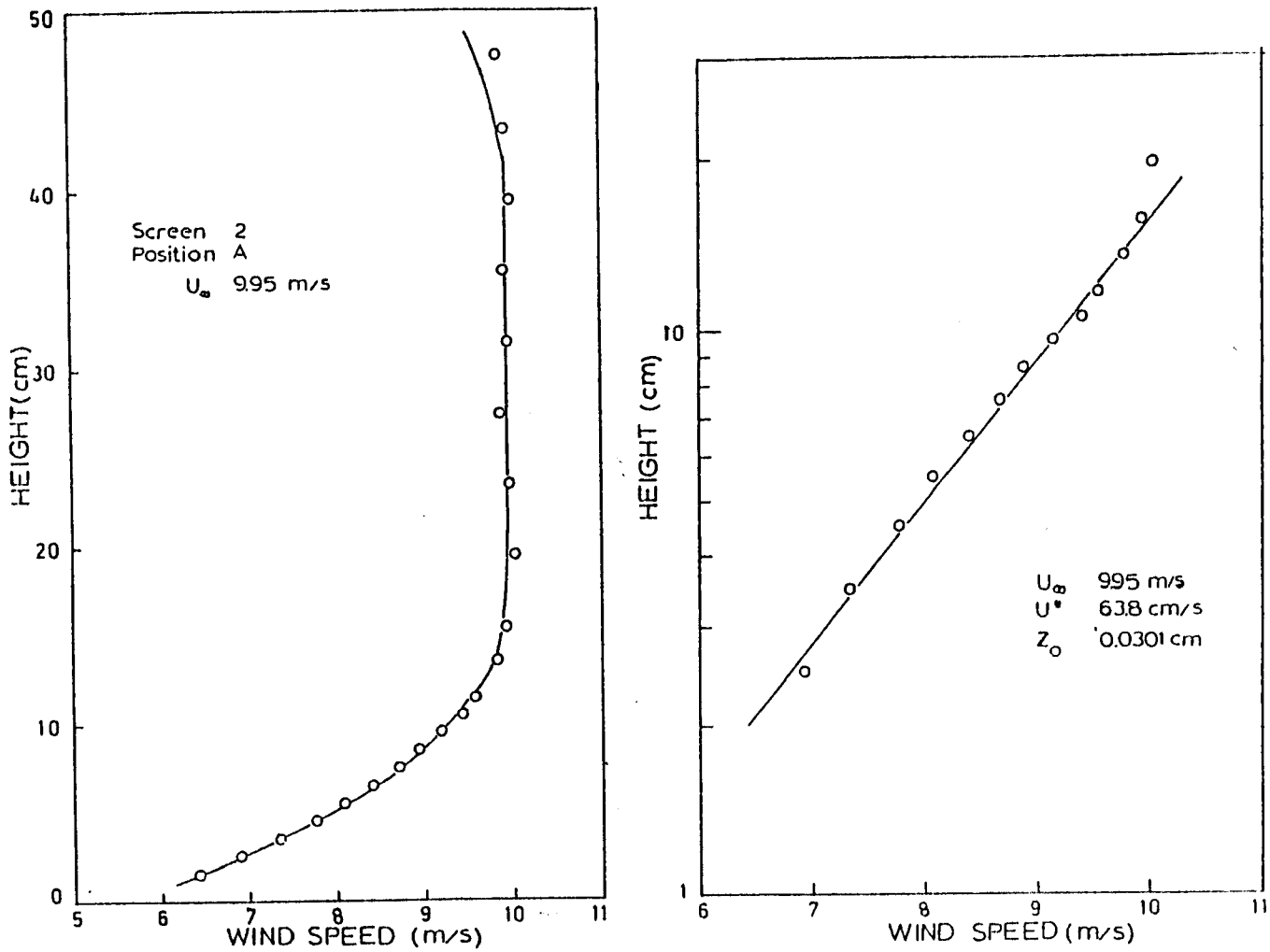

FIGURE 25

VARIATION OF SURFACE DRIFT VELOCITY WITH FETCH IN THE WIND WAVE TANK

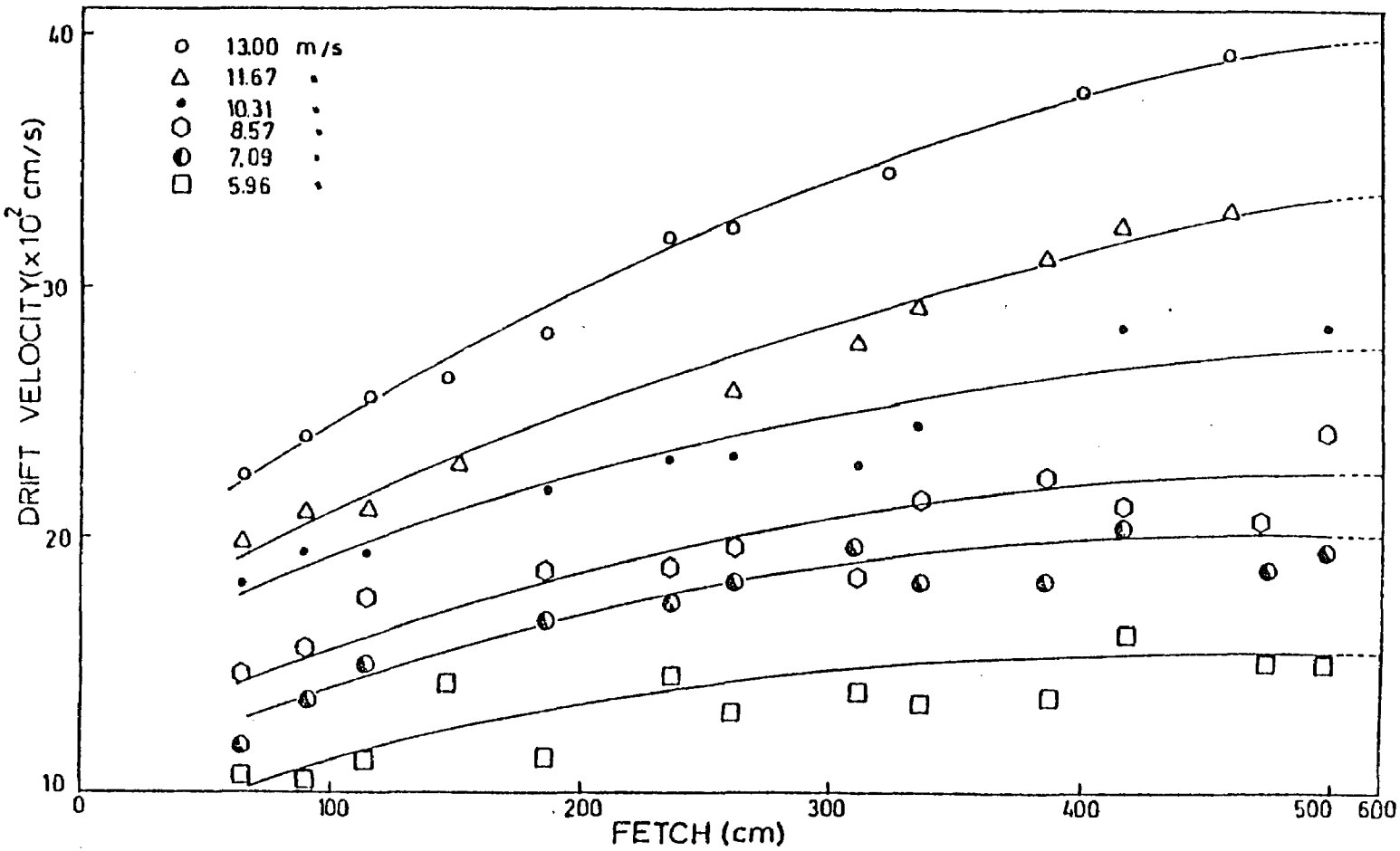

FIGURE 26

PLOT OF FINAL WATER SURFACE DRIFT VELOCITY VERSUS WIND SPEED FOR THE WIND WAVE TANK ILLUSTRATING A DRIFT VELOCITY OF 2.82% OF WIND SPEED.

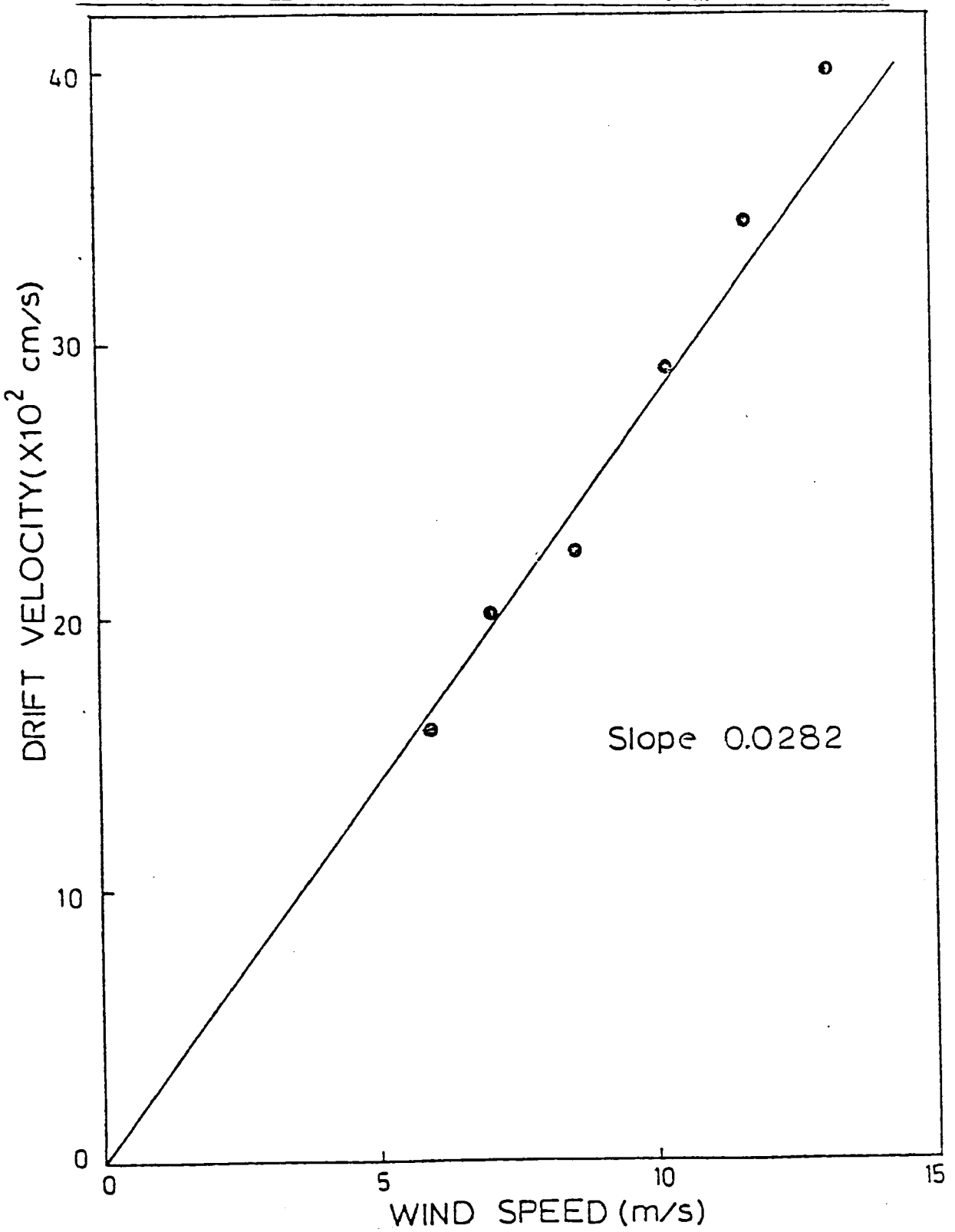

is established.

The first two stages of wave formation could be easily identified in the tank but the small fetch of the wind wave tank prohibits the transition into the non-linear growth region. A glassy surface could be identified only at low wind speed (< 5 m/s). Up to a wind speed of 3 m/s, no waves appeared on the water surface. As the wind speed increased, small ripples appeared and were separated by relatively calm water. When the wind speed reached 5 m/s significant waves developed from the small ripples and the amplitude increased with fetch. Wave heights up to 4 cm were observed and small ripples could be seen riding on the dominant waves at higher wind speed. Although the air speed U_∞ reached values exceeding 13 m/s, breaking waves i.e. white caps, were not observed. At high air velocities small droplets of spray were observed to be shedding from crests of the larger waves on the downwind end but the waves did not become sharp-created as is found in a "fully developed" sea.

Volatilization Tests

A component mass balance during volatilization from the tank gives,

$$K_{OL}A(C - P/H) = - V \frac{dC}{dt}$$

where C is the average concentrations in the water phase (mol/m^3), P is the air partial pressure (atm), H the Henry's Constant, A and V are the surface area in m^2 and the volume in m^3 of the water in the tank respectively. Integrating the differential equation gives

$$(C-P/H) = (C_0-P/H) \exp(-K_{OL}A\ t/V)$$

where C_0 is the initial concentration.

Recalling the equations derived earlier for various laboratory air-water contacting systems it is clear that conditions are either liquid or gas phase diffusion controlled since G/A is of the order of 2 m/s thus assuming a K_G of 0.01 m/s the group G/K_GA is of the order of 200. Inclusion of a liquid phase resistance adds to this group thus it exceeds unity (the criterion for near equilibrium conditions by at least two orders of magnitude). It follows that the exit gas is at the most 1% saturated i.e. P/H < 0.01C thus P can be assumed to be zero without significant error and

$$C = C_0 \exp(-K_{OL}A\ t/v) = C_0 \exp(-K_{OL}\ t/h)$$

FIGURE 27

TYPICAL PLOT OF LOG CONCENTRATION VERSUS TIME FOR

A VOLATILE COMPOUND (BENZENE) IN THE WIND WAVE TANK

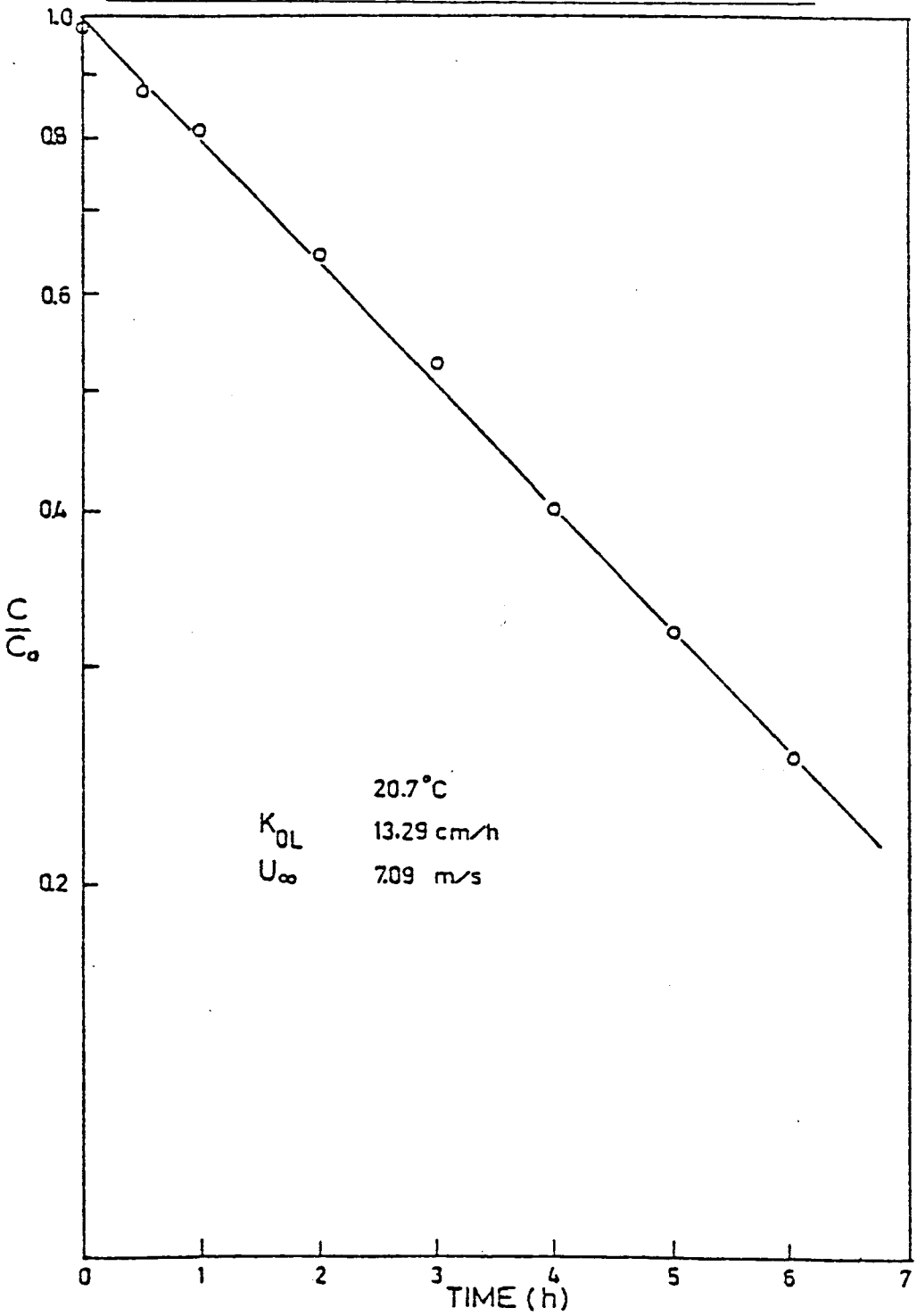

FIGURE 28

PLOT OF LOG CONCENTRATION VERSUS TIME FOR VOLATILIZATION OF A LOW VOLATILITY COMPOUND (1 BUTANOL) IN THE WIND WAVE TANK

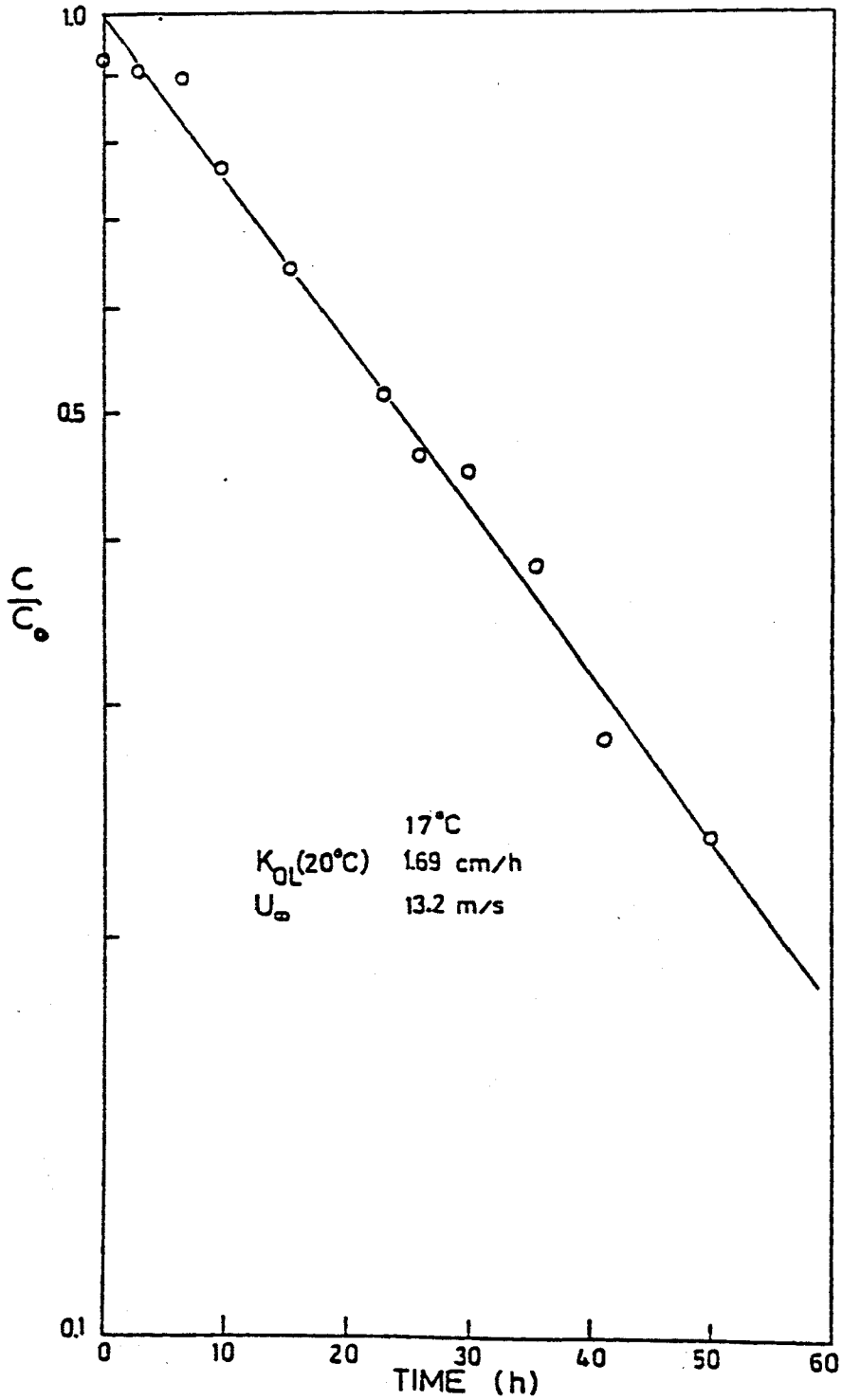

FIGURE 29

PLOT OF K_{OL} VERSUS WIND SPEED FOR VOLATILIZING SOLUTES OF VARIOUS H VALUES IN THE WIND WAVE TANK

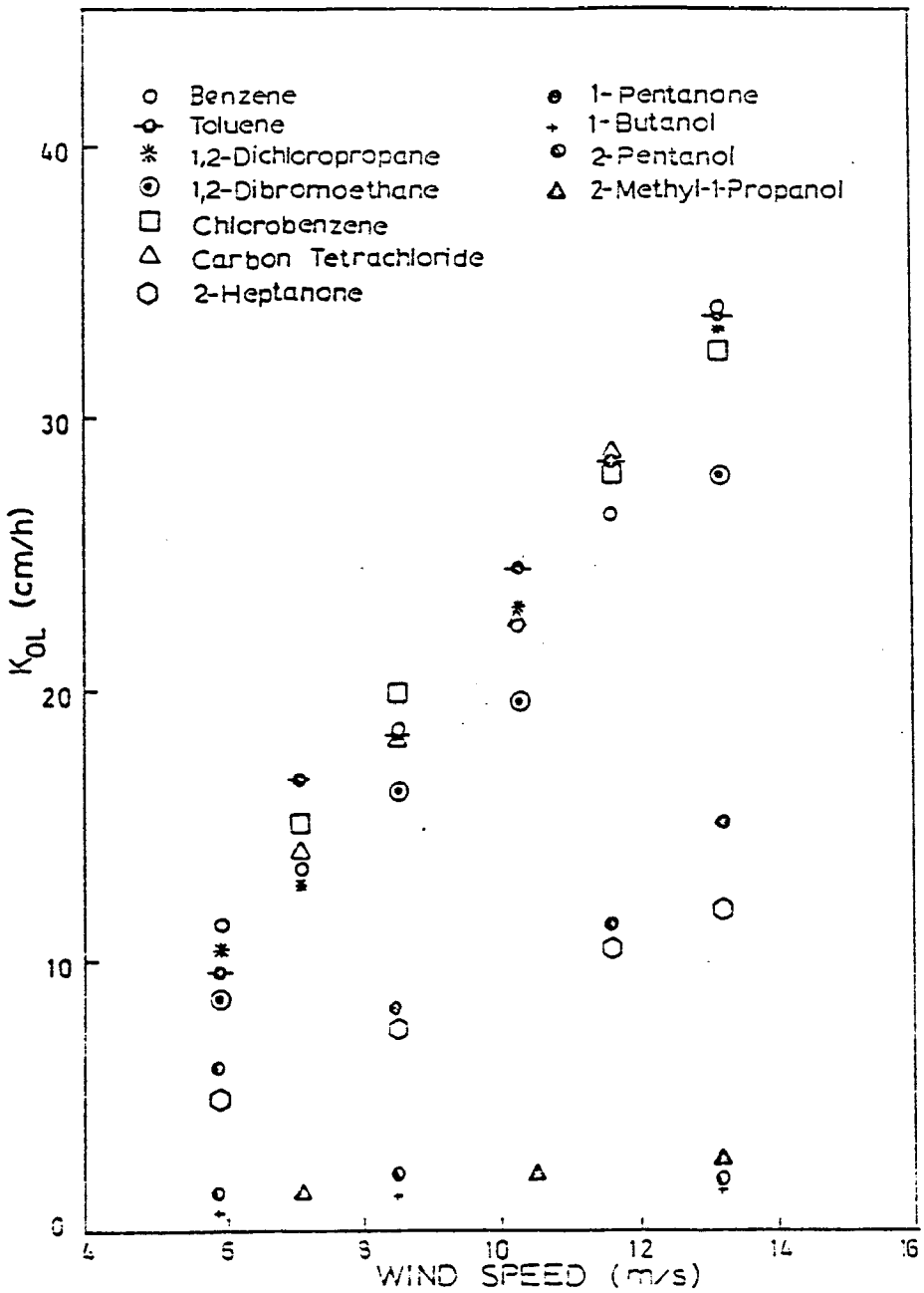

where h is V/A and is the mean height of water in the tank. The data from the mass transfer runs were analyzed using linear regression to calculate the overall mass transfer coefficient from the ln(C) versus t graph. The fitted line was not forced through the origin and the intercept can have values greater or less than the concentration measured at time zero. Figure 27 shows the results of a typical benzene run.

The data obtained for less volatile compounds show more scatter, Figure 28 being the results of a n-butanol run. The reason for this is believed to be the difficulties encountered in analytical techniques, and since the stripping efficiency for alcohols and ketones at room temperatures is low and more variable. The accuracy was however sufficient for the present purposes.

During a volatilization run, the temperature of the water and the humidity of the room were reasonably constant. However, a temperature difference of 5°C between runs carried out in the winter and in the summer necessitated some correction. The temperature dependence of K_{OL} on temperature is normally represented as,

$$K_{OL2}/K_{OL1} = \theta^{(T_2 - T_1)}$$

Dobbins (48) reported that the range of θ varied from 1.017 to 1.044. Metzger (74) has shown that the numerical value of θ depends on the mixing conditions in the water, with values being generally in the range 1.005 to 1.030. A value of 1.016 was suggested by Thackston and Krenkel (75) and was employed by Cohen (58) to make the adjustment. The same value is used in the present study to correct all the mass transfer data to 20°C.

Exchange coefficients obtained for the solutes at different wind speeds are plotted in Figure 29. Their properties are given in Table 7.

In setting up the mass balance equation a uniform concentration in the tank is assumed. Mixing experiments with dye showed that water was recirculating at a speed about 1 cm/s which was relatively fast compared to the time between sampling. Mixing in the vertical direction was enhanced by the two stirrers located along the tank. Preliminary runs indicated that the concentrations taken in three positions of the tank were all within the accuracy of experimental measurements, and the value of mass transfer coefficients obtained were relatively close. At wind speeds greater than 3 m/s, the wind drags the surface water to the downwind end of the tank and piles it up which produces a hydraulic head which causes a bottom flow to occur in the opposite direction. The experimental evidence showed that uniform mixing was attained in the tank at a time scale much shorter than the duration of the experiment.

Several runs were carried out using a mixture of compounds in which the individual mass transfer coefficients were measured to study if any interactions between the compounds exist. The results are listed in Table 11 along with the individual K_{OL} for comparison. The difference is within experimental error and no significant deviation can be detected.

The evaporation rate of water is controlled by the water in air concentration difference between the air close to the interface (which is assumed to be saturated with water vapor), and the bulk air phase. The water content of the air phase was measured by monitoring the humidity both at the upwind and the downwind ends of the tunnel. By measuring the flux of water vapor and the concentration difference in the air, K_G for water may be calculated. A total mass balance of water in the tank gives the following equation,

$$\frac{Pw}{M} = \frac{dV}{dt} /v = K_G A \ (C_i - C_b)$$

where v is the molar volume of water (18×10^{-6} mol/m^3) C_i and C_b are the interfacial and bulk air concentrations of water (mol/m^3) and K_G is the gas phase mass transfer coefficient of water (m/s). During a short interval, this equation can be rewritten in the form,

$$K_G = \Delta V/(vA(C_i - C_b)_{AV}\Delta t)$$

from which K_G can be calculated. Water evaporation experiments were carried out over 40 hours due to the fair amount of scattering that occurred between each individual measurement. The measured K_G (which have been corrected to 20°C) are reported in Table 10.

Surface Film Tests

Decyl alcohol (Fisher Scientific 98% purity) was used to form a monolayer on the water surface. Initially, a benzene volatilization run was carried out at a wind speed of 8.5 m/s. After the experiment had run for four hours and a concentration drop was established, a layer film was formed by dripping 10 ml of the alcohol continuously onto the water surface through tubing located at the upwind end of the wind wave tank. This would give a film of average thickness 3×10^{-5} cm or 0.3 μm, ignoring dissolution. The wind and spreading forces caused the film to drift toward the downwind end of the tank and multilayers of surplus alcohol could have been formed. No special precaution was taken to remove the excess alcohol and avoid the possible accumulation due to the constraints of the tank. The experiment was continued for another three hours during which observations were made and samples were taken to establish a new concentration - time curve.

The water surface turned glassy smooth immediately after the addition of decyl alcohol which could be attributed to the damping effects of the layer. The surface stayed calm for over 8 minutes then waves of much smaller amplitude started to form. However, the appearance of waves only lasted for a short duration and the surface returned to the glassy state afterwards. This cyclic behavior continued for the rest of the experiment. The reason was probably the periodic suction of the alcohol accumulated at the downwind end into the recirculation system. When the alcohol came out at the other (upwind) end, it formed a more coherent layer and damped out the wave formation more effectively.

The mass transfer coefficient was observed to be 16.6 cm/h prior to addition of the alcohol, then it fell to approximately 3.3 cm/h, a factor of five drop. The effect on the hydrodynamics was obviously very significant.

It is impossible to separate the effects of "blocking" and "damping."

TABLE 10

MASS TRANSFER COEFFICIENTS FROM THE WIND WAVE TANK

EXPRESSED IN m/s x 10^6 WITH CORRELATED* VALUES IN PARENTHESES.

Compound	Air Speeds (m/s) 13.2	11.67	10.31	8.57	7.09	5.96
Benzene	94.4 (99.1)	73.3 (82.4)	62.5 (68.4)	51.1 (51.8)	36.9 (39.0)	31.6 (30.0)
Toluene	93.6 (93.4)	79.4 (77.6)	68.9 (64.4)	51.6 (48.9)	46.9 (36.7)	26.6 (28.3)
1,2 dichloro-propane	93.9 (89.2)		63.9 (61.6)		35.8 (35.1)	28.9 (27.0)
chlorobenzene	89.7 (89.7)	78.0 (74.6)		55.0 (46.9)	41.9 (35.3)	
1,2 dibromo-methane	77.2 (83.1)		54.7 (57.4)	45.3 (43.5)		23.6 (25.2)
carbontetra-chloride		79.4 (77.5)	63.3 (64.4)	51.1 (48.8)	39.1 (36.7)	
2 pentanone	33.1 (28.6)	29.7 (23.8)		21.1 (14.9)		13.3 (8.67)
2 heptanone	42.7 (44.9)	31.6 (37.3)		23.0 (23.5)		16.9 (13.6)
1 pentanol	8.11 (8.06)			5.75 (4.22)		3.80 (2.45)
2 methylpropanol	7.30 (10.5)		5.75 (7.28)		3.81 (4.15)	
n butanol	4.69 (7.64)			3.58 (3.99)		2.02 (2.31)
Water evaporation	71100	55200	39200	29700	22200	19400

*See later discussion of correlating equations.

TABLE 11

VOLATILIZATION RESULTS OF MIXTURES IN THE WIND WAVE TANK

VALUES IN PARENTHESIS ( ) ARE FOR COMPOUNDS ALONE.

Mixture Run	Wind Speed m/s	K_{OL} values (cm/h) for stated compounds		
		2-Butanol	2-Methyl-Propanol	2-Heptanone
1	6.0	0.820 (0.724)	1.06 (ca 1.2)	5.71 (6.07)
2	8.6	1.36 (1.26)	1.66 (ca 1.6)	8.77 (8.26)
		Benzene	Chlorobenzene	1,2 Dichloropropane
3	6.0	12.50 (11.40)	11.50 (ca 11.0)	11.20 (10.35)
4	8.6	16.7 (18.4)	15.7 (19.8)	15.6 (ca 18.0)
		Benzene	Toluene	
5	10.7	24.6 (22.5)	24.1 (24.8)	

RELATIVE VOLATILITY APPARATUS

As is outlined earlier in Section 4, this apparatus operates on the principle that if a solution of a slightly volatile solute is distilled to a known extent the relative concentrations in the residue and distillate can be used to calculate the relative volatility and hence the ratio of solute to water Henry's Law Constants.

Several systems were designed and tested. The first and simplest was a direct batch distillation of a volume of solution. Unfortunately this necessarily occurs at a temperature of 100°C at atmospheric pressure and yields data which must be extrapolated down to environmental temperature conditions. This extrapolation may be inaccurate because of uncertainties about the temperature dependence of solute vapor pressure and solubility. Distilling at low temperatures requires vacuum or low pressure operation with the possibility of vapor loss. Finally it was decided to operate at atmospheric pressure and induce distillation by recirculating air through the solution in a "scrubber" and condensers using a sealed metal bellows pump.

The apparatus used is illustrated in Figure 30 . The first vessel in which the feed solution is placed, has a narrow section of 10 cm long and 2 cm in diameter, a wider section of 8 cm long and 3.5 cm in diameter, with gas inlet tubing of 0.5 cm diameter. It was immersed in a Neslab Tamson constant temperature bath. The second vessel was a condenser 24 cm long, 3.5 cm in diameter and had gas inlet tubing of 0.75 cm in diameter. It was immersed in an ice bath. The cold finger trap in the third vessel was 32.5 cm long, 6.5 cm inside diameter and 8 cm outside diameter. It was cooled with liquid nitrogen. The collecting bottle was 10 cm long, 2.8 cm in diameter and had a teflon stopcock at the side and was immersed in a liquid nitrogen bath. Teflon sleeves were used instead of grease on the glass ground joints to avoid contamination. The air flow was provided by a Metal Bellows Corp., Model MB-21 pump. The units were connected with tygon tubing. The electrical heating tape at the front section was used in order to avoid condensation and restore the air to the required temperature.

The feed solution of normally 20 to 40 g of 10 to 30 g/m^3 concentration was obtained by serial dilution of a standard solution prepared gravometrically. A known mass of the feed solution was introduced into the first vessel. The initial level of the solution was in the lower part of the wide section to ensure a larger interfacial area. The solution was then stripped by a moderate flow of air of approximately 2 cm^3/s. Most of the water content in the air stream was condensed in the ice condenser. The remaining moisture and remaining chemical content was solidified on the wall of the cool-finger trap using liquid nitrogen. The air was then warmed up to room temperature and was recycled. The residue and the distillate were collected after 3 to 5 hours depending on the properties of the compound, warmed to room temperature, combined and diluted prior to analysis.

Analysis was by either purge and trap gas chromography as described later or by total organic carbon analysis using a Beckman Instrument.

FIGURE 30

SCHEMATIC DIAGRAM OF THE RELATIVE VOLATILITY

SYSTEM FOR MEASURING HENRY'S LAW CONSTANTS

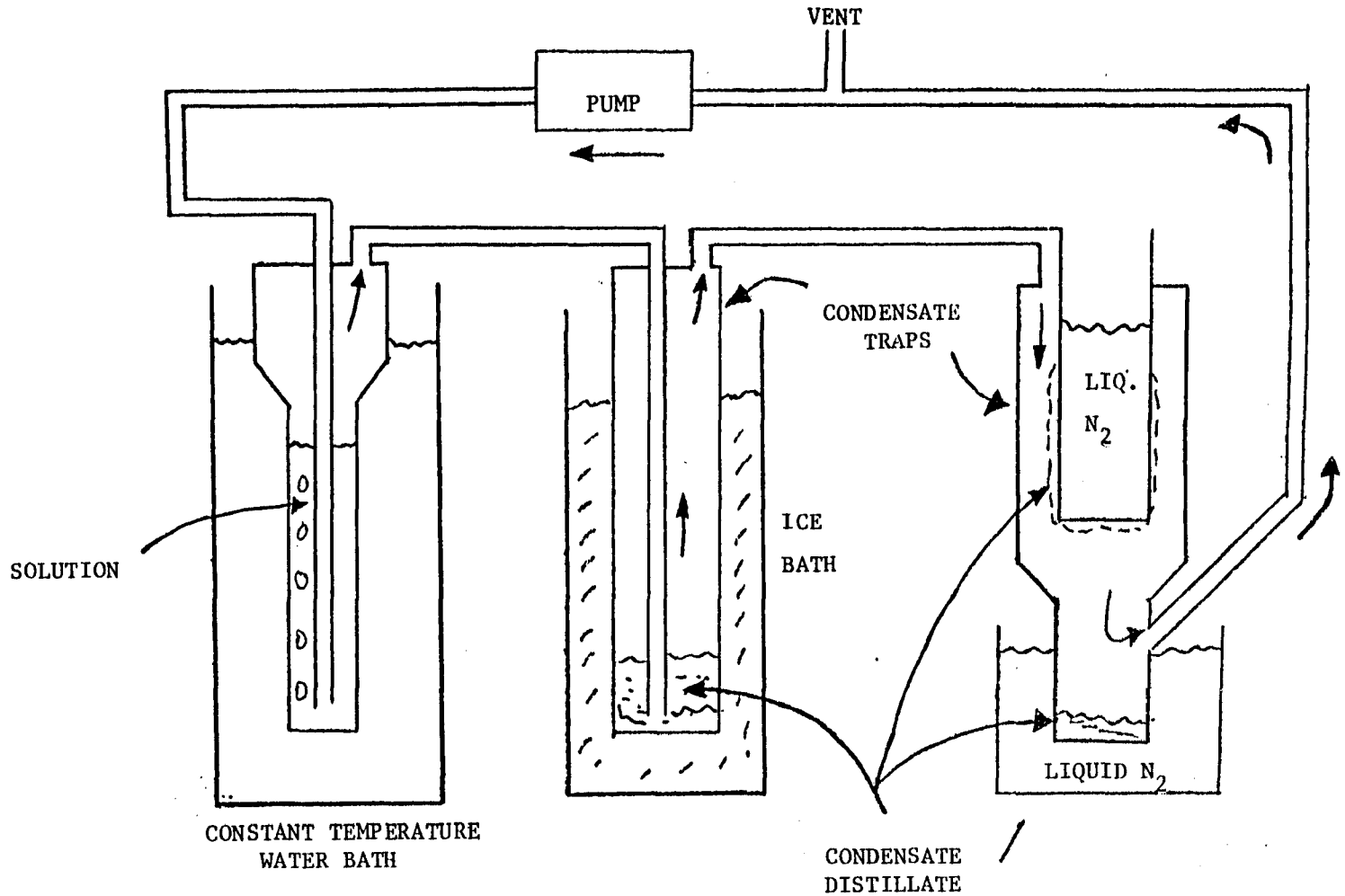

The materials used were ACS Reagent Grade (or equivalent) methanol ethanol, n propanol, n butanol, n pentanol, 2 butanol, isobutanol, 2 butanol, 2 pentanone, 2 heptanone, 3 heptanone and acetophenone. This range of compounds have Henry's Law Constants in the range of interest, i.e. up to a factor of 100 times that of water. It was normally necessary to alter the extent of distillation to obtain satisfactory concentrations.

A mass balance on the compound was determined and any obviously unsatisfactory results discarded. This mass balance check is a particularly useful feature of the technique. Generally the mass balance results were within 5%.

A sample calculation with n propanol at 25°C illustrates this procedure.

Feed 25.15 g (or $m^3 \times 10^{-6}$) concentration 24.7 g/m^3 (621 μg solute)
Residue 21.83 g concentration 6.65 g/m^3 (145 μg solute)
Distillate 3.20 g concentration 155 g/m^3 (496 μg solute)
Total solute recovered 641 μg or 103.2% of initial amount
$\alpha = 1 + \ln(C_1/C_2)/\ln(V_1/V_2) = 10.27$

The Henry's Constant of n propanol is thus 10.27 times that of water at 25°C. The vapor-pressure of water at 25°C is 0.0313 atm (Weast [76]) and its density is 0.997 g/cm^3 thus its molar concentration is 55400 mol/m^3 and H_w is 5.65×10^{-7}. It can thus be inferred that H for n proponol at 25°C is 5.8×10^{-6} atm m^3/mol. Note that this value can not be obtained accurately from solubility and vapor pressure data.

A series of determinations were done at 25°C, there being 3 or 4 replicates per compound. The results are summarized in Table 12 and show the steady increase in α as molecular weight increases.

A series of tests was undertaken at 15,25 and 35°C with 2 butanol and 2 butanone which showed that α increases slightly as temperature increases due, it is believed, to the reduction in γ_w (corresponding to the increase in water solubility). This is offset to some extent by the increase in the ratio of water to solute vapor pressure, the solute always having a lower enthalpy of vaporization.

TABLE 12

RESULTS FROM THE RELATIVE VOLATILITY APPARATUS AT 25°C

Compound	Mean Solute Mass Balance Percent	Experimental Relative Volatility
methanol	- 0.8	9.62
ethanol	+ 1.6	7.66
n propanol	- 1.0	10.7
n butanol	+ 7.3	16.3
2 butanol	- 2.3	17.5
isobutanol	+ 3.3	22.7
n pentanol	+ 3.9	22.0
2 butanone	- 1.4	62.9
2 pentanone	+17.2	51.8
2 heptanone	+18.6	35.8
3 heptanone	+26.0	28.8
acetophenone	+20.0	31.8
2 butanol (15°C)	+ 9.0	14.0
2 butanol (35°C)	+ 4.7	24.5
2 butanone (15°C)	-11.4	51.5
2 butanone (35°C)	-14.8	54.1

SOLUBILITY MEASUREMENTS WITH CO-SOLUTES

As was indicated earlier there remains some doubt about the extent to which a co-solute such as ethanol influences the solubility (and hence Henry's Law Constant) of a hydrophobic organic solute such as phenanthrene. Accordingly, a series of experiments was undertaken to determine the magnitude of this effect using phenanthrene as a model hydrophobic solute and ethanol, butanol, hexanol, octanol, and fulvic acid as co-solutes. Under the experimental conditions applicable here the solute and co-solute are truly in solution, there being no micelle or suspended phase. Concentrations of co-solutes used were mainly in the range below 5000 g/m^3 which is high environmentally but low compared to concentrations used in analytical procedures to "solubilize" the hydrophobic solutes.

The experimental procedure used was essentially that of May et al (77) in which double distilled water or a co-solute solution was pumped through a generator column containing glass beads coated with phenanthrene. The column was 6 mm outside diameter by 10 cm long containing 40-60 mesh beads. The pump was a Beckman Solution metering Pump Model 746 operated at 5 cm^3/min. The column was thermostatted at 23 C ± 0.5 C. Samples of the effluent were weighed, extracted with spectro-grade cyclohexane and analysed for phenanthrene content using an Aminco-Bowman Spectr photometer by measurement of fluorescence intensity in the linear response region.

The co-solutes used were of the purest grade commercially available and were used without purification. The fulvic acid which was obtained from Aldrich Chemical was dissolved in double distilled water and filtered prior to use, the dissolved fulvic acid content being measured by difference of amount introduced and the filter residue.

The absolute solubility of phenanthrene was determined to be 1.03 ± 0.03 g/m^3 which compares well with 1.002 ± 0.011 measured by May et al (77). Results are reported here as the ratio of the solubility in the co-solute solution to that in pure water, the objective being to determine the magnitude of this ratio as a function of co-solute concentration. The results are given in Table 13 for the five co-solutes at various co-solute concentrations. It should be noted that since there is an absolute error in the two solubilities comprising the ratio of 3%, the absolute error in the ratio is quite high. Since the experiments were done at the same time with the same instrument settings the precision is better than the accuracy and is believed to be approximately ± 0.02 of the ratio.

The results show that as expected there is generally a solubilizing effect which amounts to approximately 10% at co-solute concentrations of approximately 2000g/m^3 of alcohols. The limited solubility of octanol and fulvic acid prevented such concentrations being reached.

It is concluded from these results that at typical environmental concentrations of dissolved organic matter of 10 g/m^3, possibly reaching 100 g/m^3 in exceptional cases, that the solubilizing effect is negligible. At 1000 g/m^3 an 8% increase in solubility is indicated. It is of course possible that other solutes and co-solutes behave differently but this seems unlikely in the absence of specific interactions such as ionization or complexing. A further analysis of these data is presented later.

TABLE 13

SOLUBILITY RESULTS

Ratio of solubility of phenanthrene in solution to that in pure water at 23° (R_s), experimentally and calculated from

$$\log R_s = 0.10\ M \times 10^{-6}\ C$$

where C is co-solute concentration (g/m^3) and M is co-solute molecular weight, a value of 1000 being assumed for fulvic acid.

	Ethanol		Butanol		Hexanol		Octanol		Fulvic Acid	
C	exp.	calc.	exp.	calc.	exp.	calc.	exp.	calc.	exp.	calc.
0	1.0	1.0	1.0	1.0	1.0	1.0	1.0	1.0	1.0	1.0
7	-	-	-	-	1.02	-	-	-	1.05	-
14	-	-	-	-	1.01	-	-	-	1.05	-
24	-	-	-	-	1.01	-	-	-	-	-
60	-	-	-	-	1.02	-	-	-	1.05	-
80	1.01	-	1.04	-	1.03	-	-	-	-	-
100	-	1.001	-	1.002	-	1.002	-	1.003	-	1.02
270	-	-	-	-	-	-	1.01	-	-	-
540	-	-	-	-	1.02	-	1.01	-	-	-
800	1.06	-	1.07	-	-	-	-	-	-	-
1000	-	1.01	-	-	-	1.02	-	1.03	-	1.25
1600	1.08	-	1.08	-	-	-	-	-	-	-
3000	-	-	-	-	1.08	1.05	-	-	-	-
16000	1.18	1.15	1.35	1.31	-	-	-	-	-	-
32000	1.36	1.3	1.72	1.72	-	-	-	-	-	-
48000	1.53	1.6	-	-	-	-	-	-	-	-
64000	1.70	1.9	2.83	2.97	-	-	-	-	-	-
80000	2.00	2.3	-	-	-	-	-	-	-	-

HENRY'S LAW CONSTANTS

The apparatus used here for measuring Henry's Law constants was essentially that described previously by Mackay et al. (28) and is shown in Fig. 31 . Nitrogen was introduced through a sintered glass disk into the bottom of the gas stripping vessel filled with an aqueous solution of the compound of interest. Two versions of the system were built: one with a water jacket for coolant circulation and a second which could be immersed in a temperature bath. In the second system, samples were withdrawn from a sampling port near the top. Originally the glass vessel was made to contain 4.5 L of liquid in order that the total liquid volume change would be insignificant with larger samples taken for liquid extraction. It was later found that since the rate of concentration change was inversely proportional to the volume of liquid, a larger liquid volume tended to make the concentration change smaller and thus subject to greater error. Consequently the volume of the glass vessel was reduced to 1 L and more satisfactory results were obtained. In both cases, the system was maintained at $25^{o} \pm 1^{o}C$. The exit gas flow rate was measured by a soap bubble flow meter. The concentration of the solute in water was determined by either gas chromatography or fluorescence depending on the characteristics of the solute.

Experimental procedure:

Aqueous solutions were prepared by stirring an excess amount of the compound in a 1 L Erlenmeyer flask containing doubly distilled with a Teflon coated magnetic stirring bar for 1 day. Since it was not necessary to use a saturated solution for the experiment, a certain amount of the aqueous solution was drawn off from the flask and added to the stripping vessel, usually diluted with water. The amount was determined previously by determining an appropriate GC response or fluorescence intensity.

After the desired experimental temperature and gas flow rate were obtained, samples were taken periodically for analysis. When using the fluroescence method, the fluorescent intensities of the aqueous polynuclear aromatic hydrocarbon solutions or their cyclohexane extracts were measured. Since the fluorescent intensity is linearly related to concentration (a calibration line was prepared prior to the experiment to ensure that the concentration in the stripping apparatus was in the linear region), a plot of logarithm of fluorescent intensity versus time gives a straight line, and the Henry's law constant can be calculated from the slope. For halogenated hydrocarbons, alcohols and ketones the concentration of the aqueous solution was determined by the vapor extraction technique followed by gas chromatographic analysis. Similarly, a plot of logarithm of peak area versus time yields a straight line.

To study the effect of sorption, a sorbent, such as humic acid, fulvic acid or bentonite, was added to the stripping vessel after enough experimental points were obtained to determine the Henry's law constant of the pure solute in water. Since the sorbent materials are insoluble in water and were obtained in powder form, they formed cloudy suspensions in water. Any larger heavier particles tended to sink to the bottom in a few minutes while the smaller ones remained in the water column for a long time (a few

FIGURE 31

DIAGRAM OF HENRY'S LAW APPARATUS

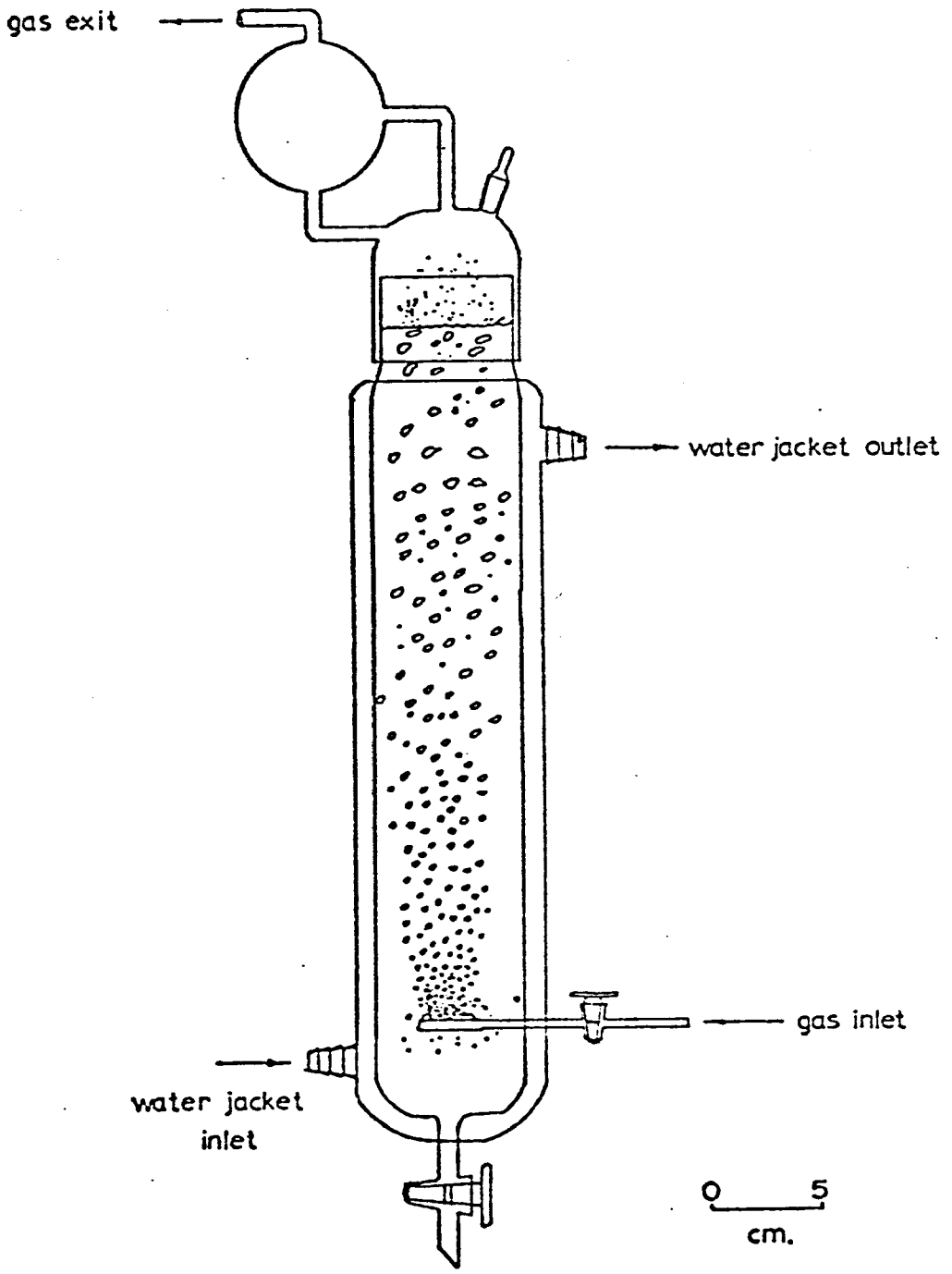

hours) before settling, leaving a slightly opaque solution. To prepare a humic acid solution, 5 g of humic acid was added to 1 L of water. At the start of the experiment, the prepared humic acid solution was shaken vigorously then allowed to settle. Approximately 10 mL of the cloudy solution was introduced to the stripping vessel. Aqueous samples were taken immediately for 10 minutes every two minutes after addition to observe the sudden drop in concentration due to sorption. Afterwards samples were collected at the same time intervals as previously.

After the experiment, the aqueous solution in the vessel was drained and collected. This solution was then filtered through a preweighted 5.0 μm Millipore filter and the filter paper dried and weighted. By taking account of the loss due to sample collection and handling, the amount of sorbent added could be estimated.

It should be noted that as samples of the aqueous solution were removed, the total volume was reduced, hence the latter part of the log (concn) - time plot became nonlinear.

The experimental difficulties involving compounds with Henry's law constant less than $1x10^{-4}$ atm-m^3/mol, as discussed in Section 4, were the small concentration changes which were comparable to accepted experimental errors when samples were taken four hours or even eight hours apart during high flow rates. It is believed that the Henry's law constant thus obtained, for example with pyrene, have higher error. For the more hydrophilic compounds, the situation was more complex since stripping efficiency, prior to GC, was low even at elevated temperature and long purging time. However, it was possible to follow the concentration change reproducibly using a specified purged time at ambient temperature.

The set of results obtained with this apparatus are given in Table 14.

TABLE 14

RESULTS OF HENRY'S LAW CONSTANT DETERMINATIONS USING THE STRIPPING APPARATUS WITH DISTILLED WATER AND IN THE PRESENCE OF FULVIC ACID (FA), HUMIC ACID (HA) AND BENTONITE (B) SORBENTS AT 25°C.

Compound	Literature Data	Experimental Henry's Law Constants atm m^3/mol		Sorbent Concentration g/m^3
		Water	Water + Sorbent	
Naphthalene	MW=128.2	4.40×10^{-4}		
	$P^s = 1.08 \times 10^{-4}$ atm	4.43×10^{-4}	3.73×10^{-4}	28.6 FA
	$C^s = 31.7 g/m^3$	4.31×10^{-4}	4.24×10^{-4}	10.0 FA
	$= 0.247 mol/m^3$	4.38×10^{-4}	3.93×10^{-4}	14.3 FA
	$H = 4.37 \times 10^{-4}$ atm m^3/mol	4.66×10^{-4}	4.18×10^{-4}	28.6 FA
	$H = 4.83 \times 10^{-4}$ atm m^3/mol (28)	4.13×10^{-4}	4.18×10^{-4}	14 HA
		4.47×10^{-4}	3.70×10^{-4}	14 HA
		4.38×10^{-4}	3.87×10^{-4}	28 HA
		4.18×10^{-4}	3.58×10^{-4}	7.71 HA
		4.42×10^{-4}	4.35×10^{-4}	19.14 HA
		4.68×10^{-4}	4.63×10^{-4}	22.3 HA
		4.56×10^{-4}	4.24×10^{-4}	36.7 HA
		4.44×10^{-4}	4.22×10^{-4}	54.1 HA
		4.50×10^{-4}	4.28×10^{-4}	20 B
		4.85×10^{-4}	4.49x10-4	100 B
		4.34×10^{-4}	4.18×10^{-4}	50 B

TABLE 14 CONTINUED

Compound	Literature Data	Experimental Henry's Law Constants atm m^3/mol		Sorbent Concentration g/m^3
		Water	Water + Sorbent	
Biphenyl	MW=154.21	3.0×10^{-4}		
	P^s=7.45x10^{-5}* atm	2.95x10^{-4}	2.96x10^{-4}	12.0 HA
	C^s=7.1g/m^3	3.23x10^{-4}	2.75x10^{-4}	12.14 HA
	=0.0460mol/m^3	3.12x10^{-4}	2.82x10^{-4}	12.0 HA
	H =4.08x10^{-4}atm m^3/mol (28)			
o-Dichlorobenzene	MW=147.01	1.90x10^{-3}		
	P^s=0.00193 atm	1.89x10^{-3}	1.88x10^{-3}	1.36 HA
	C^3=145g/m^3	1.98x10^{-3}	2.01x10^{-3}	9.52 HA
	=0.986mol/m^3			
	H =1.95x10^{-3}atm m^3/mol			
p-Dichlorobenzene	MW=147.01	2.40x10^{-3}		
	P^s=8.9x10^{-4}* atm	2.34x10^{-3}	2.44x10^{-3}	20.6 HA
	C^s=83.1g/m^3	2.48x10^{-3}	2.44.10^{-3}	13.6 HA
	=0.565 mol/m^3			

* extrapolated values

TABLE 14 CONTINUED

Compound	Literature Data	Experimental Henry's Law Constants atm m^3/mol		Sorbent Concentration g/m^3
		Water	Water + Sorbent	
1,2,3-Trichlorobenzene	MW=181.5	1.25×10^{-3}		
	$P^s=5.23\times10^{-4}$* atm	1.245×10^{-3}	$1.195.10^{-3}$	41.3 HA
	$C^s=31.5 g/m^3$	1.26×10^{-3}	1.12×10^{-3}	63.03 HA
	$= 0.170 mol/m^3$			
1,2,3,5-Tetrachlorobenzene	MW=215.9	1.57×10^{-3}		
	$P^s=1.836\times10^{-4}$* atm	1.59×10^{-3}	1.49×10^{-3}	11.6 HA
	$C^s=3.57 g/m^3$	1.57×10^{-3}	1.55×10^{-3}	31.8 HA
	$=0.0165 mol/m^3$			
Bromobenzene	MW=157.02	2.48×10^{-3}		
	$P^s=5.45\times10^{-3}$ atm	2.51×10^{-3}	2.53×10^{-3}	10.71 HA
	$C^s=410 g/m^3$	2.44×10^{-3}	2.37×10^{-3}	13.6 HA
	$=2.61 mol/m^3$			
	$H = 2.06\times10^{-3}$ atm m^3/mol			

* extrapolated values

TABLE 14 CONTINUED

Compound	Literature Data	Experimental Henry's Law Constants atm m^3/mol		Sorbent Concentration g/m^3
		Water	Water + Sorbent	
2-Pentanone	MW=86.14 P^s=1.58x10^{-2} atm C^s=43070 g/m^3 =500 mol/m^3 H = 3.16x10^{-5} atm m^3/mol	8.80x10^{-5} 8.71x10^{-5}		
2-Heptanone	MW=114.18 P^s=3.42x10^{-3} atm C^s=4340 g/m^3 =38.0 mol/m^3 H = 9.0x10^{-5} atm m^3/mol	1.74x10^{-4} 1.81x10^{-4} 1.75x10^{-4}		
Acetophenone	MW=120.16 P^s=1.32x10^{-3} atm C^s=5500 g/m^3 =45.8 mol/m^3 H =2.87x10^{-5} atm m^3/mol	1.02x10^{-5} 1.11x10^{-5} 1.07x10^{-5}		

TABLE 14 CONTINUED

Compound	Literature Data	Experimental Henry's Law Constants atm m^3/mol		Sorbent Concentration g/m^3	
		Water	Water + Sorbent		
2-Methyl-1-propanol	MW=74.12	$2.67x10^{-5}$			
	P^s= $1.32x10^{-2}$atm	$2.58x10^{-5}$			
	C^s=94875 g/m^3	$2.81x10^{-5}$			
	= 1280 mol/m^3				
	H = $1.3x10^{-5}$ atm m^3/mol				
1-Heptanol	MW=116.2	$5.3x10^{-5}$			
	P^s=$1.32x10^{-3}$atm	$5.82x10^{-5}$			
	C^s=1975 g/m^3				
	=17 mol/m^3				
	H =$7.6x10^{-5}$atm m^3/mol				
Acenaphthene	MW=154.2	$1.55x10^{-4}$			
	P^s=$3.97x10^{-5}$* atm	$1.60x10^{-4}$	$1.51x10^{-4}$	10.71	HA
	C^s=3.88 g/m^3	$1.58x10^{-4}$	$1.59x10^{-4}$	21.3	HA
	=0.0252 mol/m^3	$1.50x10^{-4}$	$1.64x10^{-4}$	15.0	HA
	H =$1.46x10^{-4}$ atm m^3/mol (28)	$1.67x10^{-4}$	$1.52x10^{-4}$	25.3	HA

* extrapolated values

TABLE 14 CONTINUED

Compound	Literature Data	Experimental Henry's Law Constants atm m^3/mol		Sorbent Concentration g/m^3	
		Water	Water + Sorbent		
Fluorene	MW=166.2	1.0×10^{-4}			
	P^s=1.64×10^{-5}* atm	9.47×10^{-5}	9.53×10^{-5}	22.8	HA
	C^s=1.90 g/m^3	9.52×10^{-5}	9.48×10^{-5}	10.5	HA
	=0.0114 mol/m^3	9.68×10^{-5}	9.58×10^{-5}	25	HA
		9.45×10^{-5}	8.8×10^{-5}	24.6	HA
Phenanthrene	MW=178.23	3.6×10^{-5}			
	P^s=4.53×10^{-5}* atm	3.55×10^{-5}	6.42×10^{-5}	17.0	HA
	C^s=1.29 g/m^3	3.71×10^{-5}	5.38×10^{-5}	15.4	HA
	=0.00724 mol/m^3	3.52×10^{-5}	6.88×10^{-5}	34.3	HA
	H =3.93×10^{-5} atm m^3/mol (28)	3.55×10^{-5}	8.29×10^{-5}	46.86	HA
Anthracene	MW=178.23	7.20×10^{-4}			
	P^s=5.04×10^{-5}* atm	7.50×10^{-4}	2.46×10^{-4}	14.0	HA
	C^s=0.075 g/m^3	8.8×10^{-4}	4.89×10^{-4}	14.0	HA
	=4.2×10^{-4} mol/m^3	6.67×10^{-3}			
	H = 6.67×10^{-3} atm m^3/mol (28)				

* extrapolated values

TABLE 14 CONTINUED

Compound	Literature Data	Experimental Henry's Law Constants atm m^3/mol		Sorbent Concentration g/m^3
		Water	Water + Sorbent	
Pyrene	MW=202.3 C^s=0.135g/m^3 =0.00067 mol/m^3	1.10×10^{-5}	pts scattered	
1-Methylnaphthalene	MW=142.2 p^s=7.8x10^{-5} atm C^s=28.5 g/m^3 =0.20 mol/m^3 H =3.54x10^{-4} atm m^3/mol	2.6 x10^{-4} 2.22x10^{-4} 2.27x10^{-4} 2.49x10^{-4}	2.01x10^{-4} 2.19x10^{-4}	9.43 HA 20.3 HA 18.7 HA
1,5-Dimethylnaphthalene	MW=156.23 C^s=3.38 g/m^3 =2.16x10^{-2} mol/m^3	3.5 x10^{-4} 3.73x10^{-4} 3.81x10^{-4} 3.62x10^{-4}	3.38x10^{-4} 3.62x10^{-4} 3.54x10^{-4}	28.7 HA 14.0 HA 25 HA
1-Chloronaphthalene	MW=162.6 C^s=22.4 g/m^3 =0.138 mol/m^3	3.55x10^{-4} 3.67x10^{-4} 3.54x10^{-4}	3.76x10^{-4} 3.65x10^{-4}	15.7 HA 25.7 HA

TABLE 14 CONTINUED

Compound	Literature Data	Experimental Henry's Law Constants atm m^3/mol		Sorbent Concentration g/m^3
		Water	Water + Sorbent	
2-Chloronaphthalene	MW=162.6	3.20×10^{-4}		
	C^s=11.67 g/m^3	3.10×10^{-4}	3.57×10^{-4}	27.4 HA
	=7.18 mol/m^3	3.24×10^{-4}	3.25×10^{-4}	20.43 HA
		3.28×10^{-4}	3.40×10^{-4}	23.6 HA
Chlorobenzene	MW=112.56	3.77×10^{-3}		
	P^s=0.0156 atm	3.1×10^{-3}		
	C^s=472 g/m^3	3.14×10^{-3}	3.0×10^{-3}	32.0 HA
	=4.19 mol/m^3	3.04×10^{-3}	3.07×10^{-3}	19.9 HA
	H =3.71×10^{-3} atm m^3/mol	3.17×10^{-3}	3.02×10^{-3}	15.6 HA
	H =3.77×10^{-3} atm m^3/mol (28)			

ANALYTICAL METHODS

The determination of the concentration of the aqueous solution was obtained by several methods. Previously UV absorption was employed to measure the concentration change of some aromatic hydrocarbons in a flow system. However, the addition of sorbents interfered with the UV adsorption, hence other methods were tested which were mainly static in nature in which small samples were removed at specified time intervals. Liquid scintillation counting was considered but rejected because of the availability of the instrument, chemicals and the disposal problems of the aqueous solution after experiments.

Fluorescence method was chosen for the analysis of polynuclear aromatic hydrocarbons because of its high sensitivity (1000 times higher than that of UV adsorption) and the sorbent did not interfere with the fluorescent intensity in the wavelength range (250 to 350 nm) and amount added (<50 ppm). Gas chromatographic analysis following vapor extraction (purge and trap technique) was used for the halogenated and more hydrophilic compounds. It was the obvious choice for the former groups of compound because of their relatively high vapor pressure and is a much simpler technique than solvent extraction for ketones and alcohols. The experimental details are given below.

1. Fluorescence

The analysis was performed on an Aminco-Bowman Spectrophotofluorometer (American Instrument Ltd). As stated earlier, the fluorescent intensity of most aqueous solutions (except pyrene) was measured using the compound specific excitation wavelength. It was not always necessary to prepare calibration solutions although the solubility of the compound under investigation should be known so that a suitable concentration giving a proper signal could be prepared before starting the experiment. 1-2 mL samples were taken from the stripping apparatus after the experiment had started, and their emission fluorescent intensity was recorded.

Since the light source of the instrument was a xenon lamp with a variation in lamp intensity sometimes greater than 10% during the course of the entire experiment (even when the light source was equipped with a magnetic arc stablizer), a standard solution was then required to use as a reference to correct for the unstable light intensity resulting in a fluctuation of fluorescent intensity. In the case of a sparingly soluble compound, such as pyrene, the fluorescent spectra of the aqueous solution was significantly different than that in a solvent, possibly due to impurities which were more soluble in water. Therefore the fluorescent intensity of cyclohexane extracts were measured for the determination of Henry's Law constants.

2. Gas chromatography

A conventional method of analyzing aqueous solution is by solvent extraction which involves several extracts and subsequent concentration of solvent until the concentration reaches a level suitable for gas

chromatography. Vapor extraction is more convenient when applied to the more volatile compounds.

A Hewlett-Packard GC Model 5840A with a 7675A Purge and Trap Sampler was employed for this analysis. The GC was equipped with both dual flame ionization detector and an electron capture detector. The analytical column was a 50 m long, 0.5 mm I.D. glass open tubular column coated with SE 30. Nitrogen was used both as carrier and purge gas. Initially, nitrogen bubbled the aqueous sample carrying the purgable content onto a Tenax-GC trap. After the purge cycle, the Tenax-GC column was heated to 200°C and the sorbed material was swept directly onto the analytical column by the carrier gas. The oven temperature was determined by the physical properties of the compound under investigation. For single compound analysis the isothermal mode was used, while for multicomponent mixture, the temperature programming mode was used if the isothermal mode did not give satisfactory resolution. The FID detector was set at 300°C.

The concentration of the sample was recorded as an area count in the chromatogram. With suitable calibration the concentration could be obtained.

SECTION 8

DISCUSSION

INTRODUCTION AND ORGANIZATION

This section consists of a discussion of the experimental results obtained

(i) in the small scale volatilization apparatus where the aims were to verify the two film model by studying 20 compounds covering a wide range in Henry's Law Constants, and to devise a test procedure which may be useful for testing the volatilization behavior of compounds of unknown volatility.

(ii) in the wind wave tank, where the primary objective was to develop correlations for mass transfer coefficients as a function of wind speed, fetch, and molecular properties.

(iii) by the relative volatility systems which is believed to be suitable for measuring Henry's Law Constants for involatile compounds.

(iv) by the measurement of Henry's Law Constants by gas stripping, which is essentially an extension of a previously devised system.

(v) by the measurement of solubility in the presence of co-solutes.

It should be noted that in the discussion of (i) and (ii) the aim is to develop correlations for K_L and K_G as a function of wind speed or turbulence solute properties and temperature. The experimental K_L and K_G values discussed apply to the specific solutes used and the initial correlations obtained apply only to these solutes. Later, general correlations are developed which, it is believed, apply to all solutes.

SMALL SCALE VOLATILIZATION APPARATUS

Characteristics as a Test Apparatus

The first objective was to devise and test a relatively simple small scale system which could be used in the laboratory to study the air-water exchange rates of compounds under various conditions of temperature, turbulence and in the presence of other dissolved and suspended materials. It is believed that the nature of the interfacial turnbulence generated by stirrers or shakers may be quite different from that which occurs at natural air-water interfaces and thus it is inherently better to generate the turbulence using air flow. If the air flow is directed linearly over a water surface it causes water drift and circulation at a rate dependent on the depth and configuration of the containing vessel. Any surface films tend to be driven to the downwind end where they are trapped. It becomes impossible to generate waves because of the short fetch. The circular swirling geometry overcomes many of these problems, permits waves to develop and turbulence levels to be achieved such that oxygen transfer rates can be achieved in the apparatus equivalent to those in the environment under various wind and fetch conditions. The 10 liter volume is convenient in that only small quantities of solute are required but substantive sample volumes can be taken without disturbing the system. Since the apparatus is closed there is minimal risk to operators of exposure to toxic substances.

The disadvantages include the inability to specify a meaningful air velocity since it varies radially, the possibility of volatilization from liquid splashed on the vessel walls and a degree of non-reproducibility of wave action which was observed between tests. This may be due to the presence of trace quantities of surface active materials which act to damp capillary waves (Davies and Rideal (18)) or to inadvertant changes in the location of the entry and exit pipes. Apparently minor changes in the flexible piping from the apparatus appeared at times to influence wave characteristics and it is possible that some acoustic resonance phenomena controlled by the nature of the upstream and downstream flow resistances may influence air flow in the apparatus. An obvious approach is to define the dimensions of the apparatus and its connecting piping in great detail such that it could be reproduced between laboratories. This may not be necessary if the transfer rates of a common solute such as oxygen are measured along with the solute of interest.

It is believed that with some refinement and closer definition the system could be used as a standard volatilization test, designed to yield kinetic information. It would thus be complementary to the thermodynamic (Henry's Law Constant) information obtained in the gas stripping or relative volatility systems. Because of the radial variation in velocity the apparatus is inherently unsuited for fundamental studies of turbulence pheonomen. The mass transfer coefficients are averages of undoubtedly varying local values.

Correlation of the Results

The results presented earlier in Table 8 show that the overall mass transfer coefficient is a strong function of the orifice plate pressure drop ΔP and hence of the air velocity. Although the actual air velocity in the pipe can be calculated the velocity over the water surface varies radially and no single value can be established. It is thus convenient to characterise the level of turbulence by the orifice plate pressure drop alone. This value depends on the dimensions of the orifice which would have to be reproduced exactly to obtain similar turbulence levels in different sets of apparatus.

It is also apparent that the lower Henry's Constant compounds volatilize more slowly as the gas phase resistance becomes significant. The effect of solute diffusivity is entirely masked by these larger effects. To analyse the data it is first convenient to fit an expression for the effect of turbulence level. This was done using a regression program to fit constants C_1, C_2, n, m and q equations of the form given below.

$$1/K_{OL} = 1/K_L + RT/HK_G$$
$$K_L = C_1 D_L^{\,n} (\Delta P - 2.0)^q$$
$$K_G = C_2 D_G^{\,m} (\Delta P - 2.0)^q$$

Here D_L and D_G are the solute molecular diffusivities. This equation implies that K_L and K_G are zero when P is 2.0 cm H_2O which is outside the experimental range. The constant q was found to have a value of 0.86. Actually a slightly lower value may be appropriate for q in the K_G equation but it can not be determined precisely. The values of n and m were determined to be 0.70 and 0.59 but the sum of squares deviation is quite insensitive to variations in the range 0.5 to 0.8 in both. Examinations of the data suggests that the variance in the data attributable to changes in D_L and D_G is so small compared to the turbulence and H effects that no accurate values can be assigned. Fortunately there are other experimental studies and theoretical predictions which strongly suggest that n should be 0.50 and m should be 0.67.

Inserting these values gives a correlation which is entirely consistent with the data. The constants C_1 and C_2 can then be determined yielding finally

$$K_L = 2990\ D_L^{0.5} (\Delta P - 2.0)^{0.86}$$
$$K_G = 19500\ D_G^{0.67} (\Delta P - 2.0)^{0.86}$$

In these equations K_L and K_G are in cm/h and D_L and D_G are in cm^2/s. The calculated K_{OL} values are given earlier in Table 8 in which the experimental and correlated values can be compared. The satisfactory fit of the data indicates that the two resistance model is valid. Another approach would be to plot $1/K_{OL}$ versus RT/H as discussed earlier. Such a plot is not as illustrative as had been hoped because of the effect of turbulence level and solute diffusivity. A precise fit in such a plot is impossible because of (i) experimental error (ii) errors in H especially for the alcohols and ketones (iii) variations in K_L and K_G between solutes because of the diffusivity effect and (iv) wave damping effects of the more polar solutes. There is clearly no need to invoke a resistance for the interface. If such a resistance exists, it can not be measured with this system. This is supported by results quoted by Sherwood et al (42) to the effect that the interfacial resistance for water evaporation

(equivalent to the "delay" as the solute leaves the liquid phase) exceeds the K_G values reported here by a factor of 1000, thus when the reciprocals of the transfer coefficients are added the interfacial resistance term is negligible.

Although it may appear that this validation of the two resistance model is unnecessary in view of the overwhelming evidence, it is believed to be justified since it is the key assumption in all volatilization calculations.

For experimental purposes it is suggested that a series of solutes including cyclohexanol, 1 pentanol, 4 methyl 2 pentanone, 2 butanone, bromoform, chlorobenzene, toluene and oxygen provide a good range of H values.

The oxygen transfer results are puzzling in that the rates are higher than are predicted from the solute data. The water diffusivity of oxygen is approximately twice that of benzene, thus one would expect an increase in K_L by a factor of 1.41 ie $\sqrt{2}$. In fact the factor is about 1.7 at low turbulence levels but falls to about 1.4 at high turbulence levels. This may be experimental error or an indication of a fundamental dependence of the power or turbulence level as is suggested by unsteady state theory. In principle, this uncertainty can be avoided by measuring the solute volatilization rate directly and not relying on ratios to oxygen transfer rates. It is probably better to use a solute such as toluene for volatilization studies and ratio transfer rates to it, rather than use oxygen which has an unusually high diffusivity. Admittedly much oxygen transfer data apparently exists for environmental conditions but there are few reliable in situ measurements because of oxygen's formation and consumption biologically.

A noteworthy observation during the data analysis was that some Henry's Law constants calculated from published data were exposed as being erroneous. For example a literature value for 3 heptanone of 1.54×10^{-5} is clearly a factor of about 10 too low. A determination was made yielding a value of 2.0×10^{-4} which gives much better agreement. Likewise cyclohexanol appears to have a value of 1.2 to 2.5×10^{-6} instead of the initially estimated value of 8.7×10^{-6} based on a suspected low published solubility. The implication is that although the system is kinetically controlled it can be used to some extent to validate thermodynamic data. This suggests that when elucidating the volatilization characteristics of new compounds it is useful to obtain kinetic data from a system such as is described here and check the consistency of the data against predictions based on correlations, which include an assumed value for H. If an error has been made in determining or calculating H by a factor of about two this will become apparent provided that H is in the gas phase controlled regime.

Multicomponent Results

Within the experimental error, it appears that solutes in mixtures behave as they would individually. A test of the validity of this claim would require a series of tests using solutes alone and in mixtures with a high degree of precision between tests. The results obtained are sufficient to indicate that any interacting effect, if present, is fairly small and certainly there is no possibility of "additive" effects. This conclusion is not surprising and greatly simplifies environmental volatilization calculations since each compound can be treated individually.

Effect of Solute Molecular Size, Diffusivity and Temperature

In these results, the effect of solute molecule size has been characterised by using the molecular diffusivity in each phase raised to an empirically determined power. Other approaches are possible, for example Tsivoglou (69,70) Rathbun (71) Smith et al (72), and Paris et al (78) have used molecular diameter. Liss and Slater (79) used molecular weight. Frequently Schmidt number is used for engineering applications to similar geometries. A brief review of the relationships between these quantities is useful.

Gas Phase

In the gas phase there is a clear relationship between molecular weight, molar volume and diffusivity which is expressed in the various correlations by Gilliland, Chapman and Enskog or Slattery and Bird as reviewed by Sherwood et al (42). The Gilliland correlation (97) is probably most convenient and is used in this study, details being given later. The diffusivity is proportional to absolute temperature to the power 1.5. When the gas Schmidt Number (Sc or $\mu/\rho D$) is calculated as a function of temperature, fortuitously it is relatively insensitive to temperature since the viscosity μ is proportional to $T^{0.5}$ and the density ρ is proportional to $T^{-1.0}$ thus when combined with the $T^{1.5}$ dependence of D the temperature effect tends to cancel.The molecular weight or volume effect thus dominates.

Liss and Slater (79) suggested using the inverse square root of molecular weight to account for solute effects on K_G but this can be criticised on two counts. First the dependence of D on molecular weight is not precisely to the power -0.5 since the size (cross sectional area) of the solute also affects the diffusivity. Second a considerable volume of experimental mass transfer coefficient data suggest a power of 0.5 to 1.0 on D, averaging approximately 0.67 hence a more accurate dependence is probably the inverse cube root of molecular weight. For example Tamir and Merchuk obtained a value recently of 0.684 for the power dependence of K_G on D_G(95,96).

The best overall approach to both solute molecular size and temperature is believed to be to use the Schmidt Number. This implies that K_G is relatively insensitive to temperature. Experiments to test this sensitivity are very difficult because varying temperature causes large changes in vapor pressure and hence in evaporation rate thus any effect on K_G will be swamped by the larger vapor pressure effect.

Liquid Phase

For liquid diffusion the most convenient correlating approach is to use the Stokes-Einstein equation as a basis and correct it for solvent differences, as for example in the Wilke-Chang correlation (Sherwood et al 42) which for dilute water solution has the form

$$D_{AB} = (\text{Constant})T/\mu_B \, V_A^{0.6}$$

where μ_B is the viscosity of water and V_A is the solute molar volume. For relating D_{AB} between solutes the molar volume is the best quantity. The temperature effect is best estimated using published data for water viscosity, which approximately halves from 1.79 cp at 0°C to 0.89 cp at 25°C. This is usually expressed in the form of an "activation energy" expression

$$\mu = \mu_o \exp(E\ (1/T - 1/T_o))$$

where E is an activation energy divided by the gas constant (approximately 2250 K for water) and the subscript refers to a reference temperature.

Diffusivity is thus a very strong function of temperature since the term T increases and μ decreases as temperature rises. A factor of approximately 2.18 applies between 0^oC and 25^oC. If a power function in T is forced, then D is proportional to T to the power 9. If an exponential function is used E is approximately -2540 when the extra dependence on T is included.

The liquid phase Schmidt number is also useful, however, unlike the gas phase Schmidt number it is very temperature dependent, the values falling rapidly with increasing temperature as μ falls and D increases, the overall effect being equivalent to an activation energy quantity E of 4790 K, i.e., the sum of 2250 for μ and 2540 for D.

Again the difficulty lies in the dependence of K_L on D, a similar power expression being invoked usually of the form

$$K_L \alpha D^n$$

where n is generally believed to lie between 0.5 and 1.0 but usually lies in the range 0.5 to 0.67.

There is often some difficulty in determining the exact value of powers in expressions of this type as is illustrated below. If experimental measurements are made for two solutes differing in molar volume by a factor of 4 then D will differ by a factor of 2.3 and K_L by a factor of 1.74 when the power is 0.67 and by a factor of 1.52 when the power is 0.50. Accurate determination of the power thus requires very accurate values of K_L preferably over a wide range of molecular sizes.

For K_L, Liss and Slater (79) suggested that the dependence be expressed as square root of molecular weight. Tsivoglou showed that ratio of molecular diameter gave an adequate correlation for the inert gases, a result found by Paris et al (78) to fit PCB data. Penetration theory suggests a power of -0.5 on Schmidt number or the equivalent 0.5 on diffusivity. Since diffusivity is proportional to molar volume to the power -0.6 and molar volume is proportional to molecular diameter to the power 3.0 it follows that diffusivity is proportional to diameter to the power -1.8 (i.e. 3.0 times -0.6). It follows that Tsivogolou's observation is in close agreement with penetration theory since it predicts a power of -0.9 (i.e. 0.5 times -1.8). The Liss assumption implies that the power on Schmidt number is near unity which could occur only during steady state near stagnant-diffusion. The experimental data obtained here support a power of 0.5 on diffusivity and it is thus concluded that the evidence favors adoption of this value, at least until evidence to the contrary is forthcoming. It is possible that more refined experimentation involving simultaneous volatilization of compounds with a wide range of diffusivities could produce a more accurate value. Further, it should be noted that there are theoretical fluid mechanical reasons for suggesting that the power may be a function of level of turbulence.

The effect of temperature on K_L is more easily measured than that of K_G and such data indirectly give an indication of the likely value of the power on D or Sc. In this study the values of K_L for benzene and toluene fell from 15 cm/h at 25°C to 12 cm/h at 15°C, a variation of 2.2% per degree around the mean temperature of 20°C. Downing and Truesdale (80) in a more exhaustive study of temperature found that K_L varied by from 1.52 to 3.12% per degree around 20°C and with an average of 2.21% with a standard deviation of 0.5%.

A solute with a liquid Schmidt Number of 1000 at 20°C will have a Schmidt Number at 19°C of

$$1000 \exp(-4790(1/293 - (1/293 - 1/292)) = 1058$$

i.e. a 5.8% increase. Raising Sc to the power -0.5 thus reduces K_L by a factor equivalent ot 2.8% for this one degree change. This is in excellent agreement with the present work and that of Downing and Truesdale thus it is concluded that the use of the Schmidt Number characterises both molecular size and the temperature effect. No separate temperature correction is thus necessary.

There remains a possibility that temperature may influence volatilization under conditions of water condensation from the atmosphere as may occur at night when the relative humidity rises due to surface radiative cooling. This effect has not been investigated here.

WIND WAVE TANK

The general aim in this section is to interpret the experimental results in the light of recent observations of wind-wave hydrodynamics and develop reliable prediction procedures for environmental volatilization calculations. Specifically, the aim is to obtain equations for K_L and K_G as a function of wind speed, fetch and solute Schmidt Number.

It is believed that a dual approach is required. Many environmental scientists undertaking volatilization calculations are primarily concerned about the processes which comprise the overall fate of the solute, thus there is insufficient time to obtain a deep understanding of the fluid mechanics at the air-water interface. For them a simple expression in terms of 10 m wind speed is sufficient. To oceanographers this approach is excessively simplistic and an adequate understanding requires evaluation of drag coefficients, friction velocities, Reynolds and Froude Numbers. An attempt is made to satisfy both.

The hydrodynamic results are examined first. Velocity profiles were measured at wind speeds from 5 to 14 m/s free stream velocities. Profile differences were encountered with distance along the tank and to accommodate this effect the individual profiles were fitted to the logarithmic velocity profile by plotting velocity against logarithm of height to obtain the friction velocity U^* and Z_o the surface roughness as was described earlier in the experimental section. The values of U^* and Z_o were then averaged as shown in Table 15. The drift velocities were measured as the final values at the end of the tank. Examination of these velocities showed that they were an average of 2.82% of the wind speed in excellent agreement with other studies.

The 10 cm drag coefficient C_D as calculated from the free stream velocity U_∞ and U^* show a distinct trend of becoming smaller at low velocities, in general agreement with oceanic observations. The absolute values are high compared to oceanic values (which rarely exceed 3×10^{-3}) due, it is believed, to the short fetch.

The constant "a" in the Charnock relationship calculated as $Z_o g/U^{*2}$ shows remarkable constancy apart from the lowest wind speed point which is possibly in error due to a low value of Z_o. It appears that above a wind speed of 6 m/s a mean value of 0.0093 applies. This is in excellent agreement with Smith's (61) suggestion of 0.01 and is somewhat lower than the value of 0.0156 suggested by Wu (60). The accuracy here is probably no better than 20%. An implication of these results is that the Froude scaling law appears to apply.

The roughness Reynolds Numbers are in the transition and rough regions (the boundary being at approximately 2.0) thus it is possible that this analysis breaks down at lower velocities when the water surface becomes very smooth. This transition to another regime was suggested by Cohen et al (58).

Hidy and Plate (81) proposed a relationship between U_∞ and U^* for

laboratory tanks of the form

$$U^* = (3.41 \times 10^{-4}\ U_\infty)^{0.5}\ U_\infty$$

which is equivalent to the statement that C_D is given by $3.41 \times 10^{-4}\ U_\infty$. This is in satisfactory agreement with the values obtained here.

Consideration of these results leads to the conclusion the wind wave tank results are consistent with other studies in that the drag coefficients C_D calculated from the friction velocity and the free stream velocity U_∞ (which is close to the 10 cm velocity) are in range 2×10^{-3} to 6×10^{-3}, values which are higher than oceanic or lake values. A correlation of C_D for these results is

$$C_D = 4.0 \times 10^{-4}\ U_\infty$$

It is thus possible to estimate U* from U as

$$U^* = U_\infty C_D^{\ 0.5} = 2.0 \times 10^{-2}\ U_\infty^{\ 1.5}$$

Using a value of 0.01 for the Charnock constant "a", the surface roughness Z_o can thus be deduced as being

$$Z_o = 0.01\ U^{*2}/g = 4 \times 10^{-6}\ U_\infty^{\ 3}/g = 4.08 \times 10^{-7} U_\infty^{\ 3}$$

since g is 9.81 m/s^2.

The only serious discrepancy is at low wind speeds where Z_o appears to be lower than expected, possibly due to a more "glassy" surface. In a similar study with a smaller tank Cohen et al (58) obtained larger roughness heights which may be attributable to different aerodynamic conditions. When the wind speed is below 5 m/s it appears that the roughness height becomes negligible and thus probably can not be measured accurately.

The roughness Reynolds Number Re^* in the tank can be estimated as

$$Re^* = \rho U^* Z_o/\mu = 8.16 \times 10^{-9} U_\infty^{\ 4.5} \rho/\mu = 5.40 \times 10^{-4} U_\infty^{\ 4.5}$$

For air at 20°C is 0.00120 g/cm^3 and μ is 181×10^{-6} poise (g/cm.s) thus ρ/μ is 6.62 s/cm^2 or 6.62×10^4 s/m^2.

Under lake or oceanic conditions it is necessary to use another expression for the drag coefficient, Smith's (61) correlation being suitable namely

$$C_D = 10^{-4}(6.1 + 0.63\ U_{10})$$

It follows that

$$U^* = 10^{-2}(6.1 + 0.63\ U_{10})^{0.5}\ U_{10}$$

and

$$Z_o = a\ U^{*2}/g = 1.02 \times 10^{-5}\ U_{10}^{\ 2}(6.1 + 0.63)\ U_{10}^{\ 0.5}$$

since g is 9.81 m^2/s and

TABLE 15. HYDRODYNAMIC RESULTS FROM THE WIND WAVE TANK

Screen No.	Position A (1.4 m)			Position B (4.2 m)			Drift Velocity	Average					
	U_∞ m/s	U* m/s	Z_o m x 10^3	U_∞ m/s	U* m/s	Z_o m x 10^3	m/s	U_∞ m/s	U* m/s	Z_o m x 10^3	Re*	C_{D10} x 10^3	a
0	12.84	0.884	0.522	13.53	1.102	1.290	0.395	13.20	0.993	.906	54.2	5.66	0.00900
1	11.59	0.737	0.355	11.78	0.960	1.070	0.344	11.67	0.849	.713	36.5	5.29	0.00970
2	9.95	0.638	0.301	10.66	0.712	0.556	0.290	10.31	0.675	.429	17.5	4.29	0.00924
3	8.59	0.422	0.185	8.55	0.487	0.232	0.222	8.57	0.455	.209	5.73	2.82	0.00990
4	6.89	0.357	0.084	7.28	0.406	0.169	0.200	7.09	0.381	.127	2.91	2.89	0.00858
5	-			5.96	0.271	0.044	0.158	5.96	0.271	.044	0.72	2.06	0.00587

$$Re^* = 1.02 \times 10^{-7}\ U_{10}{}^3(6.1 + 0.63\ U_{10})^{1.5}\rho/\mu$$
$$= 6.75 \times 10^{-3} U_{10}{}^3(6.1 + 0.63\ U_{10})^{1.5}$$

In principle it should be possible to relate mass transfer coefficients in the tank to those in the environment using U*, Z_o and Re* as defined above.

Liquid Phase Controlled Mass Transfer

The liquid phase mass transfer data can be interpreted in isolation by examining the K_L values for benzene and toluene volatilization which are almost totally liquid phase resistant systems. Table 16 gives these data. The benzene and toluene values are within experimental error of each other which is not surprising given their similar molar volumes. To assist interpretation, the mean value of K_L is calculated, converted to m/s and its ratio to U* calculated. These values are tabulated and show remarkable constancy in the range 94 to 110. An important inference from this is that the friction velocity U* is the primary determinant of K_L. There is an apparent tendency for K_L/U^* to increase at low velocities which implies that there will be a small but negative power on the roughness Reynolds Number in a Stanton Number correlation.

The simplest correlation is

$$St_L^* = K_L/U^* = 1.02 \times 10^{-4}$$

Table 16 gives the correlated values which compare well with the experimental values especially in the mid range but there are deviations at the high and low wind speeds. An improved correlation, obtained at the expense of another term is

$$St_L^* = K_L/U^* = 1.09 \times 10^{-4}\ Re^{*-0.03}$$

Table 16 gives the correlated values for this equation. Use of the Re^* equation tends to give higher K_L values at low wind speeds but the maximum difference between the correlations is 8% which is not large considering the experimental error and the uncertainty about mean environmental wind speeds. Which correlation is preferable is a matter of judgement.

The mean Schmidt Number Sc_L for these systems is 1118 thus forcing a -0.5 power on Sc_L and gives the general correlation

$$St_L^* = 34.1 \times 10^{-4}\ Sc_L{}^{-0.5}$$

or

$$St_L^* = 36.4 \times 10^{-4}\ Re^{*-0.03} Sc_L{}^{-0.5}$$

These correlations can be converted to forms involving U_{10} by substituting the equations for U* and Re* in terms of U_{10} for the environment or U_∞ for experimental tanks.

TABLE 16

WIND WAVE TANK MASS TRANSFER RATES FOR BENZENE AND TOLUENE

U_∞ m/s	U* m/s	Re*	Benzene K_L cm/h	Benzene K_L m/sx10^{6}	Toluene K_L cm/h	Toluene K_L m/sx10^{6}	Mean K_L/U^*x10^6	Correlated K_L (m/s) x10^6 (1)	Correlated K_L (m/s) x10^6 (2)
13.2	0.993	54.2	34.0	94.4	33.7	93.6	94.7	101.3	96.0
11.67	0.849	36.5	26.4	73.3	28.6	79.4	90.0	86.6	83.1
10.31	0.675	17.5	22.5	62.5	24.8	68.9	97.3	68.9	67.5
8.57	0.455	5.73	18.4	51.1	18.6	51.7	112.9	46.4	47.1
7.09	0.381	2.91	13.3	36.9	16.9	46.9	101.1	38.9	40.2
5.96	0.271	0.72	11.4	31.6	9.6	26.7	107.6	27.6	29.8

Equation (1) $K_L = 1.02 \times 10^{-4}\ U^*$

Equation (2) $K_L = 1.09 \times 10^{-4}\ U^*\ Re^{-0.03}$

Environmental Conditions, U_{10} is 10 metre wind speed

$$U^* = 10^{-2}(6.1 + 0.63\ U_{10})^{0.5}\ U_{10}$$

$$Re^* = 6.75 \times 10^{-3}\ U_{10}^{3}(6.1 + 0.63\ U_{10})^{1.5}$$

Simple version

$$K_L = 34.1 \times 10^{-4}\ U^*\ Sc_L^{-0.5}$$

$$= 34.1 \times 10^{-6}\ (6.1 + 0.63\ U_{10})^{0.5}\ U_{10}\ Sc_L^{-0.5}$$

Reynolds Number version

$$K_L = 36.4 \times 10^{-6}\ U^*\ Re^{*-0.03}\ Sc_L^{-0.5}$$

$$= 42.3 \times 10^{-6}\ (6.1 + 0.63\ U_{10})^{0.455}\ U_{10}^{0.91} Sc_L^{-0.5}$$

since $Re^{*-0.03} = 1.16\ U_{10}^{-0.09}\ (6.1 + 0.63\ U_{10})^{-0.045}$

Laboratory conditions, U_∞ is free stream velocity

$$U^* = 2.0 \times 10^{-2}\ U_\infty^{1.5}$$

$$Re^* = 5.4 \times 10^{-4}\ U_\infty^{4.5}$$

Simple version

$$K_L = 34.1 \times 10^{-4}\ U^*\ Sc_L^{-0.5}$$

$$= 68.2 \times 10^{-6}\ U_\infty^{1.5} Sc_L^{-0.5}$$

Reynolds Number version

$$K_L = 36.4 \times 10^{-4}\ U^*\ Re^{-0.03} Sc_L^{-0.5}$$

$$= 91.0 \times 10^{-6}\ U_\infty^{1.365} Sc_L^{-0.5}$$

since $Re^{*-0.03} = 1.25\ U_\infty^{-0.135}$

Strictly, the temperature variation of Re* should be included but the effect is negligible because of the low power.

Table 17 gives calculated environmental values of K_L using these equations for a compound of Schmidt Number 1000. The effect of lower temperature is to increase Sc_L thus reducing K_L. The magnitude of this effect has been discussed earlier.

These equations are markedly different in form from those of Bank (82,83) and Sivakumar (84) which were developed from data at lower velocities. They are in good agreement with the form suggested by Deacon (85).

Gas Phase Controlled Mass Transfer

The K_G data obtained from water evaporation measurements given earlier in Table 11 are presented in Table 17 in which the ratios of K_G to U^*_∞, U , and $U_\infty^{0.78}$ are also calculated. The K_G/U^* group shows no significant trend the average value being 65.0×10^{-3} with a maximum deviation of 7.3×10^{-3} or 11%. The other groups show what is believed to be a significant trend for the ratio to be lower at low wind speeds. Following the procedure used for K_L it is proposed that the data be represented by an equation of the type

$$St_G^* = K_G/U^* = 65.0 \times 10^{-3} \text{ for water } (Sc_G = 0.6)$$

$$\text{or } St_G^* = K_G/U^* = 46.2\, Sc_G^{-0.67} \times 10^{-3}$$

The reason for introducing the $U_\infty^{0.78}$ term was that Mackay and Matsugu(64) developed a correlation for gas phase controlled evaporation which included this term, however the data were obtained at lower wind speeds and that correlation severely underestimates K_G at high wind speeds, probably due to the wave action. That correlation also included a fetch term which is necessary in any correlation using U_∞ to take into account the change in evaporation rate as the flow becomes steady and C_D falls at high fetch. It is postulated here that including the variable C_D term (for calculating U* from U_∞) removes the necessity to include a fetch term.

The values of K_G calculated from the above correlation are given in Table 18.

The correlation can be expressed in terms of U_{10} and U_∞ as follows

$$U^* = 10^{-2}(6.1 + 0.63\, U_{10})^{0.5} U_{10}$$

$$K_G = 46.2\, U^* Sc_G^{-0.67} \times 10^{-3}$$

$$K_G = 46.2 \times 10^{-5}(6.1 + 0.63\, U_{10})^{0.5} U_{10} Sc_G^{-0.67}$$

Laboratory conditions, U_∞ is free stream velocity.

$$U^* = 2.0 \times 10^{-2} U_\infty^{1.5}$$

$$K_G = 92.4 \times 10^{-5} U_\infty^{1.5} Sc_G^{-0.67}$$

TABLE 17

WIND WAVE TANK GAS PHASE CONTROLLED MASS TRANSFER COEFFICIENTS FOR WATER

U_∞	U^*	Re^*	K_G m/sx10 ^{3}	K_G/U^* x10^3	K_G/U_∞ x10^4	$K_G/U_\infty^{0.78}$ x10^4	K_G(Eq1) x10^3
13.20	0.993	54.2	71	71.5	53.8	94.9	64.5
11.67	0.849	36.5	55	64.8	47.1	80.9	55.2
10.31	0.675	17.5	39	57.7	37	63.2	43.9
8.57	0.455	5.73	29.7	65.3	34.6	55.6	29.6
7.09	0.381	2.91	22.2	58.3	31.3	48.2	24.8
5.96	0.27	0.72	19.4	71.8	32.5	48.2	17.6

Eq(1) $K_G/U^* = 65.0 \times 10^{-3}$

TABLE 18

ENVIRONMENTAL AND LABORATORY VALUES

OF K_L AND K_G FOR A COMPOUND OF $Sc_L = 1000$ AND $Sc_G = 0.6$

U_∞ or U_{10}	K_L environmental		K_L laboratory		K_G environment		K_G laboratory	
	$m/s \times 10^6$	cm/h	$m/s \times 10^6$	cm/h	$m/s \times 10^3$	cm/h	$m/s \times 10^3$	cm/h
0	0	0	0	0	0	0	0	0
2.0	5.8	2.1	6.1	2.2	3.5	1270	3.68	1325
5.0	16.4	5.9	24.1	8.7	9.9	3560	14.5	5236
8.0	28.8	10.4	48.8	17.6	17.4	6250	29.4	10600
10.0	37.9	13.7	68.2	24.5	22.9	8250	41.1	14800
13	52.9	19.1	101	36.4	32.0	11500	61.0	22000
15	63.7	22.9	125	45.1	38.5	13900	75.6	27200
20	93.2	33.6	192	69.4	56.3	20300	116	41900
25	126	45.3	269	97.0	76.0	27400	162	58500
30	161	58.2	354	127	97.6	35100	213	77000

Entire K_{OL} Data Set

Having established the two equations for K_L and K_G it is possible to apply them to the entire set of K_{OL} data for the compounds of various values of Henry's Law Constant. This is essentially a test of the validity of the two resistance model. The equation used is

$$1/K_{OL} = 1/K_L + RT/HK_G$$

$$K_L = 68.2 \times 10^{-6}\ U^{1.5}\ Sc_L^{-0.50}$$

$$K_G = 92.4 \times 10^{-5}\ U^{1.5}\ Sc_G^{-0.67}$$

The correlated K_{OL} values are given earlier in Table 10 in the experimental section. Comparison of these experimental and correlated values is a test of the K_L and K_G correlations both as a function of Schmidt number and wind speed and of the two resistance theory. Agreement is excellent for the compounds of higher volatility. Somewhat poorer agreement is apparent for the alcohols, partly it is suspected because the Henry's Law Constants are in error and partly because of wave damping. The agreement is regarded as sufficient to lend further confidence to using the two resistance model in volatilization calculations.

Comparison with Other Studies

A number of studies have reported K_L and K_G values obtained in wind wave tanks and in the environment. It is instructive to compare the correlations derived here with these data notably those in wind wave tanks by Liss(86), Downing and Truesdale (80), Kanwisher (87), Hoover and Berkshire (88) and Cohen et al (58) and for the environment by Broecker and coworkers (89,90,91), Emerson (92,93,94) and Schwartzenbach et al (2).

Gas Phase Resistance (K_G)

Liss (86) measured K_G for water and K_L for oxygen in a wind wave tank and reported friction velocities, the conditions being at lower wind speeds than were used in this study.At a 10 cm velocity of 6.0 m/s Liss obtained a friction velocity of 0.31 m/s which compares well with the 0.27 m/s obtained in this study. Under these conditions,and as shown in Figure 32, Liss obtained a K_G of 7451 cm/h or 20 x 10^{-3} m/s which compares well with the 19.4 x 10^{-3} m/s in this study. The ratio of K_G/U^* obtained by Liss from 1.6 to 8.2 m/s averaged 63 x 10^{-3} which is in remarkable agreement with the present 65 x 10^{-3}. Again there was no trend in K_G/U^* with wind speed.

Sverdrup (98) reported oceanic evaporation rates over a range of velocities. The trend was for K_G to rise from 6 x 10^{-3} m/s at 3 m/s wind speed to 14 x 10^{-3} m/s at 8.5 m/s. Pond et al (99) also obtained data which agree with these values, being 8.7 x 10^{-3} m/s at 6.8 m/s wind speed. Applying the correlation to these environmental conditions yields K_G values of 5.5 x 10^{-3} m/s at 3 m/s to 18.6 x 10^{-3} m/s at 8.5 m/s in very satisfactory agreement. Pond's velocity of 6.8 m/s should yield a friction velocity of 0.22 m/s (0.256 was obtained experimentally) and a K_G of 14.2 x 10^{-3} m/s (8.7 x 10^{-3} m/s was observed). Clearly the correlation agrees well with both other wind wave tank studies and oceanic data although at very low wind speeds, ie below 3 m/s the laboratory data seem unusually high. The most important point is that analysing the data in this way predicts a considerable difference between laboratory and oceanic data which is borne out by observation. These data are shown in Figure 32.

Liquid Phase Resistance (K_L)

The laboratory data are plotted in Figure 33 corrected to 20°C and a Schmidt Number of 1000. Essentially this involves multiplying the O_2 and CO_2 data by 0.75, the benzene and toluene data by 1.06. There is a fairly wide scatter in the data attributable to differences in tank geometries, the smaller tanks tending to have larger coefficients, probably as a result of larger drag coefficients. The line given by the equation gives a good fit of the present data but tends to underestimate the high velocity data and overestimate the low velocity data, especially those of Liss. A better fit to all these data could be obtained by making the drag coefficient fetch dependent and forcing a lower drag coefficient at low wind speeds. A one-constant equation for C_D is thus too simple and it is necessary to use different expressions at high and low wind speeds. The most serious discrepancy is between the present work and that of Liss (79) at 6 to 8 m/s where there are similar friction velocities but the mass transfer coefficients differ by a factor of two. For example at 8 m/s Liss obtained coefficents of about 30 x 10^{-6} while in the present work a value of about 50 x 10^{-6} m/s was obtained, Cohen et al (58) obtaining about 60 x 10^{-6} m/s and Kanwisher (87) 85 x 10^{-6} m/s, the values being corrected for Schmidt Number. The reasons for this discrepancy are not known although it may be related to the shallowness of Liss's tank (10 cm) but the weight of evidence favours the higher values as suggested by the correlation. It seems likely that the correlation overestimates K_L in the low wind speed range of 0 to 4 m/s when the water surface is fairly calm.

The best available environmental data are from radon flux measurements in Atlantic (BOMEX), Pacific (Papa) by Broecker and Peng (89), Peng et al (91), for small lakes by Emerson (92,93) and for p dichlorobenzene in Lake Zurich by Schwartzenbach et al (2). The oceanic radon data give values of K_L of approximately 40 x 10^{-6} m/s at 12 m/s and 21 x 10^{-6} m/s at 7 m/s which are in good agreement with the environmental prediction. Emerson's lake data range from 0.07 to 0.25 m/day (0.8 to 2.9 x 10^{-6} m/s) at a probable wind speed of 1 to 2 m/s. At 1 m/s the environmental correlation predicts 3 x 10^{-6} m/s which is in fair agreement.

Paradichlorobenzene has a water solubility of approximately 83 g/m^3 and a vapor pressure of 9 x 10^{-4} atm thus H is approximately 1.6 x 10^{-3} atm m^3/mol. At a wind speed of 2 m/s K_L will be approximately 5 x 10^{-6} m/s and K_G 3.3x10^{-3} m/s thus with RT equal to 0.024

$$1/K_{OL} = 1/K_L + RT/K_G$$

$$= 0.20 \times 10^6 + 0.02 \times 10^6 = 0.22 \times 10^6$$

$$\text{and} \quad K_{OL} = 4.5 \times 10^{-6} \text{ m/s or } 1.6 \text{ cm/h},$$

with the system being 90% liquid phase resistant. Schwartzenbach et al (2) obtained a value of 1 cm/h but did not quote on average wind speed for this long but narrow lake. The discrepancy could be due to wind speed, diurnal effects, mass balance errors or of course the correlation. It is also possible that an appreciable water column resistance may be present. Given these uncertainties the agreement is encouraging.

The principal concern is that the laboratory and environmental equations overestimate K_L at low wind speeds. It appears that at low function velocities the relationship suggested here may break down because of onset of smooth conditions in a manner analogous to the laminar-turbulent transition in pipe flow. Support for this is found in the observation that the environmental prediction equation yields higher K_L values at 2 to 4 m/s than are found in tanks. Further careful K_L measurement at low wind speed is required in long tanks and in ponds to resolve this problem. Given this uncertainty the error limits on the predicted environmental values are placed at +10% and -40% i.e. a predicted value of 10 is believed to lie between 6 and 11.

The general conclusion is that these equations provide satisfactory methods of correlating both laboratory and environmental mass transfer coefficient data. The apparent discrepancy between laboratory and environment is attributed to a difference in drag coefficient which is higher in small tanks. The key scale-up variable is believed to be the friction velocity for which a K_L and K_G relationship is suggested. It is possible that roughness Reynolds number "corrections" may be necessary but given the present level of accuracy it is doubtful if they are needed. The most useful data to improve these correlations are

(i) further tank measurements of K_L at low wind speeds where there is an apparent discrepancy
(ii) pond measurements with varying wind speed
(iii) a systematic study of the effect of Schmidt number for a range of solutes including oxygen, inert gases, CO_2 and organic solutes over a range of temperature
(iv) studies of the effects of additional resistances provided by organic microlayers, as discussed earlier.

FIGURE 32

EXPERIMENTAL AND CORRELATED VALUES OF K_G

FOR SCHMIDT NUMBER 0.60

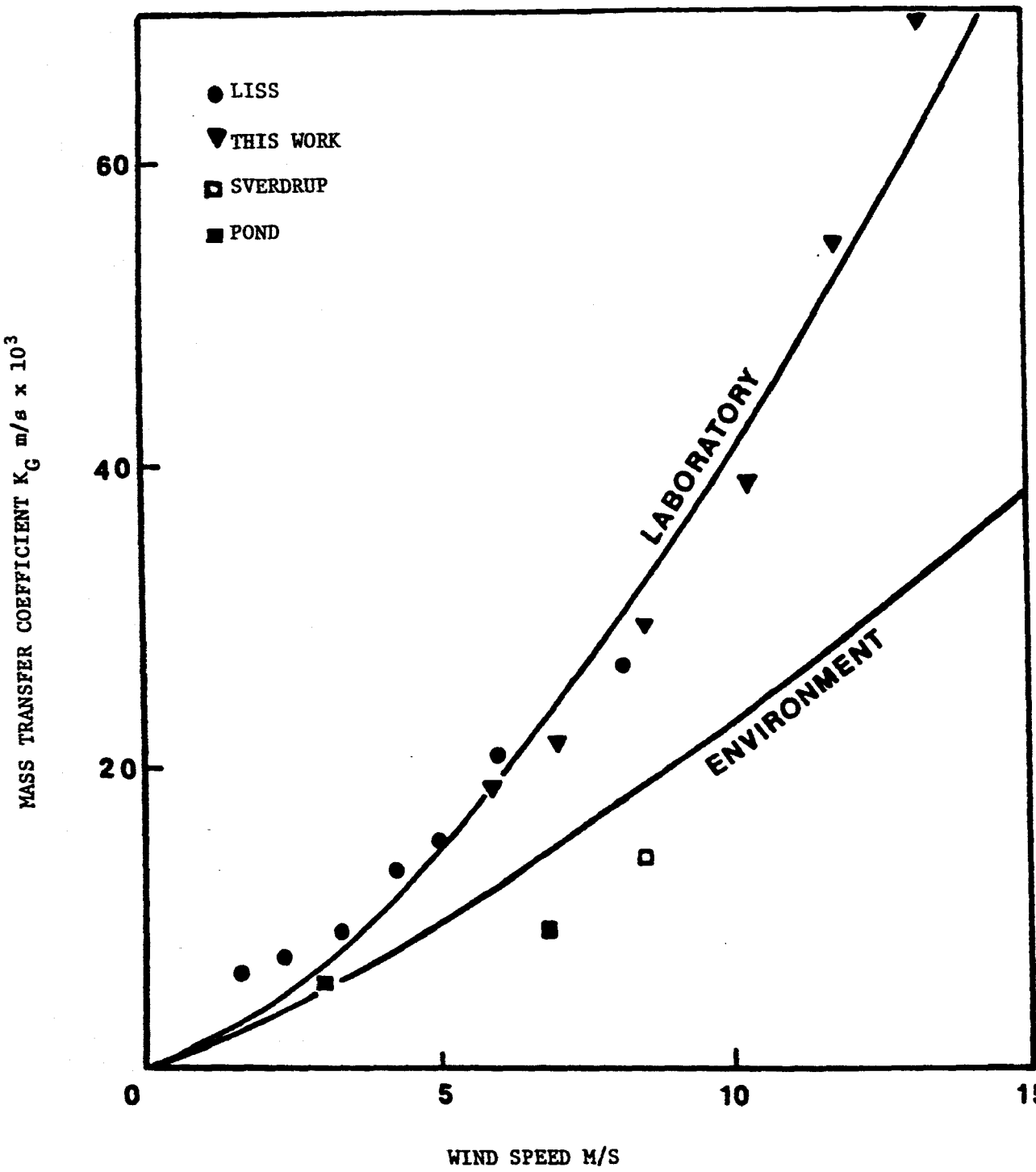

FIGURE 33

EXPERIMENTAL AND CORRELATED VALUES OF K_L

CORRECTED TO A SCHMIDT NUMBER OF 1000

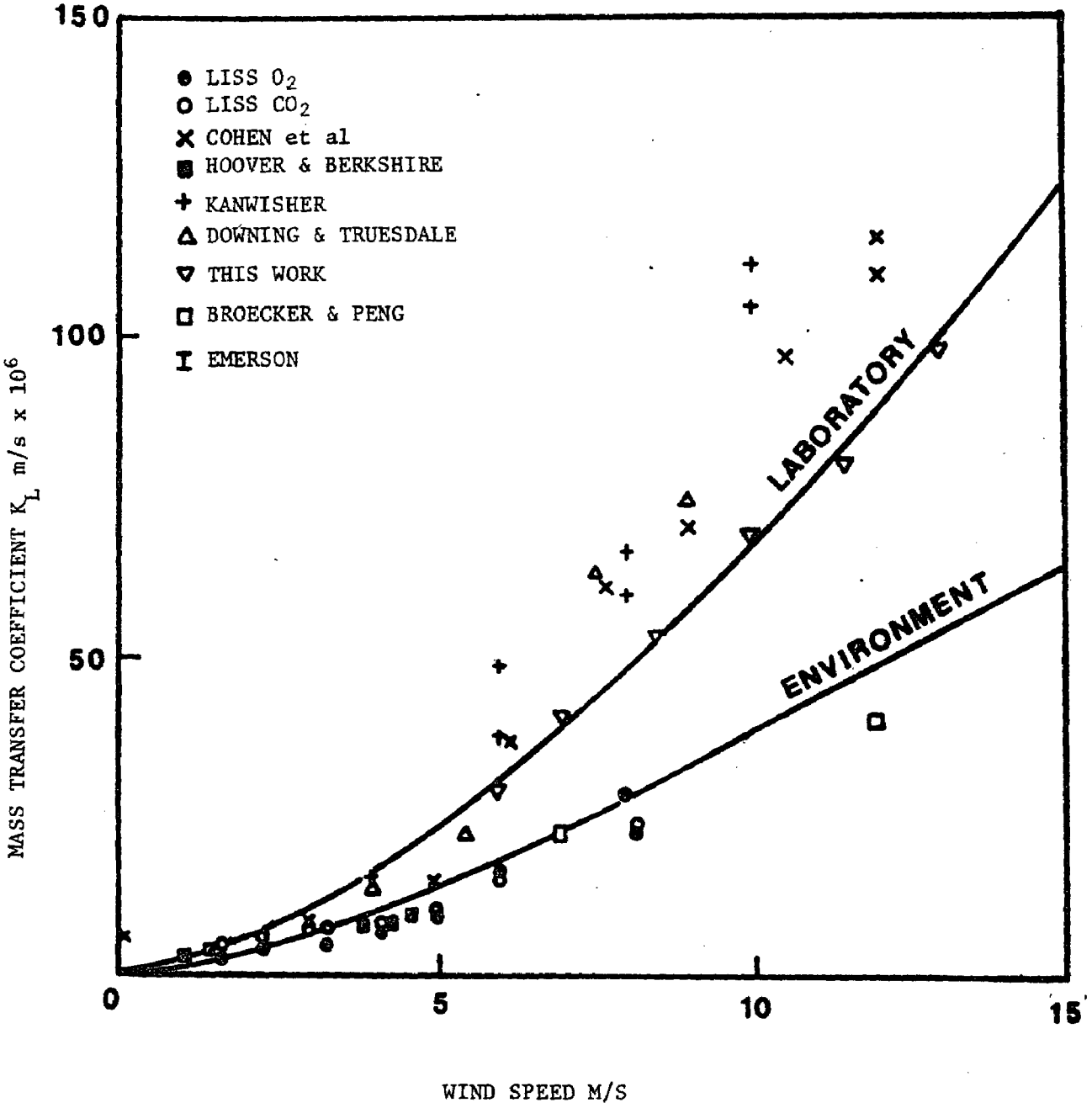

RELATIVE VOLATILITY APPARATUS

The results given earlier in Table 12 suggest that the method is capable of yielding solute mass balances better than 10% in most cases, but for higher molecular weight sparing soluble compounds there is less satisfactory recovery of the solute. The reasons for this are not clear and it is believed that further investigation could result in improved techniques and correspondingly better recoveries.

Since most of these compounds are fairly soluble in water the solute Henry's Law Constant (H_s) can not be expressed meaningfully as a ratio of vapor pressure to solubility. The fundamental definition of H is the ratio of solute partial pressure to concentration which, it has been shown is given by:

$$H_s = \gamma_s v_w P_s^s = H_w \alpha = \alpha P_w^s v_w$$

$$\text{and } \alpha = \gamma_s P_s^s / P_w^s$$

where γ_s is the infinite dilution activity coefficient of the solute in water, v_w is the molar volume of water (18×10^{-6} m^3/mol), P_s^s and P_w^s are the solute and water vapor pressures (atm), α is the relative volatility and Hw is the Henry's Law constant for water between air and pure water.

Values of γ_s can be obtained from vapor liquid equilibrium data and have been correlated by Pierotti et al as reviewed by Reid et al (14). The usual approach is to use an equation of the form

$$\log \gamma^s = A + BN + C/N$$

where N is the carbon number and A,B and C are constants applicable to a homologous series. Selected values of these constants are given in Table 19 below (Reid et al 14).

TABLE 19

CONSTANTS FOR INFINITE DILUTION ACTIVITY

COEFFICIENTS IN WATER AT 25°C

Solute	A	B	C
n Acids	-1.00	0.622	0.490
n Primary alcohols	-0.995	0.622	0.448
n Secondary alcohols	-1.220	0.622	0.170
n Tertiary alcohols	-1.740	0.622	0.170
Aldehydes	-0.780	0.622	0.320
Ketones	-1.475	0.622	0.500
Ethers (20°)	-0.770	0.640	0.195
Esters	-0.930	0.640	0.260

Using these correlations it is possible to estimate γ if vapor pressure data for the solute and water are available. This is done in Table 20 which shows that

α tends to increase with increasing carbon number. This effect is not clear since α depends on γ^{∞} (which increases with carbon number by about a factor of 3 per carbon added) but also on the vapor pressure of the solute P^s (which tends to decrease by a similar factor) thus the net effect is not large or immediately obvious.

Also given in Table 20 are the experimental values reproduced from Table 12. Agreement is good for compounds of α less than 20 but there are severe descrepancies for the Ketones. The reasons for this are not clear but probably are associated with the poor mass balances. There is also a possibility that there are errors in the calculated values. It can be concluded that the method is satisfactory for compounds which have α values up to 20 which corresponds to H_s lying in the range of 5×10^{-7} atm m^3/mol (i.e. that of water) to 10^{-5} atm m^3/mol. It should be noted that for compounds of higher H_s the ratio of vapor pressure to solubility is a satisfactory method of determination. The relative volatility method is satisfactory for solutes which are miscible with water. It can also be used to give a rapid, qualitative estimation of H which may show that H_s is so small that volatilization is unimportant.

The effect of temperature is interesting in that it is experimentally more convenient to measure α at atmospheric pressure, and hence higher temperatures than ambient.

Taking n pentanol as an example, the vapor pressures at 25, 60 and 100°C are respectively 0.0034, 0.034 and 0.25 atm (Reid et al 14) while the γ values are relatively unchanged at 168, 178 and 162. Since the water vapor pressures are respectively 0.031, 0.20 and 1.0 atm, the values of α become 18.4, 30.3 and 40 i.e. doubling in the range from environmental temperatures to 100°C where the solution can be boiled at atmospheric pressure. This behaviour is not generalizable to other compounds and depends on the solute enthalpy of vaporization which controls the variation of vapor pressure with temperature. It is thus unwise to use high temperature atmospheric data to estimate α, and hence H, at the lower environmental temperatures. If this estimation is attempted it is probably best to use the value of α at 100°C to estimate γ at 100°C then assume γ to be equal at 25°C. This is true for athermal solutions (i.e. those of zero excess enthalpy of mixing). The other extreme approach is to assume that the solution is regular (zero excess entropy of mixing) in which case $\ln\gamma$ varies inversely with absolute temperature. Thus if γ is 100 at 100°C (373 K), $\ln\gamma$ will increase from 4.61 at 100°C to 5.76 at 25°(298 K) giving an γ of 319. The aqueous solubility of such a solute should decrease from a mole fraction of 0.01 (i.e. 1/100) to 0.0031 (i.e. 1/319) over this temperature range. A convenient method of estimating the change in γ with temperature is thus to measure the variation in solubility and apply the same factor to γ but inversely. Unfortunately this approach is of greatest relevance to miscible systems for which solubility data are of cours not available. The principal merit of the method is as a rapid screening approach to H determination for solutes which are suspected to be involatile relative to water.

TABLE 20

CALCULATED AND EXPERIMENTAL RESULTS FROM

THE RELATIVE VOLATILITY APPARATUS AT 25°C

Compound	Vapor Pressure (atm) at 25°C	γ^{∞}	Calculated α	Experimental α
methanol	0.15	1.53	7.3	9.62
ethanol	0.072	3.37	7.8	7.66
n propanol	0.026	11.4	9.5	10.7
n butanol	0.010	42.9	13.7	16.3
2 butanol	0.023	20.4	14.9	17.5
isobutanol	0.016	42.9	21.9	22.7
n pentanol	0.0034	168	18.4	22.0
2 butanone	0.13	13.7	57	62.9
2 pentanone	0.016	54.3	28	51.8
2 heptanone	0.0019	892	54	35.8
3 heptanone	0.0018	892	51	28.8
acetophenone	0.0005	-	-	31.8
water	0.0313	-	-	-

SOLUBILITY MEASUREMENTS WITH CO-SOLUTES

The experimental data presented earlier in Table 13 indicate that, as expected, the presence of an organic co-solute tends to increase the aqueous solubility of a hydrophobic organic compound such as phenanthrene but the effect is unlikely to be significant. Exceptions may occur if the co-solute is a strong complexing agent such as EDTA, a surfactant, the co-solute is not truly in solution or ionization occurs. Such exceptional cases can be treated using conventional procedures. It is interesting to examine the theoretical basis for suspecting a solubilizing effect.

It may be convenient to visualize triangular diagrams of ternary systems consisting of water, a hydrophobic solute (here phenanthrene) and a co-solute such as an alcohol. The co-solute may not be totally miscible with water, as occurs with higher alcohols but the solubility of alcohol in water greatly exceeds that of the phenanthrene. In the case of fulvic acid there is a solid phase region which is not of direct interest here. The area of interest is the water apex and particularly how the phase envelope corresponding to the cloud point or solubility lies as the co-solute concentrations rises. If it is parallel to the water-co-solute side there will be no effect on solubility. If it diverges from the side there will be solubilization, as of course must occur eventually at high co-solute concentrations when the co-solute and water are miscible. The basis for suspecting solubilization is that the presence of co-solute molecules, of largely organic character, will reduce the hydrophobic solute activity coefficient and thus increase its solubility, i.e. it will become more soluble since the matrix which it encounters has more organic character. The difficulty lies in determining the magnitude of this effect at low co-solute concentration.

One approach is to attempt to quantify the degree of non-ideality using an excess Gibbs Free Energy Equation for the ternary system, the simplest of which is the symmetrical or two-suffix Margules equation (Hala et al 100) For a ternary system the activity coefficient γ becomes

$$\log \gamma_1 = x_2^2 A_{12} + x_3^2 A_{13} + x_2 x_3 (A_{12} + A_{13} - A_{23})$$

with similar symmetrical expressions for γ_2 and γ_3. The constants A_{12}, A_{23} and A_{13} are binary interaction parameters, the possible existence of a ternary constant being ignored here for simplicity. If subscript 1 refers to the hydrophobic solute, 2 to water and 3 to the co-solute, the region of interest is that where x_1 is very small thus $(x_2 + x_3)$ is essentially unity. Rearranging yields

$$\log \gamma_1 = x_2 A_{12}(x_2 + x_3) + x_3 A_{13}(x_2 + x_3) - x_2 x_3 A_{23}$$
$$= x_2 A_{12} + x_3 A_{13} - x_2 x_3 A_{23}$$

Now the solubility of compound 1 will be approximately $(1/\gamma_1)$ on a mole fraction basis or $(M_1/18\gamma_1)$ on a mass/volume (g/cm^3) basis where M_1 is the molecular weight of the compound and 18 is the molecular weight of water.

The ratio (R_s) of the solubility in the presence of co-solute to that in pure water (where x_3 is zero and x_2 is unity) is thus the inverse ratio of activity coefficients

$$\text{thus } \log R_s = A_{12}(1 - x_2) - x_3(A_{13} - x_2 A_{23})$$

But since x_3 and $(1 - x_2)$ are nearly equal and x_2 is nearly unity

$$\log R_3 = x_3(A_{12} - A_{13} + A_{23}) = x_3\bar{A}$$

This suggests that co-solutes with the greatest solubilizing effect will be those which cause γ_1 to be reduced rapidly as x_3 increases which occurs when A_{13} is small i.e. the co-solute is similar in organic character to the hydrophobic compound and thus miscible with it and when A_{23} is large, i.e. there is relatively high nonidentity between the co-solute and water. This latter effect suggests that higher molecular weight organic co-solutes will be more effective solubilizers than low molecular weight compounds, i.e. they should have higher $\bar{A}$ values.

The form of these equations suggests plotting $\log R_s$ against the co-solute concentration, which should yield straight lines of slope $\bar{A}$ dependent on the A values. Interestingly this is the same form as the Setchenow Equation for electrolytes in which the group consisting of the summed A values is termed the salting-out parameter.

Writing the equation in terms of mass concentration units as used here yields at high dilution

$$\log R_s = x_3\bar{A} = 18 \times 10^{-6} C_3\bar{A}/M_3 = \bar{A}_M C_3$$

where 18 is the molecular weight of water, M_3 is the molecular weight of the co-solute and C_3 is in units of g/m^3 and $\bar{A}_M$ has units of m^3/g. The molecular weight dependence of $\bar{A}_m$ is thus the combination of two competing trends; high molecular weights lead to high C_3 values at equivalent x_3 values thus if $\bar{A}$ is constant $\bar{A}_M$ should fall with increasing molecular weight; however as indicated earlier it is probable that the greater the organic character of the co-solute the greater the value of $\bar{A}$ and hence of $\bar{A}_M$.

An approximate value for $\bar{A}_M$ can be estimated from the present data using the higher co-solute concentration values. For example for ethanol, $\bar{A}_M$ is approximately 3.8×10^{-6}, for butanol 7.1×10^{-6} m^3/g, for hexanol 1.3×10^{-5}, for octanol 3×10^{-5} and for fulvic acic 3.5×10^{-4}, all in units of m^3/g. There is a trend of increasing $\bar{A}_M$ with molecular weight approximately expressed as

$$\bar{A}_M = 0.10\ M_3 \times 10^{-6}\ m^3/g$$

Using this simple relationship R_s values were calculated for the data in Table 13 assuming (arbitrarily) a molecular weight of 1000 for fulvic acid. Fairly good agreement is obtained especially at higher co-solute concentrations, the significant conclusion being that at co-solute concentrations of 100 g/m^3 and lower no appreciable solubilization occurs. The agreement at low concentrations of co-solute is less satisfactory probably as a result of experimental error, however non adherence to the equation can not be ruled out. An interesting observation is that although compounds such as octanol and fulvic acid are more effective per gram they are less soluble thus it is impossible to achieve high degrees of solubilization with them. For example the highest achievable concentration of fulvic acid was 60 g/m^3.

It is interesting to compare these results with those of Ueda et al (101, 102) who determined the effect of the polyhydric alcohols sorbitol and inositol on toluene solubility. These co-solutes decreased the solubility of toluene, typically by 25% at a concentration of 0.4 to 1.0 mol/liter. Urea on the other hand increases solubility by about 10% at 1 mole/liter. Boehm and Quinn (103) reported data on hydrocarbon solubilization in seawater and concluded that the effect was due to association of the hydrocarbon with organic matter, possibly in micellar form. That the effect is some form of sorption into a separate phase is indicated by the dependence of the magnitude of the effect on the hydrophobicity of the hydrocarbon, isoprenoids having a greater effect than aromatics. Phenanthrene showed little solubilization at the dissolved organic carbon levels from 0 to 17.5 g/m^3 but n hexadecane solubilities varied by about a factor of 50 over this range reaching .535 g/m^3 at 17.5 g/m^3 of dissolved organic matter, the pure water solubility being estimated to be 0.0009 g/m^3 (Sutton and Calder104). This six hundred fold increase must be due to partitioning into a separate phase. Boehm and Quinns' data can be interpreted as indicating that truly dissolved organic matter does not increase solubility significantly but colloidal organic matter, submicron in size, can sorb approximately 5% of its own mass of hydrophobic organic material. This amount of sorbate (e.g. $1g/m^3$) may be very large compared to the solubility in the case of a substance such as hexadecane but is relatively smaller in the case of aromatic compounds such as phenanthrene or naphthalene which thus do not display a significant increase in solubility.

The conclusion is that at normal environmental concentrations of organic matter there is no significant effect on solubility. The effect may be to increase or decrease solubility depending on the nature of the co-solute. Any solubilizing effect is likely to be small compared to sorption into suspended organic matter, some of which may be non-filterable and thus wrongly designated as being truly dissolved.

HENRY'S LAW CONSTANTS

This work had two primary objectives, the determination of Henry's Law Constants (H) for selected compounds including those used experimentally in the volatilization studies and the determination of the extent to which H is likely to be reduced by the presence of dissolved and particulate natural organic matter.

The data presented earlier in Table 14 for the hydrophobic compounds show good agreement between calculated and experimental values for those compounds for which reliable vapor pressure and solubility data are available. The deviations are approximately: naphthalene 3%, chlorobenzene 2%, o dichlorobenzene 3% and bromobenzene 20%. This, coupled to the satisfactory agreement obtained earlier (Mackay et al28) indicates that the method is fundamentally reliable and can be used to

(i) estimate H in isolation
(ii) estimate H and vapor pressure if the solution is known
(iii) estimate H and solubility if the vapor pressure is known or
(iv) estimate H and check reported values of solubility and vapor pressure.

Clearly the last approach is preferred.

The data for the ketones and alcohols are less satisfactory, although it is clear that the values are reasonable i.e. generally within a factor of two. It is suspected that some of the vapor pressure data are suspect and since water is appreciably soluble in the solutes this effect tends to change the solute vapor pressure and H is not simply the ratio of pure solute vapor pressure to solubility. The discrepancy appears to be highest for the more soluble solutes. Because of the low H values the stripping method is inconveniently slow and it is possible that there is an error in the procedure in that the exit gas is not fully saturated with the solute. This seems unlikely as is discussed below.

Consider a bubble of gas of diameter D_m, initially containing no solute, rising during time t s through perfectly mixed water containing solute of concentration C mol/m^3. The bubble, if spherical, will have an area A of πD^2 m^2 and a volume V of $\pi D^3/6$. If the overall mass transfer coefficient is K_{OG} and the solute partial pressure is P atm then during time dt the amount transferred will be

$$K_{OG}\, A(HC - P)dt/RT = VdP/RT$$

thus $$dP/(HC - P) = K_{OG}Adt/V$$

integrating from P = 0 to P = P at time t gives

$$\frac{HC - P}{HC} = \exp(-K_{OG}At/V)$$

$$P = HC(1 - \exp(-K_{OG}At/V))$$

Now $$A/V = 6/D$$

thus $$P = HC(1 - \exp(-6K_{OG}t/D))$$

The critical group is $6\,K_{OG}t/D$ which should be at least 3.0 to ensure a 95% approach to equilibrium. This is best achieved by having D small (finely

dispersed bubbles) and t large (a deep pool of water). As H becomes very low K_{OG} should approach K_G since

$$1/K_{OG} = 1/K_G + H/RTK_L$$

For example if the system is "calibrated" with a substance such as benzene with a H value of approximately 5×10^{-3} atm m^3 to assure a 98% approach to equilibrium then the group $6\ K_{OG}t/D$ will be 3.9 which may consist of values of 2s for t, 0.002 m for D and thus K_{OG} is 6.5×10^{-4} m/s. Since the system is liquid phase controlled K_{OG} is approximately equivalent to RTK_L/H and K_L is 1.36×10^{-4} m/s. This is a reasonable value for K_L (Sherwood et al 42). It seems likely that K_G will be higher, possibly 10^{-2} m/s. It follows that

$$1/K_{OG} = 1/K_G + H/RTK_L = 100 + 1532 = 1632 = 1/6.5 \times 10^{-4}$$

illustrating that only 100/1632 or 6% of the resistance lies in the gas phase.

If H is reduced to 5×10^{-4} (e.g. naphthalene) but K_L and K_G remain constant, as is likely given the constant fluid mechanical conditions, the K_{OG} breakdown becomes:

$$1/K_{OG} = 100 + 153 = 253 = 1/4 \times 10^{-3}$$

and $6K_{OG}t/D$ becomes 24 thus an even closer approach to equilibrium is achieved.

It thus appears that as H falls the system should give more accurate results.The only difficulty here may be if the less hydrophobic solutes cause changes in interfacial tensions and thus affect the flow conditions in the vicinity of the bubbles. Comparison of the calculated and experimental results for the five solutes shows that in three cases the experimental results are higher than calculated and in two cases they are lower, thus no systematic error is apparent. Further, the reproducibility is much better than the discrepancy between experimental and calculated data.

It is recommended that the gas stripping method be validated for compounds with H in the range less than 10^{-4} atm m^3/mol.

The tests with fulvic and humic acids in the concentration range up to 54 g/m^3 showed a significant reduction in H following addition of the acid. These tests involved measuring the change in slopes of the concentration - time curve before and after addition. The precision between experiments was insufficient to permit the change in H to be determined between tests. The naphthalene results showed that the reduction in H was an average of 1.7×10^{-6} atm m^3/mol per g/m^3 of sorbent. The error on this quantity is no better than a factor of three but it is significantly greater than zero.

Taking an average value for H of 440×10^{-6} it appears that at 1 g/m^3 sorbent there is 0.39% sorption which is equivalent to a partition coefficient of 3900 (µg solute per g sorbent) per (g solute per m^3 water or mg solute per liter water).

It is interesting to compare these results with the sediment sorption work of Karickhoff et al (8). Naphthalene has a K_{OW} of 2300 and a K_{OC} of 1300. In a suspension containing Sg/m^3 of organic carbon sorbent in equilibrium with

a dissolved solution of concentration C g/m^3 the sorbed concentration will be 1300 C µg solute/g organic carbon or 1.3×10^{-3} CSg solute/m^3. The ratio of sorbed to dissolved solute is thus 1.3×10^{-3}S.

Assuming that the sorbents have 65% carbon, the ratio becomes $0.85 \times 10^{-3} S_T$ where S_T is the total sorbent concentration.

Taking H for naphthalene as 440×10^{-6}, it is expected that at a low concentration S_T of say 10 g/m^3 the ratio would be 8.5×10^{-3} and H would be reduced by that ratio i.e. by 3.7×10^{-6}. The experimental data indicate a reduction of 17×10^{-6} or 4.6 times the amount calculated above. The conclusion is that reduction in H is attributable to a partition coefficient which is greater than K_{OW} by a factor of 1.7. It must be emphasized that the accuracy of this "K_p" determination is no better than a factor of three thus it is possible that the experimental results are consistent with Karickhoff's. It had been hoped that other solutes with higher K_{OW} values such as pyrene would permit the "K_p" to be determined more accurately but this proved to be impossible because of the low concentrations.

The implications of these results is that the presence of high molecular weight natural organic matter in suspension and/or solution apparently causes a reduction in H but the effect is small at normal environmental concentrations. A procedure for calculating the likely magnitude of the effect is to assume that the sorbent is octanol then calculate the extent of sorption using K_{OW} as K_p. This will probably give a result within a factor of three of the correct value.

For example at a sorbent concentration S_T g/m^3 the fractional reduction in H will be approximately $10^{-6} S_T K_{OW}$. This "rule" should not be used when the fraction sorbed exceeds 10%.

This result is in accord with the results of the solubility measurements in the presence of co-solutes in that it is very unlikely that concentrations of dissolved organic matter can be achieved which will significantly enhance solubilities or reduce Henry's Law Constants. The most effective organic matter is probably material such as fulvic or humic acids which have high molecular weights and structures which can incorporate molecules of hydrophobic solutes thus reducing the water cavity area requirements. Precise measurement of this effect is desirable, especially for high K_{OW} compounds but this is difficult experimentally since the magnitude of the effect is of the same order of magnitude as the error.

SECTION 9

CALCULATION OF ENVIRONMENTAL VOLATILIZATION RATES

The primary purpose of this work was to devise procedures for calculating environmental volatilization rates. Some general features of this procedure are reviewed below. The required data fall into several categories.

PHYSICAL CHEMICAL DATA

A knowledge of the Henry's Law Constant is essential, but the required accuracy varies depending on the absolute value. In the liquid phase control regime only an approximate value is necessary, provided that the atmospheric concentration is low. If experimental solubility and vapor pressure data are available, they can be used to calculate H provided that they refer to the same state. Ideally the "May-Wasik" generator column method should be used for solubility and the "Spencer-Cliath" method for vapor pressure. K_{OW} data can be used to check the solubility. If solubility and vapor pressure data are not available, one of the correlation techniques can be used. If experimental determination is necessary either the gas stripping or relative volatility approaches can be used to measure H or the small scale volatilization system can be used to measure K_{OL} and from it infer H.

Examination of the H value with others for a homologous series provides a useful check. Experimental values should be checked against the correlation.

A partition coefficient to any suspended mineral or organic matter in the water phase should be estimated either directly or from K_{OW} and used to estimate the fractions of dissolved and sorbed material as discussed earlier. Only the dissolved material exerts a driving force for volatilization.

A similar calculation may be necessary for atmospheric particulates.

ENVIRONMENTAL CONCENTRATIONS

Estimates of the temperature and water and air concentrations and their breakdown into solution (or gaseous) and sorbed forms are required. When juxtaposed with the Henry's Law Constant, the direction of transfer will become apparent as will the sensitivity of the flux estimates to the concentrations and H. This calculation can be done using concentrations or fugacities. In many cases the air phase fugacity will be negligible but in cases where the air and water phase solute fugacities are close, accurate values of both

concentration and H may be necessary. Examination of the absolute values enables the required accuracy to be estimated.

MASS TRANSFER COEFFICIENTS

Depending on the value of H, either or both of K_G and K_L may be required. The correlation equations derived earlier for these quantities as a function of wind speed, fetch, current (for rivers), and Schmidt Number (or diffusivity) can be used.

If surface films are present, an allowance may be made for their presence although quantifying this effect may be difficult.

A time average mass transfer coefficient is most useful. This requires an estimate of the diurnal variation of temperature and wind speed, possibly in 4 or 6 hour increments. The relevant temperature is that of the water surface, not the bulk. This temperature may fall during the night due to radiative cooling. In principle it is better to calculate K_L and K_G rather than average temperature and wind speed. It should be noted that temperature influences K_L, K_G and H, and thus K_{OL}, and it also affects (C-P/H) the driving force for volatilization.

The correlation equations presented in Section 8 can be used to calculate mass transfer coefficients, using either the versions in which 10 meter wind speed is used directly or the dimensionless groups (Reynolds and Stanton numbers) are evaluated. Both methods require use calculation of the Schmidt number which includes the effect of solute molecular size or diffusivity and temperature. For most purposes the simpler wind speed correlations are probably preferred.

Although in most cases the partial pressure P of the solute in the atmosphere is small and can be assumed to be zero, there may be situations (for example PCB's) where this is not valid. The simplest test is to calculate the fugacities of the solute in the water and in the atmosphere and compare their magnitudes and difference. In certain cases, volatilization may create a significant solute concentration in the atmosphere above a lake, especially if the ventilation rate is slow. An approximate mass balance-atmospheric dispersion calculation can be done to elucidate the influence of such an effect.

CALCULATION OF SCHMIDT NUMBERS

The calculation of Schmidt numbers for air and water is straightforward but procedures are reviewed here for completeness.

The water Schmidt number Sc_w is given by

$$Sc_w = \mu_w/\rho_w D_w$$

where μ_w is the viscosity of water, ρ_w is the density of water and D_w is the diffusivity of the solute in water. Rarely does the solute concentration reach a level that μ_w and ρ_w are significantly different from that of pure water. The values of μ_w and ρ_w are of course temperature dependent and can be obtained from Handbooks. The preferred SI units are Pas for viscosity and kg/m^3 for water.

The diffusivity D_w is best obtained by the Wilke Chang correlation which is given by Sherwood et al (42) for water systems as

$$D_w = 7.4 \times 10^{-8} [(\phi M)^{0.5} T/\mu_w V_s^{0.6}]$$

D_w has units of cm^2/s

Here M is the molecular weight of water.

ϕ is an association parameter which is 2.6 water

T is temperature (K)

μ is water viscosity (cp)

V_s is solute molar volume at its normal boiling point

This reduces to

$$D_w = 5.06 \times 10^{-7} T/\mu_w V_s^{0.6} \ cm^2/s \quad (\mu_w \text{ in cp})$$

Since 1 cp is equivalent to 10^{-3} P_{as} this becomes

$$D_w = 5.06 \times 10^{-10} T/\mu_w V_s^{0.6} \ cm^2/s \quad (\mu_w \text{ in Pas})$$

Finally, if D_w is required in m /s to be consistent with the other SI quantities the equation becomes

$$D_w = 5.06 \times 10^{-14} T/\mu_w V_s^{0.6} \ m^2/s$$

A typical diffusivity is 10^{-5} cm^2/s or 10^{-9} m^2/s which, when combined with a density of $10^3 kg/m^3$ and a viscosity of 10^{-3} Pas yields a dimensionless Schmidt number of typically 10^3.

The air Schmidt Number Sc_A is given similarly as

$$Sc_A = \mu_A/\rho_A D_A$$

where μ_A is the viscosity of air, ρ_A is the density of air and D_A is the diffusivity of the solute in air values of μ_A and ρ_A are available in Handbooks.

The air diffusivity D_A can be obtained from one of several correlations as reviewed by Reid et al (14) for example the Fuller Schettler and Giddings correlation is often used. Although regarded as somewhat obsolete the Gilliland correlation (97) is attractive in that it uses the same molar volume as the Wilke Chang correlation.

$$D_A = \frac{4.3 \times 10^{-3} T^{1.5} (1/M_A + 1/M_B)^{0.5}}{P\ (V_A^{1/3} + V_B^{1/3})^2}$$

where D_A has units of cm^2/s

P is total pressure (atm)

M_A and M_B are the molecular weights of air and the solute

V_A and V_B are the molar volumes at the normal boiling point.

When expressed in SI units of m^2/s the constant 10^{-3} is replaced by 10^{-7}.

A typical diffusivity is 0.1 cm^2/s or 10^{-5} m^2/s which when combined with a density of 1 kg/m^3 and a viscosity of 2×10^{-5} P_{as} (i.e. 2×10^{-2}cp) yields a Schmidt number of 2.0. Water vapor has a lower Schmidt number of 0.6 at 0°C because of its unusually high diffusivity of approximately 0.3 cm^2/s.

An attractive feature of the Schmidt Number is that it combines in a rigorous manner the effect of both molecular size (i.e. diffusivity) and of temperature in the correlation for mass transfer coefficients. It is more theoretically justified than equations invoking fictitious activation energies or power dependencies of temperature. Since correlating equations are available, or can be easily devised for densitites, viscosities and diffusivities in air and water it is relatively easy to incorporate the Schmidt Number in computer programs used for environmental prediction purposes.

OTHER TRANSFER PROCESSES

The possibility of other transfer processes such as sedimentation or wet or dry atmospheric deposition should also be examined since these processes may counteract or enhance that of volatilization. The role of sedimentation is discussed briefly in a later section.

Of particular interest are the processes of volatilization from lakes and rivers which are also discussed in more detail separately. In these cases, the hydrodynamic regimes strongly influence volatilization processes.

ROLE OF SEDIMENTATION AND SORPTION

If a diffusing solute is present in dissolved and sorbed forms in water, the calculation of water column transfer rates becomes more complex. This has been discussed by Mackay et al (105) in some detail and only the salient points are reviewed here.

If the suspended matter has a negligible settling (or rising) velocity, the sorbed material will diffuse with the water, equal diffusivities apply, and Fick's First Law can be used with the total (dissolved and sorbed) concentration. The fugacities are reduced by sorption but the resistances are also reduced.

If the suspended matter has a velocity with respect to the water column, the net velocity becomes the algebraic sum of the diffusion and particle velocities. These velocities are best calculated as the invidual mass flux ($mol/m^2.s$) divided by the relevant concentration (mol/m). It is possible for upward diffusion to be exactly balanced by downward sedimentation. The diffusive velocity is N/C where the mass flux N is $D_V \Delta C/\Delta Y$ where D_V is vertical diffusivity, C is concentration and Y is depth. The sedimentation velocity is simply the particle velocity which can be estimated from sedimentation or particle size observations.

SORPTION-DESORPTION KINETICS

In this analysis, we have assumed that equilibrium exists between the dissolved and sorbed forms, but this may not always apply. Sorption experiments generally show a fairly fast initial "outer surface" or "labile" sorption (half life of minutes) superimposed on a slower penetration of solute into interstices (half life of hours). Desorption is similar with fast "labile" desorption with slower release of the solute trapped more deeply in pores. These rates are of importance in volatilization since they may control whether or not the sorbed solute is volatilized from an element of water which eddies to the surface and remains there for a short time. If the "volatilization exposure half life" at the surface is much shorter than the desorption time, it can be assumed that only the dissolved solute will volatilize during exposure; thus the "driving force" for volatilization is derived only from the dissolved state. If desorption is fast the sorbed material could also be volatilized after having been desorbed. Unsteady state theory suggests that the mass transfer coefficient K_L will be related to diffusivity D and exposure time t by an equation of the form

$$K_L = \sqrt{4D/\pi t}$$

A typical diffusivity is 10^{-5} cm^2/s and typically K_L is 0.003 cm/s; thus the exposure time t is typically 1.4 s . It seems unlikely that appreciable desorption will occur during this short period. Under quiescent conditions when K_L is smaller, i.e., 0.001 cm/s, t will be approximately 13 s and some desorption may occur.

The general conclusions are (i) that usually only the dissolved solute will volatilize at the surface with the sorbed material desorbing later in the bulk of the water column to establish a new equilibrium, and (ii) the sorbed material will probably not influence the transfer rate in the water "film", i.e., it will not lower the resistance as may occur in the water column.

Kinetics may also influence the behaviour of solids falling through the water column. If the falling velocity is low,it is likely that the sorbent will maintain close to its equilibrium amount of sorbate;whereas if the velocity is high (as may occur with mineral particles), there may be insufficient time for equilibrium to be reached.

The role of sedimenting sorbents is thus usually to act counter to upward diffusion (or to enhance downward diffusion) at a rate depending on sorbed concentration and settling velocity and to some extent on the sorption-desorption kinetics.

VOLATILIZATION FROM RIVERS

The issue of volatilization rates from rivers has been discussed by Mackay and Yuen (106) as part of this project. The following is a review and expansion of that material.

Rivers are a particularly important component of the aquatic environment, being widely used as a source of drinking water, they provide commercial and sport fisheries and recreational ecosystems as well as supporting intrinsically valuable ecosystems. It is very desirable that the extent of contamination be known and controlled to an acceptably low level.

Examples of contamination problems include; the presence of haloforms (notably chloroform) generated during chlorination of wastes and of electrical and other plant cooling waters; contaminants introduced by groundwater inflitration from nearby landfill or industrial sites, and especially from leaking storage tanks or pipelines; chronic emissions from industrial and domestic sources; water runoff containing pesticides from agricultural land; hydrocarbon and other product contamination from accidental and chronic spills including releases from submerged oil and product pipelines, outboard motor exhausts, and from vessels which have been accidentally holed. In many of these cases volatilization is an important, or even the most important, pathway for decontamination.

Of some concern is the issue of the extent to which ice alters the volatilization rate. It is suspected for example that an oil or chemical spill into an ice-covered river could have a greater impact than a spill into an ice-free river because the rapid loss of toxic volatile compounds is inhibited, resulting in greater exposure in the water column.

Fortunately the problem of oxygen depletion or "sag" in rivers has lead to a considerable volume of information on transfer rates of oxygen between the atmosphere and the river. Many correlations have been developed to quantify this rate.

The usual approach is to express the oxygen uptake rate as a first order rate constant or reaeration constant termed K_2 . Thus if C is the oxygen concentration in the river and C^s is the saturation value (approximately $10 g/m^3$) then the flux N into unit area of water is expressed as

$$N = K_2(C^s - C) = dC/dt$$

hence

$$C = C^s - (C^s - C_o) \exp(-K_2 t)$$

where t is time (usually hours or days) and C_o is an initial concentration. K_2 has units of reciprocal time and is typically 0.1 to 0.2 h^{-1} for a 1 m deep river. Comparison of this equation with the mass flux equation derived earlier shows that K_2 is equivalent to K_L/Y where Y is the river depth. It is perhaps unfortunate that K_2 was used as the correlating quantity in the early reaeration literature because it is "less constant" than K_2. As is discussed later, it is found that K_2 is approximately inversely proportional to depth.

It is worth laboring this point by an example because there has been an unfortunate tendency to apply K_2 to lakes. Suppose that K_L is 0.1 m/h in a river of depth 2m. K_2 then becomes 0.05 h^{-1}. If this water flows into a

region where the depth decreases to 1 m it is likely that K_2 will increase slightly to say 0.12 m/h because of the closer proximity of the bottom to the surface. K_2 then becomes 0.12 m/h, which is a substantial increase. If this water enters a lake of depth 10 m it is probable that K_2 will drop to say 0.05 m/h and if a K_2 is to be defined it will be 0.005 h^{-1}. Since lakes are very variable in depth it is unwise to express "average" or "typical" K_2 values since it can vary by orders of magnitude. It is better to use K_L which is relatively more constant.

For rivers it is likely that in moving from the bulk of the water to the atmosphere, the contaminant experiences three diffusive processes, each with a resistance. Normally one of these resistances will dominate.

The first resistance (r_1) is that of diffusion from the bulk of the river to the interface. This is approximately Y/D where Y is river depth (m) and D is the vertical diffusivity (m^2/s). In a reasonably turbulent river the diffusivity can be approximated as Y^2 divided by the average time t (s) for an element or eddy of water to move from bottom to surface. In a river of depth 2 m, it is likely that this time is of the order of 100 s, thus r_1 is t/Y or 50 s/m. In shallow fast flowing rivers r_1 may be as low as 1 s/m and in deep sluggish rivers it may be as large as 1000 s/m.

The second resistance r_2 is that for diffusion through the near-surface liquid to the interface. Typical reaeration constants K_2 are 0.1 to 0.2 h^{-1} for 1 m deep rivers thus K_L is typically 4×10^{-5} m/s and r_2 is thus 25,000 s/m. It thus appears that except in deep slow moving rivers the resistance r_1 will usually be negligible compared to r_2 and can thus be neglected.

The third resistance r_3 is that for diffusion through the atmosphere in the layer close to the water surface. From the considerable body of information on water evaporation this resistance can be estimated as corresponding to a mass transfer coefficient K_G of approximately 0.01 m/s. It has been shown that the term r_3 is given by

$$r_3 = RT/HK_G$$

The overall resistance r_T is thus approximately

$$r_T = r_1 + r_2 + r_3 \approx 50 + 25000 + 2.4/H$$

It follows that a number of regimes can be identified in which differing resistances dominate.

If H is greater than 10^{-3}, r_2 will dominate by a factor of approximately 10, i.e. the overall rate is controlled by the diffusion rate through the water film at the interface. The substance will generally volatilize rapidly. This is the regime in which oxygen diffuses (since H for oxygen is approximately 0.65 atm m^3/mol) thus an estimate can be made of volatilization rate of substances in this class from reaeration data. The simplest (and rather inaccurate) approach is to assume that K_2 or K_L are equal for solute and oxygen. A correction for the usually slower diffusivity of the solute should be applied as is discussed later.

If H lies between 10^{-3} and 10^{-5} both resistances r_2 and r_3 are important and volatilization will be less rapid but still possibly significant. Reaeration data can not be used alone to estimate solute volatilization.

In the regime where H is 10^{-7} to 10^{-5} the substance will volatilize slowly and at a rate dependent on H. The gas phase resistance r_3 will dominate by a factor of over 10 and the rate is controlled by the slow diffusion through the air phase. Reaeration data become irrelevant.

In the regime of H less than 10^{-7} the compound can be regarded as involatile or less volatile than water.

The driving force for volatilization is the difference between the water column concentration C (mol/m^3) and the water concentration in equilibrium with the atmospheric concentration or partial pressure (P) of the contaminant, and is thus (C-P/H). The overall mass flux (N) equation becomes

$$N = (C-P/H)/(r_1 + r_2 + r_3)\ mol/m^2.s$$

River Concentration Profiles

It is instructive to set up and solve the steady state differential equation which applies to the decay of concentration in a river both attributable to volatilization and to other processes. The easiest situation is that of a continuous point source. If the average river depth is Y(m), the velocity is V (m/s) and the concentration C is homogeneous laterally (being C_o at the source point) then a mass balance on a volume of water of area 1 m moving downstream in time t (s) gives

$$YdC/dt = -N = -(C-P/H)/r_T$$

Usually P/H will be negligible compared to C thus

$$YdC/dt = -C/r_T$$

Integrating gives

$$C = C_o \exp(-t/Yr_T) = C_o\ (-L/YVr_T)$$

where L (m) is the distance downstream and is equal to t/V.

If the contaminant is subject to another first order decay process of rate constant $K_D(s^{-1})$ then it can be included yielding

$$dC/dt = -C(1/Yr_T + K_D)$$

thus

$$C = C_o \exp\left(-\frac{L}{V}\left(\frac{1}{Yr_T} + K_D\right)\right)$$

The group $(1/Yr_T)$ for oxygen transfer is the reaeration constant K_2. Since oxygen has a high H value in this case r_2 dominates thus r_T is r_2 and becomes $1/K_L$, and $(1/Yr_T)$ becomes K_L/Y which is K_2.

A plot of logarithm of concentration ratio (C/C_o) against distance downstream should thus give a straight line as illustrated in Figure 34. The slope is $(1/Yr_T + K_D)$ which becomes steeper the lower the resistance r_T, the shallower the river, and the greater the value of K_D. Comparison of the values of K_D and $(1/Yr_T)$ indicates whether or not volatilization is a significant competitive process.

It may be useful to calculate a volatilization "half life" or "half distance" in which the concentration drops by half. It can be easily shown that this is

$$\text{half life} = 0.69\ Yr_T\ \text{s}$$

$$\text{half distance} = 0.69\ YVr_T\ \text{m}$$

For example a volatile hydrocarbon such as benzene ($H = 5 \times 10^{-3}$) with a typical K_L value of 4×10^{-5} m/s in a river of depth 1 m of velocity 1 m/s will have a half life of 4.7 hours and a half distance of 17 km. Clearly very shallow rivers have the potential to lose volatile contaminants very rapidly.

It is instructive to examine the plot of half life or half distance as a function of H for the river described above. Ignoring the resistance r_1 and adopting the typical values r_2 of 25000 and r_3 of 2.4 /H the expression becomes as illustrated in Figure 35.

$$\text{half life} = 0.69Y\ (25000 + 2.4/H)\ \text{s}$$

$$\text{half distance} = 0.69YV\ (25000 + 2.4/H)\ \text{m}$$

Clearly only if H is greater than 10^{-5} is volatilization likely to be significant except in very shallow rivers where the lower limit of interest is 10^{-6}.

This analysis suggests that the critical quantities necessary for the determination of volatilization rates from rivers are: -

(i) r_2, the liquid phase near surface resistance (which can be obtained from reaeration coefficient data);

(ii) H, the Henry's constant

and of lower priority and needed only in certain situations

(iii) r_3 the gas phase resistance (which can be obtained from existing correlations such as that of Mackay and Matsugu (64) or those developed earlier in this report.

(iv) r_1 the river bulk resistance (which is needed only in very deep slow moving waters which can almost be regarded as lakes)

Review of Reaeration Data

There is a considerable literature on reaeration rates of rivers with numerous correlations as a function of river velocity, depth and slope. Excellent, comprehensive, critical reviews have been compiled by Rathbun (107),Holley (108),Lau(109)and Bennett and Rathbun (110). Studies by Mattingly (111) and Downing and Truesdale (80) have shown that wind also has a significant effect of reaeration rates, a result entirely in accord with the present work which has shown that these rates are influenced by

wind speed, which generates near-surface turbulence. This wind effect is difficult to characterise because it depends on fetch which in turn depends on the wind direction relative to river direction and on river width.

Rathbun (107) after a detailed review of some 19 equations showed that the equations of Tsivoglou-Wallace (112), Parkhurst-Pomeroy (113) and Churchill et al (114) gave the best overall predictions although it must be recognized that other equations may give better predictions for specific streams. These equations are

Tsivoglou-Wallace	$K_2 = 638VS$
Parkhurst-Pomeroy	$K_2 = 1.08\ (1.0 + 0.17F^2)\ (VS)^{0.375}\ Y^{-1}$
Churchill et al	$K_2 = 0.00102V^{2.695}Y^{-3.085}S^{-0.823}$

where S is the river slope (m/m) and F is the Froude Number $V/(gY)^{0.5}$.

If no slope data are available the similar Isaacs-Gaudy (115) or Langbein (116) equations can be used.

Isaacs Gaudy	$K_2 = 0.223VY^{-1.5}$
Langbein Durum	$K_2 = 0.241VY^{-1.33}$

It is likely that for a given river application of these equations would give an estimate of K_2 with an average error between 10 and 50%. One practical approach is to apply all the equations, discard the outlying result and take an average of the remainder.

From the oxygen transfer coefficient or resistance it is then necessary to calculate the effect of the difference in molecular size or diffusivity preferably using the Schmidt number approach.

Tracer Techniques

Of particular interest and relevance is the recent development of tracer techniques for measurement of stream reaeration capacity. Tsivoglou (70) used radioactive krypton as tracer, but this presents licensing difficulties. Rathbun et al (71) have developed an ingenious technique using ethylene or propane as indicator of volatilization and Rhodamine WT dye as indicator of dispersion and dilution. Any change in the ratio of hydrocarbon to the non-volatile dye concentration is largely attributable to volatilization. In essence this technique provides a direct measurement of the volatilization rate of high H contaminants from rivers. The solubilities of ethylene and propane at 1 atm are 131 and 62 g/m^3 (4.7 and 1.5 mol/m^3) thus the H values are 0.21 and 0.67 atm m^3/mol, well in the liquid phase control range. It is interesting to note that the tracer technique was developed to enable oxygen transfer data to be predicted whereas in this case it is the reverse which is being attempted.

Ice, Aeration and Volatilization

In their comprehensive review of the literature on ice behaviour in rivers and lakes Ficke and Ficke (117) have described several situations in which ice cover has significantly altered water quality including by oxygen

depletion. It seems very likely that volatilization will be severely reduced, if not eliminated, when a continuous ice cover is present. Of particular concern is the situation which may exist when there is an accidental release of a toxic compound into an ice covered river. In such cases it may prove beneficial to break the ice cover or bubble air under it in order to promote volatilization. There may be a case for installing permanent submerged bubbling or aerating systems in locations such as pipeline river crossings. This raises the issue of whether or not situations may exist in which artificial aeration and thus volatilization may be feasible or desirable.

In many oxygen depleted rivers it may be advantageous to install artificial aerating devices such as surface diffusers, submerged bubblers or even artificial weirs . Such devices would also serve to increase volatilization rates. The following order of magnitude analysis illustrates the feasibility of this approach.

If air is bubbled into water at any significant depth (i.e. > 1 m) it is likely that it will become nearly saturated with any dissolved volatilizing gas of reasonably high H. If an increament of air rate dG m^3/s is introduced then the exit volatilization rate will be dGHC/RT mol/s when the water concentration is C mol/m^3. If the river volumetric flowrate is Fm^3/s then

$$FdC = - dG\ HC/RT$$

integrating gives

$$C = Co\ \exp(-GH/RTF)$$

A reasonable target would be to reduce C to 27% of Co which would occur when GH/RT is unity or when G/F = 0.024/H. If it is feasible to bubble air into a river at a rate equal to the volumetric river flow than a reduction to 37% is possible only if H is 0.024 or greater. This suggests that the minimum condition at which artificial aeration could be contemplated is when H is 10^{-2}. At 10^{-1} and above it becomes very attractive. Examination of solute H values indicates that alkanes and haloforms are attractive candidates but aromatics such as benzene are marginal, and the polynuclear aromatics are definitely not feasible.

Another method of viewing an artificial aerating device is to consider the natural river length to which the device is equivalent. This length is obtained by equating L/YVr_T to GH/RTF i.e.

$$L = GHYVr_T/RTF$$

but since ZVW is F where W is the river width (m)

$$L = GHr_T/RTW = G'Hr_T/RT$$

where G' is the air rate in cubic meters per meter width per second. Since r_T is typically 25000 s/m and RT is 0.024 this length becomes 10^6 G'H m. To achieve 1 km of natural volatilization for a compound with an H of 10^{-2} would require 0.1 $m^3/m^3.s$ which seems feasible. Higher values of H would require correspondingly smaller values of G'.

It is concluded that situations may exist for toxic compounds of high

Henry's Constant in which artificial voltatilization is a feasible approach to stream decontamination. Since the artificial volatilization efficiency increases steadily with increasing H (whereas the natural rate becomes independent of H above 10^{-3}) the most attractive situations are those in which H is largest, i.e. low solubility highly volatile compounds.

Comparison with Literature Data

The most accurate reported data are those of Rathbun et al (71) and Rathbun and Grant (118) who obtained dye, ethylene and propane concentration profiles over river lengths in the U.S. from 4 to 9 km. The results were plotted by Mackay and Yuen(106) as the ratio of volatile tracer to dye concentration as a function of flow time, which is approximately proportional to distance. The drop in concentration of a factor of 2 occurs in approximately 200 minutes or 3 to 4 km, indicating that Zr_T has a v ue of 17400 s, which for a depth of 1 m corresponds to a mass transfer coefficient of 5×10^{-5} m/s and a reaeration constant K_2 of approximately 5 $days^{-1}$, in good agreement with the earlier theoretical predictions.

Zurcher and Giger (119) and Giger et al (120) have presented some precise data on trichlorethylene tetrachloroethylene, 1,1,2,2 tetrachloroethane, 1,4 dichlorobenzene, benzene and other contaminant profiels for a 30 km stretch of the Glatt river in Switzerland which flows from the Greifensee to the Rhine. In the 12 km stretch after Dübendorf the concentrations of trichlorethylene, tetrachloroethylene and 1,1,2,2, tetrachloroethane showed reductions of factors of approximately 8, 50 and 20, all probably attributable to volatilization. These data are broadly consistent with the earlier predictions. The 1,4 dichlorbenzene and benzene profiles showed little drop possibly because of the low H values and the presence of continuous inputs. It is interesting to note that the disagreement between predicted and observed concentrations may indicate the presence of unknown sources. Data reported by Helz (121) on haloform concentrations in the estuary of the Back River, Maryland also suggest that this class of compounds may be useful as tracers.

Finally, the comprehensive laboratory and computer prediction work of Smith et al (4) on eleven contaminants provides an interesting assessment of the importance of volatilization in rivers, relative to other processes. In two cases (benzo (b) thiophene and mirex) volatilization was judged to be the most significant pathway. In the case of benzo (a) pyrene volatilization was second in importance after photolysis, assuming summer sunlight conditions.

Agreement with the available literature data is clearly satisfactory and lends support to the methodology developed here.

VOLATILIZATION FROM LAKES

The simplest approach for calculating volatilization rates from lakes is to assume that the water volume is well mixed in a time scale which is short compared to the volatilization tine, and that the resistance to volatilization lies at the interfacial region. Mathematically, if V is the lake volume (m^3), A is the area (m^2), thus the mean depth is (V/A)m, F is the water inflow and outflow (m^3/h), K_{OL} is the overall liquid phase mass transfer coefficient (m/h), C is the solute dissolved concentration (mol/m^3) and the total solute input rate is I mol/h it follows that for a nonreacting solute

$$I - FC - K_{OL}\ A(C - P/H) = V\ dC/dt$$

The atmospheric concentration P can usually be assumed to be zero.

Two solutions are of interest, the first being the steady state value when the derivative becomes zero at which

$$C = I/(F + K_{OL}A)$$

The relative magnitudes of F and $K_{OL}A$ control the solute fate, i.e., by outflow if F dominates and by volatilization if K_{OL} A domeinates. A reaction term could also be included in the denominator which would have the form K_R V where K_R is the total first order reaction rate constant. The mean residence time τ of the solute in the lake becomes

$$\tau = VC/I = V/(F + K_{OL}A) \qquad (h)$$

If F is small compared to $K_{OL}A$, τ becomes V/K_{OL} Z or Y/K_{OL} where Y is the mean depth.

Second, is the first order decay equation corresponding to an initial concentration C_o with no subsequent input.

$$-FC - K_{OL}\ A\ C = V\ dc/dt$$

or $$C = C_o \exp\ (-(F + K_{OL}A)t/v)$$

The half life for small values of F becomes 0.69 $V/K_{OL}A$ or 0.69 $Y/K_{OL}A$, similar to the mean residence time introduced earlier.

In assessing the role of volatilization compared to flow (advection) and reaction the characteristic half lives or residence times are thus useful indications. These are

Volatilization	Y/K_{OL}	
Flow	V/F	all in units of hours
Reaction	$1/K_R$	

Examination of thier magnitudes provides a useful indication of relative importance.

This simple approach is likely to break down when the lake is sufficiently deep that there is some thermal stratification and thus vertically restricts diffusion. Calculation of volatilization rates from water bodies with significant vertical diffusive resistance is very difficult since it requires knowledge about the exact vertical variation in diffusivity and the vertical location of solute introduction. A comprehensive analysis is probably best done using finite difference solution of equations set up for a multi-layer system. In many cases it is suspected that relatively simple expressions can be derived which elucidate where the dominant resistance lies. To do this it is first desirable to discuss briefly the magnitudes and dependencies of vertical and horizontal diffusivities.

Horizontal Diffusion

The usual approach is to assume that Fick's Law applies horizontally and attributes any departure from that Law to a variation in diffusivity. In fact, the departures are so large that horizontal diffusivities become very scale dependent. In a typical determination a volume of dye is injected into the water and its horizontal expansion followed with time. It tends to spread in a Gaussian manner with a standard deviation S (or width L = 3S) at time t. The diffusivity D_H is then given as $S^2/2\ t$ or $L^2/18\ t$. Results are usually expressed in a logarithmic diffusion diagram of D_H versus L and a typical relationship is (Murty and Miners 122)

$$D = 0.02\ L^{1.2} \quad \text{(units of cm and s)}$$

The implication is that for a small lake of diameter 100 m D_H will be approximately 10^3 cm^2/s whereas for a larger 1000 m lake D_H will be 10^4 cm^2/s and at 10 km D_H will exceed 10^5 cm^2/s. Oceanic values reported by Okubo (123) have reached nearly 10^6 cm^2/s.

This marked dependence of D_H on L indicates that simple diffusion does not apply. A better conceptual model may simply be to assume a constant spreading velocity (dL/dt) which can be estimated as follows:

$$D = 0.02\ L^{1.2} = L^2/18\ t$$

thus $$L^{0.8} = 0.36\ t$$

and $$(dL/dt) = 0.45\ L^{0.20} = 0.35\ t^{0.25}$$

The powers on L and t are quite low indicating that constant velocity is a better assumption than constant diffusivity. For a 1 km lake ($L = 10^5$ cm) the velocity becomes 4.5 cm/s with a characteristic diffusion time of 2.2×10^4 s or 6 hours. A useful "rule of thumb" is then that horizontal diffusion occurs at a rate of the order of 1 km/day. This rate is very rapid compared to that of vertical diffusion discussed below, the implication being that in most lakes it can be assumed that horizontal concentration gradients in surface waters are eliminated quite rapidly.

Vertical Diffusion

The vertical diffusivity D_V is controlled by the presence of currents (which tend to induce eddying and thus promote diffusion) and the damping effect of density differences which arise from temperature and occasionally salinity variations. When the fluid density decreases with increasing height any eddy propelled upwards will tend to sink back because of its negative buoyancy. The balance between these tendencies is characterised by the Richardson Number which can be used to correlate D_V as reviewed by Thibodeaux (44). Thibodeaux also discusses the work of Koh and Fan (124) who correlated D_V with vertical density (ρ) gradient Ω where

$$\Omega = (d\rho/dY)/\rho \quad (m^{-1})$$

yielding

$$D_V = (cm^2/s) = 10^{-4}/\Omega$$

A form which does not give infinite D_V at $\Omega = 0$ is

$$D_V = 10^{-4}/(10^{-6} + \Omega)$$

At 10°C the density of water varies by approximately 0.0001 g/cm^3 per °C thus a 1°C temperature difference over a 1 m depth corresponds to $\Omega = 10^{-4}$ with a resultant D_V of 1 cm^2/s which is orders of magnitude smaller than D_H. For surface waters (epilimmion) D_V may be 1 to 100 cm^2/s with a mean value of 10 cm^2/s being a useful estimate. The characteristic diffusion time in surface waters is thus Y^2/D_V. A typical epilimmion depth in late summer may be 10 m thus this time is 10^5 s or 1 day. A mean mass transfer coefficient K_{OL} may be 10 cm/h thus the characteristic volatilization time is Y/K_{OL} or 100 h or 4 days. It follows that vertical mixing will generally be faster than volatilization thus in an epilimmion the usual situation will be that of a vertically well mixed layer with little concentration gradient. Expressed in another but equivalent form introduced earlier, the vertical diffusive resistance ($\Delta Y/D_V Z$) is small compared to the interfacial resistance ($1/K_{OL}$ Z) where Z is the fugacity capacity which for water is (1/H).

At the thermocline temperature gradients of 5 to 10°C may exist over depths of a few meters thus Ω may reach 10^{-3} m^{-1} resulting in D_V falling to 0.1 to 0.01 cm^2/s. If this applies over 2 m the characteristic diffusion time becomes 10^5 s to 10^6 s or 4 to 10 days which implies a significant resistance. It is probably better to combine the uncertainties in D_V and ΔY over the thermocline into a single term K_T the exchange coefficient equivalent to $D_V/\Delta Y$ which can be compared directly with the volatilization mass transfer coefficient K_{OL}. Snodgrass (125) for example has shown that thermocline vertical exchange coefficients for Lake Ontario have varied from 0.07 to 0.15 m/day which corresponds to a mean diffusivity of say 0.05 cm^2/s over a 3 to 6 m diffusion distance. From thermal observations Snodgrass has deduced that D_V varies from 0.1 to 0.4 cm^2/s in this region. The thermocline usually acts as a significant barrier to diffusion thus the simplest approach may be to assume negligible diffusion during the time that it applies.

In the hypolimmion below the thermocline there is usually negligible current action and very low vertical diffisivities apply. Thibodeaux (44) quotes

values of 0.73 m /day (0.08 cm^2/s) but values as low as 0.01 cm^2/s may occur. Snodgrass and O'Melia (126) have reviewed data on mean vertical diffusivities in various hypolimnetic waters and obtained the correlation

$$D = 0.0142\ Y^{1.49} \quad (D \text{ in } m^2/day, \quad Y \text{ the depth in m})$$

$$\text{or } D = 0.00164\ Y^{1.49} \quad (D \text{ in } cm^2/s, \quad Y \text{ in m})$$

Thus for lakes of depth 10 to 30 m diffusivities in the range 0.05 to 0.26 cm^2/s are expected. For a hypolimmion of depth 20 m with a D_V of 0.05 cm^2/s the characteristic diffusion time is 2.5 years implying that the mixing process is very slow.

The topic of modelling stratified lakes has been reviewed more fully by Imboden and Lerman (127) and Thibodeaux (44) who give details of more complex modelling approaches.

In summary, for estimating the volatilization rate from a lake it is essential to first obtain an approximate picture of its annual vertical stratification characteristics using temperature data as a guide. If dissolved oxygen or phosphorus data are also available these may also be useful. The simplest approach is to first regard the surface waters (which may be variable in volume as the thermocline descends) as a vertically and horizontally well mixed volume into which solute flows and from which solute is depleted by volatilization, advection and reaction. Exchange with deeper waters can be considered if necessary. It is unlikely that the transport, reaction, concentration and flow quantities will be known to a sufficiently high degree of accuracy to justify complex numerical models. For most purposes a simple intuitive model quantifying the dominant process will be adequate. The analysis by Schwartzenbach et al (2) for Lake Zurich is a good example of such an approach.

REFERENCES

1. Neely, W. B., Sci. of the Total Environ., 7, 117 (1977).

2. Schwartzenbach, R. P., Kubica, E. M., Giger W. and Wakehorn, S. G., Envir. Sci. Technol., 13, 1367 (1979).

3. Baughman, G. L. and Lassiter, R., "Prediction of Environmental Pollutant Concentrations", ASTM STP 657, p. 35, Philadelphia, PA (1978).

4. Smith, J. H., Mabey, W. R., Bohonos, N., Holt, B. R., Lee, S. S., Chou, T. W., Bomberger, D. C. and Mill, T., "Environmental Pathways of Selected Chemicals in Freshwater Systems", Parts I and II, EPA Reports 600/7-77-113 and 600/7-78-074.

5. USEPA, "Prospectus: Research and Development on an Exposure Analysis Modeling Systme (EXAMS)", USEPA Environmental Research Laboratory, Athens GA 1979.

6. Prausnitz, J. M., "Molecular Thermodynamics of Fluid Phase Equilibrium", Prentice Hall, Engelwood Cliffs, NJ (1973).

7. Mackay, D., Envir. Sci. Technol., 13, 1218 (1979).

8. Karickhoff, S. W., Brown, D. S. and Scott, T. A., Water Res., 13, 241 (1979).

9. Leo, A. J., Hansch, C. and Elkins, D., Chem. Res., 71, 525 (1971).

10. Hansch, C. and Leo, A. J., "Substituent Constants for Correlation Analysis in Chemistry and Biology", J. Wiley, New York (1979).

11. Yalkowsky, S. H., Ind. Eng. Chem. Fundam., 18, 108 (1979).

12. Yalkowsky, S. H., and Valvani, S. L., J. Chem. Eng. Data, 24, 127 (1979).

13. Mackay, D., Mascarenhas R., Shiu, W. Y., and Yalkowsky, S. H., Chemosphere, 9, 257 (1980).

14. Reid, R. D., Prausnitz, J. M., and Sherwood, T.K., "The Properties of Gases and Liquids", McGraw Hill, New York (1977).

15. Setschenow, J, Z. Physik. Chem. 4, 117 (1889).

16. McDevit, W. F. and Long, F. A., J. Am. Chem. Soc., 74, 1773 (1952).

17. Aquan Yeun, M., Mackay, D. and Shiu, W. Y. , J. Chem. and Eng. Data, 24, 30 (1979).

18. Davies J. T. and Rideal E. K., "Interfacial Phenomena" Academic Press, NY (1963).

19. Mukerjee P. and Mysels, K. J., "Critical Micelle Concentrations of Aqueous Surfactant Systems" Natl. Bur. Stds. Ref. Data Sev. No 36 (1971)

20. Almgren, M. Grieser, F., Powell, J. R., Thomas J. K., J. Chem. Eng. Data. 24 285 (1979).

21. Peake, E., and Hodgson, G. W. J., J. Amer. Oil. Chem. Soc., 43, 212 (1966) and 44, 696 (1967).

22. Spencer, W. F., Cliath, M. M., J. Agric. Food Chem.,18, 539 (1970).

23. Sinke, G. C., J. Chem. Thermo. 6. 311 (1974).

24. MacKnick, A. O., Prausnitz, J. M., J. Chem. Eng. Data, 24, 175 (1979).

25. Schwartz, F. P., J. Chem. Eng. Data, 22, 273 (1977).

26. Acree, F., Beroza, M., and Bowman, M. C., J. Agric. Food Chem., 11, 278 (1963).

27. Mackay, D., Wolkoff, A. W., Envir. Sci. and Technol., 7, 611 (1973).

28. Mackay,D., Shiu, W. Y. and Sutherland, R. P., Envir. Sci. and Technol, 13, 333 (1979).

30. Hansch, C., Quinlan, J.E. and Lawrence, G. L., J. Org. Chem., 33, 347 (1967).

31. Neely, W. B., Branson, D. R., Blau, G. E., Envir. Sci. Technol., 8, 1113, (1974).

32. Chiou, C. T., Freed, V. H., Schmedding, D. W. and Kohnert, R. L., Envir. Sci. Technol. 11, 475 (1977).

33. Mackay, D., Envir. Sci. Technol., 11, 1219 (1977).

34. Tulp, M. T. M., and Hutzinger, O., Chemosphere, 10, 849 (1978).

35. Kenega, E. E. and Goring, C. A. I., Paper given at ASTM Third Aquatic Toxicology Symposium, October 1978, New Orleans (ASTM STP 707 March 1980), Philadelphia, PA.

36. Zitko , V., Bull. Envir. Contam. Toxic., 12, 406 (1974).

37. Albro, P. W. and Fishbein, L., Biochem. Biophys. Acta, 214, 437 (1970).

38. Hansch, C., Accts. Chem. Res., 2, 232 (1960).

39. Sugihara, K., Ito, N., Matsumoto, N., Mihara, Y., Murata, K., Tsukakoshi, Y., and Goto, M., Chemosphere, 9, 731 (1978).

40. Csanady, G. T., "Turbulent Diffusion in the Environment", Reidel, Boston, (1973).

41. Bird, R. B., Stewart, W. E., Lightfoot, E. N., "Transport Phenomena", Wiley, NY (1960).

42. Sherwood, T. K., Pigford, R. L., Wilke, C. R., "Mass Transfer", McGraw Hill, NY, (1975).

43. Whitman, W. G., Chem. Metal Engrg., 29, 146-48 (1923).

44. Thibodeaux, L. J., "Chemodynamics", Wiley, NY (1979).

45. Lewis, W. K., Whitman, W. G., Ind. Eng. Chem., 16, 1215 (1924).

46. Higbie, R., Trans. Amer. Inst. Chem. Eng., 31, 365 (1935).

47. Danckwerts, P. V., Ind. Eng. Chem., 43, 1460 (1951).

48. Dobbins, W. E., J. San. Eng. Div. ASCE 90 SA3, 53 (1964), also in "Mechanisms of Gas Absorption by Turbulent Liquids," MacMillan Co., N.Y. (1964).

49. Toor, H. L., Marchello, J. M., Ind. Eng. Chem. Fundam., 2, 8 (1963).

50. King, C. J., Ind. Eng. Chem. Fund., 4, 125 (1965).

51. Harriot, P., Chem. Eng. Sci., 17, 149 (1962).

52. Ruckenstein, E., Chem. Eng. Sci., 18, 223 (1903).

53. Fortescue, G. E., and Pearson, J. R. A.., Chem. Eng. Sci., 22, 1163 (1967).

54. Ruckenstein, E., Sucier, D. G., Chem. Eng. Sci, 24, 1395 (1969).

55. King, C. J., AIChEJ 10, 671 (1964).

56. Goodgame, T. H., Sherwood, T. K., Chem. Eng. Sci., 3, 37 (1954).

57. Kinsman, B., "Wind Waves", Prentice-Hall, Inc., Englewood Cliffs, NJ, (1965).

58. Cohen, Y., Cocchio, W., Mackay, D., Envir. Sci. and Technol., 12, 553 (1978).

59. Schlichting, H., "Boundary Layer Theory", McGraw Hill, NY, 1968.

60. Wu, J., J. Geo. Res., 74, 444 (1969).

61. Smith, S. D., J. Phys. Oceanogr., 10, 709 (1980).

62. Wu, J., "Wind Stress Coefficients over Sea Surfaces - a Revisit", Unpublished Paper (1979).

63. Charnock, H., Quart, J.. Roy. Met. Soc., 81,639 (1955).

64. Mackay, D., Matsugu, R., Can. J. Chem. Eng., 51, 434 (1973).

65. Liss, P. S., Rap. P.-v. Reun. Cons. int. Explor. Mer., 171, 120 (1977).

66. Hunter, K. A. and Liss, P. S., Marine Chem. 5, 361 (1977).

67. Liss, P. S., Martinelli, F. N., Thalassia Jugoslavica, 14, 215 (1978).

68. Nguyen Ly L. Carbonell R. G., McCoy, B. J., AIChEJ 25, 1015 (1979).

69. Tsivoglou, E. C., J. Water Poll. Contr. Fed., 37, 1343 (1967).

70. Tsivoglou, E. C., "Tracer Measurement of Stream Reaeration". Fed. Water Poll. Contr. Admin. US Dept. of Interior (1967).

71. Rathbun, R. E., Shultz, D. J., Stephens, D. W., Tai, D. Y., 17th. Congress Intl. Assoc. for Hydr. Res 483 (1977).

72. Smith, J. H., and Bomberger, D. C., "Prediction of Volatilization Rate of Chemicals in Water" in "Hydrocarbons and Halogenated Hydrocarbons in the Aquatic Environment", p. 445 Ed. by B. K. Afghan and D. Mackay, Plenum Press, NY (1978).

73. Mackay, D., Nadeau, S., and Ng, C., "A Small Scale Laboratory Dispersant Test", ASTM STP 659, Philadelphia, PA (1979).

74. Metzger, I, ASCE J. San.Eng. Div. 94 SA6 1153 (1968).

75. Thackston, E. L., Kneckel, P. A., ASCE J. San. Eng. Div. 95, SA1 65 (1969).

76. Weast, R. C., Handbook of Chemistry and Physics, 53rd. Ed. CRC Press 1972.

77. May, W. E., Wasik, S. P., Freeman, D. M., Anal. Chem. 50, 175 and 997 (1978).

78. Paris, D. F., Steen, W. C., Baughman, G. L., Chemosphere 4, 319 (1978).

79. Liss, P. S., Slater, P. G., Nature (Lond), 247, 181 (1974).

80. Downing, A. L., Truesdale, G. A., J. Appl. Chem., 5, 570 (1955).

81. Hidy, G. M., Plate, E. J., J. Fluid Mech, 26, 4 651 (1966).

82. Bank, R. B., ASCE J. Envir. Eng. Div.,101, 813 (1975).

83. Bank, R. B., ASCE J. Envir. Eng. Div., 103, 489 (1977).

84. Sivakumar, M., Herzog, A., "A Model for the Prediction of Reaeration Coefficients in Lakes from Wind Velocity" in Developments in Water Science, 11, Hydrodynamics of Lakes Elsevier Pub. Coy, NY 1979.

85. Deacon, E. L., Tellus, 29, 363 (1977).

86. Liss, P. S., Deep Sea Res., 20, 221 (1973).

87. Kanwisher, Deep Sea Res., 10, 195 (1963).

88. Hoover, T. E., Berkshire, D. C., J. Geophys. Res., 74, 456 (1969).

89. Broecker, W. S. and Peng, T. H., Tellus, 26, 21 (1974).

90. Broecker, W. S. and Peng, T. H., Earth Planet. Sci. Letters, 11, 99 (1971).

91. Peng, T. H., Takahashi, T. and Broecker, W. S., J. Geophys. Res., 79, 1772 (1974).

92. Emerson, S., Limnol and Oceanogr., 20, 743 (1975).

93. Emerson, S., Limnol and Oceanogr., 20, 754 (1975).

94. Emerson, S. and Broecker, J. Fish Res. Board Can., 30, 1475 (1973).

95. Tamir, A., Merchuk, J. D., Chem. Eng. Sci., 33, 1371 (1978).

96. Tamir, A., Merchuk, J. C. and Virkar, P. D., Chem. Eng. Sci., 34, 1077 (1979).

97. Gilliland, E. R., Ind. Eng. Chem., 26, 681 (1934).

98. Sverdrup, H. V., J. Marine Res., 1, 3 (1937).

99. Pond, S., Phelps, G. T., Paquin, J. E., McBean, G. and Stewart, R. W., J. Atmos. Sci., 28, 901 (1971).

100. Hala, E., Pick, J., Fried, V., Vilim, O., "Vapour Liquid Equilibrium" Pergamon Press (1967).

101. Veda, M., Katayama, A., Urahata, T. and Kuroki, N., Colloid and Polymer Sci., 256, 1032 (1978).

102. Veda, M., Katayama, A., Kuroki, N., Urahata, T., Progr. Colloid and Polymer Sci., 63, 116 (1978).

103. Boehm, P.D., and Quinn, J. G., Geochim et Cosmochem. Acta, 37, 2459 (1973).

104. Sutton, C., Calder, J. A., Environ. Sci. and Technol., 8, 654 (1974).

105. Mackay, D., Shiu, W. Y. and Sutherland, R. J., Chapter 11 of "Dynamics Exposure and Hazard Assessment of Toxic Chemicals", R. Hague Ed., Ann Arbor Science, Ann Arbor, Mich. (1980).

106. Mackay, D. and Yuen, A., Water Poll. Res. J. of Canada, 15, (1), 83 (1980).

107. Rathbun, R. E., "Reaeration Coefficient of Streams - State of the Art." J. Hydraulics Div., ASCE, 103 (HY4):409, (1977).

108. Holley, E. R., "Oxygen Transfer at the Air Water Interface", Transport Processes in Lakes and Oceans, (Ed.) R. J. Gibbs, Plenum Press, New York (1977).

109. Lau, Y. L., "A Review of Conceptual Models and Prediction Equations for Reaeration in Open-Channel Flow", Tech. Bull. 61, Inland Waters Branch, Department of the Environment, Ottawa, (1972).

110. Bennett, J. P. and Rathbun, R. E., "Reaeration in Open Channel Flow", U.S. Geol. Survey, Open File Report, Bay St., St. Louis, Miss., (1971).

111. Mattingly, G. E., J. Hydraulics Div. ASCE, 103 (HY3):311, (1977).

112. Tsivoglou, E. C., and Wallace, J. R., "Characterization of Stream Reaeration Capacity", EPA Report R3-72-012, Washington, DC (1972).

113. Parkhurst, J. D. and Pomeroy, R. D., J. Sanit. Eng. Div. ASCE, 98, No. SA1 Paper 8701:101, (1972).

114. Churchill, M. A., Elmore, H. L. and Buckingham, R. A., J. Sanit. Eng. Div., ASCE, 88, No. SA4 paper 3199 1, (1962).

115. Isaacs, W. P. and Gaudy, A. F., J. Sanit. Div., ASCE, 94, No. SA2 paper 5905 319, (1968).

116. Langbein, W. B. and Durum, W. H., "The Aeration Capacity of Streams", U. S. Geol. Survery, Circ. No. 542, Reston, VA , (1967).

117. Ficke, E. R. and Ficke, J. F., "Ice on Rivers and Lakes - A Bibliographic Essay",U. S. Geol. Survey, Water Res. Div. Rep. 77-95, Reston, VA, (1977).

118. Rathbun, R. E. and Grant, R. S., "Comparison of the Radioactive and Modified Techniques for Meaurement of Stream Reaeration Coefficients:, U.S. Geol. Survey, Water Res. Investigations 78-68, (1978).

119. Zurcher, F. and Giger, W., Fluchtige Organische Spurenkomponenten in der Glatt, Vom Wasser, 47:37, (1976).

120. Giger, W., Reinhard, M., Schaffner, C., and Zurcher, F., "Analysis of Organic Constituents in Water by High Resolution Gas Chromatography in Combination with Specific Detection and Computer Assisted Mass Spectrometry", Identification and Analysis of Organic Pollutants in Water, (Ed.) L. H. Keith, Ann Arbor Sci., Ch. 26:433, (1976).

121. Helz, G. R., "Anthropogenic C_1 and C_2 Haloforms: Potential Application as Coastal Water Mass Tracers", Presented: Int. Symp. Anal. Hydroc. Halogenated Hydroc. Aquatic Environ., Hamilton, Ontario, (1978).

122. Murty, C. R. and Miners, K. C., "Turbulent Diffusion Processes in the Great Lakes", Scientific Series No. 83, Inland Waters Directorate Environment Canada (1978).

123. Okubo, A., Deep Sea Res., 18, 789 (1977).

124. Koh, C. Y. and Fan, L. N. USEPA Water Pollution Control Research Series 16130 DW 016 Washington, DC, (1970).

125. Snodgrass, W. J., "Relationship of Vertical Transport Across the Thermocline to Oxygen and Phosphorus Regimes: Lake Ontario as a Prototype", p. 179 of Transport Processes in Lakes and Oceans, (Ed.) R. J. Gibbs, Plenum Press, NY, (1977).

126. Snodgrass, W. J. and O'Melia, C. R., Environ. Sci. and Technol., 10, 937 (1975).

127. Imboden, D. M. and Lerman, A., "Chemical Models of Lakes", Chapter 11 in "Lakes: Chemistry Geology Physics" (Ed.) A. Lerman, Springer Verlag, NY (1978).

128. Valvani, S. C., Yalkowsky, S. H., and Amidon, G. J., J. Phys. Chem. 80, 829 (1976).

129. Yalkowsky, S. H., Orr, R. J., Valvani, S. C., Ind. Eng. Chem. Fundam 18, 351 (1979).

SYMBOLS

The symbols used in this report are given below with dimensions, which are generally in SI units. Pressures were expressed in atm rather than Pascals. In some cases where an existing correlation is quoted, for example for diffusivity or reaeration constant, the original units used by the author have been retained, thus the dimensions may differ from those stated below. Where this occurs, it is noted in the text.

A	area	m^2
a	Charnock constant	dimensionless
C	concentration	mol/m^3
C^s	solubility	mol/m^3
C_D	drag coefficient	dimensionless
C_H	heat concentration	J/m^3
C_O	initial concentration	mol/m^3
D	molecular diffusivity	m^2/s
D_F	" in film	m^2/s
D_G	" in gas	m^2/s
D_L	" in liquid	m^2/s
D_H	horizontal turbulent diffusivity	m^2/s
D_V	vertical turbulent diffusivity	m^2/s
F	Froude Number	dimensionless
F	water flow rate	m^3/s

F	$\ln (x_s \gamma_s)$	dimensionless
f	fugacity	atm
f_L	liquid fugacity	atm
f_R	reference fugacity (of subcooled liquid)	atm
f_S	solid fugacity	atm
G	volumetric flow rate	m^3/s
g	gravitational constant	$9.81\ m/s^2$
H	Henry's law constant	atm m^3/mol
H_w	Henry's law constant of water	atm m^3/mol
ΔH^F	enthalpy of fusion	J/mol
ΔH^S	enthalpy of sublimination	J/mol
ΔH^V	enthalpy of vaporization	J/mol
I	input rate	mol/h
K	various constants	
K_{12}	partition coefficient	dimensionless
K_D	decay constant	s^{-1}
K_P	sorption coefficient	m^3/Mg
K_{OW}	octanol water partition coefficient	dimensionless
K	mass transfer coefficient	m/s
K_G	" in gas	m/s
K_L	" in liquid	m/s
K_{OG}	" overall gas	m/s
K_{OL}	" overall liquid	m/s

K	Von Karman constant	dimensionless
K_2	reaeration constant	h^{-1}
L	distance downstream	m
M	amount	mols
M	molecular weight	g/mol
N	mass flux	mol/m^2s
n	amount	mols
P	partial pressure	atm
P^S	saturation vapor pressure	atm
P_T	total pressure	atm
R	gas constant	$(82 \times 10^{-6}$ atm m^3/mol K)
Re	Reynolds' Number	dimensionless
r	mass transfer resistance	atm m^2s/mol
S	solubility	mol/L
S	surface renewal rate	s^{-1}
ΔS	entropy change	J/mol K
Sc_A	Schmidt Number in air	dimensionless
Sc_L	Schmidt Number in liquid	dimensionless
St	Stanton Number	dimensionless
T	temperature	K
T_B	boiling point temperature	K
T_C	critical temperature	K
T_M	melting point temperature	K
TSA	total surface area	$Å^2$
t	time	s

U	wind velocity	m/s
U_{10}	wind velocity at 10 m height	m/s
U_{∞}	free stream velocity	m/s
U^*	friction velocity	m/s
V	volume	m^3
V	river velocity	m/s
V	molar volume	m^3
v	molar volume	m^3/mol
w	river width	m
X	fetch	m
x	mole fraction in liquid	dimensionless
Y	water or river depth	m
y	diffusion path length	m
y	mol fraction in vapor	dimensionless
Z_A	fugacity capacity in air	mol/m^3 atm
Z_F	fugacity capacity in film	mol/m^3 atm
Z_O	fugacity capacity in octanol	mol/m^3 atm
Z_S	fugacity capacity in sorbed state	mol/m^3 atm
Z_W	fugacity capacity in water	mol/m^3 atm
Z_H	volumetric heat capacity	J/m^3 K
Z	length dimension in Froude Number	m
Z	height above water surface	m
Z_0	surface roughness	m

α	relative volatility	dimensionless
γ	activity coefficient	dimensionless
γ_o	activity coefficient in octanol	dimensionless
γ_s	activity coefficient in solvent	dimensionless
γ_w	activity coefficient in water	dimensionless
ρ	density	kg/m^3
μ	viscosity	Pa s
ϕ	fugacity coefficient	dimensionless
ϕ	association parameter	dimensionless
τ	stress	N/m^2
Ω	density gradient	kg/m^4

GLOSSARY

Activity Coefficient(γ) A dimensionless factor applied to a solute's "ideal" or Raoult's Law fugacity or vapor pressure to correct it to the observed experimental value. It is thus the ratio of the actual pressure to that "predicted" by Raoult's Law.

Drag Coefficient (C_D) A dimensionless quantity relating the drag or stress on a surface to the speed of the wind passing over the surface.

Fetch Distance over water which wind has passed and thus has had an opportunity to establish waves. Low fetch situations are sheltered from wind and wave action.

Friction Velocity(U^*) A hypothetical velocity which is a measurement of the force, stress, or "friction" which air exerts when flowing over water.

Froude Number (F) A dimensionless number (velocity)/(length x g)$^{0.5}$ used to scale-up velocities over a range of system sizes.

Fugacity (f) The "escaping tendency" of a solute from a phase and thus an indication of equilibrium in multiphase systems. It has units of pressure.

Fugacity capacity (Z) A constant relating fugacity to concentration analogous to a volumetric heat capacity.

Logarithmic Velocity Profile A commonly used equation relating velocity of air to height above a surface. It contains the von Karman constant and two empirical constants, the friction velocity and surface roughness.

Mass Transfer Coefficient (K) A constant expressing the ease with which mass diffuses in a defined region. It can be regarded as the piston velocity with which the solute in solution diffuses near an interface.

Reynolds Number (Re) A dimensionless number (velocity x density x length/viscosity) used to correlate turbulent flow conditions.

Schmidt Number (Sc) A dimensionless number (viscosity/[diffusivity x density]) which can be regarded as the ratio of the ease with which a fluid transports momentum and mass by diffusion. It is used to introduce diffusivity into correlation.

Stanton Number (St) A dimensionless number which is a ratio of a mass transfer coefficient to a velocity.

Surface Roughness (Z_0) A constant obtained from a logarithmic velocity profile. It can be regarded as an indication of the roughness of the surface.

Total Surface Area (TSA) A calculated area of a molecule in units of square Angstroms used to correlate solubility.

INDEX

Activity Coefficient, 4-15, 4-45, 8-22
Aeration, 9-11
Alcohols, 4-20
Antoine equations, 4-8
Aqueous solubility, 4-10, 4-45
Bioconcentration, 4-7
Charnock constant, 5-20, 8-9
Consistency tests, 4-45
Co-solutes, 4-13, 8-25
Diffusion processes, 5-4
Diffusivity, 8-5
Drag Coefficient, 5-19, 8-8
Epilimmion, 9-16
Fetch, 5-20
Fick's first law, 5-4
Froude number, 5-20
Fugacity in atmosphere, 4-4
Fugacity in biota, 4-7
Fugacity capacity, 4-2
Fugacity in octanol, 4-7
Fugacity ratio, 4-10
Fugacity in sorbed phases, 4-6
Fugacity in water, 4-4
Henry's law constant, 4-29, 4-45, 8-28, 9-1
Horizontal Diffusion, 9-15
Hypolimmion, 9-16
Ice, 9-11
Lakes, 9-14
Logarithmic velocity profile, 5-16
Mass transfer coefficient, 5-6, 5-12
Mass transfer coefficient K_G, 8-14
Mass transfer coefficient K_L, 8-11, 8-18
Mass transfer coefficient overall, 8-17
Mass transfer mechanism, 5-1
Molecular size, 8-5
Octanol-water partition coefficient, 4-38, 4-45
Reaeration constant, 9-7, 9-10
Relative volatility, 4-29
Resistances, 5-8
Rivers, 9-7
Roll cell, 5-13
Small scale volatilization apparatus, 7-2
Solubility, 8-25
Stanton Number, 5-22
Surface active, 4-14
Surface films, 5-24
Surface roughness, 5-19

Temperature, 8-5
Thermocline, 9-16
Total surface area, 4-11, 4-15
Tracer techniques, 9-11
Turbulence, 5-5
Two resistance, 5-15
Vapor pressure, 4-23
Vertical Diffusion, 9-16
Volatilization systems, 5-25
von Karman constant, 5-19
Waves, 5-16
Whitman, 5-12
Whitman Two Resistance Theory, 5-8
Wind Velocity, 5-16
Windwave tank, 7-21